SYNTHESIS AND CHARACTERIZATION OF CONDUCTING POLYMERS WITH NEW ARCHITECTURAL MOTIFS

by

Paul D. Byrne

B.S., Chemistry
University of Vermont, 2000

SUBMITTED TO THE DEPARTMENT OF CHEMISTRY IN PARTIAL FULFILLMENT OF THE REQUIREMENT FOR THE DEGREE OF

DOCTOR OF PHILOSOPHY IN CHEMISTRY

AT THE

MASSACHUSETTS INSTITUTE OF TECHNOLOGY

JUNE 2006

Signature of Author: _____
Department of Chemistry
April 13, 2006

Certified by: _____
Timothy M. Swager
Professor of Chemistry
Thesis Supervisor

Accepted by: _____
Robert W. Field
Chairman, Department Committee on Graduate Students

This doctoral thesis has been examined by a Committee of the Department of Chemistry as follows:

Professor Stephen L. Buchwald: _____
Chairman

Professor Timothy M. Swager: _____
Thesis Adivsor

Professor Gregory C. Fu: _____

To my persistent family.

Synthesis and Characterization of Conducting Polymers with New Architectural Motifs.

by

Paul D. Byrne

Submitted to the Department of Chemistry on April 13, 2006 in partial fulfillment of the requirement for the degree of Doctor of Philosophy in Chemistry

Abstract

Chapter one has a brief discussion of polythiophene and the important factors to consider with polythiophene synthesis and characterization. In chapter two, a variety of polythiophene derivatives that incorporated 2,2'-biphenyl units into the polymer main chain were synthesized. The potential utility of the 2,2'-biphenyl unit as a scaffold to facilitate the π-π interactions between thiophene oligomers was explored. The linkage of the thiophene to the biphenyl was varied between the α- or β-positions to assess how this variable affected the overall properties of the resulting polymers. The β-linked thiophene monomers produced highly cross-linked polymers and the electroactivity of these polymers depended on the length of the thiophene fragment in the corresponding monomer. The α-linked thiophene monomers produced segmented linear conjugated polymers and the polymers' segmentation dominated the resulting electroactivity. A model study demonstrated that through-space interactions between the oligothiopene fragments of the 2,2'-biphenyl monomers did occur. In chapter three, a synthetic scheme was developed to generate 2,2'-biphenyl monomers with long alkyl chains from which soluble polymers could be generated. The synthetic scheme was also utilized to produce a monomer that could be electrochemically cross-linked in a controlled fashion. In chapter four, a variety of polythiophene derivatives that incorporated azaferrocenes complexes into the main polymer chain were synthesized. These polymers were then used to ascertain the effect of a π-bound metal on the main chain of a conducting polymer. The oxidation of the metal centers in the polymer produced a significant change in the conductivity of the polymer film. Changing the length and oxidation potential of the polythiophene section of the monomer appeared to alter the charge delocalization of the polymers. In chapter five, a series of polythiophene derivatives containing cyclobutadiene cobalt cyclopentadiene complexes in the main polymer chain were synthesized. The viability of the electropolymerization of the complexes was determined by the relative position of organic section's oxidation potential versus the oxidation of the metal centers. The metal coordinated cyclobutadiene ring of the complex appeared to have a modest charge transport ability.

Thesis Supervisor: Timothy M. Swager
Title: Professor of Chemistry

Table of Contents

Chapter 1:

Introduction to Polythiophene Derivatives

Introduction

Since the discovery of a purely organic conducting polymer, these materials have been the center of intense research.[1] One conducting polymer in particular that has attracted strong interest is polythiophene.[2] A reason for this material's preeminence is the ease of synthesis and modification of the monomers and polymers.[3] The derivatization of polythiophene can take the form of either substitution on the α- or β-positions of the thiophene monomer, as shown in Chart 1.

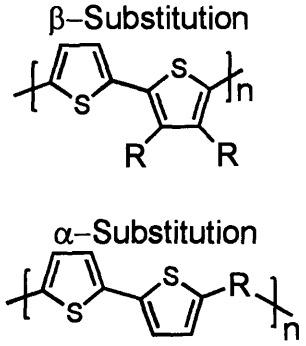

Chart 1.

Substitution at the β-position of the thiophene keeps the main polymer chain un-interrupted; and therefore, the π-conjugation of the polymer remains intact. The effect of a β-substituent on polythiophene will be determined by several factors such as electronic polarization and sterics. Substitution at the α-position of the thiophene creates a break in the main polymer chain and disrupts the original π-conjugation. How this disruption affects the π-delocalization of the polymer will depend on the relative energy and molecular orbital alignment of the substituted group. Since β-substitution is a subtle perturbation of the polymer structure that can be used to substantially alter the electroactive properties of the polymer, β-substitutions are more common than α-substitutions.

All the substitutions in this introduction involve only organic compounds or main group elements. Transition metals were not included in this summary since their incorporation into conducting polymers gives rise to complicated interactions involved in that are beyond this simple introduction.[4]

Applications

The specific modifications of polythiophene are driven by the properties that need to be optimized for a desired application. Polythiophene derivatives have applications in sensors, supercapacitors, batteries, actuators, LED's, and electrochromic devices.[5] The design of polythiophene derivatives can be divided into three categories: tuning the chemical relationships between the polymer and other compounds, tuning the ionic and electrical transport, and tuning the optical properties. Both α- and β-substitutions have been used as methods for modifying polythiophene. A brief discussion with a few examples will demonstrate the important design principles. The design of sensors using polythiophene is an example of tuning the chemical relationships between the polymer and other compounds. Polythiophene-based sensors utilize receptors that are either attached to or built into the polymer structure.[6] Designing a polymer for sensor applications is not dependent on improving the electroactivity of the polymer but on shifting this electroactivity with a particular analyte. The α-substituted **p-1** is an example of a simple receptor, in this case a Lewis acidic aryl boryl, being built into the

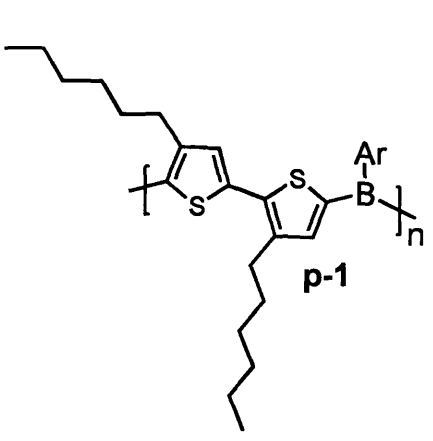

p-1

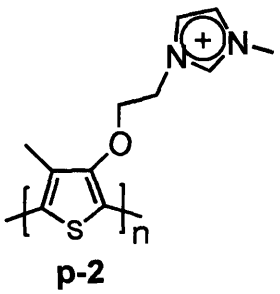

p-2

polythiophene structure. The boryl group serves as a binding site for Lewis bases of interest such as pyridine.[6a] The β-substituted **p-2** has a cationic group attached to the polymer so that the polymer can serve as a fluorescent transducer for the binding of an anionic oligonucleotide probe.[6b] Supercapacitors are capacitors that can store larger amounts of charge than typical capacitors, and optimization for this application involves tuning the ion transport of a polymer.[7] The design of polythiophene based supercapacitors involves maximizing the charge storing ability of the polymer. For supercapacitors, the material of the capacitor must allow significant p-doping (oxidation of the polymer) and n-doping (reduction of the polymer) to occur. One method to

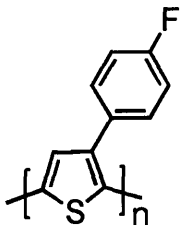

p-3

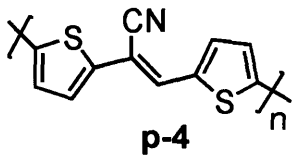

p-4

accomplish this task is to use both a p-dopable polymer and n-dopable polymer in the capacitor. The n-dopable and β-substituted **p-3** along with the p-dopable native polythiophene was used to a create supercapacitor device.[8] The α-substituted polymer **p-4** allows the simplification of the supercapacitor system since the a polymer can be significantly p- and n-doped.[9] This effect is due in the low bandgap (E_g) of **p-4**.[10]

Electrochromic applications require the tuning of the optical properties of polythiophene. Polymeric electrochromic devices utilize the visible colors of conjugated polymers that change with an electric stimulus.[11] In this application, the substituents are used to tune the absorption of polymer. (i.e. modify the E_g of the polymer). One α-

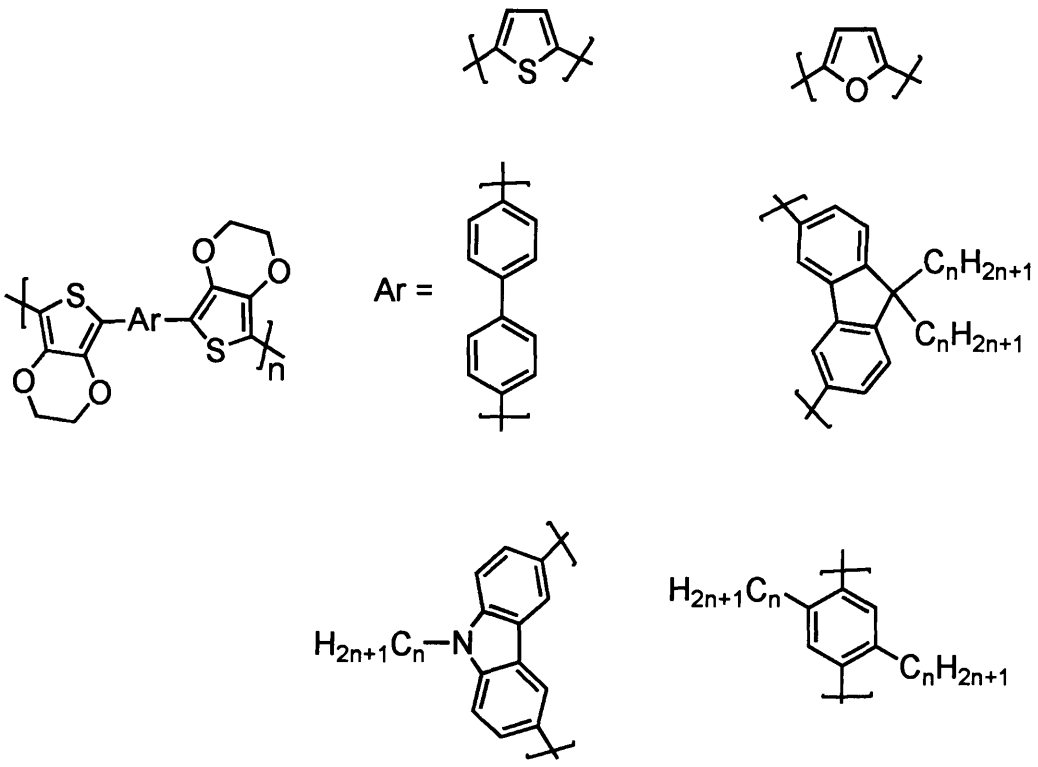

Chart 2

substituted system that has been utilized to produce a wide variety of colors is shown in Chart 2. The aryl group in the polymer chain is varied to achieve a wide range of bandgaps and therefore the resulting polymers absorb or reflect a variety of colors.[5f] One drawback to the α-substituted system was the difficulty in producing the color green. The β-substituted **p-5** was developed to address this problem. In the case of **p-5**, the backbone contains two well-defined conjugated systems that absorb blue and red light.[12] This mix of absorptions causes the polymer to reflect green light. An electrochemical polymerization at a low electrochemical potentials polymerizes the terthiophene unit of the monomer. This produces the low band-gap red absorbing portion and illustrates the importance of the extent of the π-conjugation within the polymer chain.[13] Although not

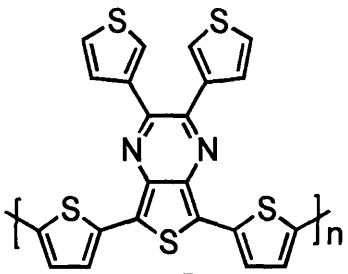

p-5

all manipulations of polythiopene involve the extended π-conjugation of the polymer, a significant portion of the manipulations are focused on this aspect.

Electrochemical Measurements of Polythiophene

In determining the extent of π-conjugation in a polymer, different types of measurements are useful. In particular the E_{pa} (peak anodic or peak oxidation potential from the neutral polymer), the λ_{max} (the absorbance maximum of the neutral polymer), and the conductivity of the polymer in the fully doped state give a good measure of the polymer properties that are controlled by π-delocalization. Each measurement has its advantages and limitations. The E_{pa} provides a good estimate of the relative energy of the valence band (HOMO) in the polymer. This is an important measurement of any polythiophene derivative since most applications of polythiophene require the oxidation (p-doping) of a film. The E_{pa} value is not an equilibrium value and E_{pa} value is dependent on other factors such as the transfer coefficient and the diffusion coefficient of the electrolyte for the electrochemical process. These factors are in turn affected by macroscopic elements such as the density, morphology, polarity, and thickness of the polymer film. A more appropriate value is the half wave potential, $E_{1/2}$. Yet, the $E_{1/2}$ values are not often reported due to the electrochemical irreversibility of most conducting polymers.[14] The E_{pc} (peak cathodic or peak reduction potential of the neutral polymer) is reported less often since the reduction of polythiophenes requires potentials lower than allowed in typical electrochemical solvents, such as acetonitrile or methylene chloride. The reduction of polythiophenes also tends to be chemically irreversible as well.[15] The

λ_{max} of the neutral polymer is useful if it corresponds to a pure $\pi \rightarrow \pi^*$ transition because it then can provide a measure of the extent of conjugation.[16] The λ_{max} for all the polymers reported in this introduction correspond to these $\pi \rightarrow \pi^*$ transitions. The neutral polymer's bandgap, E_g, can be determined from UV-vis absorption spectroscopy and electrochemistry of the polymer. This value can be determined from the absorption onset of the UV-vis spectrum (minimum energy of the absorption of the polymer). Electrochemically, the E_g is determined by the difference between the onsets of E_{pa} and E_{pc}. This energy difference between the valence and conduction bands is affected by the extent of π-conjugation and E_g is often considered the ultimate measurement of the extent of longest π-conjugation. The value λ_{max} is also important and reflects the most abundant conjugation length. The fact λ_{max} is off set from λ_{onset} is due to the inherent conformational disorder in most conducting polymers. For many applications, the bulk conductivity is the most important measurement and it is also the measurement that often has the greatest experimental variation. The polymer must be cast into a film or pressed into a pellet then oxidized chemically to determine its bulk conductivity. The stability of the polymer can be a problem and decomposition or de-doping can significantly affect

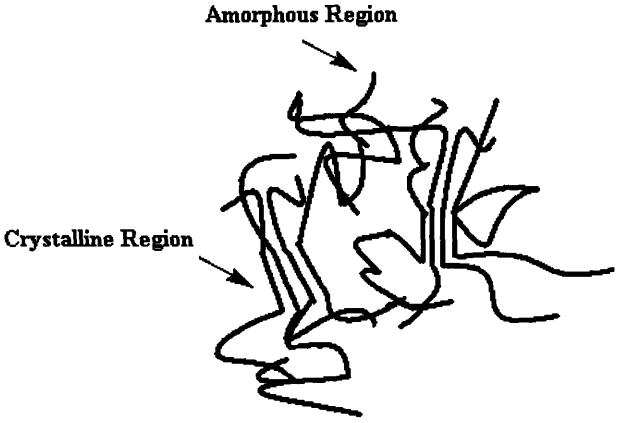

Chart 3.

the conductivity measurement. *In situ* conductivity with electrochemical doping often avoids this problem but requires a correction for the resistance of leads and the non-uniform film coverage. Another factor that affects the conductivity is the degree of order within the polymer film. Conducting polymers are effectively amorphous semiconductors with some crystalline regions, as shown in Chart 3.[17] The conductivity of a conjugated polymer and the bulk conductivity is limited by the ability of a charge (an electron or hole) to hop between localized sites in the amorphous domains. The higher carrier mobility in the crystalline domain is universal and the bulk conductivity of material is noticeably affected by the amount of crystalline order.[18] Although the extent of π-conjugation within a conjugated polymer will affect the hopping between the localized sites, the amount of order in the film will sometimes be the dominate factor that determines the bulk conductivity.

The properties of the polythiophene can vary significantly, as shown in Chart 4.[2] This variance is due the sensitivity of polythiophene to the polymerization and doping conditions. The typical E_{pa} for reported for polythiophene is 0.72 V vs. Fc/Fc^+ (Referenced to the $E_{1/2}$ of the ferrocene/ferrocenium redox couple, 0.22 V versus Ag/Ag^+) but an E_{pa} as low as -0.53 V has been reported.[19, 20]

To understand polythiophene, many different oligomers of polythiophene have been studied. The oligomers in solution display two waves in their CVs and their E_{pa}'s decreased linearly with the reciprocal number of thiophenes rings. This trend is the expected outcome since the addition of the π-conjugated units causes an increase in the delocalization of charge.[21] This observation is also useful to understand polythiophene derivatives with significant or complete segmentation of the π-conjugation since they

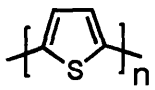

Polythiophene:

E_{pa} = -0.53-0.72 V

λ_{max} ~ 480 nm

σ_{con}=0.02-370 S cm^{-1}

E_g ~ 2.2 V

Chart 4.

often have two waves in their CV's with E_{pa}'s (or $E_{1/2}$'s) in the same potential range as the polythiophene oligomers of similar conjugation length. In the solid state, the CV's of similar oligomers displayed only one irreversible E_{pa} ($\approx$ 0.35 V).[22] This phenomenon was attributed to the stabilization of the oxidized oligomers by the formation of π-dimerized complexes of the oxidized oligomers. The phenomenon of π-dimerization involves the cofacial bonding of two radical cation oligomers to form a lower energy species, a diamagnetic species with unconventional multicenter binding between the π-systems.[23] This phenomenon has been observed in solution and in the solid state.[24] The irreversible solid state CV's of the oligomers of polythiophene in some cases may also be due to a secondary reaction (e.g., reactions through the β-position of the thiophene) between oligomer units.[25]

For the purpose of this summary, the E_{pa} value for a fully π-conjugated polythiophene was assumed to be 0.5 V or lower. The typical conductivity of polythiophene produced by electrochemical polymerization is the range of 0.02-370 S cm^{-1}.[2] The typical solid state neutral absorption of any polythiophene grown by oxidative polymerization typically has at λ_{max} at 480 nm and a band gap for polythiophene of 2.20 eV.[3]

β-Substitutions

There are numerous examples of β-substituted polythiophene derivatives, so only the important trends will be highlighted herein. The most common β-substitutent is an alkyl chain. The β-substitution of a methyl group into polythiophene poly(3-methylthiophene) affects the electroactivity of the resulting polythiophene derivative in multiple ways.[26] The methyl group has an inductive electron donating effect on the thiophene monomer, and this effect increases the relative energy of the HOMO of the thiophene. This in turn increases the energy of the valance band of polythiophene and lowers the E_g of the polymer. The addition of the methyl group also decreases the number of unwanted β-couplings in an oxidative synthesis and thereby gives a more regular structure that increases the ordering of the polymer chains.[27] The combination of these effects is the origin of poly(3-methylthiophene)'s higher bulk conductivity relative to polythiophene polymerized under similar conditions.[26] Adding long alkyl chains at the β-position of the thiophene monomer produces soluble polythiophenes.[28] A complicating factor is the head-to-tail and head-to-head nature of the thiophene monomers in the polymer. A

Poly(3-alkylthiophenes), regioirregular

E_{pa}=0.34 V; σ_{con}= 10 to 100 S cm^{-1}

λ_{max} = 438 nm (solution); 480 nm (solid state)

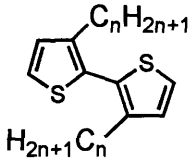

Head-to-Head Coupling

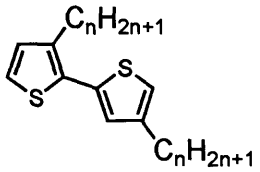

Head-to-Tail Coupling

Scheme 1.

completely defined regiochemistry is referred to as a regioregular polythiophene. In electrochemical or chemical oxidative polymerizations the coupling of two thiophenes at the 2-position, will give a combination of head-to-tail and head-to-head coupling, as shown in Scheme 1. The head-to-head coupling creates a steric interaction between the alkyl groups and the sulfur atom of thiophene that reduces the effective planar π-

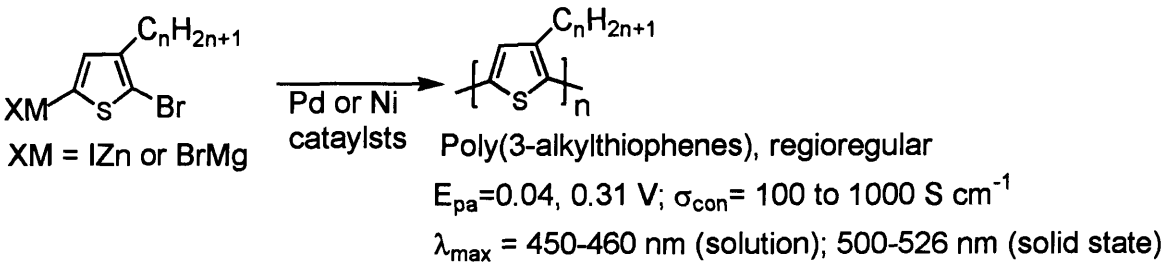

Scheme 2.

conjugation of the polymer.[3c] An organometallic cross-coupling polymerization of 2-bromo-5-metallohalide-thiophene monomers eliminates this problem and thus produces regioregular polythiophene, as shown in Scheme 2.[29] In addition to the decreased steric interactions, the regioregularity of these polymers increases the ability of the polymer strands to align and form large crystalline regions.[30] The electrochemical measurements of the polymers confirmed the improvement in electroactivity of these polymers.[29a,31] Unfortunately, this polymerization produces polymers of significantly lower molecular weights than the polymers from oxidative polymerizations and this property limits the use of these polymers in some applications. The 3,4-substituted thiophene monomers would completely eliminate the possibility of β-couplings and symmetric monomers have no possibility of regioirregularity, yet as expected the resulting polymers have significant steric interactions between the adjacent thiophene units. The electroactive properties of

most 3,4-substituted polythiophenes are generally worse than the 3-substituted polythiophenes.[2] However by tying back the 3,4-substituents into a ring structure these steric effects can be reduced. In fact, one of the most widely used polythiophene derivatives is poly(3,4-ethylenedioxythiophene), **p-6** in Chart 5.[32] This polymer has significantly improved electrochemical activity and durability in comparison to polythiophene,[32b,33] and has found a wide variety of applications.[3d,3e] The electron donating ability of oxygen substituents of **p-6** lowers the E_{pa} of the polymer and this effect in turn lowers the bandgap of the polymer.[34]

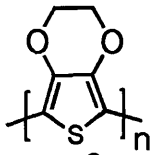

p-6

E_{pa}= -0.2 V; σ_{con}= 300 S cm^{-1}

λ_{max} = 496 nm, E_g ~1.5 eV

Chart 5.

As observed in **p-3**, the substitution of electron withdrawing groups in the β-positions of the thiophene monomer produces polymers that are stable in a reduced anionic state. This effect thereby creates n-dopable polythiophene derivatives, and an example is **p-7** in Chart 6.[35] The replacement of an alkyl group in the β-position of the thiophene monomer with a fluoroalkyl group produces a polymer with a higher electron affinity that is stable when reduced. Consequently, the E_{pc} of **p-7** is observed at -1.18 V while the E_{pc}'s for poly(3-alkylthiophene)'s cannot be observed under standard conditions.[35,36]

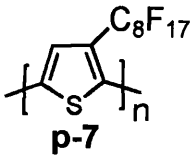

p-7

E_{pa}= 1.19 V, E_{pc}= -1.18 V

λ_{max} = 326 nm (solution); 338 nm (solid state)

Chart 6.

Structures that enforce planarity between monomers can be useful and should lower the E_g of the polymer. The resultant planarity increases the effective π-conjugation of the polymer which in turn enhances the intrachain polymer interactions. A planar structure will also increase π-stacking therefore there will be more interchain polymer interactions. One simple example of a polymer with a enforced planarity is poly(cyclopentadithiophene), **p-8**. The λ_{max} of the polymer suggests that the polymer has a lower E_g than pure polythiophene and the electrochemical data also shows a lower oxidation potential in Chart 7.[37]

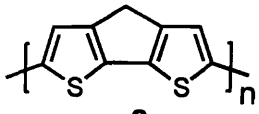

p-8

$E_{1/2}$ (oxidation) = -0.10 V

σ_{con}= 40 S cm^{-1} λ_{max} = 545 nm

Chart 7.

Another important β-substitution trend has been to produce fused ring systems that disrupt the aromaticity of the thiophene system. The first example of this type of polythiophene derivative was poly(isonapthiophene), **p-9** in Chart 8.[38] The monomer in this case was designed to create competing aromaticity between the fused benzene ring and the thiopene ring. The E_g of the polymer is lowered by this disruption of the aromaticity of thiophene unit and electrochemical measurements confirm this effect.[39]

These highlighted general trends of β-substitution show that this modification can have significant effects on the electrochemical properties of the polymer.

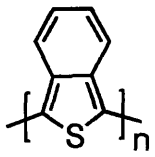

p-9

E_{pa}= -0.01 V; E_{pc}= -0.41

σ_{con}= 10^{-3} S cm^{-1}(undoped) 50 S cm^{-1}(doped) λ_{max} = 886 nm

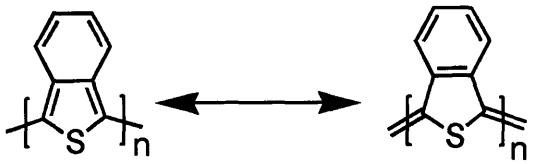

Aromaticity Competition

Chart 8.

α-Substitution

The α-substitution of polythiophene can create a far more dramatic change in the polymer's π-electron system. The placement of a substituent directly into the π-electron system of the polymer causes the effect of the substitution to be highly dependent on the geometries and relative energy of the molecular orbitals of the substituted group. Therefore, α-substitution requires more specific discussions for different classes of substituents. A brief summary of a variety of α-substituted polythiophene derivatives provides a perspective on the overall effects of the various α-substituted compounds on the molecular and bulk electroactive properties of the resulting polymers. Three elements are used to focus this summary. First, most of the polythiophenes derivatives considered have no β-substitutions on the thiophene units. Only polymers produced by an oxidative electrochemical or chemical polymerization will be discussed. The Oxidative polymerizations tend to produce some β-couplings between thiophene monomers.[40]

Finally in all the polymers considered, the longest π-conjugation segment is the polythiophene section with at least two thiophene units..

Most often α-substitution of the polythiophene disrupts the π-conjugation of polymer but there are cases where this substitution can produce an increase in the π-conjugation of the polymers. The types of α-substitutions can be divided into three categories. One category includes α-substituted groups that show no or little π-conjugation because these groups do not have π-electrons (alkyl chains) or the geometrical alignment of the group's molecular orbitals does not allow for significant conjugation. In another category are substituted groups that allow moderate π-conjugation. This category includes *para*-phenylene, which has the appropriate geometrical alignment of the molecular orbitals, but, because of the strong tendency of phenyl groups to maintain their aromatic character, delocalization is reduced. An important category includes α-substituents that allow significant π-conjugation. The members of this category have both the appropriate geometrical alignment and relative energy of the molecular orbitals. . The extent of π-conjugation is often a determining factor in the polymer's electrochemical properties.

The values of σ_{con}, λ_{max}, E_{pa}, and E_g polythiophene listed in Chart 7 are a useful reference for the π-conjugations in α-substituted polythiophene derivatives. If a polythiophene derivative had significant π-delocalization, then it was expected to have an E_{pa} that is near or lower than 0.5 V, a λ_{max} of the undoped polymer that is near or higher than 480 nm and a conductivity maximum that is near or higher than 0.1 S cm^{-1}. For moderate π-delocalization, at least two of the three values are close to the polythiophene values. Any polythiophene derivative that did not meet these criteria is described herein as poorly delocalized.

Alkyl, Vinyl and Alkyne Substitutions

Substitutions containing alkyl, vinyl, and alkyne produce very different extents of π-conjugation. Consequently, the data from these types of substitutions can be used as a representative examples of a poor, moderate and significant levels of π-conjugation.

Polymers comprised of alternating oligomeric thiophenes alkyl chains have been investigated. The insertion of the alkyl chain into the polymer creates a break in the π-conjugation since the alkyl groups do not possess any π electrons. This segmented polymer is of interest to establish the length of the thiophene oligomer needed for effective interchain charge transport. The polymers listed in Chart 9, are examples of alkyl α-substituted polythiophenes derivatives.[41] As expected the electroactive properties of **p-10**, **p-11**, and **p-12** behave in a similar electrochemical manner as simple oligmeric thiophenes. Short thiophene sections resulted in instabilities and **p-10** degraded during the polymerization. For polymer **11,** its CV was reported to display only wave at around

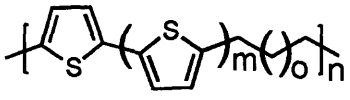

p-10: σ_{con}= 7-9 x 10^{-3} S cm^{-1}

p-11:E_{pa}=0.3, 0.4 V; σ_{con}= 0.1 to 2.5 x 10^{-4} S cm^{-1}

p-12: σ_{con}= 2.5 x 10^{-6} S cm^{-1}; λ_{max} = 339-399 nm

p-10: m=3, o=0
p-11: m=5, o=0
p-12: m=3, o=1

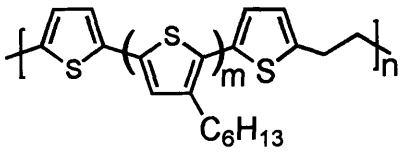

p-10a: m=2
p-11a: m=4

Chart 9.

0.3 V but the CV of **p-11** did contain the start of another oxidation near the highest potential of the CV experiment. The *in situ* conductivity was reported at 5 x 10^{-3} S cm^{-1} which was not significantly less than some types of polythiophene. Analogue **p-12** has a longer alkyl chain between the thiophene fragments and was synthesized chemically by $FeCl_3$. The increase in the alkyl chain length gave a decrease in the conductivity (measured by a four point probe) in comparison to the other polymers.[42] Soluble polymers of **p-10**a and **p-11**a were prepared by addition of alkyl groups to the β-positions of the thiophenes. The conductivities (four point probe, doped with $FeCl_3$) of these polymers (9 x 10^{-3} and 0.4 S cm^{-1} for **p-10**a and **p-11a**, respectively.) were significantly higher than the insoluble versions.[43] These values are also high considering the low π-conjugation lengths. This effect may be due to the improved solubility of the polymers, which ultimately allowed higher quality films to be prepared for conductivity measurements. The *in situ* conductivity of **p-11**a recorded a significantly lower conductivity value of 2.5 x 10^{-4} S cm^{-1}.[44] The CV of **p-11**a did possess the two waves expected for a segmented polymer and the values were in the same potential regions as those of a sexithiophene oligomer.[21]

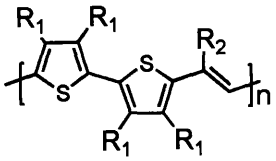

p-13: R_1= H, R_2=H
p-14: R_1= -OC_4H_9, R_2=H
p-4: R_1= H, R_2=CN

p-13:
E_{pa}= 0.3 V
E_{pc}= -1.95 V
λ_{max} = 490-505 nm
σ_{con}= 40 S cm^{-1}

p-14:
λ_{max} = 539 nm
σ_{con}= 0.03 S cm^{-1}

p-4:
E_{pa}= 0.3 V
E_{pc}= -0.7 V
σ_{con}= 0.07 S cm^{-1}
E_g = 0.5-0.6 eV

Chart 10.

In direct contrast to saturated alkyl chains, which break the π-conjugation in the polythiophene backbone, the addition of a vinyl group to the polythiophene main chain actually improves the delocalization of the π electrons along the polymer backbone. Polymer **p-13**, as shown in Chart 10, has been extensively studied and has a high conductivity (40 S cm^{-1}, four point probe and *in situ*).[45,46] The oxidation potential of the polymer is similar to polythiophene, around 0.30 V. The polymer can be reduced at accessible potentials (E_{pc} = -1.95 V) thereby indicating that the introduction of the ethylene group decreases the band gap of polymer. Consistently the reported neutral UV-vis absorption of **p-13** (λ_{max} = 490-505 nm) is also at a longer wavelength than polythiophene.[46,47] The addition of the dibutoxy groups to the 3 and 4 positions of the thiophene, as in **p-14,** red shifted the UV-vis absorption of the polymer to 539 nm, however the conductivity decreased to 0.03 S cm^{-1} (four point probe, $FeCl_3$ doped). The reasons for the low conductivity were not given but, as discussed earlier, the decrease was probably due to an increase in the dihedral angle between the thiophene units caused by a steric interaction between the β-substituents.[48] As discussed earlier, the band gap of **p-4** was decreased relative to **p-13** by the introduction of a cyano group on the double bond. The E_{pa} of 0.3 V **p-4**, , did not differ from **p-13** but the E_{pc} was lower (-0.7 V).[10,49] The optical band gap corresponded to 0.50-0.60 eV and was consistent with the

electrochemical band gap of 0.54 eV. Yet, the conductivity of the polymer was low (0.07 S cm^{-1}).[10]

The substitution of an ethyne in polythiophene produces a polymer that has less electronic delocalization than either polythiophene or poly(dithiopheneethylene). The polymer **p-15**, shown in Chart 11, was produced by electrochemical polymerization.[50]

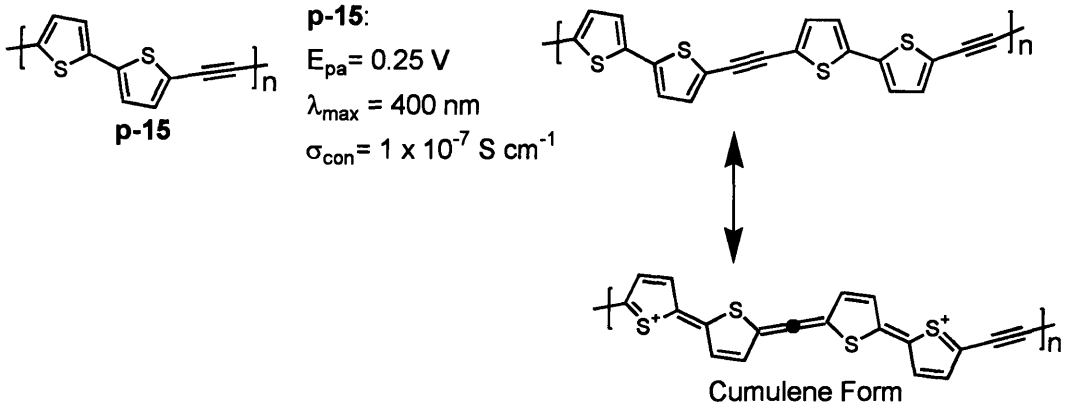

Chart 11.

The peak oxidation of the polymer was in the same region as **p-13**, (0.25 V). However, the UV-vis absorption of the polymer was at a much lower wavelength (400 nm). The reported conductivity of **p-15** was very low (1 x 10^{-7} S cm^{-1}, four point probe, doped with $NOPF_6$).[51] This low conductivity was attributed to defects created during the polymerization and/or dedoping as well as to the localization of charges caused by the disfavored cumulene form of this polymer. Injection of charges in these systems results in bipolarons that require the formation of these cumulene structures shown in Chart 11.

Phenyl Substitutions

Phenyl rings have a strong tendency to localize the electronic states in polymers because increased delocalization is only achieved at the cost of aromaticity. Another

important factor to consider is the substitution pattern of the thiophene units around the

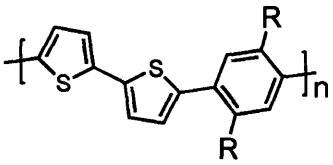

p-16: R = H
p-17: R=OMe
p-18: R = F

p-16:
E_{pa}= 0.35 V
E_{pc}= -2.16 V
σ_{con}= 0.5 S cm^{-1}

p-17:
E_{pa}= 0.35 V
σ_{con}= 2 x 10^{-6} S cm^{-1}

p-18:
E_{pa}= 1.0 V
E_{pc}= -1.95 V

Chart 12

phenyl ring, i.e.; *para*, *meta*, or *ortho*.

For maximum π-conjugation with the least amount of steric interactions, the 1, 4-phenyl substitution pattern is the best. As discussed briefly in the application section, extensive research has been done on these types of polymers, as shown in Chart 12.[52] For the simple phenyl polymer, **p-16**, produced by chemical polymerization, the conductivity was relatively high (0.5 S cm^{-1}, four point probe, $NOPF_6$).[53] The E_{pa} was in the same potential region as that of polythiophene and the CV also resembled polythiophene in shape.[54] Even with the difference in energy between thiophene and phenyl π orbitals, the electrochemistry suggests a highly delocalized conjugated polymer. A subtle change to these types of polymers is to substitute the 2- and 5-positions of the phenyl group. A methoxy substituted polymer, **p-17**, had a significantly lower E_{pa} (0.00 V).[53] But this polymer had a much lower conductivity (2 x 10^{-6} S cm^{-1}). This decrease in the conductivity relative to **p-16** can probably be attributed to an increase in the dihedral angle between the thiophene units and the phenyl group similar to the steric effect of the butoxy groups on **p-14**. As expected, the oxidation potential of a fluorine substituted

polymer, **p-18**, was higher.[55] Analogous to the β-substituted polymers, the absolute value of the E_{pc} of the polymer is decreased by the addition of electron withdrawing groups (fluorine atoms, in this case), with the value of E_{pc} being -2.16 for **p-16** versus -1.95 for **p-18**.[55] It is clear that increasing or decreasing the relative energy of the orbitals of the phenyl group affects the electroactivity and conductivity of the material..[56]

Due to the molecular orbitals of benzene, the 1, 3-substitution of the phenyl ring should provide a break in the π-conjugation. This effect was observed in the pure 1, 3-phenyl substitution of bithiophene analogue, **p-19** and the distinctive two wave CV, E_{pa} = 0.30 and 0.56 V, of a segmented polymer was observed.[57] Similar to the earlier alkyl substituted polythiophene derivatives, these values were in the same potential regions as those of the corresponding polythiophene oligomer (quaterthiophene).[16] The reported conductivity (2.3 x 10^{-4} S cm^{-1}) was slightly higher than the completely segmented polymer **p-12**. A bithiophene analogue of **p-19** displayed poor electroactivity and appeared to decompose.[54] An important issue to consider is how additional substituents,

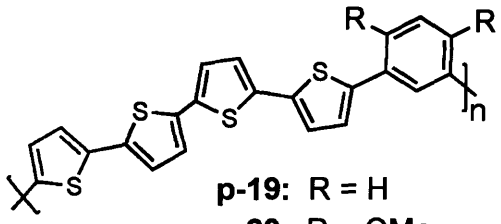

p-19: R = H
p-20: R = OMe
p-21: R = OH
p-22: R= $COCH_3$

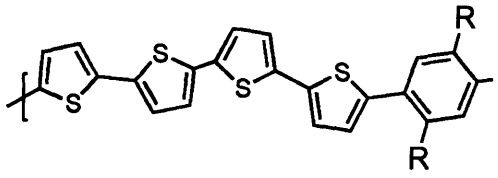

p-23: R = OH
p-24: R = $COCH_3$

p-19:
E_{pa}= 0.30, 0.56 V
σ_{con}= 2.3 x 10^{-4} S cm^{-1}

p-20: E_{pa} = 0.37, 0.61 V
p-21: E_{pa} = 0.41, 0.68 V
p-22: E_{pa} = 0.12, 1.0, 0.72 V

Chart 13.

such as OR and OH, can extend the conjugation of the *meta* substituted polymer. Since the *meta* substitution pattern places the thiophene fragments in a direct conjugation path of the phenyl R groups in the *para* position, this substitution has the optimum delocalization to the thiophene fragments and the substitution of the phenyl ring should have a greater effect on the overall effective conjugation of the polymer than in the case of the *para* substitution. A study in our group was performed to investigate these properties on a series of polymers in shown Chart 13.[58] The maximum conductivities observed for **p-21** and **p-22** were more than twice as large as those for **p-19**. The electroactivity properties of **p-21** and **p-22** were similar to the electroactivity properties of **p-23** and **p-24**.

The substitution of thiophene at the 1 and 2 positions of a phenyl group affords, a tandem cyclization and polymerization reaction with the electrochemical oxidation, as shown in Scheme 3.[59] The sequence shown in Scheme 3 was proven by systematic model studies. Since this occurs, the properties of the polymer are determined by the

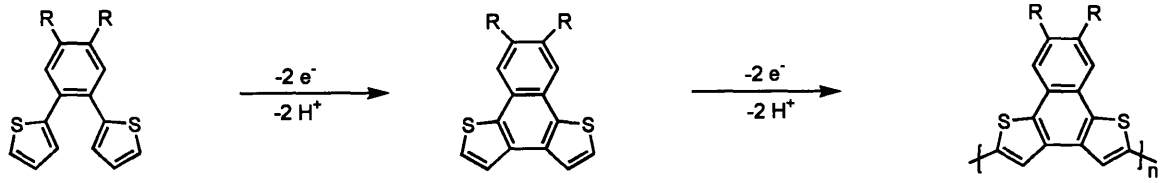

Scheme 3.

naphthodithiophene core and are not relevant to our discussion of simple α-substitution. It is noteworthy that the β-substituted analogues also exhibit the same reactivity .

Azulene Substitution

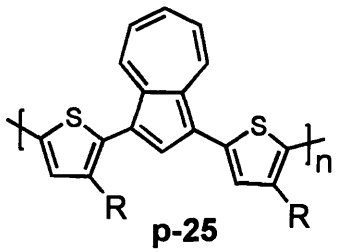

p-25

p-25:
E_{pa}= 0.04 V
λ_{max}=386 nm
σ_{con}= 0.44-49.0 S cm^{-1}
E_g=2.45 eV

Chart 14.

A polythiophene containing azulene, **p-25** in Chart 14, displayed reasonable conductivities when doped by iodine (0.44-49.0 S cm^{-1}, four point probe).[60] The E_{pa} was low, 0.04 V, but an electrochemical E_g of 2.45 eV was measured. This value for the electrochemical E_g was close in energy to the solution UV-vis measurement of the dominant $\pi \rightarrow \pi^*$ of the neutral polymer backbone (λ_{max} = 386 nm). However, the optical bandgap is actually determined by the ~600 nm absorption of the azulene unit. By definition, the optical bandgap is actually closer to 2.0 eV than 2.45 eV. The electrochemical E_g indicated a short π-conjugation for the polymer backbone yet the large bulk conductivity indicated a charge delocalized polymer. The cause of this significant charge delocalization was rationalized as the stabilization of the polaronic and bipolaronic states by azulenium ion.

Heteroatom Substitutions

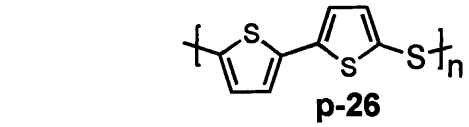

p-26

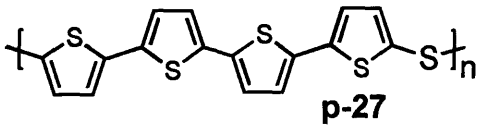

p-27

p-27:
$E_{1/2}$= 0.51 V
λ_{max}=345, 410 nm

Chart 15.

The polarizability of the heteroatom inserted into the main chain of polythiophene will greatly affect the delocalization within the polymer.[61] A sulfur bridged polythiophene derivative, **p-26**, shown in Chart 15, was synthesized by electrochemical polymerization but it was electrochemically unstable.[62] An analogue with a longer oligothiophene in the polymer structure, **p-27**, was synthesized and this polymer displayed a UV-vis absorption with the relatively short wavelengths (λ_{max}'s at 345 and 410 nm) but had a relatively low $E_{1/2}$ of 0.51 V. The electroactivity was poor since the sulfur group is only moderately polarizable. Several silyl substituted polythiophene derivatives, as shown in Chart 16, have also been synthesized,. Silyl groups do not possess the non-bonding electrons of sulfur, and ,hence, it was not expected to display significant charge migration. However, the silane and thiophene polymers can interact through the π orbitals of the thiophene and the empty d orbitals of the silicon atom. Polymer **p-28** displayed an E_{pa} at approximately 0.55 V and a λ_{max} at 390 nm.[63] A systematic study found that the conductivity of polymers composed of thiophene and alkyl silyl groups was determined by the length of the thiophene segments between silyl

groups.[64] This fact was revealed in conductivity studies (four point probe, $NOBF_4$) of **p-28** and **p-29**, which were 3 x 10^{-5} S cm^{-1} and 0.1 S cm^{-1}, respectively.

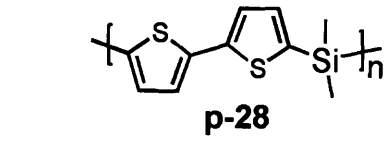

p-28

p-28:
E_{pa}= 0.55 V
λ_{max}= 390 nm
σ_{con}=3 x 10^{-5} S cm^{-1}

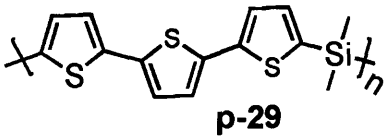

p-29

p-29:
σ_{con}=0.1 S cm^{-1}

Chart 16.

Aromatic Heterocycle Substitutions

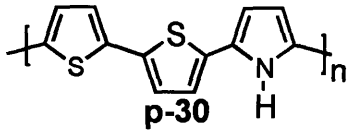

p-30

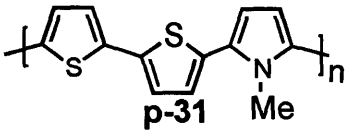

p-31

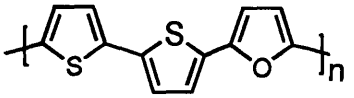

p-32

p-30:
E_{pa}= -0.51
λ_{max}= 477 nm
σ_{con}=2.7 x 10^{-3} to 280 S cm^{-1}

p-31:
E_{pa}= 0.18-0.22 V
λ_{max}= 419 nm
σ_{con}=1 S cm^{-1}

p-32:
E_{pa}= -0.50 to -0.48 V
λ_{max}= 475 nm
σ_{con}=0.3 S cm^{-1}

Chart 17.

The insertion of an isoenergic heterocycle into the polythiophene backbone should not affect the overall π-conjugation of the polymer. The introduction of a pyrrole unit into polythiophene, as shown in Chart 17, has received considerable attention.[65] The conductivity of **p-30** varied significantly depending on the dopants (2.7×10^{-3} to 280 S cm^{-1}, four point probe). Nevertheless, the E_{pa} was low at -0.51 V and the λ_{max} of the neutral polymer occurred at long wavelengths, 477 nm. Changing of the N-H of pyrrole, **p-30**, to the N-Me of N-methylpyrrole, **p-31**, caused the electroactive properties of the polymer to decrease significantly (E_{pa} = 0.18-0.22 V, $\sigma_{con.}$ = 1 S cm^{-1}, λ_{max} = 419 nm).[65c,66] This effect was attributed to the steric interactions of the methyl group, which caused the dihedral angle between the thiophene units and the pyrrole to increase. A polymer incorporating a furan into the main chain, **p-32**, was also synthesized.[65c] The electroactivity of this polymer resembled a highly delocalized polymer (E_{pa} = -0.50 to -0.48 V, $\sigma_{con.}$ = 0.3 S cm^{-1} four point probe with electrochemical doping, λ_{max} = 475 nm).

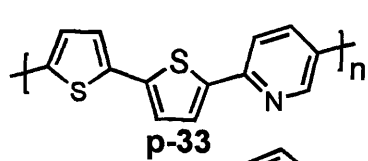

p-33

p-33:
E_{pa}= 0.34 V
σ_{con}=3 x 10^{-4} S cm^{-1}

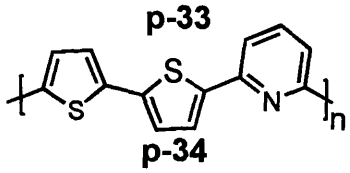

p-34

p-34:
E_{pa}= 0.44 V
σ_{con}=7 x 10^{-6} S cm^{-1}

Chart 18.

The substitution of pyridine into the polythiophene has the same molecular orbital consequences as the phenyl substitution. The 2, 5- and 2, 6- substituted pyridine polymers, **p-33** and **p-34** in respectively Chart 18, were synthesized.. The E_{pa} for

p-33 (0.34 V) was slightly lower than **p-34** (0.44 V). The conductivities for **p-33** (3 x 10^{-4} S cm^{-1}) was significantly higher than **p-34** (7 x 10^{-6} S cm^{-1}, impedance spectroscopy).[67] These trends suggested that the pyridine substituted polymers follow the phenyl substituted polymers in that the *para* linked, **p-33**, are more electroactive than the *meta*-linked, **p-34**. Second, it appears that these polymers have less π-conjugation than α-substituted phenyl polymers due to the higher electron affinity of pyridine which creates additional localization.

Conclusions

Table 1. Summary of the relative delocalization in α-substituted polythiophene derivatives.

Non/Poor	Moderate	Significant
p-10, p-11, p-12, p-18, p-19, p-20, p-25, p-26, p-27, p-28, p-29, p-34	**p-14, p-15, p-16, p-17, p-21, p-22, p-23, p-24, p-33**	**p-13, p-4, p-23, p-30, p-32**

The qualitative degrees of delocalization in the various α-substituted polythiophene derivatives are summarized in Table 1. As expected, the typical α-substitution of polythiophene produces either a complete or partial loss of the π-conjugation in comparison to polythiophene. The few examples of increased or comparable conjugation were limited to a few compounds where the thiophenes sequences are interrupted by alkenes or aromatic heterocycles possessing molecular orbitals with similar or lower energy levels. The moderate delocalized systems, like phenyl or pyridine, conform to typical organic trends of meta and para substitutions.. The example of the *ortho* substitution of thiophenes about a phenyl results in cyclization reaction to give very

different materials. Overall, the values contained in this summary will be used throughout this thesis as a guide to evaluate the electroactivity displayed in α-substituted polymer.

References

[1] Shirakawa, H.; Louis, E. J.; MacDiarmid, A. G.; Chiang, C. K.; Heeger, A. J. *J. Chem. Soc. Chem. Commun.*, **1977**, 578.

[2] Roncali, J. *Chem. Rev.* **1992**, *92*, 711.

[3] (a)Roncali, J. *Chem. Rev.* **1997**, *97*, 173. (b) Higgins, S. J. *Chem. Soc. Rev.*, **1997**, *26*, 247. (c) McCullough, R. D. *Adv. Mater.* **1998**, *10*, 93. (d) Groenendaal, L.; Jonas, F.; Freitag, D.; Pielartzik, H.; Reynolds, J. R. *Adv. Mater.* **2000**, *12*, 481. (e) Roncali, J.; Blanchard, P.; Frere, P. *J. Mater. Chem.* **2005**, *15*, 1589.

[4] (a) Kingsborough, R. P.; Swager, T. M. *Prog. Inorg. Chem.* **1999**, *48*, 123. (b) Pickup, P. G. *J. Mater. Chem.* **1999**, *9*, 1641. (c) Wolf, M. O. *Adv. Mater.* **2001**, *13*, 545. (d) Holliday B. J.; Swager T. M. *Chem. Commun.* **2005**, 23.

[5] (a) McQuade, D. T.; Pullen, A. E.; Swager, T. M. *Chem. Rev.* **2000**, *100*, 2537. (b) Ferraris, J. P.; Eissa, M. M.; Brotherston, I. D.; Loveday, D. C. *Chem. Mater.* **1998**, *10*, 3528. (c) Novak, P.; Muller, K.; Santhanam, K. S. V.; Haas, O. *Chem. Rev.* **1997**, *97*, 207. (d) Madden, P. G. A.; Madden. J. D. W.; Anquetil, P. A.; Vandesteeg, N. A.; Hunter, I. W. *J. Oceanic Eng.* **2004**, *29*, 696. (e) Andersson, M. R.; Thomas, O.; Mammo, W.; Svensson, M.; Theander, M.; Inganas, O. *J. Mater. Chem.* **1999**, *9*, 1933. (f) Mortimer, R. J.; Dyer, A. L.; Reynolds, J. R. *Displays*, **2006**, *27*, 2.

[6] (a) Sundararaman, A.; Victor, M.; Varughese, R.; Jäkle, F. *J. Am. Chem. Soc.* **2005**, *127*, 13748. (b) Ho, H.A.; Dore, K.; Boissinot, M.; Bergeron, M. G.; Tanguay, R. M.; Boudreau, D.; Leclerc, M. *J. Am. Chem. Soc.* **2005**, *127*, 12673. (c) Yu, H-H.; Pullen, A. E.; Buschel, M. G.; Swager, T. M. *Angew. Chem. Int. Ed.* **2004**, *43*, 3700. (d) Marsella, M. J.; Swager, T. M. *J. Am. Chem. Soc.* **1993**, *115*, 12214.

[7] Ren, X.; Gottesfield, S.; Ferraris, J. P. In *Electrochemical Capacitors*; Delnick, F. M., Tomkiewicz, M. Eds.; The Electrochemical Soc. Inc.: Pennington, 1995; Vol. 95-29, p 138.

[8] Laforgue, A.; Simon, P.; Sarrazin, C.; Fauvarque, J-F.; *J. Power Sources*, **1999**, *80*, 142.

[9] Chen, S.; Liu, Y.; Qiu, W.; Sun, X.; Ma, Y. Zhu, D. *Chem. Mater.* **2005**, *17*, 2208.

[10] Fusalba, F.; Ho, H. A.; Breau, L. Belanger, D. *Chem. Mater.* **2000**, *12*, 2581.

[11] Sonmez, G.; Sonmez, H. B.; Shen, C. K. F.; Wudl, F. *Adv. Mater.* **2004**, *16*, 1905.

[12] Sonmez, G.; Shen, C. K. F.; Rubin, Y.; Wudl, F. *Angew. Chem. Int. Ed.* **2004**, *43*, 1498.

[13] Roth, S.; Bleier, H.; Pukacki, W. *Faraday Discuss. Chem. Soc.* **1989,** *88*, 223.

[14] Bard, A. J.; Faulker, L. R. *Electrochemical Methods: Fundamentals and Applications* 2nd Edition, Wiley & Sons: USA, 2001.

[15] (a) DuBois, C. J.; Reynolds, J. R. Adv. Mater. 2002, 14, 1844. (b) Sotzing, G. A.; Thomas, C. A.; Reynolds, J. R.; Steel, P. J. *Macromolecules* **1998**, *31*, 3750.

[16] Patil, A.O; Heeger, A. J.; Wudl, F. *Chem. Rev.* **1988**, *88*, 183.

[17] Roth, S. *One-Dimensional Metals* VCH: Weinheim, Germany,1995.

[18] Hummel, R. E. *Electronic Properties of Materials*, 2nd Edition, Springer-Verlag: New York, 1993.

[19] (a) Meerholz, K.; Heinze, J. *Electrochim. Acta.* **1996**, *41*, 1839. (b) Jin, S.; Cong, S.; Xue, G.; Xiong, H.; Mansdorf, B.; Cheng, S. Z. D. *Adv. Mater.* **2002**, *14*, 1492.

[20] The reported potentials have been corrected to the Fc/Fc^+ couple by using these reported potentials versus NHE for the following reference electrodes: 0.197 V for Ag/AgCl, 0.2360 V for SSCE, 0.2412 V for SCE, 0.799 V for Ag/Ag^+ and approximately 0.999 V for Fc/Fc^+.

[21] Guay, J.; Kasai, P.; Diaz, A.; Wu, R.; Tour, J. M.; Dao, L. H.; *Chem. Mater.* **1992**, *4*, 1097.

[22] Zotti, G.; Schiavon, G.; Berlin, A.; Pagani, G. *Chem. Mater.* **1993**, *5*, 620.

[23] Miller, L. L.; Mann, K. R. *Acc. Chem. Res.* **1996**, *29*, 417.

[24] (a) Hill, M. G.; Mann, K. R.; Miller, L. L.; Penneau, J. *J. Am. Chem. Soc.* **1992**, *114*, 2728. (b) Graf, D. D.; Campbell, J. P.; Miller, L. L.; Mann, K. R. *J. Am. Chem. Soc.* **1996**, *118*, 5480.

[25] Waltman, R. J.; Bargon, J. *Tetrahedron* **1984**, *40*, 3963. (b) Waltman, R. J.; Bargon, J. *Can. J. Chem.* **1986**, *64*, 76.

[26] Waltman, R. J.; Bargon, J.; Diaz, A. F. *J. Phys. Chem.* **1983**, *87*, 1459.

[27] Tourillon, G.; Garnier, F. *J. Phys. Chem.* **1983**, *87*, 2289.

[28] Sato, M-A.; Tanaka, S.; Kaeriyama, K. *Synth. Met.* **1987**, *18*, 229.

[29] (a) McCullough, R. D.; Tristram-Nagle, T.; Williams, S. P.; Lowe, R. D.; Jayaraman, M. *J. Am. Chem. Soc.* **1993**, *115*, 4910 (b) Chen, T.-A.; Rieke, R. D. *J. Am. Chem. Soc.*. **1992**, *114*, 10087.

[30](a) Prosa, T. J.; Winokur, M. J.; Moulton, J.; Smith, P.; Heeger, A. J. *Macromolecules*, **1992**, *25*, 4364. (b) Prosa, T. J.; Winokur, M. J.; McCullough, R. D. *Macromolecules*, **1996**, *29*, 3654.

[31] McCullough, R. D.; Lowe, R. D.; Jayaraman, M.; Anderson, D. L. *J. Org. Chem.* **1993**, *58*, 904.

[32] (a) Jonas, F.; Schrader, L. *Synth. Met.* **1991**, *41-43*, 831. (b) Heywang, G.; Jons, F. *Adv. Mater.* **1992**, *4*, 116.

[33] (a) Deitrich, M.; Heinze, J.; Heywang, G.; Jonas, F. *J. Electrochemical Chem.* **1994**, *369*, 87. (b) Sotzing, G. A. Reynolds, J. R.; Steel, P. J. *Chem. Mater.* **1996,** *8*, 882.

[34] Ahonen, H. J.; Lukkari, J.; Kankare, J. *Macromolecules* **2000**, *33*, 6787.

[35] Li, L.; Collard, D. M. *Macromolecules*, **2005**, *38*, 372.

[36] Crooks, R. M.; Chyan, O. M. R.; Wrighton, M..S. *Chem. Mater.* **1989**, *1*, 2.

[37] (a) Benincori, T.; Brenna, E.; Sannicolo, F.; Trimarco, L.; Moro, G.; Pitea, D.; Pilati, T.; Zerbi, G.; Zotti, G. *J. Chem. Soc. Chem. Commun.* **1995**, 881. (b) Coppo, P.; Turner, M. T. *J. Mater. Chem.* **2005**, *15*, 1123.

[38] Wudl, F.; Kobayashi, M.; Heeger, A. J. *J. Org. Chem.* **1984**, *49*, 3382.

[39] (a) Kobayashi, M.; Colaneri, N.; Boysel, M.; Wudl, F.; Heeger, A. J. *J. Chem. Phys.* **1985**, *82*, 5717. (b) King, G.; Higgins, S. J. *J. Mater. Chem.* **1995**, *5*, 447.

[40] Yamamoto, T.; Sanechika, K.; Yamamoto, A. *J. Polym. Sci. Polym. Lett. Ed.* **1980**, *18*, 9.

[41] Berlin, A.; Fontana, G.; Pagani, G.; Schiavon, G.; Zotti, G. *Synth. Met.* **1993**, *57*, 4796.

[42] Hoffmann, K J.; Samuelsen, E. J.; Carlsen, P. H. J. *Synth. Met.* **2000**, *114*, 167.

[43] Sato, M.-A.; Sakamoto, M.-A.; Miwa, M.; Hiroi, M. *Polymer*, **2000**, *41*, 5681.

[44] Jiang, X.; Harima, Y.; Zhu, L.; Kunugi, Y.; Yamashita, K.; Sakamoto, M.; Sato, M. *J. Mater. Chem.* **2001**, *11*, 3043.

[45] Bragadin, M. Cescon, P.; Berlin, A.; Sannicolo, F.; *Makromol. Chem.* **1987**, *188*, 1425.

[46] Berlin, A.; Zotti, G. *Synth. Met.* **1999**, *106*, 197.

[47] Ononda, M.; Iwasa, T.; Kawai, T.; Yoshino, K. *J. Phys. D: Appl. Phys.* **1991**, *24*, 2076.

[48] Blohm, M. L.; Pickett, J E.; Van Dort, P. C. *Marcomolecules*, **1993**, *26*, 2704.

[49] Ho, H.A.; Brisset, H.; Frere, P.; Roncali, J. J. *Chem. Soc. Chem. Commun.* **1995**, 2309.

[50] Zotti, G.; Schiavon, G.; Zecchin, S.; Berlin, A. S *Synth. Met.* **1998**, *97*, 245.

[51] Kossmehl, G. *Marcomol. Symp.* **1986**, *4*, 45.

[52]*Handbook of Conducting Polymers*, Skotheim, T. A.,. Elsenbaumer, R. L, Reynolds, J. R. Eds. Marcel Dekker, New York, 1998.

[53] Reynolds, J. R., Ruiz, J. P.; Child, A. D.; Nayak, K.; Marynick, D. S. *Marcomolecules*, **1991**, *24*, 678.

[54] Mitsuhara, T.; Tanaka, S.; Kaeriyama, K. *Makromol. Chem.* **1988**, *189*, 1755.

[55] Killian, J.G.; Gofer, Y.; Sarker, H.; Poehler, T.O.; Searson, P.C. *Chem. Mater.* **1999**, *11*, 1075.

[56] Irvin, D. J.; Steel, P. J.; Dudis, D. S.; Reynolds, J. R. *Synth. Met.* **1999**, *101*, 392.

[57] Sato, T.; Hori, K.; Tanaka, K. *J. Mater. Chem.* **1998**, *8*, 589.

[58] Song, C.; Swager, T. M. *Macromolecules*, **2005**, *38*, 4569.

[59] (a) Tovar, J. D.; Swager, T. M. *Adv. Mater.* **2001**, *13*, 1775. (b) Tovar, J. D.; Rose, A.; Swager, T. M. *J. Am. Chem. Soc.* **2002**, *124*, 7762.

[60] Wang, F.; Lai, Y-H.; Han, M-Y. *Macromolecules*, **2004**, *37*, 3222.

[61] Waite, J.; Papadopoulos, M. G. *J. Phys. Chem.* **1990**, *94*, 6244.

[62] Chahma, M.; Myles, D.J. T.; Hicks, R. G. *Chem. Mater.* **2005**, *17*, 2672.

[63] Mudigonda, D. S. K.; Boehme, J. L.; Brotherston, I. D.; Meeker, D. L.; Ferraris, J. P. *Chem. Mater.* **2000**, *12*, 1508.

[64] Chicart, P.; Corriu, R. J. P.; Moreau, J. J. E.; Garnier, F.; Yassar, A. *Chem. Mater.* **1991**, *3*, 8.

[65] (a) McLeod, G. G.; Mahboubian-Jones, M. G.B.; Pethrick, R. A.; Watson, S. D.; Truong, N. D.; Galin, J. C.; Francois, J. *Polymer*, **1986**, *27*, 455. (b) Ferraris, J. P.; Skiles, G. D. *Polymer*, **1987**, *28*, 179. (c) Ferraris, J. P.; Hanlon, T. R. *Polymer*, **1989**, *30*, 1319.

[66] Ferraris, J. P.; Andrus, R. G.; Hrhcir, D. C. *J. Chem. Soc., Chem. Commun.* **1989**, 1318.

[67] Jenkins, I. H.; Salzner, U.; Pickup, P. G. *Chem. Mater.* **1996**, *8*, 2444.

Chapter 2:

Polythiophene Containing 2,2'-Substituted Biphenyls: Hinge Structures in Pursuit of Better Actuating Materials

Portions of this chapter have been submitted

as a paper to Chemistry of Materials

Introduction

Conducting polymer actuators have seen intense study due to their many potential applications.[1] The majority of these studies have focused on typical conducting polymers that undergo intrinsic volume changes associated with electrochemical oxidation/reduction due to the migration of charged electrolytes and solvent into and out-of the thin polymer films.[2] We are motivated to produce new molecular mechanical mechanisms in an effort to create materials that exhibit larger dimensional changes and specific thermodynamic interactions.[3] These advances will produce larger actuation forces and enable new applications. Systems of interest include calix[4]arene derivatives of polythiophene.[4] The polythiophene sections of the calix[4]arene polymer are aligned so that the calix[4]arene can acts as a hinge to facilitate the π-stacking interactions that have been observed in polythiophene oligomers.[5] It was hypothesized that these π-stacking interactions could be utilized as the driving force for the actuation of the polymer.[6] Calculations have shown that this π-stacking can perhaps act as a driving force in molecular actuation for these calix[4]arene polymers.[7] Although the calix[4]arene platform is an attractive structure, the relatively complicated synthesis of these monomers is a potential drawback. In search for a simplified platform, we have investigated a 2,2'-substituted biphenyl unit as an alternative hinge group. The phenyl groups of a 2,2'-substituted biphenyl twist out of plane and this twist can be utilized as the hinge between aligned polythiophene sections.[8]

The development of actuating devices from conducting polymers requires the optimization of the redox potentials and conductivity of the polymers.[9] To assess how the 2,2'- biphenyl affects the overall electroactivity and the electrical transport of the resulting polymers, the linkage of the thiophene units to the biphenyl was varied to be either the α-(2-thienyl) or the β-(3-thienyl) positions. Considering that thiophenes predominantly couple though their α-positions when oxidized, we expect, as shown in Scheme 1, the biphenyl monomer with α- and β-linked

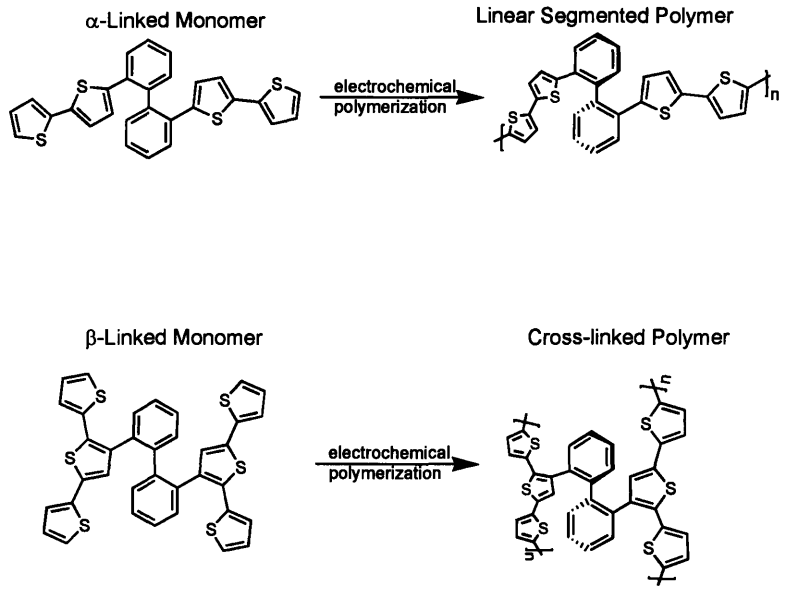

Scheme 1.

thiophenes to give linear segmented and cross-linked polymers, respectively. The α-linked monomer should produce a polymer that is physically segmented by the twist of the biphenyl and this physical segmentation may result in localized charges in the oxidized polythiophene sections. The β-linked monomer should produce a polymer that is fully π-conjugated and should delocalize charge in a similar manner as polythiophene. The systematic variation of the thiophene units per each 2,2'-biphenyl monomer will provide important information on how the number of the thiophenes per monomer and the nature of the connections affect the potential molecular actuator properties. The optimization of the electrical properties of polythiophene

derivatives has often been achieved by the addition of 3,4-ethylenedioxythiophene (EDOT) units.[10] With this idea in mind, EDOT containing monomers were synthesized to study the steric and electrical effects of this unit on the 2,2'-biphenyl system.

The π-stacking interactions can be considered a through-space electronic delocalization. [11] This effect has been observed in purely organic structures such as cyclophanes of thiophene oligomers, stacked phenyl groups, and tethered phenyl groups.[12] A model study is reported in an effort to assess the through space electronic interaction in the 2,2' biphenyl compounds. Model compounds were chosen to confirm if there is the potential for through space electronic interactions between the thiophene fragments of 2,2'-biphenyl and how this interaction depends on the α- or β- type connection of the thiophene fragments linked to the biphenyl. Our results reveal that the biphenyl hinge unit is a versatile element for the design of highly electroactive conducting polymers for future actuator applications.

Results and Discussion

Synthesis of the α- and β-Linked Thiopene Monomers

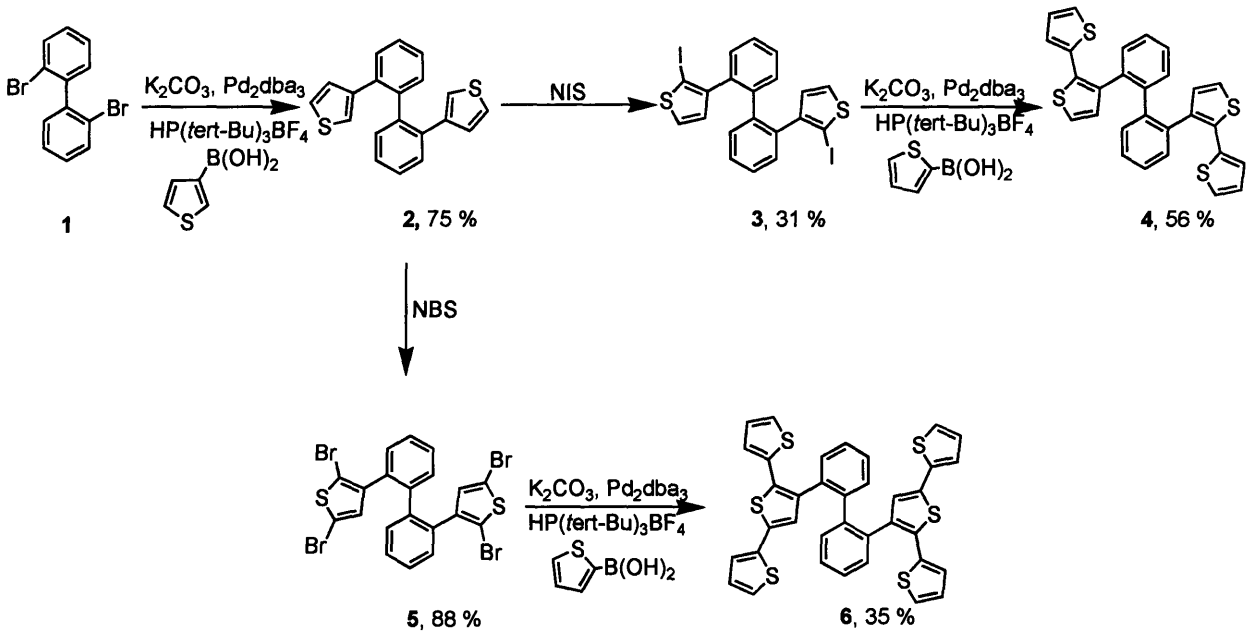

Scheme 2.

The synthesis of the β-linked thiophene monomers is shown in Scheme 2. The β-linked thiophene units were synthesized by Suzuki cross coupling between the commercially available 3-thiopeneboronic acid and 2,2' dibromobiphenyl. A catalyst system comprised of HP(*tert* -butyl)$_3$BF$_4$ and Pd$_2$dba$_3$ gave satisfactory yields.[13] The halogenation of the thiophene monomer, **2**, and subsequent cross coupling gave the bithiophene, **4**, and the terthiophene, **6**, monomers.

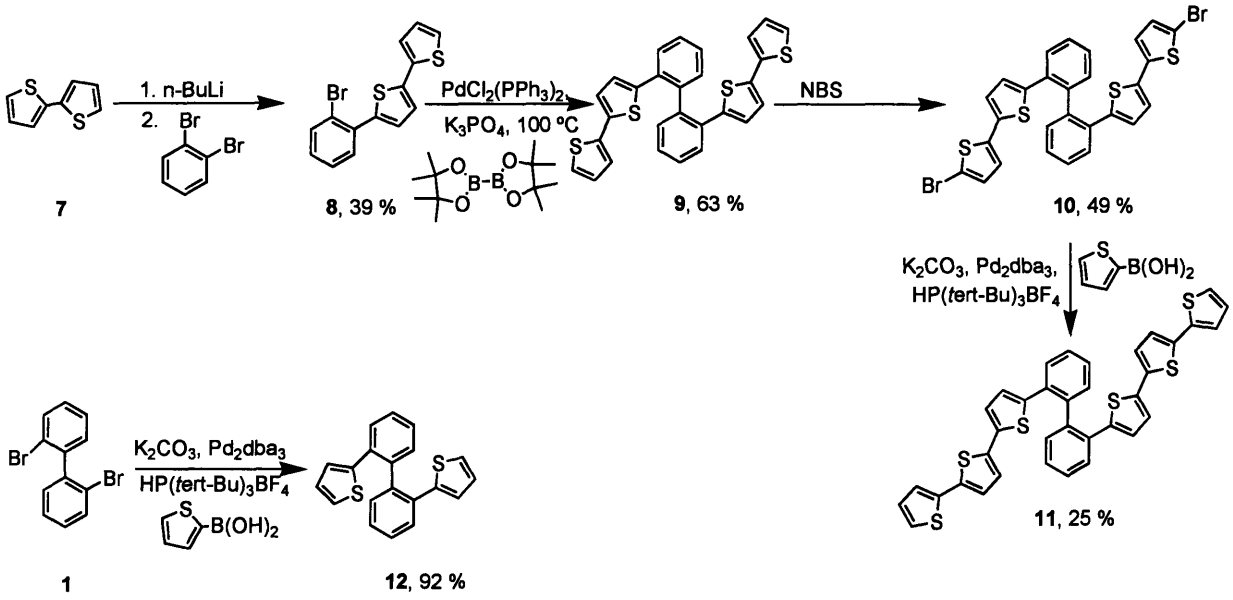

Scheme 3.

The synthesis of the α-linked monomers required variations in strategy, as shown in Scheme 3. A cross coupling synthesis produced the thiophene monomer, **12**. However a homocoupling strategy was determined to be the preferred method for the synthesis of monomer **9**. The synthesis of **11** begins with the treatment of bithiophene with n-butyl lithium and quenching of the reaction mixture with 1, 2-dibromobenzene provided **8**.[14] The homocoupling of

8 yielded the bithiophene monomer, **9**, and subsequent and bromination of **9** followed by a Suzuki cross coupling reaction gave the terthiophene monomer, **11**.

Synthesis and Electrochemistry of the β-Linked Thiophene Polymers

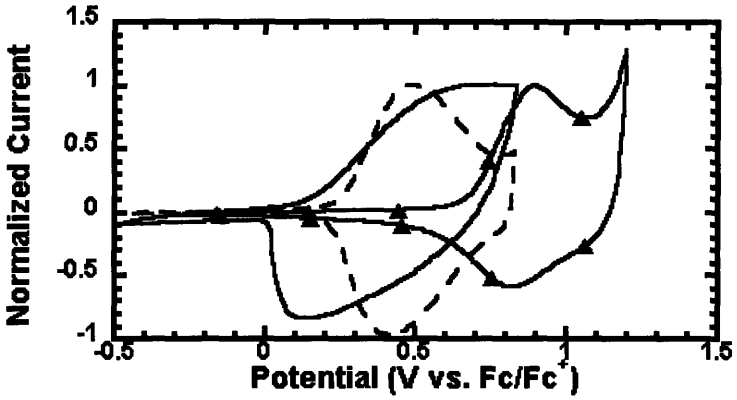

Figure 1. Cyclic voltammetry at 100 mV/s of polymer films, **p-2** (▲), **p-4** (dashed line) and **p-6** (solid line) grown onto interdigitated Pt microelectrodes with 5 μm gaps.

The β-linked thiophene monomers (**2**, **4** and **6**) were deposited onto 5 μm interdigitated microelectrodes by anodic electropolymerization utilizing cyclic voltammetry (CV). The resulting surface confined polymers displayed half waves potentials of 0.86, 0.45 and 0.41 V for **p-2**, **p-4**, and **p-6**, respectively, which reveal a pronounced potential decrease as the number of thiophenes in the monomer increases, as shown in Figure 1.

The *in situ* conductivities of the polymers show a similar trend to the half wave potentials whereby the onset of conductivity was lower as the number of thiophene units was increased, as shown in Figure 2.[15] The *in situ* conductivity of **p-2** that this polymer's conductivity ($>10^{-6}$ S cm^{-1}) was too low to be determined in the electrochemical transistor scheme used here. The difference in absolute conductivity between **p-4** and **p-6** was about an order of magnitude.[16] In

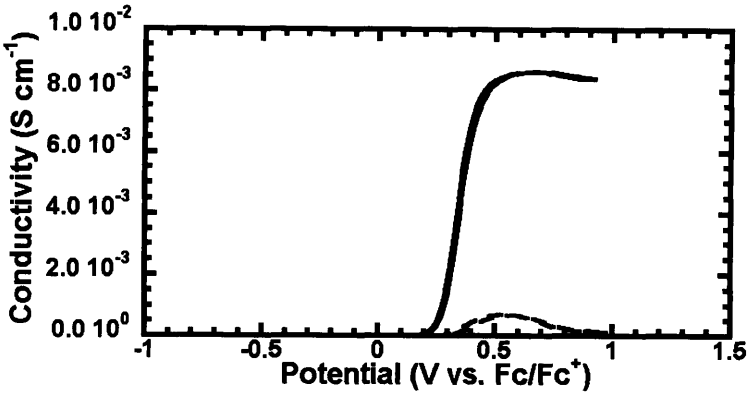

Figure 2. *In situ* conductivity profile of polymer films determined with a 40 mV offset potential between the working electrodes**p-4** (dashed line) and **p-6** (solid line). A scan rate of 10 mV/s was used for **p-4** and **p-6**.

addition, polymer **p-6** displayed a larger region of high conductivity while the conductivity profile of **p-4** was confined to the potential window of the oxidation wave in its CV.

The nature of the substitution on polythiophene and the restricted nature of the highly cross-linked polymer structures were expected to give some differences. However, the magnitude of the variation in the CV and *in situ* conductivity of these polymers was unexpected. With an efficient polymerization, the polymer structures of **p-2**, **p-4** and **p-6** should all resemble a π-conjugated polythiophenes. The likely origin for the large dependence of the redox properties on the number of thiophene units per monomer is the highly cross-linked nature of the polymers. It has been suggested that the cross-linking of conducting polymers can decrease the electrochemical activity of the polymers by reducing the effective π-conjugation length of the polymer.[17] For the β-linked monomers, the degree of cross-linking should be dependent on the number of thiophene units per monomer. Therefore, monomers with more thiophene units should have the electrochemical properties that most closely resemble polythiophene. Polymer **p-6** does in fact display a CV and *in situ* conductivity that closely resembles polythiophene.[18] It is interesting that the separation between the oxidation peak and reduction peak of **p-6**'s CV is larger than those of **p-4** and **p-2**. Given that **p-6** is slightly more conductive this kinetic

sluggishness is not the result of slow electron diffusion but is likely the result of sluggishness in the conformational/structural relaxation and/or slow ion diffusion. Polymers **p-2** and **p-4**, in contrast, may have more rigid and perhaps more open structures that allow fast ion diffusion and limit structure relaxation with changing and discharging.

The UV-vis spectroelectrochemistry of **p-2** showed very little electrochromic activity. The λ_{max} of the absorption of **p-2** in the neutral state was 420 nm. Upon full oxidation, the λ_{max} of the neutral absorption of **p-2** blue shifted from 420 nm to 402 nm with little change in the intensity of the absorption. A weak longer wavelength absorption centered at 758 nm appears when **p-2** was fully oxidized. These results are consistent with the low conductivity displayed by **p-2**. It appears that **p-2** has limited electroactivity and some thiophene units are not oxidized over the potential range of the spectroelectrochemistry experiment (-0.2 V to 1.25 V). The blue shift in the spectrum likely reflects a lowering of the conjugation length induced by mechanical

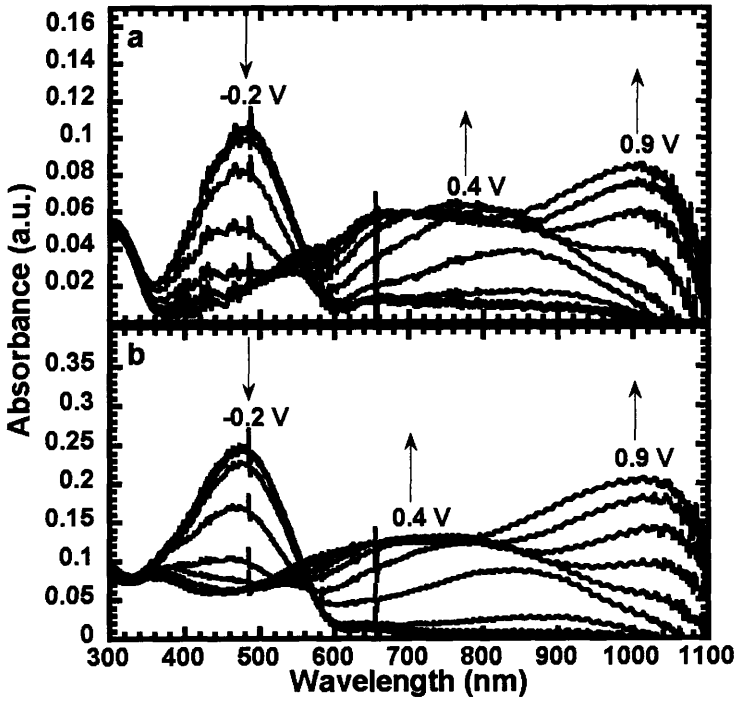

Figure 3. Spectroelectrochemistry of **p-4** (**a**) and **p-6** (**b**) deposited on ITO with applied electrochemical potential intervals from -0.2 to 0.9 V in 0.1 V intervals.

stresses from partial oxidation of the material.

Considering **p-6**'s CV and *in situ* conductivity data, it was expected that its optical spectrum in both the neutral and partially oxidized forms should be at longer wavelengths than those of **p-4**. However, the UV-vis spectroelectrochemistry of **p-4** and **p-6** were remarkably similar to each other and other polythiophenes, as shown in Figure 3. Both **p-4** and **p-6** had λ_{max} absorptions of approximately 480 nm in their neutral state, similar to electrodeposited polythiophene.[18] Upon oxidation at an applied potential of 0.4 V, a broad absorption at approximately 830 nm appears. With oxidation at higher potentials (to 0.9 V) the absorption at 830 nm shifts to shorter wavelengths and a second peak at approximately 1100 nm appears.

Synthesis and Electrochemistry of the α-Linked Thiophene Polymers

Monomer **12** did not undergo oxidative polymerization, which was consistent with the results on a similar monomer.[19] However, the other α-linked thiophene monomers polymerized under similar conditions as used for the β-linked thiophene monomers. The CV's of the films **p-9** and **p-11** display two separate waves, as shown in Figure 4. The half wave potentials for **p-9** (0.39 and 0.74 V) are at higher potentials than those of **p-11** (0.22 and 0.53 V). This CV trend is similar to the β-linked thiophene polymers, with an increase in the number of thiophenes per monomer resulting in the lowering of the half wave potentials. Specifically, the α-linked thiophene polymers should predominantly give a structure whose thiophene segments are interrupted by the hinge structure of the biphenyl, which produces a localization of charged species within the polymer. The lowering of the half wave potentials by the increase in the number of thiophenes per monomer is caused by the increase in the π-conjugation length of the polythiophene section between the biphenyl units. The presence of two waves in the CV's of the **p-9** and **p-11** is a common feature of polythiophene derivatives with segmented molecular

compositions that do not allow significant π-conjugation and therefore should have highly localized charge distributions.[4,20]

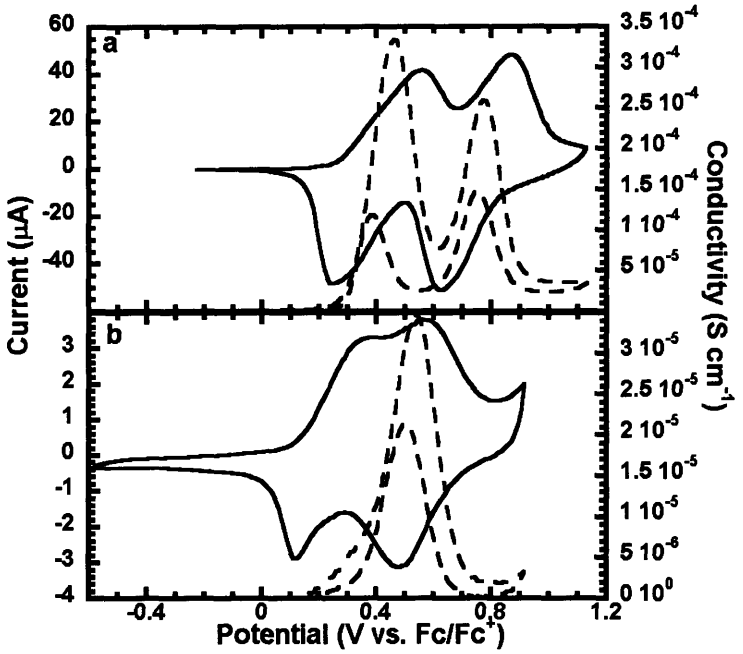

Figure 4. CV (solid line) and *in situ* conductivity (dashed line) of **p-9** (**a**) and **p-11** (**b**). *In situ* conductivity profile of polymer films determined with a scan rate of 2 mV/s and a 40 mV offset potential between the interdigitated working electrodes (5 μm spacing between the electrodes).

The *in situ* conductivities of **p-9** and **p-11** exhibited peaks in their conductivity profiles at potentials coincident with the potentials of the second wave in their CV's. The *in situ* conductivity of **p-9** differed from **p-11** in that it also displayed a peak coincident with the half wave potential of the first wave of its lower potential oxidation wave. This first peak conductivity was also the maximum observed conductivity in **p-9**. The coincidence of the maxima in the conductivity profiles with the half wave potentials is suggestive of a self-exchange or hopping type of conductivity. We have observed similar characteristics in other

segmented polymers. [21] In accord with this nature, the maximum absolute conductivities of the **p-9** and **p-11** were only 3.0×10^{-4} and 3.5×10^{-5} S cm^{-1}, respectively.

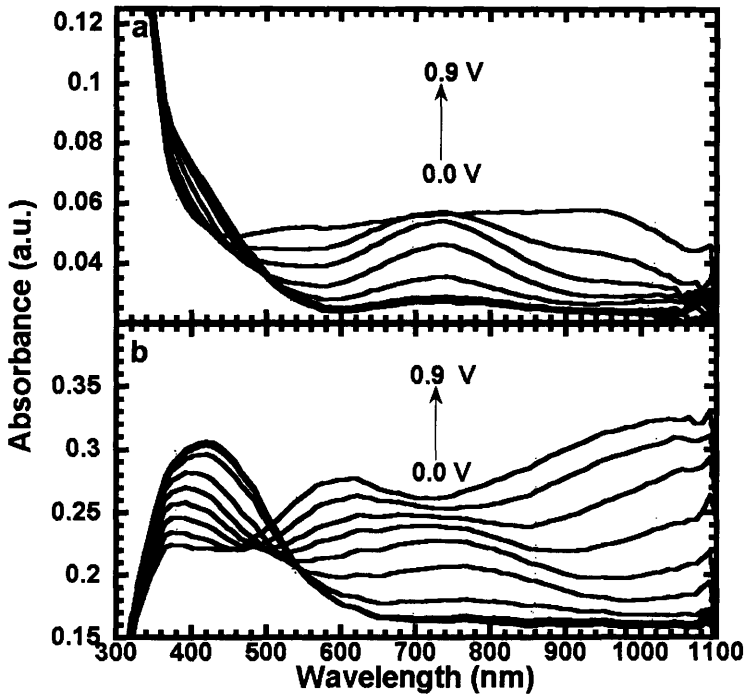

Figure 5. Spectroelectrochemistry of **p-9** (**a**) and **p-11** (**b**) deposited on ITO with applied electrochemical potential intervals from -0.2 to 0.9 V in 0.1 V intervals.

In contrast to the β-linked thiophene polymers, the spectroelectrochemistry of **p-9** versus **p-11** displayed significant differences, as shown in Figure 5. The λ_{max} **p-9** in its un-doped (neutral) state was obscured by the inherent absorbance of the ITO glass slide. Oxidation of **p-9** to 0.6 V produces a new peak centered at 738 nm. With further oxidation, **p-9**'s absorbance broadens and becomes featureless. The λ_{max} of the neutral **p-11** is 415 nm and oxidation at a potential of 0.6 V gives a new peak at 737 nm. This peak is broader and has fewer features than the corresponding oxidation induced absorption peak in **p-9**'s spectroelectrochemistry. Upon further oxidation, a new band appeares at which extends beyond 1100 nm into the near IR. The

λ_{max}'s for the absorption spectra of the neutral **p-9** and **p-11** are consistent with an increase in the conjugation length with in increasing in the number of thiophenes per monomer.[22]

EDOT Derivatives

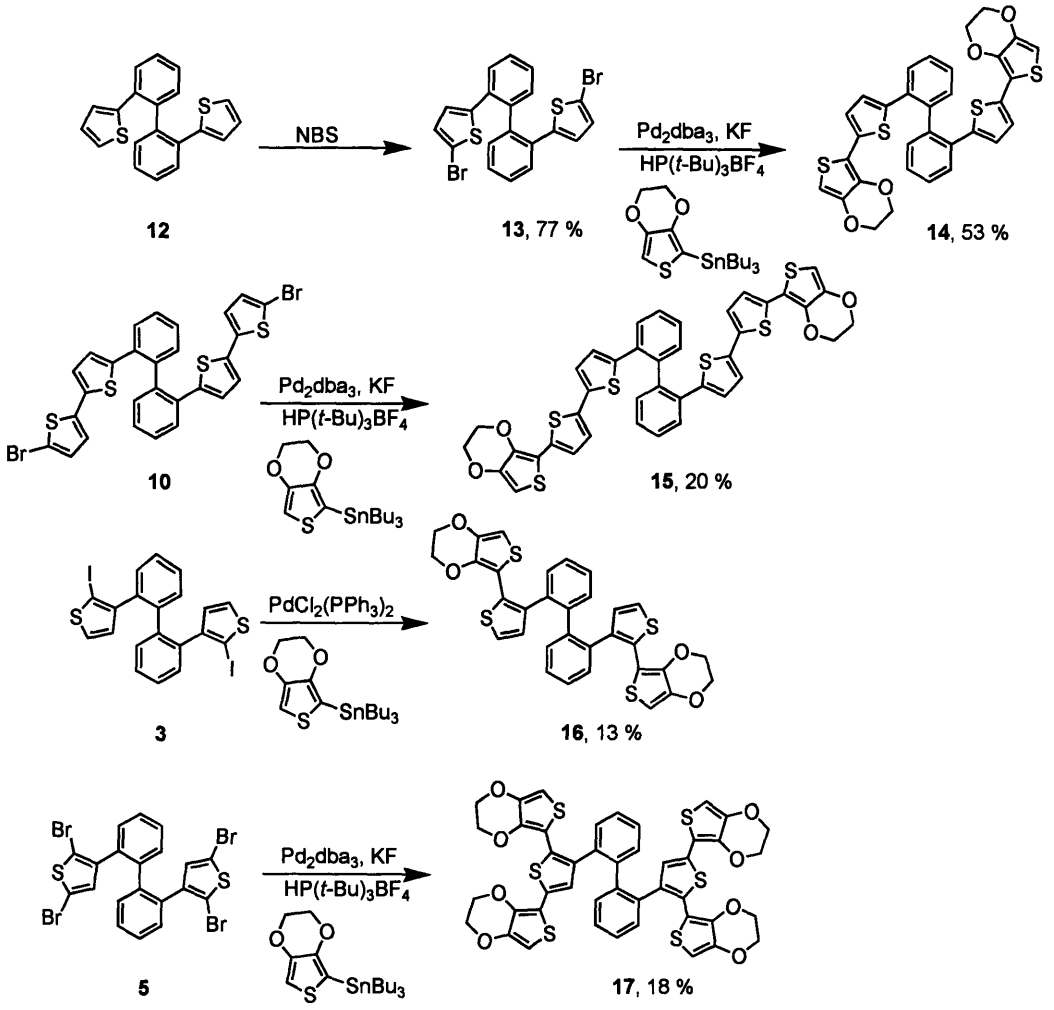

Scheme 4.

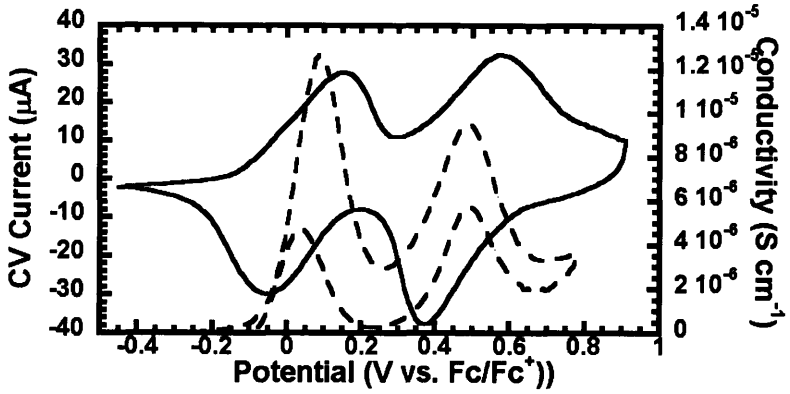

Figure 6. CV (solid line) and *in situ* conductivity (dashed line) of **p-14**. *In situ* conductivity profile of polymer films determined with a scan rate of 2 mV/s and a 40 mV offset potential between the interdigitated working electrodes (2 μm spacing between electrodes).

In an effort to improve the electroactivity of the 2,2' biphenyl incorporated polymers, monomers containing 3,4-ethylenedioxythiophene (EDOT) units were prepared, as shown in Scheme 4.[23] For the α-linked thiophenes monomers, the EDOT unit was added to the end of the thiophene or bithiophene unit of the monomer. Polymer **p-14** is the EDOT analog of **p-9** and in accord with our expectations; **p-14** displays its electroactivity at lower potentials, as shown in Figure 6. In the case of **p-14**, the two electrochemical waves are well resolved and like **p-9**, the conductivity profile exhibits maxima associated with each wave. A similar behavior was observed for **p-15,** the EDOT analogue to **p-11**, as shown in Figure 7. The CV's of **p-14** and **p-15** are strikingly similar with half wave potentials at 0.05 V and 0.47 V for **p-14**, in comparison to half wave potentials of 0.02 V and 0.46 V for **p-15**.

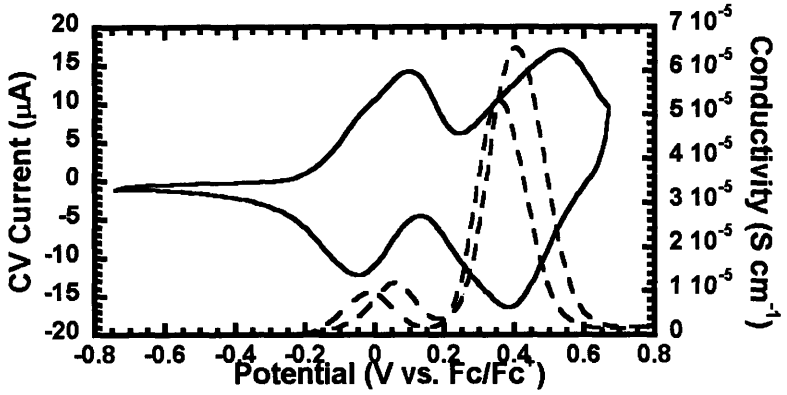

Figure 7. CV (solid line) and *in situ* conductivity (dashed line) of **p-15**. *In situ* conductivity profile of polymer films determined with a scan rate of 2 mV/s and a 40 mV offset potential between the interdigitated working electrodes (5 μm spacing between electrodes).

The lowering of the oxidation potentials with EDOT incorporation was expected, yet the similarities of the electroactivity of **p-14** and **p-15** were a surprise considering our results on **p-9** and **p-11**. The similarities of **p-14** and **p-15** extend to their *in situ* conductivity profiles as well as their maximum conductivities of 1.5×10^{-5} and 7.0×10^{-5} S cm^{-1}, respectively. The ability of an EDOT substitution to produce such similar behavior reflects the fact that a great deal of the charge is likely localized on this unit. Similarly, the coincidence of the conductivity maxima with the half wave potentials and the modest conductivity suggests a hopping/self-exchange conduction mechanism.

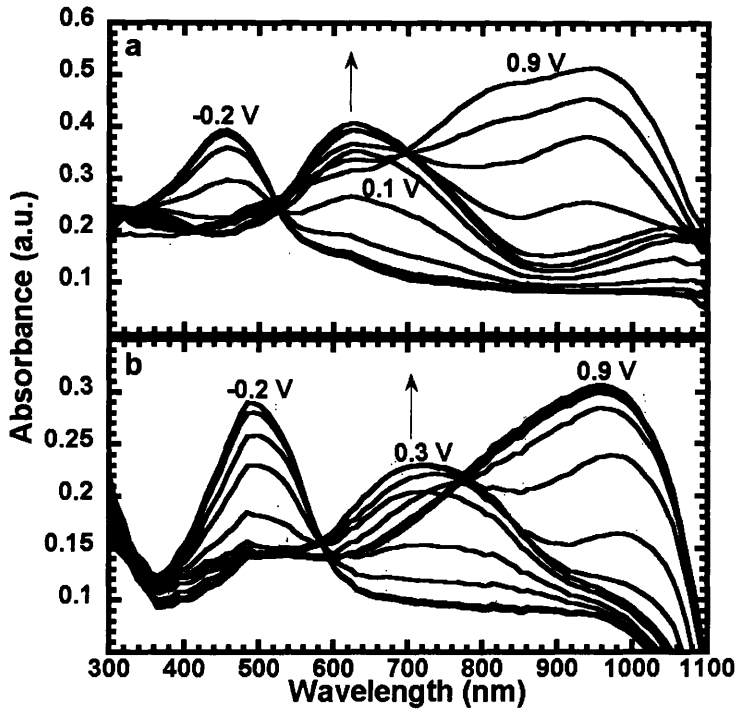

Figure 8. Spectroelectrochemistry of **p-14** (**a**) and **p-15** (**b**) deposited on ITO with applied electrochemical potential intervals from -0.2 to 0.9 V in 0.1 V intervals.

It was useful to compare the λ_{max}'s of the neutral absorptions of the EDOT analogues of the α-linked thiophene polymers to each other and to their pure thiophene analogues. The EDOT substitution caused a red shift in neutral λ_{max}'s absorptions (460 nm for **p-14** and 493 nm for **p-15**) relative to the native thiophene polymers, as shown in Figure 8.[24] The difference in these λ_{max}'s of these EDOT analogues was 33 nm, which was less than half the 71 nm difference between the pure thiophene analogues, **p-9** and **p-11**. These spectroscopic observations are consistent with the CV and *in situ* conductivity results in which the substitution of an EDOT unit into the polymers caused a leveling of the differences between the α-linked thiophene polymers. The spectroelectrochemistry of profile **p-14** displays two features that are different from that of **p-9**. When **p-14** was oxidized at a potential of 0.4 V, the absorption of the polymer had a very

prominent λ_{max} at 606 nm. When fully oxidized, the absorption of **p-14** had two features at 817 nm and 960 nm in direct contrast to the very broad absorption of **p-9** when fully oxidized. The spectroelectrochemistry profile of **p-15** was similar to the profile of **p-11** with only minor differences.

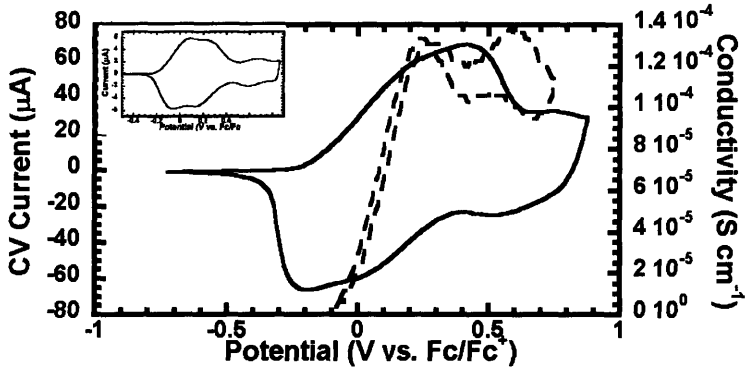

Figure 9. CV (solid line) and *in situ* conductivity (dashed line) of **p-16**. Inset is the CV of **p-16** on a 2 mm^2 Pt button. *In situ* conductivity profile of polymer films determined with a scan rate of 2 mV/s and a 40 mV offset potential between the interdigitated working electrodes (5 μm spacing between electrodes).

For the EDOT analogue of β-linked monomer **4**, the outer thiophene was exchanged with an EDOT unit to provide monomer **16**. For the EDOT analogue of monomer **6**, the two outer thiophene units were exchanged with two EDOT units to give monomer **17**.

The electrochemical results of the EDOT analogues of the β-linked thiophene monomers and the resulting polymers were not as straightforward. The CV of **p-16** occurred at lower potentials, but the profile of the CV profile was significantly different from **p-4**'s CV, as shown in Figure 9. We achieved our most informative CV's of **p-16** on a Pt button working electrode, which clearly displays two waves with half wave potentials at approximately 0.26 and -0.02 V(inset of Figure 9). The *in situ* conductivity of **p-16** displayed an onset of conductivity near -

0.1 V but reached a relative maximum after 0.3 V then another relative maximum in conductivity was displayed at 0.57 V.

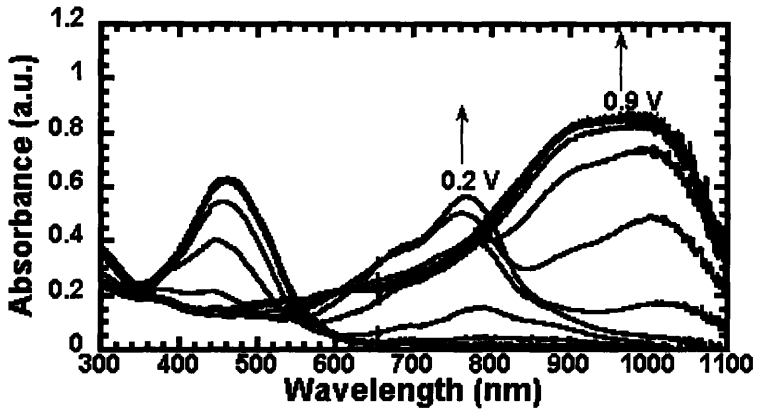

Figure 10. Spectroelectrochemistry of **p-16** from -0.2 to 0.9 V in 0.1 V intervals.

The spectroelectrochemistry of **p-16** had some unusual features, as shown in Figure 10. The λ_{max} of the neutral absorption of **p-16** was 460 nm, which is blue shifted from the λ_{max} of the neutral absorption of **p-4**. With the oxidation of **p-16** at 0.2 V, the absorption spectrum had two features at 689 and 769 nm. Again, these absorptions were slightly blue shifted to the corresponding absorptions in the spectroelectrochemistry of **p-4**. When fully oxidized, the absorption of **p-16** possessed a broad feature from 900 to 1050 nm. These spectroelectrochemistry results were not expected. As stated earlier, we expected a red shift in the UV-vis absorption spectrum of the EDOT analogue relative to the absorption spectrum of the native polythiophene derivative, yet the absorption spectrum of **p-16** actually showed a blue shift relative to **p-4**. The CV, *in situ* conductivity and spectroeletrochemistry results would suggest that the effective neutral π-conjugation in **p-16** is actually lower than in the effective π-conjugation in **p-4.**

The CV of **p-17** had only one wave with a half wave potential at -0.07 V with a small separation between the oxidation and reduction peaks, as shown in Figure 11. The smaller separation between the oxidation and reduction peaks demonstrates that the EDOT groups improve the electrochemical kinetics in **p-17** relative to the native polythiophene, **p-6**. As expected, the half wave potential of the **p-17** occurred at much lower potential than **p-6** and the *in situ* conductivity of **p-17** had a lower onset of conductivity, ≈ -0.22 V. The maximum absolute conductivity of **p-17** was slightly higher than **p-6**'s.

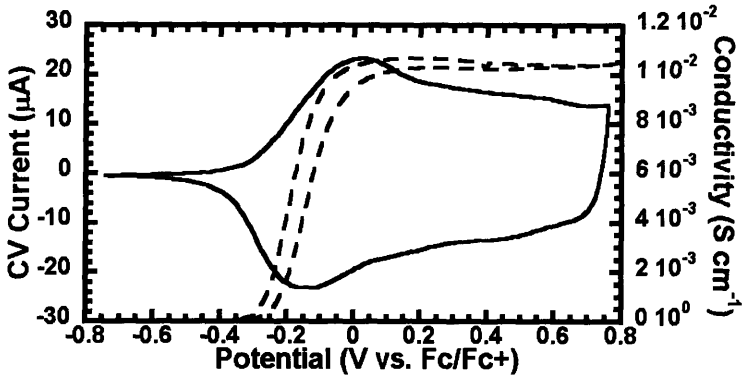

Figure 11. CV (solid line) and *in situ* conductivity (dashed line) of **p-17.** *In situ* conductivity profile of polymer films determined with a scan rate of 10 mV/s and a 40 mV offset potential between the interdigitated working electrodes (5 μm spacing between electrodes).

The λ_{max} (509 nm) of the UV-vis spectrum for the neutral form of **p-17** was red shifted from the λ_{max} of the neutral form of **p-6** by 29 nm shift was observed (Figure 12). This small red shift in λ_{max} of the absorption is not consistent with the expected result of the inclusion of EDOT into the monomer. The spectroelectrochemistry of **p-17** when oxidized at potential of -0.2 V showed a broad absorption that was centered near 800 nm and the absorption of **p-17** when fully oxidized had only a broad peak near the end of the detection limit of the instrument.

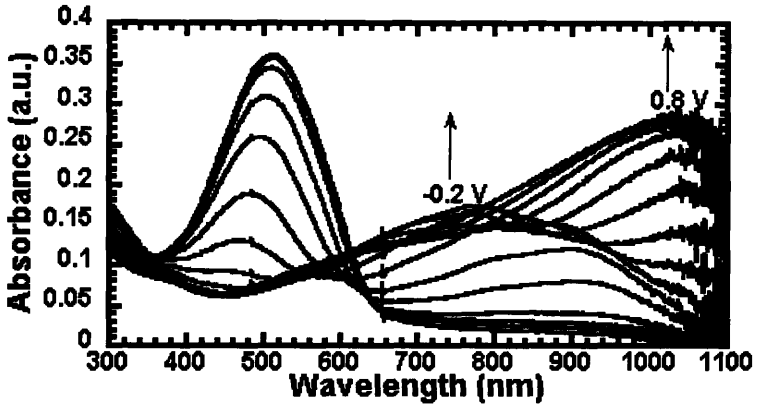

Figure 12. Spectroelectrochemistry of **p-17** from -0.5 to 0.9 V in 0.1 V intervals.

The electrochemical results from **p-16** and **p-17**'s results indicate that the expected significant improvement in charge delocalization by inclusion of the EDOT unit in the polymer does not occur. The reason for this result was attributed to the steric interactions between the ethylene dioxy bridge of EDOT and the phenyl groups of the biphenyl. This interaction may have increased the energy needed for co-planarity between the EDOT units of polymer. The inability to achieve this preferred conformation in turn decreases the charge delocalization throughout the polymer. Overall, the EDOT derivatives of the β-linked thiophene polymers had lower oxidation potentials but provided limited delocalization.

Asymmetric Monomer

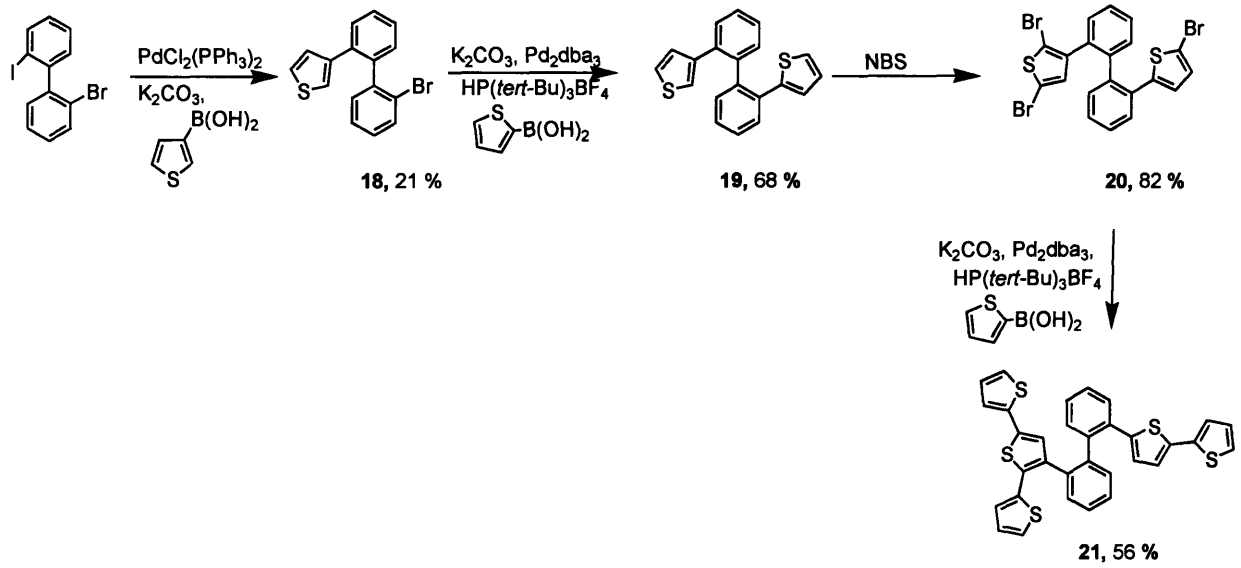

Scheme 5.

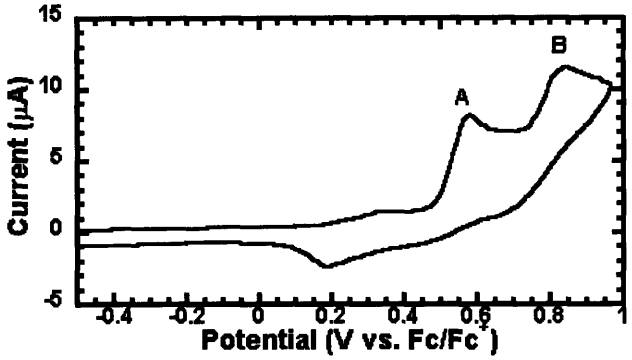

Figure 13. An initial cyclic voltammetry scan of **21**. A 2 mm^2 Pt button was used as the working electrode.

Given the extremely different properties displayed by the α- and β-linked thiophene polymers, we set out to produce a polymer with both types of linkages. Hence, monomer **21** was synthesized as shown in Scheme 5. Monomer **21** displays two oxidations, one at approximately 0.5 V (A in Figure 13) and another at approximately 0.9 V (B in Figure 13). The effectiveness of the electrochemical polymerization of **21** depended on which potential was utilized for the polymerization, as shown in Figure 14. The polymerization at point A was very inefficient, in

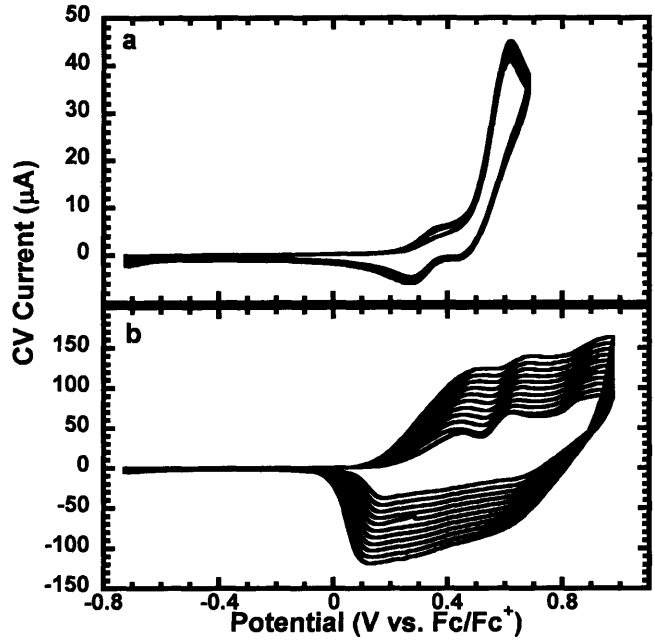

Figure 14. The polymerization of **21** at 0.5 V (**a**) and the polymerization of **21** at 0.9 V by CV.

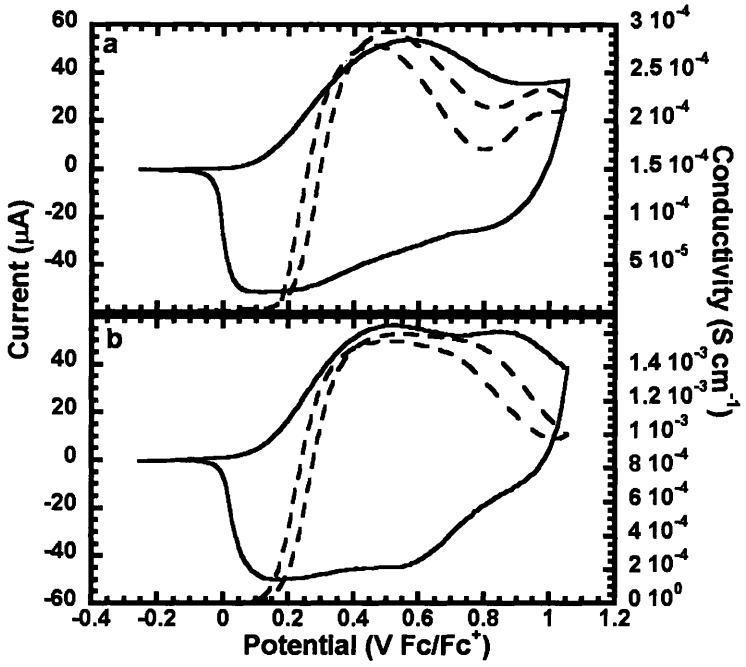

Figure 15. CV (solid line) and *in situ* conductivity (dashed line) of **p-21** synthesized from a potentiostatic polymerization at 0.5 V (**a**) and **p-21** synthesized by cycling between -0.2 and 0.9 V using cyclic voltammetry (**b**). *In situ* conductivity profile of polymer films determined with a scan rate of 10 mV/s and a 40 mV offset potential between the interdigitated working electrodes (5 μm spacing between electrodes).

that it required five times the number of CV scans to deposit a film at 0.5 V than to deposit a film at 0.9 V. This property produced problems in reproducibility and instead a potentiostatic polymerization at 0.5 V was utilized. A direct comparison of the CV and *in situ* conductivity of polymers polymerized at 0.5 V and 0.9 V shows the subtle differences in the electroactivity, as shown in Figure 15. The polymer deposited at 0.5 V shows just one peak oxidation (E_{pa}) at 0.57 V in the CV and the *in situ* conductivity of the polymer has small window of high conductivity with two local maxima. The polymer deposited at 0.9 V shows two E_{pa}'s (0.49 V and 0.87 V) and the *in situ* conductivity shows one broad region of high conductivity.

The dissimilar electroactivities observed in the polymers that resulted from differing polymerization voltages can be rationalized by assigning the waves in the initial CV of **21** to a section of the monomer. Assuming that the bithiophene section will not have significant π-

orbital donation from the phenyl unit of the biphenyl, then the terthiophene section should have the longest π-conjugation length and the lowest oxidation.[25] Therefore, the oxidation at 0.5 V is assigned to the terthiophene section of monomer **21** and the oxidation at 0.9 V is the bithiophene section. The polymerization at the lower potential includes only the terthiophene sections of the monomer, while the polymerization at 0.9 V includes both the terthiophene section and the bithiophene sections. This rationalization would answer why the polymerization at 0.5 V produces a polymer with only E_{pa} present in its CV while the polymerization at 0.9 V produces a polymer with two E_{pa}'s in its CV. However, if the polymer produced at a lower potential consists mainly of the terthiophene sections of the monomer than the unpolymerized bithiophene sections should produce a large irreversible wave in the initial CV of the polymer over the potential range shown in Figure 15. This event does not occur. Due to the small difference in the polymerization potentials and the inefficiency of the low potential polymerization, the oxidation/polymerization of the bithiophene sections may occur under of these conditions. If this event does occur in the low potential polymerization then the dissimilar electroactivity between the polymers derived from monomer **21** is caused by how the bithiophene fragments of the polymer are incorporated into the polymer.

Model Study

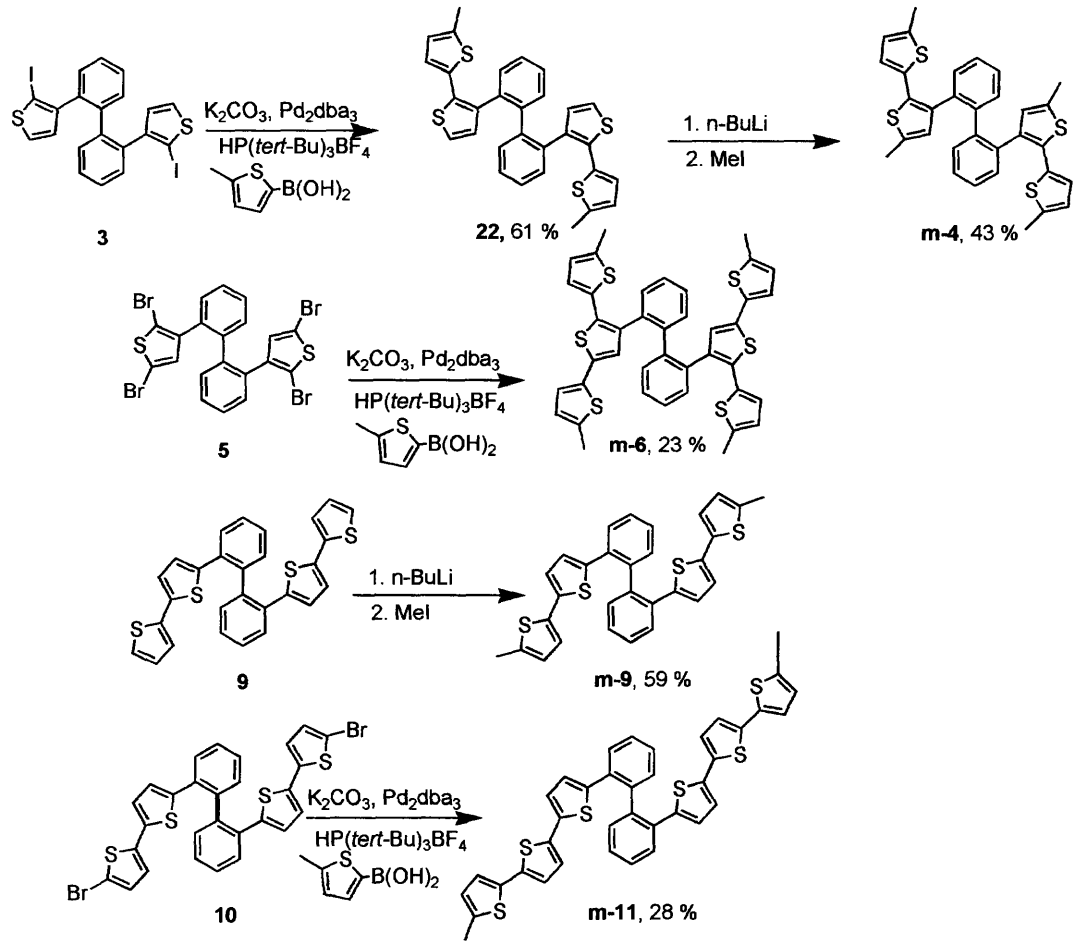

Scheme 6.

We designed model systems to test if the 2,2'-biphenyl unit will align the thiophene units so that π-π interactions between the thiophene fragments are maximized. To fully explore this possibility, several model compounds were synthesized that resemble α- or β-linked monomers, as shown in Scheme 6. The model compounds have methyl groups at the terminal positions α-positions of the thiophene fragment to prevent polymerization. For the β-linked thiophene model compounds, the bithiophene model (**m-4**) had a CV that was irreversible while the terthiophene model compound (**m-6**) exhibited a CV that was reversible. This result was consistent with

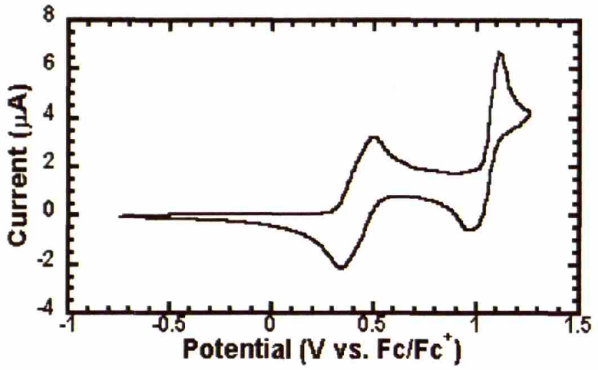

Figure 16. Cyclic voltammetry of **m-6** at 100 mV/s with a 2 mm^2 Pt button as the working electrode.

previous results that found non-polymerizable bithiophenes had irreversible CV's while the methyl end-capped terthiophenes had reversible CV's.[25] The CV of **m-6** displays a lower potential wave that appeared to have unresolved structure suggesting a second wave (Figure 16). Differential pulse voltammetry, DPV, revealed this wave indeed consisted of two waves with a separated by 51 mV, *vide infra*. This result suggested the possibility that the spatial orientation of

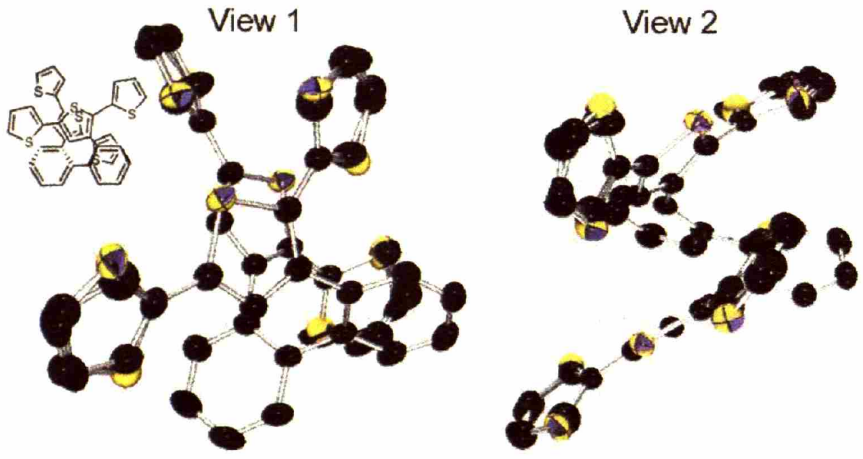

Figure 17. ORTEP of the X-ray structure of compound **6**. Structure generated with 50 % probability thermal ellipsoids. Elements were assigned a color for identification: C (black) and S (yellow/blue).

the 2,2'-substituted biphenyl facilitated a through-space π-π interaction between the two thiophene fragments. Examination of the X-ray structure of **6** revealed that although the twist of the biphenyl does not give the optimum molecular alignment of the thiophene fragments, it appears there is some molecular overlap (Figure 17). This was consistent with the modest coupling potential observed in the DPV of **m-6**.

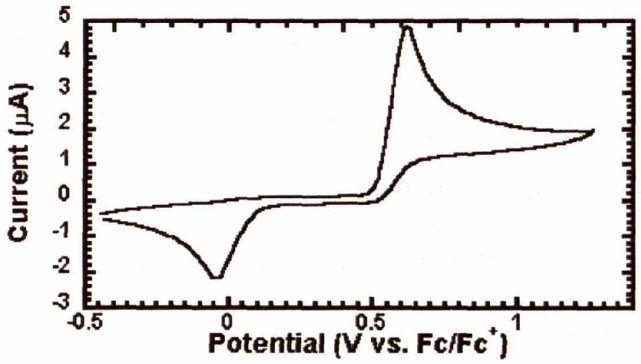

Figure 18. Cyclic voltammetry of **m-9** at 100 mV/s with a 2 mm^2 Pt button.

For both of the α-linked model compounds, the CV was highly electrochemically irreversible but chemically reversible, as represented by the CV of **m-9** in Figure 18.

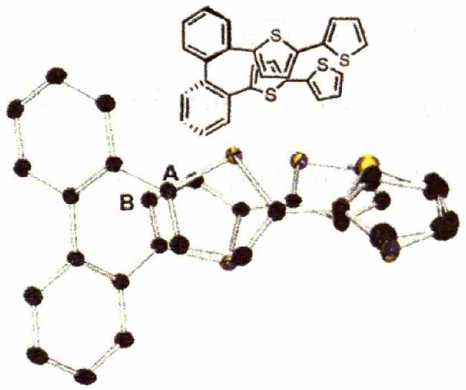

Figure 19. ORTEP of the X-ray structure of compound **9**. Structure generated with 50 % probability thermal ellipsoids. Elements were assigned a color for identification: C (black) and S (yellow/blue).

These results led us to postulate that if the thiophene were in such an optimum position for a through-space interaction that the adjacent thiophene units can actually react to form a weak σ bond. The reasoning behind this suggestion was based on the X-ray structure of compound **9**, as shown in Figure 19. The X-ray structure showed that the thiophene fragments were orientated in such a way that there was a possibility that the α-carbon (A in the Figure 19) of one thiophene attached to the biphenyl could react with the β-carbon (B in Figure 19) of the other thiophene attached to the biphenyl. Similar electrochemical behavior has been observed in thiophene oligomers containing bis(thioxanthyl) dications, which undergo reversible C-C bond breaking/formation upon oxidation/reduction.[26]

A 3-phenyl substituted terthiophene, **23**, and a 3-biphenyl substituted terthiophene, **26**, were synthesized to explore the nature of splitting in the first wave in the CV of **m-6** and to see if this splitting in **m-6** was due to interaction between the phenyl and the thiophene sections, as shown in Scheme 7. The CV and DPV of these compounds revealed no splitting in the lower potential peak, as shown in Figure 20. Therefore it was concluded that the splitting observed in **m-6** was not due to an interaction between the biphenyl and the thiophene sections. The half wave potential of the first wave in the CV of **23** and **26** were extremely close to each other, which was consistent with our primary assumption that the phenyl and biphenyl groups did not significantly affect the π -conjugation of the terthiophene fragments.

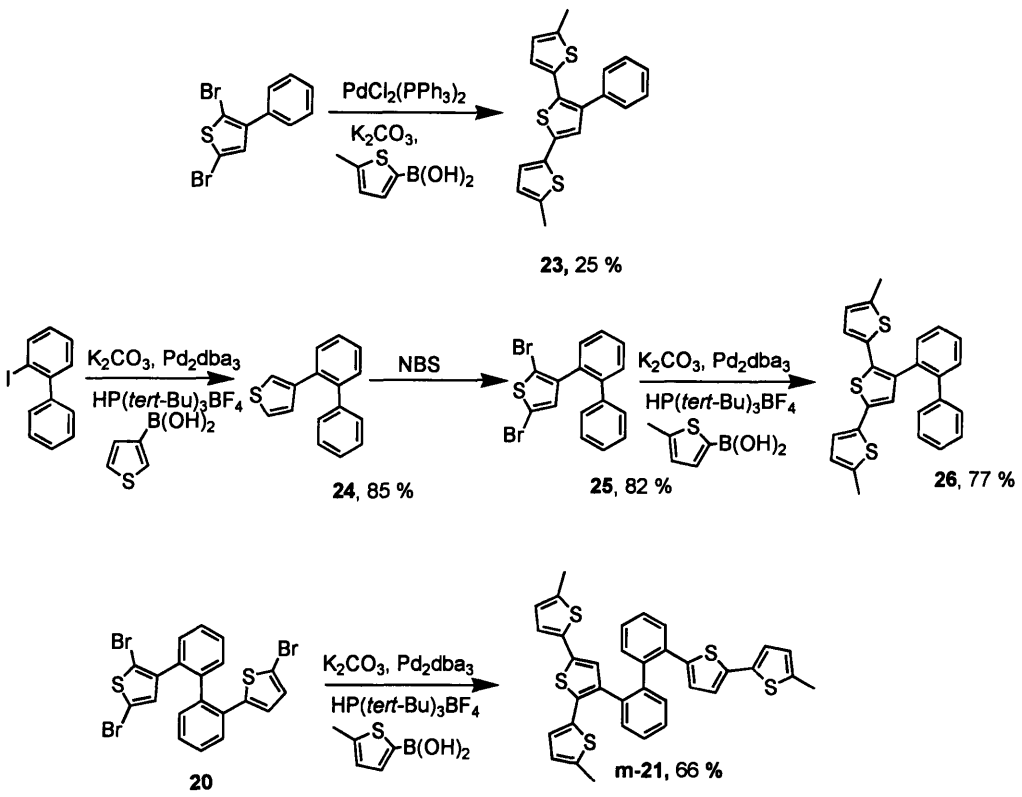

Scheme 7.

A model of **21** also was synthesized to answer the important question about the electrochemical data of **m-6** and **23**. Since the twist of the biphenyl should cause a break in the π-conjugation through the biphenyl, the oxidations of **m-6** and **23** should be close in potential. However, the DPV of **m-6** and **23** showed that the first wave of **23** occurred at a higher potential than **m-6**. The half wave potential of **m-21** was extremely close to the half wave potential of one of the waves in the DPV of **m-6**. This information suggested that a through-space interaction is responsible for the low half wave potential in **m-6**.

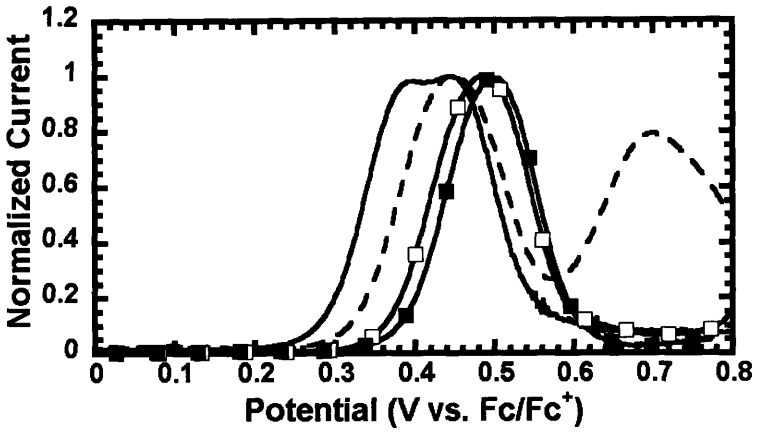

Figure 20. DPV of **m-6** (solid line), **m-21** (dashed line), **23** (□) and **26** (■). A pulse height of 10 mV, a scan rate of 2 mV/s and a 2 mm^2 Pt button as the working electrode were utilized.

Conclusions

In summary, a series of 2, 2'-substituted biphenyl thiophene monomers and their respective polymers were studied. The β-linked thiophene monomers produced a highly cross-linked polymer while the α-linked thiophene monomers produced segmented polymers with limited charge delocalization. The electrical properties for the resulting polymers were dependent on the number of thiophenes per monomer for both the α- or β-linked thiophene monomers. For the α-linked thiophene monomers, the increase in the number of thiophenes in the monomer increased the π-conjugation length of the thiophene oligomers between the biphenyls. For the β-linked thiophene, the increase in the number of thiophene units per monomer reduced the effective cross-linking within the polymer, thus raising the effective π-conjugation of the polymer. As expected, the EDOT homologues all had lower oxidation potentials and lower onsets of conductivities. For the β-linked thiophene monomers, there appears to be steric interactions between the EDOT units and the biphenyl groups. A hybrid monomer of the α- and β- linked thiophene monomers exhibited a modular behavior in that the electroactivity of the polymer was dependent on the potential under which the polymerization was performed. A model study showed that β-linked terthiophene 2, 2'-biphenyl displays through-space electronic interaction

between thiophenes. The model compound of the α-linked monomers displayed CV's with a large hysteresis suggesting reversible σ-bonding between radical cation units. The mapping of the electrochemical properties of these polymers and the understanding of their through space interactions will help guide the design of new conducting polymer molecular mechanical based actuators.

Experimental

General Comments ^{1}H and ^{13}C NMR spectra were recorded on a Bruker 400 MHz spectrometer and are referenced to residual $CHCl_3$ (7.27 ppm for ^{1}H and 77.23 ppm for ^{13}C) or $CHDCl_2$ (5.32 ppm for ^{1}H and 54.00 ppm for ^{13}C). Melting points are uncorrected. High-resolution mass spectra (HRMS) were determined on a Bruker Daltonics APEX II 3 Tesla FT-ICR-MS. All commercial chemicals were purchased from Aldrich. The solvents were purified by a SPS-400-5 solvent purification system (Innovative Technologies). Air sensitive manipulations were performed using standard Schlenk techniques. The 2-bromo-2'-iodo-biphenyl starting material was synthesized according to published procedures.[27] A Discovery model (CEM) microwave reactor was used for reactions involving heating by microwaves.

Electrochemistry Electrochemical measurements with an Autolab II with PGSTAT 30 potentiostat (Eco Chemie) were performed in a nitrogen glovebox or in air for the spectroelectrochemistry measurements. The electrolyte solution for all the electrochemical measurements was 0.1 M $(n\text{-}Bu)_4NPF_6$ in dry CH_2Cl_2, which was prepared and stored over 4 Å molecular sieves in a glovebox. The quasi-internal reference electrode was a Ag wire submersed in 0.01 M $AgNO_3$/ 0.1 M $(n\text{-}Bu)_4NPF_6$ in anhydrous acetonitrile and a Pt wire or gauze was used as a counter electrode. All potentials were referenced to the Fc/Fc^{+} couple. The working electrodes were 2 mm^2 Pt button (Bioanalytical), 2 or 5 μm Pt interdigitated microelectrodes (Abtech Scientific, Inc.), or indium tin oxide coated unpolished float glass slides (Delta

Technologies). Absorption spectra were collected on an Agilent 8453 diode array spectrophotometer. A Dektak 6M stylus profiler (Veeco) was used to measure the film thickness of the polymers grown onto interdigitated microelectrodes.

2,2'-bis(3-theinyl)biphenyl (2) To a 100 mL Schlenk flask was placed 0.560 g of 2,2'dibromobiphenyl, 0.85 g of 3-thiophene boronic acid, 2.6 g of K_2CO_3, 20 mL of THF, 10 mL of ethanol, and 5 mL of water. The solution was de-oxygenated by purging with Ar for 30 minutes. To the solution was then added 0.089 g of Pd_2dba_3 and 0.045 g of $HP(tert\text{-}Bu)_3BF_4$ and the solution was stirred for 48 hours. The organic layer was filtered through a short silica column using ethyl acetate as an eluent, and the solvent was removed in vacuo. Column chromatograph with silica gel was performed using 10 % CH_2Cl_2 in hexanes as an eluent. After evaporation of the solvent under reduced pressure, 0.419 g (75 %) of the product was obtained as a white solid, mp 103.3-105.1 °C. ^1H NMR (CD_2Cl_2): δ 7.36 (m, 8 H), 7.02 (dd, J = 2.8, 4.8 Hz, 2 H), 6.58 (dd, J = 2.8, 1.2 Hz 2 H), 6.50 (dd, J = 4.8, 1.2 Hz 2 H) ppm. ^{13}C NMR (CD_2Cl_2): δ 142.1, 140.6, 136.3, 131.7, 129.8, 128.7, 128.1, 127.7 124.3, 122.9 ppm. HRMS calcd for $C_{20}H_{14}S_2$ $[M]^+$: 318.0531. Found 318.0521.

2,2'-bis(3-[2-iodothiophene])biphenyl (3) To a 100 mL round bottom was added 0.275 g of **2**, 0.58 g of N-iodosuccimide, 20 mL $HCCl_3$, and 20 mL acetic acid The solution was stirred for 26 hours. After stirring, water was added to the reaction mixture and the product was extracted with CH_2Cl_2. The organic layer was washed 2 x 20 mL with a 2 M KOH solution. The solvent was dried with $MgSO_4$ and the solvent was removed in vacuo. Column chromatograph with silica gel was performed using hexanes as an eluent. After evaporation of the solvent under reduced pressure, 0.154 g (31 %) of the product was obtained as a white solid, mp 88.4-90.7 °C. ^1H NMR (CD_2Cl_2): δ 7.38 (m, 8 H), 7.23 (d, 2 H), 6.27 (d, 2 H) ppm. ^{13}C NMR (CD_2Cl_2): δ 146.8, 140.7,

136.1, 132.3, 131.5, 130.5, 130.0, 128.1, 127.6, 76.4 ppm. HRMS calcd for $C_{20}H_{12}S_2I_2$ $[M]^+$: 569.8464. Found 569.8437.

2,2'-bis(3-[2,2']bithiophene])biphenyl (4) To a 25 mL Schlenk flask was added 0.177 g of **3**, 0.130 g of 2-thiopheneboronic acid, 1.0 g of K_2CO_3, 5 mL of THF, 1 mL of ethanol, and 0.5 mL of water. The solution was de-oxygenated by purging with Ar for 30 minutes. To the solution was then added 0.029 g of Pd_2dba_3 and 0.015 g of $HP(tert\text{-}Bu)_3BF_4$ were added and the solution was stirred for 48 hours. The reaction mixture was cooled and filtered through silica gel using ethyl acetate as an eluent. The solvents were removed in vacuo. Column chromatograph with silica gel was performed using 10 % CH_2Cl_2 in hexanes as an eluent. After evaporation of the solvent under reduced pressure, 0.084 g (56 %) of the product was obtained as a white solid, mp 162.1-164.1 °C. ^1H NMR (CD_2Cl_2): δ 7.21 (m, 8 H), 6.99 (broad d, J = 7.2 Hz, 2 H), 6.95 (d J = 5.2 HZ, 2 H), 6.89 (dd, J = 7.2, 3.6 Hz 2H), 6.55 (broad d, J = 3.6 Hz, 2 H), 6.37 (d J = 5.2 Hz, 2 H) ppm. ^{13}C NMR (CD_2Cl_2): δ 141.1, 138.3, 136.5, 135.2, 132.9, 131.7, 131.5, 131.3, 127.6, 127.5, 127.2, 126.2, 125.5, 123.3 ppm. HRMS calcd for $C_{28}H_{18}S_4$ $[M]^+$: 482.0286. Found 482.0289.

2,2'-bis(3-[2,5-dibromotheinyl])biphenyl (5) To a 100 mL round bottom flask was added 0.396 g of **2**, 1.19 g of N-bromosuccimide (NBS) and 30 mL of DMF and the reactants were stirred together in absence of light for 72 hours. After stirring, 30 mL of water was added and the product was extracted with ethyl ether. The organic layer was dried with $MgSO_4$ and solvent was removed in vacuo. Column chromatograph with silica gel was performed using hexanes as an eluent. After evaporation of the solvent under reduced pressure, 0.690 g (88 %) of the product was obtained as a white solid, mp 156.3-157.4 °C. ^1H NMR (CD_2Cl_2): δ 7.45 (m, 8 H), 6.16 (s, 2 H) ppm. ^{13}C NMR (CD_2Cl_2): δ 142.7, 140.6, 133.4, 132.6, 132.4, 130.9, 128.9, 128.0, 110.6, 110.2 ppm. HRMS calcd for $C_{20}H_{10}Br_4S_2$ $[M]^+$: 629.6952. Found 629.6982.

2,2'-bis(3'-[2,2',5',2"]terthiophene])biphenyl (6) To a 50 mL Schlenk flask was added 0.298 g of **5**, 0.690 g of 2-thiopheneboronic acid, 2.4 g of K_2CO_3, 15 mL of THF, 3 mL of ethanol, and 1 mL of water. The solution was de-oxygenated by purging with Ar for 30 minutes. To the solution was then added 0.110 g of Pd_2dba_3 and 0.051 g of $HP(tert\text{-}Bu)_3BF_4$ and the solution was heated to 50 °C for 24 hours. The reaction mixture was stirred an additional 24 hours at room temperature. The reaction mixture was filtered through silica gel using ethyl acetate as an eluent. The solvents were removed in vacuo. Column chromatography with silica gel was performed using 10 % CH_2Cl_2 in hexanes as an eluent. After evaporation under reduced pressure of the solvent, the product was recrystallized from hexanes and the minimum amount of CH_2Cl_2. The product was obtained as yellow crystals, 0.109 g (35 %) mp 200 °C. ^1H NMR (CD_2Cl_2): δ 7.23 (m, 6 H), 7.11 (dd apparent triplet, 2 H), 7.07 (d J = 5.1 Hz, 2 H), 6.89 (m, 6 H), 6.76 (dd J = 3.7, 5.1 Hz, 2 H), 6.43 (m, 4 H) ppm. ^{13}C NMR (CD_2Cl_2): δ 141.3, 138.7, 137.4, 136.1, 135.0, 131.9, 131.7, 131.0, 128.1$_9$, 128.1$_5$, 128.0, 127.6, 127.6, 126.4, 125.7, 124.8, 123.9 ppm. HRMS calcd for $C_{36}H_{22}S_6$ $[M]^+$: 646.0042. Found 646.0072.

5-(2-bromo-phenyl)-bithiophene (8) To a 100 mL Schlenk flask was added 3.01 g of [2, 2']bithiophene which was dissolved in 50 mL of THF. The solution was cooled to -78 °C and then 8 mL of 2.2 M n-butyl lithium solution was added drop wise. The reaction mixture was stirred at -78 °C for 1.5 hours. After this stirring, 2.2 mL of 1,2-dibromobenzene was added syringe. The solution was allowed to warm up to room temperature and stirred overnight. At that time 50 mL of brine was added and the organic layer was separated and dried with $MgSO_4$. The solvent was removed in vacuo and the product was purified by column chromatography on silica gel using hexanes as an eluent. After evaporation of the solvent under reduced pressure, 2.27 g (39 %) of the product was obtained as a colorless oil. ^1H NMR (CD_2Cl_2): δ 7.74 (dd J = 1.2, 8.0 Hz, 1 H), 7.56 (dd J = 1.6, 7.5 Hz, 1 H), 7.41 (dd J = 1.2, 7.5 Hz, 1 H), 7.31 (dd J = 1.1,

5.1 Hz, 1 H), 7.25 (m, 4 H) 7.09 (dd J = 3.6, 5.1 Hz, 1 H) ppm. ^{13}C NMR (CD_2Cl_2): δ 140.8, 138.5, 137.4, 135.1, 134.2, 132.1, 129.6, 129.1, 128.3, 128.0, 125.1, 124.3, 124.0, 122.7 ppm. HRMS calcd for $C_{14}H_9BrS_2$ $[M]^+$: 319.9324. Found 319.9326.

2,2'-bis(5-[2,2']bithiophene)biphenyl (9) To a 100 mL Schlenk flask was added 2.20 g of **8**, 0.960 g of bis(pinacolato)diboron, 3.1 g of K_3PO_4 which were dissolved in 50 mL of DMF. The solution was de-oxygenated by purging with Ar for 30 minutes. To the solution was then added 0.16 g of $Pd(PPh_3)_2Cl_2$, the solution was heated to 100 °C for 10 hours, and 25 mL of water was added. This mixture was extracted with 2 x 30 mL of CH_2Cl_2 and the organics were dried with $MgSO_4$. The solvents were removed in vacuo and column chromatography was performed with silica gel using a solution of 10 % CH_2Cl_2 in hexanes as an eluent. After evaporation of the solvent under reduced pressure, 1.10 g (63 %) of the product was obtained as a yellow solid, mp 106.1-107.8 °C. ^1H NMR (CD_2Cl_2): δ 7.51 (m, 2 H), 7.42 (m, 6 H), 7.20 (dd, J = 8.4, 1.2 Hz 2 H), 7.02 (dd, J = 3.5, 1.2 Hz 2 H), 6.98 (dd, J = 8.4, 3.5 Hz 2 H) 6.89 (d, 2 H) 6.43 (d, 2 H) ppm. ^{13}C NMR (CD_2Cl_2): δ 142.2, 139.8, 138.0, 137.7, 134.0, 132.0, 129.8, 128.6, 128.2, 127.4, 124.7, 124.0, 123.9 ppm. HRMS calcd for $C_{28}H_{18}S_4$ $[M+Na]^+$: 505.0184. Found 505.0189.

2,2'-bis(5(5'-bromo[2,2']bithiophene))biphenyl (10) To a 100 mL round bottom, 0.761 g of **9** and 0.610 g of NBS were dissolved in 50 mL of DMF. The solution was stirred in the dark for 12 hours and then 50 mL of water was added to the solution. This mixture was extracted with 2 x 30 mL of CH_2Cl_2 and the organics were dried with $MgSO_4$. After evaporation of the solvent under reduced pressure, the product was recrystallized from boiling toluene, 0.496 g (49 %) of the product was obtained as a yellow solid, mp 175.2-178.6 °C. ^1H NMR ($CDCl_3$): δ 7.42 (m, 8 H), 6.91 (d J = 4.0 Hz, 2 H), 6.78 (d J = 3.8 Hz, 2 H), 6.71 (d J = 4.0 Hz, 2 H), 6.31 (d, 2 H) ppm. ^{13}C NMR ($CDCl_3$): δ 142.6, 139.7, 139.3, 137.0, 133.7, 131.9, 130.9, 129.8, 128.6, 128.4,

127.3, 124.3, 123.7, 111.0 ppm. HRMS calcd for $C_{28}H_{16}S_4Br_2$ $[M]^+$: 637.8469. Found 637.8447.

2,2'-bis-(5'''-[2,2',5',2'']terthiophene)biphenyl (11) To a 25 mL Schlenk flask was added 0.120 g of **10**, 0.200 g of 2-thiopheneboronic acid, 2.0 g of K_2CO_3, 5 mL of THF, 1 mL of ethanol, and 0.5 mL of water. The solution was de-oxygenated by purging with Ar for 30 minutes. To the solution was added 0.040 g of Pd_2dba_3 and 0.020 g of HP(*tert*-Bu)$_3BF_4$ and then the solution was stirred at room temperature for 72 hours. The reaction mixture was then filtered through silica gel with ethyl acetate an eluent. The solvents were removed in vacuo and column chromatography was performed using silica gel with a solvent gradient (10 to 20 % CH_2Cl_2 in hexanes) as an eluent. After evaporation of the solvent under reduced pressure, 0.030 g (25 %) of the product was obtained as a yellow solid, mp 200.3-202.5 °C. ^{1}H NMR ($CDCl_3$): δ 7.43 (m, 8 H), 7.22 (dd J = 1.0, 5.1 Hz, 2 H), 7.13 (dd J = 1.1, 3.6 Hz, 2 H), 7.03 (m, 4 H), 6.90 (d J = 3.6 Hz, 2 H), 6.86 (d J = 3.8 Hz, 2 H) 6.34 (d 3.8 Hz, 2 H) ppm. ^{13}C NMR ($CDCl_3$): δ 142.1, 139.6, 137.7, 137.4, 136.5, 136.1, 133.7, 131.7, 129.7, 128.4, 128.1, 127.2, 124.6, 124.5, 124.2, 123.9 123.8 ppm. HRMS calcd for $C_{36}H_{22}S_6$ $[M]^+$: 646.0040. Found 646.0031.

2,2'-bis(2-theinyl)biphenyl (12) To a 100 mL Schlenk flask was placed 0.493 g of 2,2'dibromobiphenyl, 1.2 g of 2-thiophene boronic acid, 2.3 g of K_2CO_3, 15 mL of THF, 5 mL of ethanol and 2 mL of water. The solution was de-oxygenated by purging with Ar for 30 minutes, then 0.080 g of Pd_2dba_3 and 0.040 g of HP(*tert*-Bu)$_3BF_4$ were added and then solution was heated at 50 °C for 12 hours. The organic layer was then filtered through a short silica column with ethyl acetate as an eluent. The solvent was removed in vacuo, and the product was purified by column chromatography with silica gel using 10 % CH_2Cl_2 in hexanes as an eluent. After evaporation of the solvent under reduced pressure, 0.465 g (92 %) of the product was obtained as a white solid, mp 71.0-74.7 °C. ^{1}H NMR (CD_2Cl_2): δ 7.51 (m, 2 H), 7.38 (m, 6 H), 7.16 (dd, J =

1.1, 5.1 Hz 2 H), 6.82 (dd, J = 3.6, 5.1 Hz 2 H), 6.58 (dd, J = 1.1, 3.6 Hz 2 H) ppm. ^{13}C NMR (CD_2Cl_2): δ 143.2, 140.2, 134.5, 132.0, 130.0 128.5, 127.9, 127.2 126.6, 126.0 ppm. HRMS calcd for $C_{20}H_{14}S_2$ $[M]^+$: 318.0531. Found 318.0534.

2,2'-bis(2-(5-bromo-theinyl)biphenyl (13) To a 100 mL round bottom flask was placed 0.465 g of **12** and 0.700 g of NBS which were dissolved in 50 mL of DMF. The solution was stirred in the dark for 22 hours and then 50 mL of water was added. This mixture was washed with 2 x 30 mL of ethyl ether. The organic wash was dried with $MgSO_4$ and the solvent was evaporated in vacuo. Column chromatography was performed with silica gel to purify the product using 10 % CH_2Cl_2 in hexanes as an eluent. After removal of the solvent by evaporation, 0.535 g (77 %) of the product was obtained as a white solid, mp 104.7-107.1 °C. ^{1}H NMR ($CDCl_3$): δ 7.41 (m, 8 H), 6.77 (d J = 3.9 Hz, 2 H), 6.30 (d J = 3.9 Hz, 2 H) ^{13}C NMR ($CDCl_3$): δ 144.2, 139.0, 133.3, 131.7, 129.8, 129.5, 128.5, 128.2, 126.5, 112.6 ppm. HRMS calcd for $C_{20}H_{12}Br_2S_2$ $[M]^+$: 473.8742. Found 473.8735.

2,2'-bis-(2-(5-(3,4-ethylenedioxythiophene)thiophene))biphenyl (14) To a 25 mL Schlenk flask was placed 0.0726 g of **13**, 0.50 g of 2-tributylstannyl-3,4-ethylenedioxythiophene, 0.50 g of KF, and 15 mL toluene. The solution was de-oxygenated by purging with Ar for 30 minutes, then 0.050 g of Pd_2dba_3 and 0.020 g of HP(*tert*-Bu)$_3BF_4$ were added. The solution was then heated at 50 °C for 12 hours. After stirring, water was added to the reaction mixture and the product was extracted with ethyl acetate. The organic phase was dried with $MgSO_4$, and the solvent was removed in vacuo. The products were purified with silica gel column chromatography using a mixture of 1:1 CH_2Cl_2 in hexanes as an eluent. After evaporation of the solvent under reduced pressure, 0.0484 g (53 %) of the product was obtained as a yellow-orange solid, mp 92.1-93.7 °C (dec.). ^{1}H NMR (CD_2Cl_2): δ 7.53 (m, 2 H), 7.39 (m, 6 H), 6.93 (d J = 3.8 Hz, 2 H), 6.40 (d J = 3.8 Hz, 2 H), 6.20 (s, 2 H), 4.23 (m, 8 H) ppm. ^{13}C NMR (CD_2Cl_2): δ

142.4, 141.3, 139.9, 137.9, 135.5, 134.0, 131.9, 129.7, 128.4, 127.9, 126.7, 123.1, 112.4, 96.9, 65.4, 65.1 ppm. HRMS calcd for $C_{32}H_{22}O_4S_4$ $[M+Na]^+$: 621.0293. Found 621.0290.

2, 2'-bis-(5'-(5-(3,4-ethylenedioxythiophene)[2, 2']bithiophene))biphenyl (15) To a 25 mL Schlenk flask was placed 0.126 g of **10**, 0.50 g of 2-tributylstannyl-3,4-ethylenedioxythiophene, 0.50 g of KF, and 15 mL toluene. The solution was de-oxygenated by purging with Ar for 30 minutes then 0.040 g of Pd_2dba_3 and 0.020 g of HP(*tert*-Bu)$_3BF_4$ were added. The solution was stirred for 20 hours then water was added to the reaction mixture and the product was extracted with ethyl acetate. The organic phase was dried with $MgSO_4$. The solvents were removed in vacuo. Column chromatography was performed with silica gel (the silica gel was treated with 10 % triethylamine in hexanes before the column was run.) using a mixture as 1:1 CH_2Cl_2 in hexanes as an eluent. After evaporation of the solvent under reduced pressure, 0.031 g (20 %) of the product was obtained as a yellow-orange solid, mp 112.5-114.7 °C (dec.). ^{1}H NMR (CD_2Cl_2): δ 7.51 (m, 2 H), 7.44 (m, 6 H), 7.08 (d J = 3.8 Hz, 2 H), 6.94 (d J = 3.8 Hz, 2 H), 6.89 (d J = 3.8 Hz, 2 H), 6.67 (d J = 3.8 Hz, 2 H), 6.26 (s, 2 H), 4.36 (m, 4 H), 4.26 (m, 4 H) ppm. ^{13}C NMR (CD_2Cl_2): δ 142.4, 142.0, 139.8, 138.2, 138.0, 135.7, 134.0, 133.9, 131.9, 129.7, 128.5, 128.2, 127.5, 123.8, 123.6, 112.2, 97.3, 65.5, 65.1 ppm. HRMS calcd for $C_{40}H_{26}O_4S_6$ $[M+Na]^+$: 785.0048. Found 785.0055.

2, 2'-bis-(3-(2-(3,4 ethylenedioxythiophene)thiophene))biphenyl (16) To a 10 mL microwave tube was placed 0.111 g of **3**, 0.50 g of 2-tributylstannyl-3,4-ethylenedioxythiophene, and 4 mL toluene. The solution was de-oxygenated by purging with Ar for 30 minutes. To the solution was added 0.020 g of $PdCl_2(PPh_3)_2$ and the solution was heated at 130 °C for 1 hour using a microwave reactor. A solution of 10 % KF in water was added to the reaction mixture and the product was extracted with ethyl acetate. The organic phase was dried with $MgSO_4$ and the solvents were removed in vacuo. Column chromatography was performed with silica gel (the

silica gel was treated with 10 % triethylamine in hexanes before the column was run.) using a mixture as 1:1 CH_2Cl_2 in hexanes as an eluent. After evaporation under reduced pressure of the solvent, 0.029 g of the impure product was isolated. Further purification by HPLC was performed using a reverse phase C-18 HPLC column with a gradient of acetonitrile and methanol as an eluent. After evaporation of the solvent under reduced pressure, 0.015 g (13 %) of the product was obtained as a white solid, mp 119.0-120.3 °C. ^{1}H NMR (CD_2Cl_2): δ 7.23 (m, 4 H), 7.14 (m, 2 H), 7.06 (d J = 5.2 Hz, 2 H), 7.03 (d J = 7.0 Hz, 2 H), 6.43 (d J = 5.2 Hz, 2 H), 6.19 (s, 2 H), 4.16 (apparent d, 4 H), 4.08 (broad s, 2 H) ppm. ^{13}C NMR (CD_2Cl_2): δ 141.9, 140.9, 139.2, 138.8, 135.7, 131.6, 131.5, 130.6, 129.8, 127.6, 127.0, 124.1, 111.2, 99.2, 65.2, 65.0 ppm. HRMS calcd for $C_{32}H_{22}O_4S_4$ $[M+Na]^+$: 621.0293. Found 621.0310.

2, 2'-bis-(3-(2,5-bis-(3,4-ethylenedioxythiophene)thiophene))biphenyl (17) To a 25 mL Schlenk tube was added 0.1694 g of **5**, 0.50 g of 2-tributylstannyl-3,4-ethylenedioxythiophene, 0.50 g of KF, and 15 mL toluene. The solution was de-oxygenated by purging with Ar for 30 minutes then 0.060 g of Pd_2dba_3 and 0.030 g of HP(*tert*-Bu)$_3BF_4$ were added. The solution was heated at 50 °C for 24 hours then water was added to the reaction mixture and the product was extracted with ethyl acetate. The organic phase was dried with $MgSO_4$ and the solvents were removed in vacuo. Column chromatography was performed with silica gel (the silica gel was treated with 10 % triethylamine in hexanes before the column was run.) using a mixture as 1:1 ethyl acetate in hexanes as an eluent. After evaporation of the solvent under reduced pressure, 0.0436 g (18 %) of the product was obtained as a yellow-orange solid, mp 203.0-205.9 °C. ^{1}H NMR (CD_2Cl_2): δ 7.26 (m, 4 H), 7.20 (m, 2 H), 6.94 (d J= 7.8 Hz, 2 H), 6.59 (s, 2 H), 6.12 (two s, 4 H), 4.29 (m, 4 H), 4.21 (m, 4 H), 4.12 (m, 4 H), 4.06 (m, 4 H) ppm. ^{13}C NMR (CD_2Cl_2): δ 142.3, 141.8, 141.4, 138.9, 138.4, 137.9, 135.4, 133.5, 131.6, 131.2, 127.9, 127.6, 127.1, 126.1,

113.0, 111.4, 99.1, 96.7, 65.6, 65.2 (two carbons), 65.1 ppm. HRMS calcd for $C_{44}H_{30}O_8S_6$ $[M+Na]^+$: 901.0157. Found 901.0128.

2-(3-theinyl)-2'-bromo-biphenyl (18) To a 50 mL Schlenk flask was added 0.4201 g of 2-bromo-2'-iodo-biphenyl, 0.150 g of 3-thiophene boronic acid, 0.3 g of K_2CO_3, 20 mL of THF, 10 mL of ethanol and 5 mL of water. The solution was de-oxygenated by purging with Ar for 30 minutes. To the solution was added 0.050 g of $PdCl_2(PPh_3)_2$ and the solution was heated to 60 °C for 16 hours. The organic layer was filtered through a short silica column with ethyl acetate as an eluent. The solvent was removed in vacuo. Column chromatography was performed with silica gel using 4 % CH_2Cl_2 in hexanes as an eluent. After evaporation of the solvent under reduced pressure, 0.079 g (21 %) of the product was obtained as a colorless oil. ^1H NMR ($CDCl_3$): δ 7.62 (m, 2 H), 7.50 (m, 1 H), 7.43 (m, 1 H), 7.36 (dd J = 1.3, 7.5 Hz, 1 H), 7.29 (m , 1 H), 7.21 (m, 2 H), 7.16 (dd, J = 2.9, 5.0 Hz 1H), 6.97 (dd, J = 1.3, 2.9 Hz 1 H), 6.90 (dd, J = 1.3, 5.0 Hz 1H) ppm. ^{13}C NMR ($CDCl_3$): δ 142.7, 141.5, 139.7, 135.7, 132.7, 131.9, 130.9, 129.6, 128.9, 128.8, 128.4, 127.2, 127.1, 124.7, 124.1, 123.1 ppm. HRMS calcd for $C_{16}H_{11}BrS$ $[M+Na]^+$: 336.9657. Found 336.9648.

2-(3-theinyl)-2'-(2-theinyl)-biphenyl (19) To a 50 mL Schlenk flask was added 0.078 g of **18**, 0.150 g of 2-thiophene boronic acid, 0.5 g of K_2CO_3, 20 mL of THF, 10 mL of ethanol and 5 mL of water. The solution was de-oxygenated by purging with Ar for 30 minutes. To the solution was added 0.060 g of Pd_2dba_3 and 0.030 g of $HP(tert\text{-}Bu)_3BF_4$ and the solution was heated at 60 °C for 12 hours. After heating, the organic layer was filtered through a short silica column with ethyl acetate. The solvent was removed in vacuo. Column chromatography was performed with silica gel using 4 % CH_2Cl_2 in hexanes as an eluent. After evaporation of the solvent under reduced pressure, 0.054 g (68 %) of the product was obtained as a colorless oil. ^1H NMR ($CDCl_3$): δ 7.48 (m, 1 H), 7.40 (m, 7 H), 7.13 (dd J =1.2, 5.0 Hz, 1 H), 7.03 (dd J =3.0, 5.0 Hz, 1

H), 6.81 (dd, J = 3.6, 5.1 Hz, 1 H), 6.67 (dd J = 1.2, 3.0 Hz, 2 H), 6.60 (dd, J = 1.3, 5.1 Hz, 1H), 6.48 (dd, J = 1.3, 3.6 Hz, 1 H) ppm. ^{13}C NMR ($CDCl_3$): δ 143.0, 141.6, 140.1, 139.8, 136.2, 133.9, 131.5, 129.8, 129.5, 128.5, 128.0, 127.9, 127.6, 127.4, 126.8, 126.0, 125.5, 124.2, 122.7 ppm. HRMS calcd for $C_{20}H_{14}S_2$ $[M+H]^+$: 319.0610. Found 319.0605.

2-(3-(2,5-dibromotheinyl))-2'-(2-(5-bromotheinyl))-biphenyl (20) To a 100 mL round bottom flask was placed 0.022 g of **19**, 0.150 g of NBS and 30 mL of DMF and stirred for 24 hours. After stirring, 50 mL of water was added to the solution and the product was extracted with ethyl ether. The solvent was dried with $MgSO_4$ and removed in vacuo. Column chromatography was performed with silica gel using 4 % CH_2Cl_2 in hexanes as an eluent. After evaporation of the solvent under reduced pressure, 0.032 g (82 %) of the product was obtained as a colorless oil. ^{1}H NMR ($CDCl_3$): δ 7.46 (m, 3 H), 7.35 (m, 5 H), 6.80 (d J = 3.8 Hz, 1 H), 6.25 (d J = 3.8 Hz, 1 H), 6.06 (s, 1 H) ppm. ^{13}C NMR ($CDCl_3$): δ 144.7, 141.3, 140.5, 138.9, 133.5, 132.9, 131.5, 130.7, 130.1, 129.5, 128.8, 128.4, 128.0, 127.9, 126.5, 112.4, 109.8, 109.7 ppm. HRMS calcd for $C_{20}H_{11}Br_3S_2$ $[M+Na]^+$: 574.7745. Found 574.7734.

2-(3'-[2,2',5',2"]terthiophene)-2'-(5-[2,2']bithiophene)-biphenyl (21) To a 50 mL Schlenk flask was placed 0.0323 g of **20**, 0.2 g of 2-thiophene boronic acid, 0.6 g of K_2CO_3, 20 mL of THF, 10 mL of ethanol and 5 mL of water. The solution was de-oxygenated by purging with Ar for 30 minutes. To the solution was added 0.040 g of Pd_2dba_3 and 0.020 g of HP(*tert*-Bu)$_3BF_4$ and the solution was heated at 60 °C for 26 hours. After heating, the organic layer was filtered through a short silica column with ethyl acetate as an eluent. The solvent was removed in vacuo. Column chromatography was performed with silica gel using 10 % CH_2Cl_2 in hexanes as an eluent. After evaporation of the solvent under reduced pressure, 0.054 g (68 %) of the product was obtained as a light yellow solid, m.p. 123-124.5 °C. ^{1}H NMR ($CDCl_3$): δ 7.45 (m, 3 H), 7.34 (m, 2 H), 7.18 (m, 1 H), 7.14 (dd J = 1.2, 3.5 Hz, 1 H), 7.07 (m, 2 H), 7.00 (m, 1 H), 6.93 (m, 3

H), 6.87 (dd J = 3.0, 5.0 Hz, 1 H), 6.85 (d J = 3.8 Hz, 1 H), 6.78 (dd J = 3.6, 5.0 Hz, 1 H), 6.74 (broad d J = 7.5 Hz, 1 H), 6.50 (dd J = 1.1, 3.0 Hz, 1 H), 6.31 (d J = 3.8 Hz, 1 H), 6.26 (s, 1 H) ppm. ^{13}C NMR ($CDCl_3$): δ 141.2, 137.3, 131.1$_6$, 131.1, 130.9, 127.8, 127.7, 127.4, 127.3, 127.1, 126.9, 125.6, 125.3, 124.3, 124.0, 123.9, 123.5, 123.4 ppm. HRMS calcd for $C_{32}H_{20}S_5$ $[M+H]^+$: 587.0061. Found 587.0057.

2,2'-bis(3-(5'-methyl-[2,2']bithiophene]))biphenyl (22) To a 25 mL Schlenk flask was added 0.105 g of **3**, 0.160 g of 5-methyl-2-thiopheneboronic acid, 1.0 g of K_2CO_3, 5 mL of THF, 1 mL of ethanol, and 0.5 mL of water. The solution was de-oxygenated by purging with Ar for 30 minutes. To the solution was added 0.060 g of Pd_2dba_3 and 0.020 g of $HP(tert\text{-}Bu)_3BF_4$, then the solution was stirred for 24 hours. The reaction mixture was filtered through silica gel with ethyl acetate as eluent. The solvents were removed in vacuo. Column chromatography was performed with silica gel using 10 % CH_2Cl_2 in hexanes as an eluent. After evaporation of the solvent under reduced pressure, 0.057 g (61 %) of the product was obtained as a white solid, mp 96.3-98.9 °C. ^1H NMR (CD_2Cl_2): δ 7.22 (m, 6 H), 7.06 (broad d J = 7.0 Hz, 2 H), 6.93 (d J = 5.1 Hz, 2 H), 6.55 (m, 2 H), 6.37 (m, 4 H), 2.42 (d *J* = 0.8 Hz, 6 H) ppm. ^{13}C NMR (CD_2Cl_2): δ 141.1, 140.5, 137.8, 135.6, 134.3, 133.7, 131.8, 131.6, 127.6, 127.3, 126.3, 125.8, 122.8, 15.5 ppm. HRMS calcd for $C_{30}H_{22}S_4$ $[M]^+$: 510.0599. Found 510.0590.

2, 2'-bis(3-(5,5'-dimethyl-[2,2']bithiophene))biphenyl (m-4) To a 25 mL Schlenk flaks was added 0.057 g of **22** which was dissolved in 10 mL of THF. The solution was cooled -78 °C and 0.15 mL of 2.2 M solution of n-butyl lithium was then added to the solution. The solution was stirred at -78 °C for 1.5 hours. To the solution was added 0.2 mL of MeI and the solution was stirred overnight. The solution was filtered through silica gel with ethyl acetate as an eluent and the solvent was removed in vacuo. Column chromatography was performed with 10 % CH_2Cl_2 in hexanes as an eluent. After evaporation of the solvent under reduced pressure, 0.026 g (43 %)

of the product was obtained as a white solid, mp 164.0-166.3 °C. ^{1}H NMR (CD_2Cl_2): δ 7.21 (m, 6 H), 7.00 (broad d J = 7.2 Hz, 2 H), 6.50 (m, 2 H), 6.25 (d J = 3.4 Hz, 2 H), 5.99 (s, 2 H) 2.40 (d J = 0.7 Hz, 6 H), 2.23 (s, 6 H) ppm. ^{13}C NMR (CD_2Cl_2): δ 141.2, 139.7, 137.6, 137.0, 135.8, 134.7, 131.8, 131.2, 131.1, 129.9, 127.5, 127.2, 125.7, 125.6, 15.5, 15.3 ppm. HRMS calcd for $C_{32}H_{26}S_4$ $[M]^+$: 538.0912. Found 538.0909.

2,2'-bis(3'-(5,5"-dimethyl-[2,2',5',2"]terthiophene])biphenyl (m-6) To a 50 mL Schlenk flask was added 0.094 g of **5**, 0.20 g of 5-methyl-2-thiopheneboronic acid, 2.0 g of K_2CO_3, 15 mL of THF, 3 mL of ethanol, and 1 mL of water. The solution was de-oxygenated by purging with Ar for 30 minutes then 0.055 g of Pd_2dba_3 and 0.020 g of HP(*tert*-Bu)$_3BF_4$ were added and the solution was heated to 55 °C for 48 hours. The reaction mixture was filtered through silica gel with ethyl acetate as an eluent. The solvents were removed in vacuo. Column chromatography was performed with silica gel using 10 % CH_2Cl_2 in hexanes as an eluent. After evaporation of the solvent under reduced pressure, the product was obtained as yellow crystals, 0.024 g (23 %), mp 214.1-216.0 °C. ^{1}H NMR (CD_2Cl_2): δ 7.27 (broad m, 6 H), 7.04 (broad m , 2 H), 6.73 (d J = 3.5 Hz, 2 H), 6.59 (dd J = 1.0, 2.5 Hz, 2 H), 6.44 (dd J = 1.1, 2.5 Hz, 2 H), 6.38 (s, 2 H), 6.25 (d J = 3.5 Hz, 2 H), 2.45 (s, 6 H), 2.36 (s, 6 H) ppm. ^{13}C NMR (CD_2Cl_2): δ 141.3, 140.3, 139.5, 137.9, 135.3, 135.2, 134.9, 133.9, 131.9, 131.6, 131.1, 127.8, 127.5, 127.3, 126.2$_1$, 126.1$_5$, 125.8, 123.5, 15.6, 15.4 ppm. HRMS calcd for $C_{40}H_{30}S_6$ $[M]^+$: 702.0666. Found 702.0646.

2,2'-bis (5-(5'-methyl-[2,2']bithiophene))biphenyl (m-9) To a 100 Schlenk flask was placed 0.248 g of **9** which was dissolved in 50 mL of THF. The solution was cooled -78 °C and 1 mL of 2.2 M solution of n-butyl lithium was then added to the solution. The solution was stirred at -78 °C for 1.5 hours. To the solution was added 1.4 mL of MeI was added and the solution was stirred overnight. The solution was filtered through silica gel with ethyl acetate. Solvent was

removed in vacuo. Column chromatography was performed with silica gel using 20 % CH_2Cl_2 in hexanes as an eluent. After evaporation of the solvent under reduced pressure, 0.154 g (59 %) of the product was obtained as a white solid, mp 172.5-173.4 °C. ^{1}H NMR (CD_2Cl_2): δ 7.48 (m, 2 H), 7.34 (m, 6 H), 6.79 (d J = 3.5 Hz, 2 H), 6.77 (d J = 3.5 Hz, 2 H), 6.61 (m, 2 H), 6.39 (d J = 3.5 Hz, 2 H), 2.44 (s, 6 H) ppm. ^{13}C NMR (CD_2Cl_2): δ 141.4, 139.8, 139.6, 138.4, 135.3, 134.0, 131.9, 129.6, 128.5, 128.0, 127.2, 126.3, 123.6, 123.2, 15.4 ppm. HRMS calcd for $C_{30}H_{22}S_4$ $[M]^+$: 510.0599. Found 510.0605.

2,2'-bis-(5'''-(5-methyl-[2,2',5',2"]terthiophene))biphenyl (m-11) To a 25 mL Schlenk flask was added 0.049 g of **10**, 0.040 g of 5-methyl-2-thiopheneboronic acid, 1.2 g of K_2CO_3, 5 mL of THF, 1 mL of ethanol, 0.5 mL of water. The solution was de-oxygenated by purging with Ar for 30 minutes then 0.020 g of Pd_2dba_3 and 0.010 g of HP(*tert*-Bu)$_3BF_4$ were added. The solution was heated at 50 °C for 12 hours. After stirring, the reaction mixture was filtered through silica gel with ethyl acetate. The solvents were removed in vacuo. Column chromatography was performed with silica gel using a gradient of 20 to 30 % CH_2Cl_2 in hexanes as an eluent. After evaporation of the solvent under reduced pressure, 0.0143 g (28 %) of the product was obtained as a yellow solid, mp 179.3-180.7 °C. ^{1}H NMR ($CDCl_3$): δ 7.41 (m, 8 H), 6.93 (m apparent d, 4 H), 6.88 (d J = 3.8 Hz, 2 H), 6.84 (d J = 3.8 Hz, 2 H), 6.66 (d J = 1.0, 3.8 Hz, 2 H), 6.33 (d J = 3.8 Hz, 2 H), 2.50 (s, 6 H) ppm. ^{13}C NMR ($CDCl_3$): δ 141.9, 139.6, 139.4, 137.8, 136.6, 135.8, 135.1, 133.7, 131.7, 129.6, 128.3, 128.0, 127.1, 126.2, 124.1, 123.7$_3$, 123.6$_8$, 15.6 ppm. HRMS calcd for $C_{38}H_{26}S_6$ $[M]^+$: 674.0353. Found 674.0381.

2-(3'-(5,5''-dimethyl[2,2',5',2"]terthiophene))-2'-(5-(5'-methyl-[2,2']bithiophene))-biphenyl (m-21) To a 50 mL Schlenk flask was placed 0.157 g of **20**, 0.5 g of 5-methyl-2-thiopheneboronic acid, 1.0 g of K_2CO_3, 20 mL of THF, 10 mL of ethanol and 5 mL of water. The solution was de-oxygenated by purging with Ar for 30 minutes. To the solution was added

0.060 g of Pd_2dba_3 and 0.030 g of HP(*tert*-Bu)$_3BF_4$ and the solution was heated at 60 °C for 20 hours. After heating, the organic layer was filtered through a short silica column with ethyl acetate as an eluent. The solvent was removed in vacuo. Column chromatography was performed with silica gel using 10 % CH_2Cl_2 in hexanes as an eluent. After evaporation of the solvent under reduced pressure, 0.110 g (66 %) of the product was obtained as a light yellow solid, mp 67-69 °C. ^{1}H NMR (CD_2Cl_2): δ 7.48 (m, 3 H), 7.33 (m, 2 H), 7.22 (m, 1 H), 7.06 (m, 1 H), 6.85 (broad d, 1 H), 6.79 (d *J* = 3.8 Hz, 1 H), 6.76 (m apparent broad d, 2 H), 6.63 (m, 1 H), 6.56 (m, 1 H), 6.47 (m, 1 H), 6.33 (d J = 3.5 Hz, 1 H), 6.28 (d J = 3.8 Hz, 1 H), 6.15 (s, 1 H), 2.48 (d J = 0.7 Hz, 3 H), 2.38 (d J = 0.5 Hz, 3 H), 2.37 (d = 0.5 Hz, 3 H) ppm. ^{13}C NMR (CD_2Cl_2): δ 142.4, 140.4, 139.6, 131.9, 131.8, 131.2, 129.1, 128.2, 127.7, 127.5, 127.2, 127.0, 126.3, 126.2, 125.8, 125.7, 123.7, 123.5, 123.4, 15.6, 15.5 (two carbons) ppm. HRMS calcd for $C_{35}H_{26}S_5$ $[M]^+$: 606.0633. Found 606.0635.

3'-phenyl-5, 5''-dimethyl-[2,2',5',2'']terthiophene (23) To a 100 mL Schlenk flask was added 0.5441 g of 2,5-dibromo3-phenylthiophene, 0.95 g of 5-methyl-2-thiophene boronic acid, 3.3 g of K_2CO_3, 20 mL of THF, 10 mL of ethanol, and 4 mL of water. The solution was de-oxygenated by purging with Ar for 30 minutes. To the solution was added 0.100 g of $PdCl_2(PPh_3)_2$ and the solution was heated at 60 °C for 24 hours. After stirring, the organic layer was filtered through a short silica column with ethyl acetate as an eluent. The solvent was removed in vacuo. Column chromatography was performed with silica gel using 10 % CH_2Cl_2 in hexanes as an eluent. After evaporation of the solvent under reduced pressure, 0.148 g (25 %) of the product was obtained as a yellow solid, mp 107.9-110.4 °C. ^{1}H NMR ($CDCl_3$): δ 7.40 (m, 5 H), 7.06 (s, 1 H), 7.01 (d *J* = 3.5 Hz, 1 H), 6.80 (d *J* = 3.5 Hz, 1 H), 6.70 (m, 1 H), 6.60 (m, 1 H), 2.52 (d J = 0.7 Hz, 3 H), 2.43 (d J = 0.8 Hz, 3 H) ppm. ^{13}C NMR ($CDCl_3$): δ 140.6,

139.6.6, 138.9, 136.5, 135.6, 134.8, 133.6, 130.5, 129.5, 128.6, 127.7, 126.5_3, 126.4_7, 126.3, 125.6, 123.9, 15.6, 15.5 ppm. HRMS calcd for $C_{20}H_{16}S_3$ $[M]^+$: 352.0409. Found 352.0403.

2-(3-theinyl)-biphenyl (24) To a 100 mL Schlenk flask was placed 0.4123 g of 2-iodo-biphenyl, 0.22 g of 3-thiophene boronic acid, 1.3 g of K_2CO_3, 30 mL of THF, 20 mL of ethanol and 10 mL of water. The solution was de-oxygenated by purging with Ar for 30 minutes. To the solution was added 0.060 g of $Pd_2(dba)_3$ and 0.030 g of HP(*tert*-Bu)$_3BF_4$ was added and the solution was heated to 60 °C for 16 hours. After heating, the organic layer was filtered through a short silica column with ethyl acetate as an eluent. The solvent was removed in vacuo. Column chromatography was performed with silica gel using 10 % CH_2Cl_2 in hexanes as an eluent. After evaporation of the solvent under reduced pressure, 0.306 g (85 %) of the product was obtained as a white solid, m.p. 64 °C. ^{1}H NMR ($CDCl_3$): δ 7.71 (m, 1 H), 7.59 (m, 3 H), 7.46 (m, 5 H), 7.27 (dd J = 3.0, 4.9 Hz, 1 H), 7.20 (m, 1 H), 6.94 (dd J = 1.2, 4.9 Hz, 1 H) ppm. ^{13}C NMR ($CDCl_3$): δ 142.1, 141.8, 140.7, 135.3, 130.8, 130.3, 129.7, 129.2, 128.2, 127.7, 127.6, 126.9, 124.7, 123.2 ppm. HRMS calcd for $C_{16}H_{12}S$ $[M]^+$: 236.0654. Found 236.0652.

2-3-(2,5-dibromotheinyl)-biphenyl (25) To a 100 mL round bottom flask was placed 0.304 g of **24**, 0.66 g of NBS and 30 mL of DMF and these reagents were stirred for 24 hours. After stirring, 50 mL of water was added to the solution and the product was extracted with ethyl ether. The solvent was dried with $MgSO_4$ and removed in vacuo. Column chromatography was performed with silica gel using 10 % CH_2Cl_2 in hexanes as an eluent. After evaporation of the solvent under reduced pressure, 0.417 g (82 %) of the product was obtained as a colorless oil. ^{1}H NMR (CD_2Cl_2): δ 7.57 (m, 2 H), 7.50 (m, 2 H), 7.38 (m, 3 H), 7.31 (m, 2 H), 6.69 (s, 1 H) ppm. ^{13}C NMR (CD_2Cl_2): δ 143.2, 142.2, 141.2, 133.2, 131.4, 130.9, 129.8, 129.3, 128.6, 127.8, 127.6, 110.9.4, 110.2 ppm. HRMS calcd for $C_{16}H_{10}Br_2S$ 391.8864. Found 391.8877.

2-(3'-(5, 5''-dimethyl[2,2',5',2"]terthiophene))-biphenyl (26) To a 100 mL Schlenk flask was placed 0.417 g of **25**, 0.6 g of 5-methyl-2-thiopheneboronic acid, 0.9 g of K_2CO_3, 30 mL of THF, 20 mL of ethanol, and 10 mL of water. The solution was de-oxygenated by purging with Ar for 30 minutes. To the solution was added 0.060 g of $Pd_2(dba)_3$ and 0.030 g of $HP(tert\text{-}Bu)_3BF_4$ was added and the solution was heated to 60 °C for 25 hours. The organic layer was filtered through a short silica column with ethyl acetate as an eluent. The solvent was removed in vacuo. Column chromatography was performed with silica gel using 10 % CH_2Cl_2 in hexanes as an eluent. After evaporation of the solvent under reduced pressure, 0.326 g (77 %) of the product was obtained as a white solid, m.p, 44 °C. ^1H NMR ($CDCl_3$): δ 7.50 (m, 4 H), 7.25 (m, 3 H), 7.20 (m, 2 H), 6.96 (d J =3.5 Hz, 1 H), 6.83 (s, 1 H), 6.71 (m, 1 H), 6.63 (d J = 3.5 Hz, 1 H), 6.57 (m, 1 H) 2.54 (s, 3 H), 2.49 (s, 3 H) ppm. ^{13}C NMR ($CDCl_3$): δ 142.5, 141.6, 140.7, 140.0, 138.4, 135.3, 134.9, 131.7, 130.8, 129.6, 128.2, 128.0, 127.4, 127.1, 126.6, 125.8, 124.0, 15.7, 15.5 ppm. HRMS calcd for $C_{26}H_{20}S_3$ 428.0722. Found 428.0735.

REFERENCES

[1] Electroactive Polymer Actuators as Artificial Muscles-Reality, Potential and Challenges; Bar -Cohen, Y., Ed.; SPIE Press: Bellingham, 2001.

[2] Madden, J. D. W.; Vandesteeg, N. A.; Anquetil, P. A.; Madden, P. G. A.; Takshi, A.; Pytel, R. Z.; Lafontaine, Wieringa, P. A.; Hunter, I. W. *J. Oceanic Eng.* **2004**, *29*, 706.

[3] Marsella, M. J. *Acc. Chem. Res.* **2002**, *35*, 944.

[4] Yu, H.-h.; Xu, B.; Swager, T. M. *J. Am. Chem. Soc.* **2003**, 125, 1142.

[5] (a) Miller, L. L.; Mann, K. R. *Acc. Chem. Res.* **1996**, *29*, 417. (b) Graf, D. D.; Campbell, J. P.; Miller, L. L.; Mann, K. R. *J. Am. Chem. Soc.* **1996**, *118*, 5480. (c) Graf, D. D.; Duan, R. G.; Campbell, J. P.; Miller, L. L.; Mann, K. R. *J. Am. Chem. Soc.* **1997**, *119*, 5888.

[6] Brocks, G. *J. Chem. Phys.* **2000**, *112*, 5353.

[7] Scherlis, D. A.; Marazri, N. *J. Am. Chem. Soc.* **2005**, 127, 3207.

[8] Grein, F. *J. Phys. Chem. A,* **2002**, 106, 3823.

[9] Baughman, R. H. *Synth. Met.* **1996**, 78, 339.

[10]Grienendal, L. B.; Jonas, F.; Feitag, D.; Pielartzik, H.; Reynolds, J. R. *Adv. Mater.* **2000**, 12, 481.

[11] Salhi, F.; Lee, B.; Metz, C.; Bottomly, L. A.; Collard, D. M. *Org. Lett.* **2002,** 4, 3195.

[12] (a) Kaikawa, T.; Takimiya, K.; Aso, Y.; Otsubo, T. *Org. Lett.* **2000**, *2*, 4197. (b)Sakai, T.; Satou, T.; Kaikawa, T.; Takimiya, K.; Otsubo, T.; Aso, Y. *J. Am. Chem. Soc.* **2005**, *127*, 8082. (c) Salhi, F.; Collard, D. M. *Adv. Mater.* **2003**, *15*, 81. (d) Mataka, S.; Shigaski, K.; Swada, T.; Mitoma, Y.; Taniguchi, M.; Thiemann, T.; Ohga, K.; Egashira, N. *Angew. Chem. Int. Ed.* **1998**, *37*, 2532. (e) Rathore, R.; Chebny, V. J.; Kopatz, E. J.; Guzei, I. A. *Angew. Chem. Int. Ed.* **2005**, *44*, 2771.

[13] Netherton, M.R.; Fu, G. C. *Org. Lett.* **2001**, 3, 4295.

[14] Becht, J-M.; Ngouela, S.; Wagner, A.; Mioskowski, C. *Tetrahedron*, **2004**, 60, 6853.

[15] Ofer, D.; Crooks, R. M.; Wrighton, M. S. *J. Am. Chem. Soc.* **1990**, *112*, 7869.

[16] (a) Zotti, G.; Schiavon, G. *Synth. Met.* **1990**, 39, 183. (b) Schiavon, G.; Sitran, S.; Zotti,G. *Synth. Met.* **1989**, 32, 209.

[17] Davidson, K.; Ponsonby, A. M. *Synth. Met.* **1999**, *102*, 1512.

[18] Roncali, J. *Chem. Rev.* **1992**, *92*, 711.

[19] Ni, J; Pei, J.; Chen, Z.-K.; Lai, Y.-H.; Huang, W. *Synth. Met.* **2002**, 126, 69.

[20] (a) Berlin, A.; Fontana, G.; Pagani, G.; Schiavon, G.; Zotti, G. *Synth. Met.* **1993**, 57, 4796. (b) Sato, T.; Hori, K.; Tanaka, K. *J. Mater. Chem.* **1998**, *8*, 589. (c) Jiang, X.; Harima, Y.; Zhu, L.; Kunugi, Y.; Yamashita, K.; Sakamoto, M.; Sato, M. *J. Mater. Chem.* **2001**, *11*, 3043.

[21] Kingsborough, R. P.; Swager, T. M. *J. Am. Chem. Soc.* **1999**, *121*, 8825.(

[22] Apperloo, J.J.; Groenendaal, L.; Verheyen, H.; Jayakannan, M.; Janssen, R. A.; Dkhissi, A.; Beljonne, D.; Lazzaroni, R.; Bredas, J. *Chem. Eur. J.* **2002**, 8, 2384.

[23] Kingsborough, R. P.; Swager, T. M. *Adv. Mater.* **1998**, 10, 1100.

[24] (a) Groenendaal, L.; Jonas, F.; Freitag, D.; Pielartzik, H.; Reynolds, J. R. *Adv. Mater.* **2000**, *12*, 481. (b) Roncali, J.; Blanchard, P.; Frere, P. *J. Mater. Chem.* **2005**, *15*, 1589.

[25] (a) Bauerle, P., *Adv. Mater.* **1992**, 4, 102. (b) Guay, J.; Kasai, P.; Diaz, A.; Wu, R.; Tour, J. M.; Dao, L. H. *Chem. Mater.* **1992**, 4, 1097. (c) Hill, M. G.; Mann, K. R.; Miller, L. L.; Penneau, J. *J. Am. Chem. Soc.* **1992**, 114, 2728.

[26] Nishida, J.; Miyagawa, T.; Yamashita, Y. *Org. Lett.* **2004**, 6, 2523

[27] Leroux, F.; Schlosser, M. *Angew. Chem. Int. Ed.* **2002**, *41*, 4272.

Chapter 3:

Synthesis of Polythiophene Derivatives Containing

Unsymmetrical 2,2'-Substituted Biphenyls

Introduction

In the design of the 2,2'-substituted biphenyl containing monomers in chapter 2, it was concluded that linkage of the biaryl to the β-position (3-position) of the thiophene would provide the optimum conducting polymer properties as shown in Scheme 1. The β-linked thiophene monomer will produce a fully π-conjugated polymer upon polymerization, while retaining the desired geometry for through space electronic interaction between the oligothiophene sections. Since these biphenyl monomers will have two potentially polymerizable oligothiophenes, the possibility exists that cross-linking will occur during the polymerization. Cross-linking is unwanted if soluble materials are desired since it will often produce intractable materials. [1] To avoid cross-

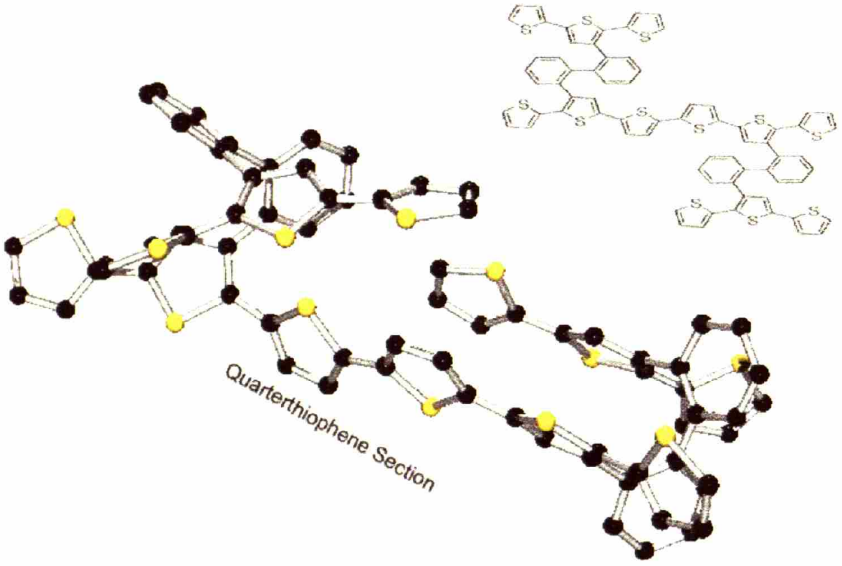

Scheme 1. Lowest energy conformer for the dimer of the β-linked terthiophene 2,2'-biphenyl compound (compound **6** from chapter 2) from a conformational analysis using Molecular Mechanics Force Field model.

linking, the terminal α-positions of one of the monomer's oligothiophene sections must be blocked. These partially blocked monomers provide synthetically accessible locations for the attachment of flexible alkyl chains or ethylene oxide chains into the monomers. Inclusion of flexible chains into the monomer units is a well known modification to render conjugated polymers soluble and hence processable.[2] In addition, soluble polymers can be synthesized by chemical polymerizations. Chemical polymerizations are more desirable given that electrochemical polymerizations require a concentrated electrolyte solution and large amounts of electrical energy to produce significant quantities of material.[3]

The α-substituted terthiophenes' stability to oxidation is a potential issue. There are many examples of α-substituted oligothiophenes that have stable oxidations in solution but the oligomers' oxidation stability in solid state is unclear.[4,5] There is also a concern about the stability of the oligothiopenes' oxidation in the polythiophene matrix in that the highly localized charges of the oxidized oligothiophene may react with the polythiophene strands.

Although avoiding cross-linking will produce processable polymers, cross-linking can be utilized to alter the properties of a polymer in valuable ways. The cross-linked conducting polymers have been used as polymer gels and may possess multi-dimensional or three dimensional conjugation pathways networks. [6,7,8] The conductivities of highly cross-linked polymers are often less than that of the non cross-linked analogues of the polymers.[9] However, the occasional cross-link in the polymer may produce an improvement in the bulk conductivity.[6c,7a] These results have been rationalized by invoking two competing mechanisms.[10] The decrease in the conductivity has been

attributed to cross-linking producing a decrease in the planarity between the monomer units, while the increase in the conductivity has been attributed to more conducting pathways provided by the cross-linking.

The Swager group has employed electrochemical cross-linking to produce unique macromolecular structures. A synthesis of a three-stranded conducting polymer was accomplished by utilizing a metallorotaxane as the scaffold for the polymerization.[11] This polymerization was accomplished with thiophene segments with different oxidation potentials. This difference in oxidation potential allowed the segments to be polymerized successively. The synthesis strategy for the unsymmetrical soluble biphenyl monomers can also be utilized to create an unsymmetrical biphenyl monomer containing two thiophene sections with different oxidization potentials. The nonplanar conformation of the biphenyl unit should prevent direct π-conjugation of the thiophene fragments and this break in the electronic communication should allow for a separate polymerization of each thiophene fragment as previously demonstrated using the metallorotaxane monomers. In contrast to the latter study, cross-linking will not lead to three stranded polymer but rather a network of polymer strands almost orthogonal to each other.

The effect of cross-linking on the polymer's actuation ability is not easily predicted. Slight cross-linking should improve the mechanically stability of electrochemically grown films. However, a highly cross-linked polymer should form a very rigid three-dimensional structure that will greatly reduce the actuation ability of the polymer.[1] These considerations suggest that a highly controlled method for cross-linking is required.

We report a synthetic strategy that demonstrates an effective method for the preparation of unsymmetrical 2,2'-substituted biphenyl polythiophene monomers. The chemical and electrochemical polymerizations of these monomers are described. In addition, the synthetic sequence was used for the synthesis of an electrochemically cross-linkable polymer. Both the unique structure and the controlled method for cross-linking should afford more information on how cross-linking affects a conducting polymer's conductive and actuating properties.

Results and Discussion

Synthesis

The synthesis of the monomers takes advantage of the inherent symmetry of the desired biphenyl monomers by dividing the biphenyl monomer into two phenyl groups, as shown in Scheme 2. All of the phenyl fragments were synthesized from either a selective Suzuki or Stille cross coupling reaction.[12] The Suzuki cross coupling reaction was found to be the best overall method to create the biphenyl unit from the two phenyl sections. For the necessary boronic ester, a modified Suzuki-Miyaura cross coupling with bis(pincalcolato)diboron was used.[13] The exchange of the Pd catalyst from $PdCl_2$(dppf) to $PdCl_2(PPh_3)_2$ was necessary in order to obtain useful yields. The subsequent Suzuki reaction to form the biphenyl linkage required extreme conditions, 100 °C in N, N'-dimethylformamide (DMF), but the monomers were produced in acceptable yields.

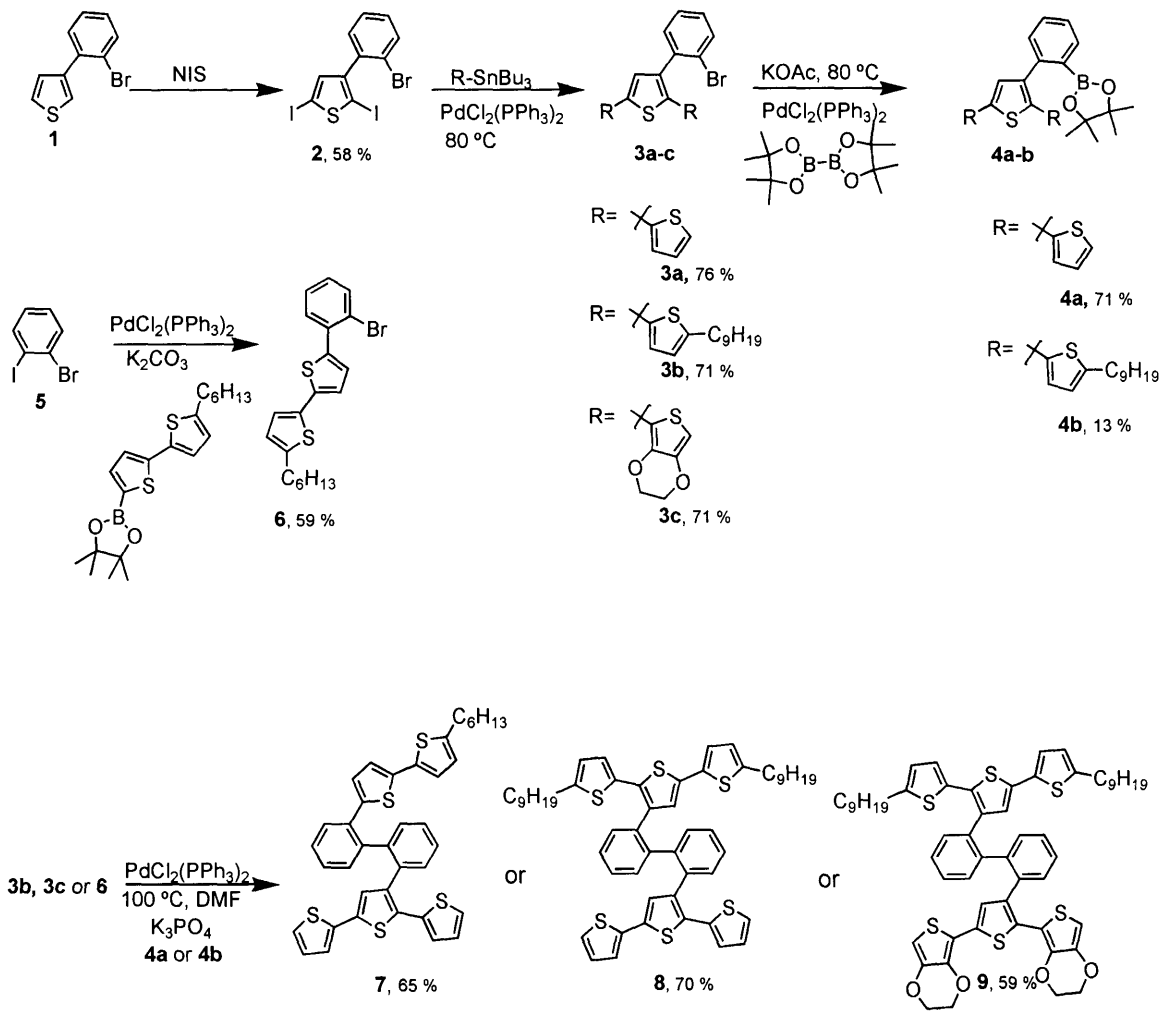

Scheme 2

The polymerization of the monomers by $FeCl_3$ in $HCCl_3$ resulted in only low molecular weight (<11000) polymers, Scheme 3.[14] Poor solubility of the high molecular weight polymers might account for this result. This explanation accounts for the low yields and the formation of a considerable amount of intractable material. Decomposition of the polymer under the relatively harsh reaction conditions is another possibility. Studies of the electrochemically polymerized polymers in the next section, *vide infra*, imply that this second explanation is the more likely.

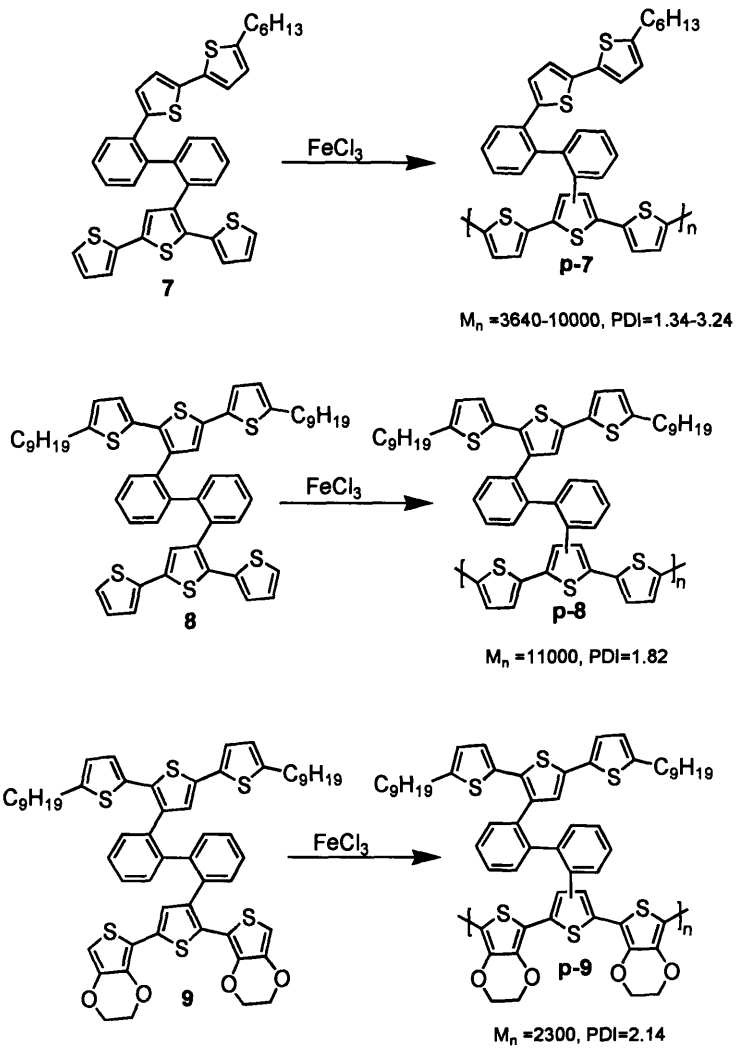

Scheme 3.

Electrochemistry

Since the initial chemical polymerizations did not provide high molecular weight polymers, electrochemical polymerization of these monomers was investigated.

Monomer **7** was polymerized with cyclic voltammetry (CV) sweeps from -0.10 to 0.90 V (vs. Fc/Fc^+) in an electrolyte solution of 0.1 M $(n\text{-}Bu)_4NPF_6$ in acetonitrile. The initial CV scan of **p-7** from -0.10 to 0.90 V had a very sharp peak oxidation (E_{pa}) at0.63 V, as shown in Figure 1. The CV of **p-7** was very sensitive to the potential window of

the CV experiment. Increasing the potential window any amount beyond 0.9 V lead to a loss of the E_{pa} at 0.63 V.

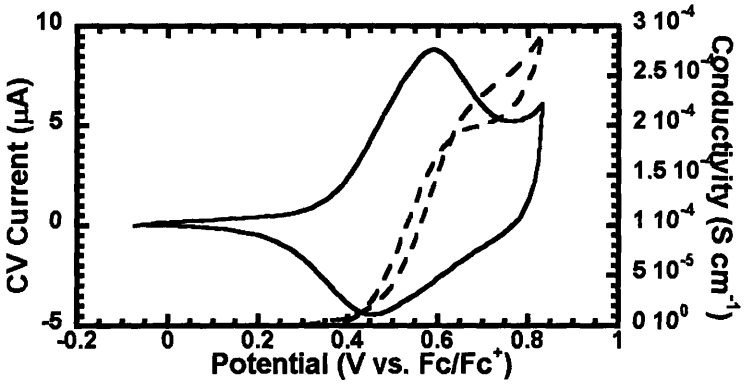

Figure 1. Cyclic voltammetry (solid line) and *in situ* conductivity (dashed line) of **p-7** from -0.10 to 0.90 V. A scan rate of 10 mV/s and a 40 mV offset potential between the interdigitated working electrodes (5 μm spacing between electrodes) were utilized for all the *in situ* conductivity measurements. The electrolyte solution was 0.1 M $(n\text{-}Bu)_4NPF_6$ in acetonitrile.

The *in situ* conductivity displayed an on set of conductivity nearly coincident with the E_{pa}. The *in situ* conductivity was unusual in that it did not display the expected plateau of fully π-conjugated polymers but instead the conductivity increased until the end of the potential window being scanned.[15]

As the potential window was extended to higher potential, the stability of **p-7** decreased significantly (Figure 2). CV scans from -0.1 to 1.3 V displayed a large E_{pa} at approximately 1.2 V, however this E_{pa} was lost with successive scans. The subsequent CV scans show a progressive decrease in electroactivity over all anodic processes. At higher potential, we propose that the non-polymerizable oligothiophene sections of the monomers, which for **p-7** is a bithiophene, undergo irreversible oxidation. As indicated

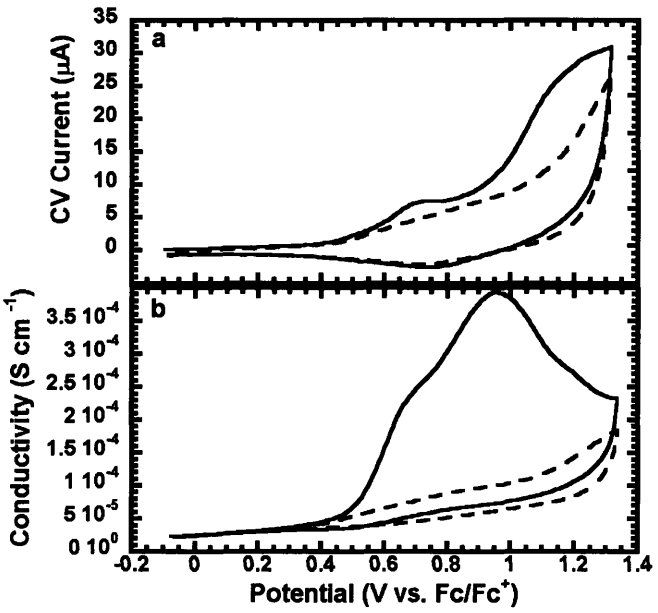

Figure 2. (a) Cyclic voltammetry of **p-7** from -0.10 to 1.30 V; scan 1 (solid line) and scan 2 (dashed line). (b) *In situ* conductivity of **p-7** from -0.10 to 1.30 V; scan 1 (solid line) and scan 2 (dashed line).

in the introduction, short oligothiophenes, such as these, are known to decompose in the oxidation. In accord with conclusion, the *in situ* conductivity gave results similar to the CV results, wherein the first scan displayed a significant peak in conductivity, but later scans displayed reduced conductivity. Therefore it can be concluded **p-7** decomposes at higher potentials to produce a less conducting material material.

Monomer **8** was polymerized at CV sweeps from -0.10 to 0.90 V. Both the CV and the *in situ* conductivity of **p-8** displayed better stability than **p-7**, with a broad E_{pa} at 0.67 V, as shown in Figure 3.

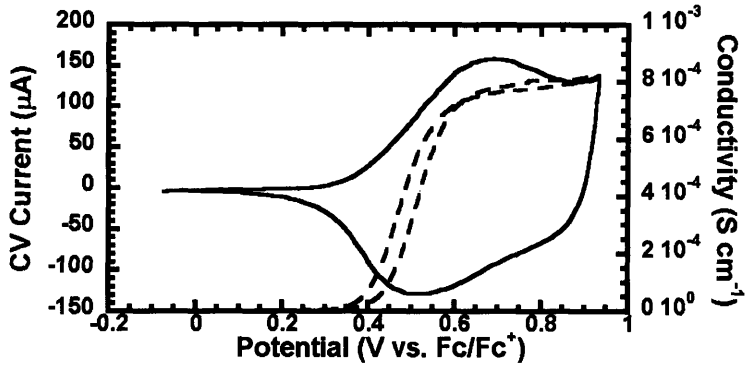

Figure 3. Cyclic voltammetry (solid line) and *in situ* conductivity (dashed line) of **p-8** from -0.10 to 0.90 V. The same *in situ* conductivity conditions for **p-7** were used for **p-8**.

The on set for *in situ* conductivity of **p-8** occurred at a potential before the E_{pa}. The *in situ* conductivity did plateau at higher potentials as expected of fully π-conjugated materials. This result suggests that there was more charge delocalization in **p-8** in comparison to **p-7**.

As the higher point in the potential window of the CV experiments was increased to 1.3 V, the CV of **p-8** showed a loss of electroactivity consistent with degradation resulting from an irreversible oxidation (Figure 4). Unlike **p-7**, however, the CV profile **p-8** did reach a quasi-stable state after successive CV scans and a certain amount of electroactivity near the lower E_{pa} did remain. The *in situ* conductivity profile of **p-8** did change significantly with the increase in the potential window of the experiment. At the higher potentials, the *in situ* conductivity displayed a very large reduction in conductivity

in the reverse sweep of measurement. A reduction in the overall bulk conductivity was observed with each successive scan as well. Overall, these results suggested that **p-8** was more stable than **p-7** but still degrades at higher potentials. Although the exact cause of the small difference in stability between **p-7** and **p-8** at higher potentials can not be determined from these experiments, it is likely due to the different non-polymerizable thiophene sections attached to the biphenyl unit.

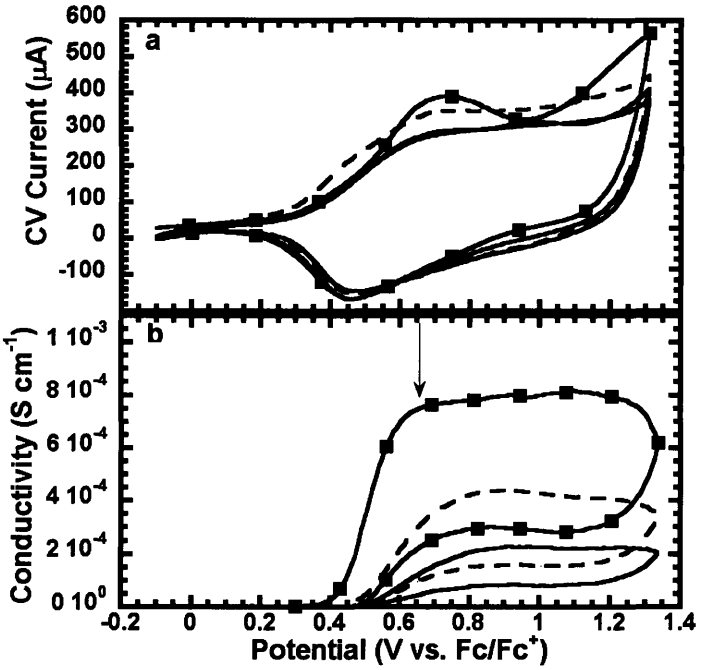

Figure 4. (a) Cyclic voltammetry of **p-8** from -0.10 to 1.30 V; scan 1 (■), scan 2 (dashed line) and scans 3-4 (solid lines). (b) *In situ* conductivity of **p-8** from -0.10 to 1.30 V; scan 1 (■), scan 2 (dashed line) and scan 3 (solid line).

Monomer **9** did not effectively polymerize under cyclic voltammetry treatment. The monomer was best polymerized using a potentiostatic method. The potential was kept at 0.4 V for a period from 100 s then the potential was decreased to -0.60 V for a period of 30 s. This process was repeated for 20 cycles. The electrolyte solution was 0.1

M $(n\text{-}Bu)_4NPF_6$ in 1:1 of mixture of CH_2Cl_2 and acetonitrile. The polymer resulting from this process had a CV and an *in situ* conductivity shown in Figure 5. Over the potential region of -0.6 V to 0.4 V, the stability of **p-9** was similar to that of **p-8**. The

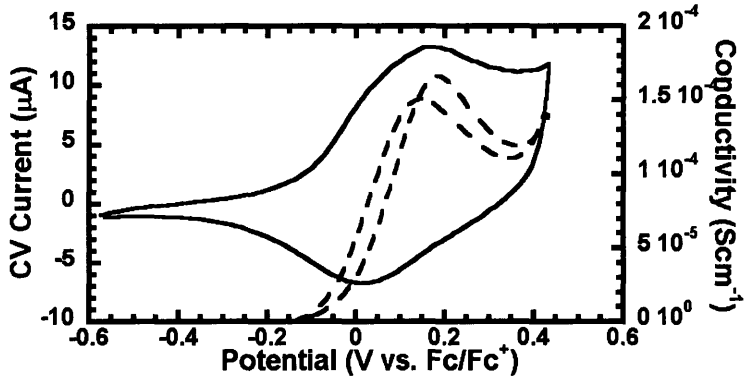

Figure 5. Cyclic voltammetry (solid line) and *in situ* conductivity (dashed line) of **p-9** from -0.60 to 0.40 V. The same *in situ* conductivity conditions for **p-7** were used for **p-9**.

first E_{pa} (0.12 V) of **p-9** occurred in a much lower potential region than **p-8** as expected by the substitution of 3,4-ethylenedioxythiophene (EDOT) groups into the polymerizable oligothiophene section of the monomer.[16] The *in situ* conductivity displayed an on set of conductivity coincident with the E_{pa} in the CV of **p-9**. The conductivity decreased significantly as the gate potential went past the potential of the E_{pa}. The small potential region of high conductivity implies that **p-9** is not as charge delocalized as **p-8**.

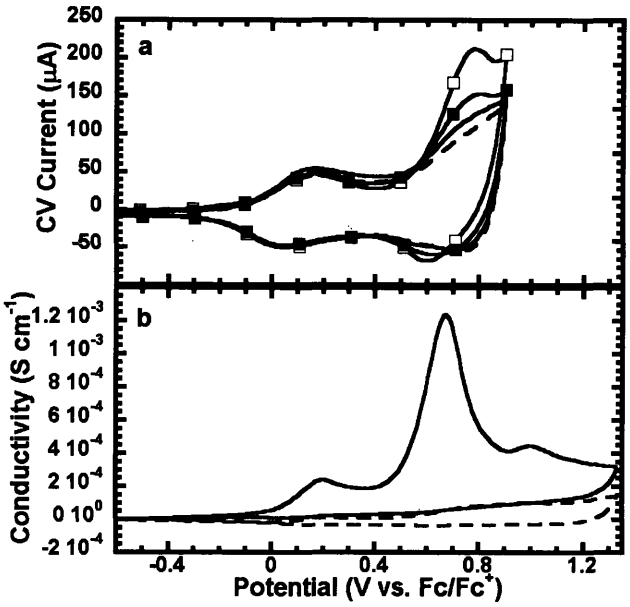

Figure 6. (a) Cyclic voltammetry of **p-9** from -0.60 to 0.90 V; scan 1 (■), scan 2 (dashed line) and scans 3 (solid line) and scan 4 (□). (b) *In situ* conductivity of **p-9** from -0.1 to 1.3 V: scan 1 (solid line) and scan 2 (dashed line).

Increasing the potential window (-0.60 to 0.90 V) revealed the typical second E_{pa} at approximately 0.78 V. As shown in Figure 6, the film of **p-9** showed the same instability that **p-7** and **p-8** displayed, however unlike **p-7** and **p-8,** the current of lower E_{pa} decreased only slightly. In this potential window, the *in situ* conductivity profile of **p-9** reveals a loss of structure and magnitude indicating degradation. .

Overall, the electrochemical results indicate that polymers, **p-7**, **p-8** and **p-9** are unstable at relatively high electrochemical potentials. These results confirmed that the oxidations of the nonpolymerized oligothiophene groups give detrimental degradation in either in the solid state or the polythiophene matrix. Since $FeCl_3$ has a relatively high

oxidation potential, ~1.1 V, this effect is a likely reason for the low molecular weights in the chemical polymerizations.[17]

Electrochemical Cross-Linking

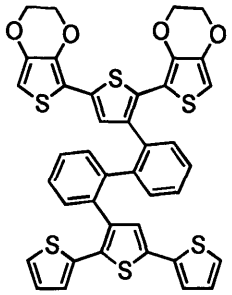

10

Scheme 4.

Monomer **10,** as shown in Scheme 10, was synthesized to explore the cross-linking affects in 2,2' biphenyl modified polythiophenes. This monomer contains two different oligothiophene sections, an EDOT containing section and a pure oligothiophene section. The EDOT based section will polymerize at a lower potentials then the thiophene based section, thereby allowing for the selective polymerization of the EDOT section.

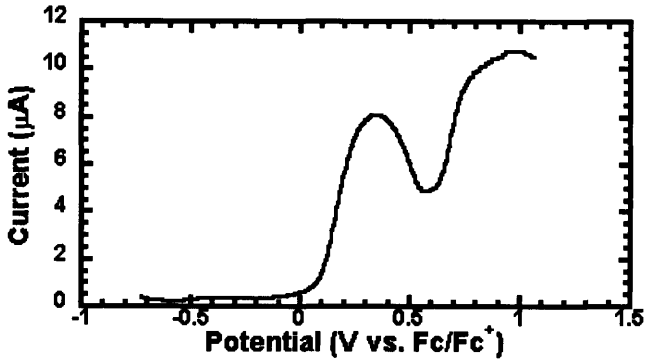

Figure 7. Square wave voltammetry of **10** at a scan rate of 0.148 V/s with a step potential of 0.005 V, amplitude of 0.025 V and a frequency of 30 Hz with 0.1 M $(n\text{-}Bu)_4NPF_6$ in CH_2Cl_2 as the electrolyte solution.

The viability of a sequential polymerization of the thiophene units in **10** was confirmed by the square wave voltammetry of the monomer, as shown in Figure 7, which clearly demonstrates two oxidations separated by approximately 0.6 V. Due to solubility issues, all the electrochemical operations were performed in 0.1 M $(n\text{-}Bu)_4NPF_6$ solution in CH_2Cl_2. Like monomer **9**, the EDOT section of **10** did not polymerize using CV

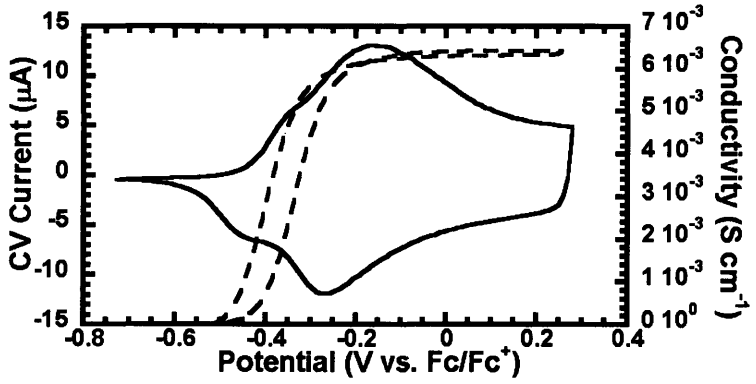

Figure 8. Cyclic voltammetry (solid line) and *in situ* conductivity (dashed line) of **lpp-10** from -0.70 to 0.30 V with 0.1 M $(n\text{-}Bu)_4NPF_6$ in CH_2Cl_2 as the electrolyte solution. The same *in situ* conductivity conditions for **p-7** were utilized.

conditions and a potentiostatic method was employed. The polymer that resulted from this deposition (low potential polymerization of **10**: **lpp-10**) had a CV profile with a half wave potential ($E_{1/2}$) at -0.21 V, as shown in Figure 8. The $E_{1/2}$ of the wave in **lpp-10**'s CV was at lower in potential than the $E_{1/2}$ of the wave in the CV of **p-9** (0.02 V). This fact is unusual since **p-9** should have very similar electroactivity to **lpp-10**. Also unlike **p-9**, **lpp-10**, had the *in situ* conductivity profile with an on set of conductivity near -0.4 V, and a large region of high conductivity which is typical of a fully π-conjugated polymer.

An irreversible wave with an E_{pa} at 0.77 V was discovered when the potential window of the CV was increased to -0.70 to 0.90 V, as shown in Figure 9. This

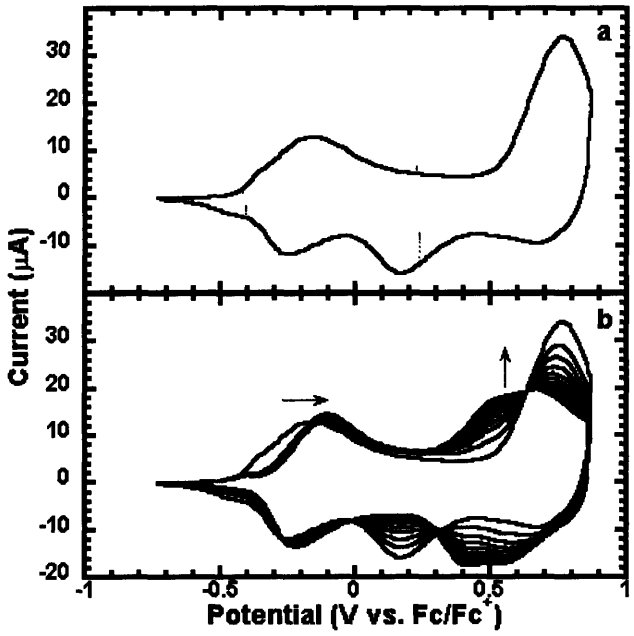

Figure 9. (a) Initial cyclic voltammetry (solid line) of **lpp-10** from -0.70 to 0.90 V. (b) Successive cyclic voltammetry scans of **lpp-10** to give **clp-10**. The polymer film is on an interdigitated 5 μm Pt microelectrodes with 0.1 M $(n\text{-}Bu)_4NPF_6$ in CH_2Cl_2 as the electrolyte solution.

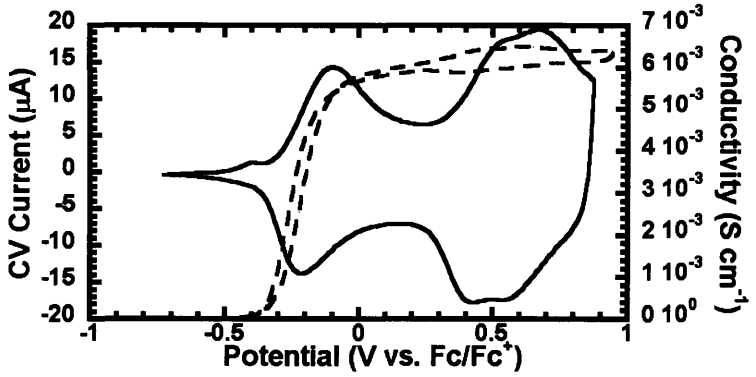

Figure 10. Cyclic voltammetry (solid line) and *in situ* conductivity (dashed line) of **clp-10** from -0.70 to 0.90 V in a CH_2Cl_2 solution of 0.1 M $(n\text{-}Bu)_4NPF_6$.

irreversible wave was attributed to the coupling of unreacted terthiophene section of the monomer. It was assumed that this section will oxidize then react with successive CV cycling at these potentials. Repeated CV scans of the polymer film produced the growth of new waves ($E_{1/2}$'s = 0.44, 0.61 V, Figure 10) that were consistent with the polymeric sections formed from the coupling of the terthiophene fragments. This process will change the previous linear polymer, **lpp-10**, to a fully cross-linked polymer, **clp-10**. The *in situ* conductivity profile of the **clp-10** did not change significantly from **lpp-10**'s profile, with only a small drop in the bulk conductivity.

The most noticeable change from **lpp-10** to **clp-10** is a shift to higher potential for the $E_{1/2}$'s of lower wave, as shown in Figure 11. There is a concurrent potential shift in the onset of conductivities. These results imply that the cross-linking increases the energy needed to oxidize the polymer and this effect may be due to the increased mechanical rigidity of **clp-10**. Since the oxidation process requires the inclusion of counterions into the polymer matrix, the decreased flexibility of the fully cross-linked can decrease the ability of the counterions to stabilize the charge on the polymer.

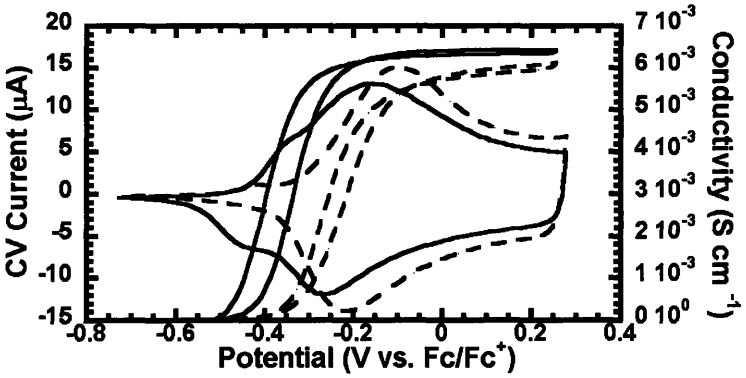

Figure 11. Cyclic voltammogram and *in situ* conductivity (solid lines) of **lpp-10** and cyclic voltammogram *in situ* conductivity (dashed lines) of **clp-10** from -0.70 to 0.30 V in a CH_2Cl_2 solution of 0.1 M $(n\text{-}Bu)_4NPF_6$.

Spectroelectrochemistry

UV-vis spectroelectrochemistry provided more information for the effect of cross-linking on the polymer. The UV-vis absorbance and response to potential changes from -0.7 to 0.3 V for **lpp-10** are displayed in Figure 12. The neutral form of **lpp-10** had two λ_{max}'s at 549 and 358 nm. The absorbance at 549 nm was assigned to the polymerized

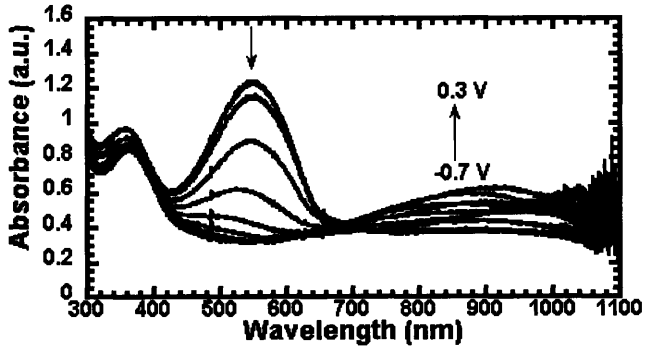

Figure 12. Spectroelectrochemistry of **lpp-10** grown onto ITO with potential changes from -0.7 to 0.3 V at 0.1 V intervals

EDOT[18] and, the absorbance at 358 nm was assigned as the unpolymerized terthiophene sections of the monomers.[12] Oxidation caused the peak at 549 nm to reduce in intensity and a new broad wave centered at 875 nm appeared. The peak at 358 nm was unaffected when the potential did not exceed 0.3 V. The same film was then subjected to CV scans from -0.7 to 0.9 V and the neutral UV-vis spectrum was recorded after each scan, as shown in Figure 13. The absorbance at 549 nm broadens with each CV scan and the peak at 358 nm is gone after two scans. The loss of the peak at 358 nm is consistent with the expected coupling of the terthiophene sections to give a cross-linked network.

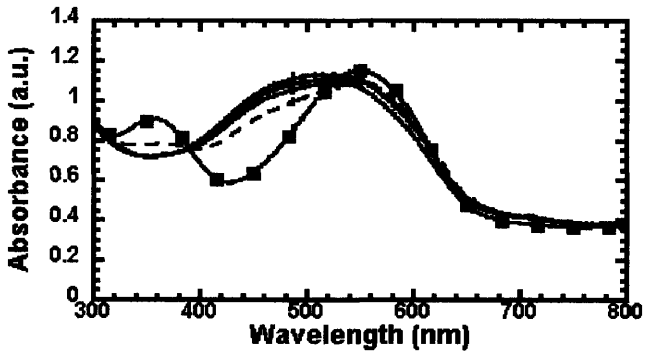

Figure 13. The initial UV-vis spectrum of **lpp-10** before cross-linking (■), the UV-vis spectrum after the first CV scan (dashed line) and the UV-vis spectrum after the CV scans 2-5 (solid lines) in the process of converting **lpp-10** to **clp-10**.

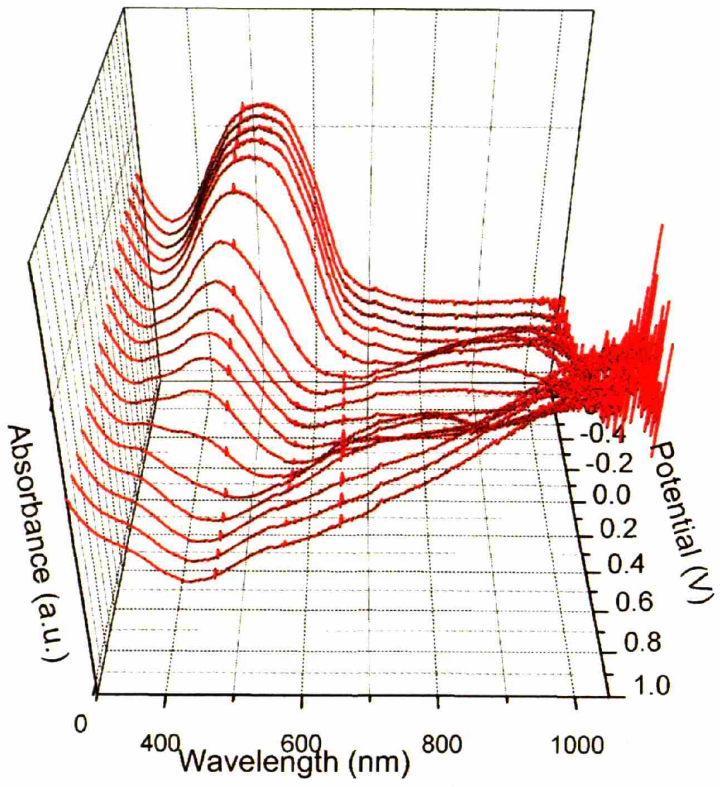

Figure 14. Spectroelectrochemistry of **clp-10** grown onto ITO with changes in potential from -0.7 to 1.0 V at 0.1 V intervals.

Due to the separation of the polymer strands by the biphenyl unit, the spectroelectrochemistry of **clp-10** behaved as two different polymers. At potentials near the first wave (-0.70 to 0.30 V), the real edge (EDOT segments) of the neutral absorbance decreased in intensity, as shown in Figure 14. The remaining absorbance displays a λ_{max} near 460 nm which close to the typical absorbance of polythiophene derivatives.[19] This remaining absorbance decreased in intensity as the potential cell approached the electrochemical potentials of **clp-10**'s second wave, 0.3 to 1.0 V. Overall, the spectroelectrochemistry confirmed the CV data that the EDOT section of monomer **10**

could be selectively polymerized and the terthiophene section could be used to electrochemically cross-link the resulting polymer in a controlled fashion. This process could be used in the future to optimize the effect of a cross-linked conducting polymer actuators.

Conclusions

A modular synthetic strategy was utilized to produce a variety of 2,2'-biphenyl substituted thiophene monomers including a set of monomers that were precursors for soluble polymers. The polymers that resulted from these monomers had low M_n's. Electrochemistry of the monomers suggested that the polymers were not stable to the high oxidation potential of $FeCl_3$. The synthetic strategy for the unsymmetrical monomers was also utilized to produce a monomer that could be selectively cross-linked via electrochemical oxidation. This electrochemical method may provide a controlled way to cross-link conducting polymers.

Experimental

General Comments ^1H and ^{13}C NMR spectra were recorded on a Bruker 400 MHz spectrometer and are referenced to residual $CHCl_3$ (7.27 ppm for ^1H and 77.23 ppm for ^{13}C) or $CHDCl_2$ (5.32 ppm for ^1H and 54.00 ppm for ^{13}C). Melting points are uncorrected. High-resolution mass spectra (HRMS) on a Bruker Daltonics APEX II 3 Tesla FT-ICR-MS. The 2-tributylstannyl-3,4-ethylenedioxythiophene, 2-tributyl stannyl-5-nonylthiophene and compound **1** was synthesized according to literature procedures.[20,21,22] Commercially available reagents were purchased from Aldrich. The solvents were dried using a SPS-400-5 solvent purification system (Innovative Technologies). Manipulations of air sensitive materials were performed using standard

Schlenk techniques. The GPC analysis was performed using a PLgel 5 μm Mixed -C column (300 x 7.5 mm) and a diode detector at 254 nm with a flow rate of 1 mL/min. in THF. The molecular weights were reported relative to polystyrene standards purchased from Polysciences Inc.

Electrochemistry Electrochemical measurements with an Autolab II with PGSTAT 30 potentiostat (Eco Chemie) were performed in a nitrogen glovebox or in air for the spectroelectrochemistry measurements. The electrolyte solution for all the electrochemical measurements was 0.1 M $(n\text{-}Bu)_4NPF_6$ in dry CH_2Cl_2 or acetonitrile which was prepared and stored over 4 Å molecular sieves in a glovebox. The quasi-internal reference electrode was a Ag wire submersed in 0.01 M $AgNO_3$/ 0.1 M $(n\text{-}Bu)_4NPF_6$ in anhydrous acetonitrile and a Pt wire or gauze was used as a counter electrode. All potentials were referenced to the Fc/Fc^+ couple. The working electrodes were 5 μm Pt interdigitated microelectrodes (Abtech Scientific, Inc.), or indium tin oxide coated unpolished float glass slides (Delta Technologies). Absorption spectra were collected on an Agilent 8453 diode array spectrophotometer. A Dektak 6M stylus profiler (Veeco) was used to measure the film thickness of the polymers grown onto interdigitated microelectrodes.

3-(2-bromophenyl)-2,5-diodothiophene (2) To a 250 mL round bottom flask was placed 8.62 g of **1**, 23.2 g of N-iodosuccimide, 50 mL of $HCCl_3$ and 50 mL of glacial acetic acid. This solution was stirred for 24 hours. After stirring, 100 mL of water was added to the mixture and CH_2Cl_2 was used to extract the product. The organic layer was washed 2 x 100 mL of 2 M KOH and then dried with $MgSO_4$. The organic layer was concentrated on a rotovap. Silica column chromatography was performed on the residue

using hexanes as an eluent. The solvent was removed in vacuo to give 10.3 g (58 %) of **2** as a brown oil. ^{1}H NMR (CD_2Cl_2): δ 7.73 (dd J = 1.1, 8.0 Hz, 1 H), 7.44 (m, 1 H), 7.33 (dd J = 1.1, 7.3, 1H), 7.29 (dd J =1.3, 7.3, 1 H), 7.12 (s, 1 H) ppm. ^{13}C NMR (CD_2Cl_2): δ 149.4, 139.3, 137.2, 133.4, 132.2, 130.5, 127.9, 123.9, 80.3, 76.8 ppm. HRMS calcd for $C_{10}H_5BrI_2S$ $[M]^+$: 489.7379. Found 489.7371.

3'-(2-bromophenyl)-[2,2',5',2"]terthiophene (3a) To a 100 mL Schlenk flask was added 0.748 g of **2**, 1.42 g of 2-tributylstannylthiophene, and 50 mL of N,N-dimethylformamide (DMF). This solution was purged with Ar for 30 minutes. To the solution was added 0.0860 g of $PdCl_2(PPh_3)_2$ was added to the solution. This solution was heated to 80 °C for 12 hours. After stirring, 50 mL of an aqueous 15 % KF solution was added to the mixture. The product was extracted with CH_2Cl_2 and the organic layer was dried with $MgSO_4$. The organic layer was concentrated by evaporation of the solvent reduced pressure. Silica column chromatography was performed on the residue with a solution of 10 % CH_2Cl_2 in hexanes as an eluent. The solvent was removed in vacuo to give 0.470 g (76 %) of **3a** as a yellow oil. ^{1}H NMR (CD_2Cl_2): δ 7.78 (d J = 7.8 Hz, 1 H), 7.43 (m, 2 H), 7.34 (m, 3 H), 7.21 (dd J = 5.1, 1.1 Hz, 1 H), 7.16 (s, 1 H), 7.12 (dd J = 4.7, 3.7 Hz 1 H), 7.07 (dd J = 4.7, 1.0 Hz, 1 H) 6.98 (dd J = 4.5, 3.7 Hz, 1 H) ppm. ^{13}C NMR (CD_2Cl_2): δ 138.2, 137.8, 137.2, 136.1, 135.2, 133.5, 133.0, 132.5, 130.4, 128.6, 128.2, 127.7, 127.3, 126.3, 126.0, 125.4, 125.0, 124.6 ppm. HRMS calcd for $C_{18}H_{11}BrS_3$ $[M]^+$: 403.9201. Found 403.9202.

3'-(2-bromophenyl)-5,5''-dinonyl-[2,2',5',2"]terthiophene (3b) To a 50 mL Schlenk flask was added 0.291 g of **2**, 0.90 g of 2-tribuylstannyl-5-nonylthiophene, and 25 mL of DMF. This solution was purged with Ar for 30 minutes. To the solution was

added 0.080 g of $PdCl_2(PPh_3)_2$ was added to the solution. This solution was heated to 80 °C for 12 hours. After stirring, 50 mL of an aqueous 15 % KF solution was added to the mixture. The product was extracted with CH_2Cl_2 and the organic layer was dried with $MgSO_4$. The organic layer was concentrated on a rotovap. Silica column chromatography was performed on the residue using a mixture of 4 % CH_2Cl_2 in hexanes. The solvent was removed in vacuo to give 0.301 g (77 %) of **3b** as a yellow oil. ^1H NMR (CD_2Cl_2): δ 7.77 (d, J = 7.2 Hz, 1 H), 7.39 (m, 3 H), 7.10 (d J = 3.6 Hz, 1 H), 7.03 (s, 1 H), 6.81 (d J = 3.1 Hz, 1 H), 6.64 (d J = 3.6 Hz, 1 H), 2.88 (t J= 7.8 Hz, 2 H), 2.74 (t J = 7.6 Hz, 2 H) 1.77 (apparent quintet, 2 H), 1.65 (apparent quintet, 2 H), 1.37 (m, 24 H), 0.99 (t, J = 7.0 Hz, 6 H) ppm. ^{13}C NMR (CD_2Cl_2): δ 147.1, 146.4, 138.1, 137.4, 135.2, 134.7, 133.6, 133.5, 132.9, 132.6, 130.3, 128.2, 126.6, 125.7, 125.6, 125.1, 124.8, 124.1, 32.6, 32.3, 32.1, 30.8, 30.6, 30.2_4, 30.2_2, 30.1, 29.8, 29.7, 23.4, 14.6 ppm. HRMS calcd for $C_{36}H_{17}BrS_3$ $[M]^+$: 654.2018. Found 654.2020.

3-(2-bromophenyl)-2,5-bis-(3,4-ethylenedioxy thiophene)thiophene (3c) To a 100 mL Schlenk flask was added 0.517 g of **2**, 1.01 g of 2-tribuylstannyl-3,4-ethylenedioxythiophene, and 50 mL of DMF. This solution was purged with Ar for 30 minutes. To the solution was added 0.107 g of $PdCl_2(PPh_3)_2$. This solution was heated to 80 °C for 12 hours. After stirring, 50 mL of an aqueous 15 % KF solution was added to the mixture. The product was extracted with CH_2Cl_2 and the organic layer was dried with $MgSO_4$. The organic layer was concentrated by evaporation of the solvent reduced pressure. Silica column chromatography was performed on the residue using a mixture of 1:1 ethyl acetate to hexanes as an eluent. The solvent was removed in vacuo to give 0.283 g (52 %) of **3c** as a yellow solid, m.p. = 86-88 °C. ^1H NMR (CD_2Cl_2): δ 7.73 (dd *J*

= 1.0 Hz, 7.9 Hz, 1 H), 7.38 (m, 3 H), 7.15 (s, 1 H), 6.29 (s, 1 H), 6.17 (s, 1 H), 4.37 (m, 2 H), 4.27 (m, 4 H) 4.21 (m, 2 H) ppm. ^{13}C NMR (CD_2Cl_2): δ 142.6, 141.8, 138.7, 138.5, 138.2, 137.2, 133.3, 133.2, 132.8, 130.3, 129.3, 128.0, 125.5, 125.3, 112.1, 111.3, 99.3, 97.5 65.7, 65.6, 65.2, 65.0 ppm. HRMS calcd for $C_{22}H_{15}BrO_4S_3$ $[M]^+$: 517.9310. Found 517.9291.

3'-(2-(4,4,5,5-tetramethyl-dioxaborane)phenyl)-[2,2',5',2"]terthiophene (4a) To a 100 mL Schlenk flask was added 0.321 g of **3a**, 0.41 g of bis(pinacolato) diboron, 0.45 g of potassium acetate, and 50 mL of dimethylsulfoxide (DMSO). This solution was purged with Ar for 30 minutes. To the solution was added 0.100 g of $PdCl_2(PPh_3)_2$. This solution was heated to 80 °C for 24 hours. After stirring, 50 mL of a brine solution was added to the mixture. The product was extracted with CH_2Cl_2 and the organic layer was dried with $MgSO_4$. The organic layer was concentrated by evaporation of the solvent reduced pressure. Silica column chromatography was performed on the residue using a gradient of 10 % to 50 % CH_2Cl_2 in hexanes as an eluent. The solvent was removed in vacuo to give 0.256 g (71 %) of **4a** as a yellow oil. ^1H NMR (CD_2Cl_2): δ 7.86 (d J = 7.3 Hz, 1 H), 7.52 (m, 1 H), 7.47 (d J = 7.3 Hz, 1 H), 7.38 (d J = 5.0 Hz, 1 H), 7.29 (m, 2 H), 7.14 (dd J = 1.2, 5.0 Hz, 1 H), 7.10 (m, 2 H), 6.97 (d, J = 3.5 Hz, 1 H), 6.92 (dd J = 3.6, 5.0 Hz, 1 H), 1.18 (s, 12 H) ppm. ^{13}C NMR (CD_2Cl_2): δ 142.4, 141.1, 137.7, 136.9, 135.6, 133.9, 131.8, 131.1, 130.5, 128.9, 128.5, 127.8, 127.5, 125.8, 125.6, 125.0, 124.0, 84.0, 25.0 ppm. HRMS calcd for $C_{24}H_{24}BO_2S_3$ $[M+H]^+$: 451.1039. Found 451.1035.

3'-(2-(4,4,5,5-tetramethyl-dioxaborane)phenyl)-5,5''-dinonyl-[2,2',5',2"]terthiophene (4b) To a 100 mL Schlenk flask was added 1.22 g of **3b**, 0.90 g of bis(pinacolato) diboron, 0.89 g of potassium acetate, and 50 mL of DMSO. This

solution was purged with Ar for 30 minutes. To this solution was added 0.100 g of $PdCl_2(PPh_3)_2$. The solution was heated to 80 °C for 16 hours. After stirring, 50 mL of a brine solution was added to the mixture. The product was extracted with CH_2Cl_2 and the organic layer was dried with $MgSO_4$. The organic layer was concentrated by evaporation of the solvent reduced pressure. Silica column chromatography was performed on the residue using a gradient of 10 % to 50 % CH_2Cl_2 in hexanes as an eluent. The solvent was removed in vacuo to give 0.166 g (13 %) of **4b** as a yellow oil. ^{1}H NMR (CD_2Cl_2): δ 7.85 (d J = 7.3 Hz, 1 H), 7.51 (m, 1 H), 7.41 (m, 2 H), 7.05 (d J = 3.6 Hz, 1 H), 6.98 (s, 1 H), 6.75 (d J = 3.5 Hz, 1 H), 6.70 (d J = 3.6 Hz, 1 H), 6.58 (d J =3.6 Hz, 1 H), 2.86 (t J = 7.5 HZ, 2 H), 2.71 (t J = 7.5 Hz, 2 H) 1.75 (apparent quintet, 2 H), 1.62 (apparent quintet, 2 H), 1.34 (m, 24 H), 1.20 (s, 12 H), 0.96 (t J = 6.5 Hz, 6 H) ppm. ^{13}C NMR (CD_2Cl_2): δ 145.9, 145.6, 142.3, 139.8, 135.2, 134.9, 134.1, 133.6, 131.4, 130.7, 130.1, 127.8, 127.2, 125.1, 125.0, 124.2, 123.2, 83.6, 32.2, 31.9, 31.8, 30.4, 30.1, 29.8_1, 29.7_9, 29.6_4, 29.5_9, 29.4, 29.3, 24.7, 23.0, 14.2 ppm. HRMS calcd for $C_{42}H_{59}BO_2S_3Na$ $[M+Na]^+$: 725.3680. Found 725.3696.

5'-(2-bromophenyl)-5-hexyl-[2,2']bithiophene (6) To a 100 mL Schlenk flaks was placed 0.385 g of 2-Iodobromobenzene, 0.5135 g of 2-(5'-hexyl-[2,2']bithiophenyl)-4,4, 5, 5-tetramethyl-dioxaborane, 25 mL THF, 5 mL ethanol, 2 mL water, and 2.0 g K_2CO_3. This solution was purged with Ar for 30 minutes. To the solution was added 0.10 g of $PdCl_2(PPh_3)_2$. This solution was heated to 65 °C for 12 hours. After stirring, the organic layer solution was filtered through a silica gel plug. The organic layer was concentrated by solvent evaporation reduced pressure. Silica column chromatography was performed on the residue using hexanes as an eluent. The solvent was removed in vacuo to give

0.326 g (59 %) of **6** as a clear oil that turned brown over time. ^{1}H NMR (CD_2Cl_2): δ 7.73 (dd *J* = 1.2, 7.0 Hz, 1 H), 7.56 (dd *J* = 1.7, 7.0 Hz, 1 H), 7.40 (m, 1H), 7.26 (d *J* =3.8 Hz, 1 H), 7.23 (dd *J* = 1.5, 7.8 Hz, 1 H), 7.14 (d *J* = 3.8 Hz, 1 H), 7.07 (d *J* = 3.5 Hz, 1 H), 6.78 (d *J* = 3.6 Hz, 1 H), 2.85 (t *J* = 7.5 Hz, 2 H), 1.72 (apparent quintet, 2 H), 1.39 (m, 6H), 0.93 (t *J* = 7.3 Hz, 3 H) ppm. ^{13}C NMR (CD_2Cl_2): δ 146.5, 140.3, 139.3, 135.4, 134.8, 134.3, 132.2, 129.6, 129.1, 128.2, 125.5, 124.1, 123.3, 122.9, 32.2, 32.1, 30.7, 29.3, 23.2, 14.4 ppm. HRMS calcd for $C_{20}H_{21}BrS_2$ $[M]^+$: 404.0263. Found 404.0226.

General Reaction Conditions for Suzuki Cross Coupling In a 100 ml Schlenk flask, 1 equivalent of the appropriate phenyl bromide, 1.5 equivalents of the corresponding aryl pinacol borane, and 3 equivalents of K_3PO_4 were dissolved in DMF to a concentration of 1mM, based on the phenyl bromide. The solution was de-oxygenated by purging with Ar for 45 minutes. The solution was then heated to 100 °C for 12 hours. After heating, brine was added to the solution and the product was extracted with ethyl acetate. The organic layer was dried with $MgSO_4$ and the solvent was removed in vacuo. Column chromatography with SiO_2 was performed on the residue and the solvent was removed in vacuo to give the desired biaryl compound.

2-(3'-[2,2',5',2"]terthiophene)-2'-(5-(5'-hexyl-[2,2']bithiophene))biphenyl (7) The crude product was purified by column chromatography was performed with a solution of 10 % CH_2Cl_2 in hexanes as an eluent to give the product as a yellow oil in 65 % yield. ^{1}H NMR (CD_2Cl_2): δ 7.52 (m, 2 H), 7.46 (dd *J* = 1.3, 7.5 Hz, 1 H), 7.38 (m, 2H), 7.23 (dd J = , 1 H), 7.13 (m, 2 H), 7.06 (d J = 7.5 Hz, 1 H), 7.03 (d J = 3.5 Hz, 1 H), 6.94 (dd J =3.6, 5.0 Hz, 1 H), 6.82 (m, 4 H), 6.67(d J =3.5 Hz, 1 H), 6.57 (dd J = 1.1, 3.6 Hz, 1 H), 6.37 (d J = 3.5 Hz, 1 H), 6.34 (s, 1 H), 2.83 (t J =7.5 Hz, 2 H), 1.73 (apparent quintet, 2

H), 1.40 (m, 6H), 0.99 (t J = 7.2 Hz, 3 H) ppm. ^{13}C NMR (CD_2Cl_2): δ 145.7, 142.4, 139.5, 132.0, 131.2, 128.8, 128.4, 128.2, 127.8_3, 127.8_1, 127.6, 127.3, 124.7, 123.8, 123.6, 123.4, 32.2_4, 32.1_7, 30.6, 29.4, 23.2, 14.5 ppm. HRMS calcd for $C_{38}H_{32}S_5$ $[M]^+$: 648.1102. Found 648.1103.

2-(3'-[2,2',5',2"]terthiophene)-2'-(3'-(5,5''-dinonyl-[2,2',5',2'']terthiophene))biphenyl (8) The crude product was purified by column chromatography on silica (pretreated with a 5 % solution of triethyl amine in hexanes), eluting with a gradient of 4 % to 10 % CH_2Cl_2 in hexanes to give the product as a yellow oil in 70 % yield. ^1H NMR (CD_2Cl_2): δ 7.28 (m, 6 H), 7.12 (m, 2 H), 7.01 (m, 4 H), 6.80 (dd *J* = 3.6, 5.0 Hz, 1H), 6.73 (d *J* = 3.5 Hz, 1 H), 6.59 (d *J* = 3.5 Hz, 1 H), 6.48 (m, 3 H), 6.36 (s, 1 H), 6.27 (d *J* = 3.3 Hz, 1 H), 2.76 (t *J* = 7.4 Hz, 2 H), 2.67 (t *J* = 7.2 Hz, 2 H), 1.64 (m, 4 H), 1.35 (m, 24H), 0.95 (m, 6 H) ppm. ^{13}C NMR (CD_2Cl_2): δ 146.5, 145.7, 135.0, 134.9, 132.0, 131.8, 131.1, 128,1, 128.0, 127.6, 127.5, 126.4, 126.0, 125.6, 125.1, 124.7, 124.6, 123.8, 123.4, 32.5, 32.3, 32.2, 30.6, 30.5, 30.2, 30.0, 29.9, 29.7, 23.3, 14.5 ppm. HRMS calcd for $C_{54}H_{58}S_6$ $[M]^+$: 898.2857. Found 898.2860.

2-(3-(2,5-bis-(3,4-ethylenedioxythiophene)thiophene)-2'-(3'-(5,5''-dinonyl-[2,2', 5',2'']terthiophene))biphenyl (9) The crude product was purified by column chromatography on silica (pretreated with a 5 % solution of triethyl amine in hexanes), eluting with a solution of 50 % CH_2Cl_2 in hexanes to give the product as a yellow oil in 59 % yield. ^1H NMR (CD_2Cl_2): δ 7.26 (m, 6 H), 6.95 (d *J* =7.5 Hz, 1 H), 6.91 (d *J* =7.0 Hz, 1 H), 6.78 (d *J* = 3.6 Hz, 1H), 6.61 (m, 2 H), 6.46 (d *J* = 3.5 Hz, 1 H), 6.43 (s, 1 H), 6.25 (d *J* = 3.5 Hz, 1 H), 6.13 (s, 1 H), 6.11 (s, 1 H), 4.23 (m, 4 H), 4.12 (m, 2 H), 4.06 (m, 2), 2.77 (t J =7.4 Hz, 2 H), 2.69 (t J = 7.4 Hz, 2 H), 1.67 (m, 4 H), 1.34 (m, 24H),

0.94 (m, 6 H) ppm. ^{13}C NMR (CD_2Cl_2): δ 146.3, 141.3, 138.5, 138.0, 135.2, 135.0, 131.8, 131.6, 131.1, 130.9, 128.0, 127.8, 127.2, 127.1, 126.3, 125.8, 125.0, 124.7, 123.1, 99.0, 96.9, 65.4, 65.2, 65.1, 65.0, 32.5, 32.3, 32.1, 30.6, 30.5, 30.1, 30.0, 29.9, 29.8, 23.3, 14.5 ppm. HRMS calcd for $C_{58}H_{62}O_4S_6$ $[M]^+$: 1014.2967. Found 1014.2966.

2-(3-(2,5-bis-(3,4-ethylenedioxythiophene)thiophene)-2'-(3'-[2,2',5',2'']terthiophene)biphenyl (10) The crude product was purified by column chromatography on silica (pretreated with a 5 % solution of triethyl amine in hexanes), eluting with a solution of 50 % CH_2Cl_2 in hexanes to give the product as a red solid oil (m. p. = 112-118 °C) in 90 % yield. ^1H NMR (CD_2Cl_2): δ 7.27 (m, 5 H), 7.16, (m, 2 H), 7.08 (dd J = 1.1, 5.0 Hz, 1 H), 6.94 (m, 3 H), 6.84 (broad d J = 7.1 Hz, 1H), 6.80 (dd J = 3.5, 5.0 Hz, 1 H), 6.58 (s, 1 H), 6.52 (s, 1 H), 6.46 (dd J = 1.1, 3.6 Hz, 1 H), 6.12 (s, 1 H), 6.11 (s, 1 H), 4.24 (m, 2 H), 4.19 (m, 2 H), 4.11 (m, 2), 4.04 (m, 2 H) ppm. ^{13}C NMR (CD_2Cl_2): δ 142.1, 141.6, 141.2, 137.4, 136.0, 131.6_3, 131.5_7, 131.0, 130.7, 128.0, 127.9, 127.8, 127.4, 127.1, 126.1, 126.0, 125.4, 124.3, 123.4, 112.4, 111.0, 98.9, 96.8, 65.3, 65.0_7, 64.9_6, 64.8_4 ppm. HRMS calcd for $C_{40}H_{26}O_4S_6$ $[M]^+$: 762.0150. Found 762.0160.

General $FeCl_3$ Polymerization Procedure In a 4 mL vial, one equivalent of the monomer was dissolved in $HCCl_3$ to a concentration of ~17 μM. Three equivalents of $FeCl_3$ were added to this solution and the entire mixture was stirred for 24 hours at room temperature. This polymerization mixture was then poured into a solution of NH_4OH and $HCCl_3$ was used to extract the product. The polymer solution was concentrated by solvent evaporation under reduced pressure. This concentrated polymer solution was filtered through a kimwipe plug and into methanol to induce precipitation. The

precipitated polymer was collected by centrifuge and dried under vacuum. The yield of all the polymerizations was less than 10 %.

References

[1] Stevens, M. *Polymer Chemistry*; 2nd Edition; Oxford University Press; New York; 1990.

[2] Sato, M-A.; Tanaka, S.; Kaeriyama, K. *Synth. Met.* **1987**, *18*, 229.

[3] (a) McCullough, R. D. *Adv. Mater.* **1998**, *10*, 93. (b) Madden, J. D.; Cush, R.A.; Kanigan, T. S.; Hunter, I. W. *Synth. Met.* **2000**, 113, 185.

[4] (a) Bauerle, P. *Adv. Mater.* **1992**, *4*, 102. (b) Guay, J.; Kasai, P.; Diaz, A.; Wu, R.; Tour, J. M.; Dao, L. H.; *Chem. Mater.* **1992**, *4*, 1097.

[5] Zotti, G.; Schiavon, G.; Berlin, A.; Pagani, G. *Chem. Mater.* **1993**, *5*, 620.

[6] (a) Nakao, K.; Morita, S.; Yoshino, K. *Synth. Met.* **1991**, *41*, 1039. (b) Siddhanta, S. K.; Gangopadhyay, R. *Polymer* **2005**, *46*, 2993. (c) Kawano, S.; Fujita, N.; Shinkai, S. *Chem. Eur. J.* **2005**, *11*, 4735.

[7] (a) Jang, S.; Sotzing, G. A.; Marquez, M. *Macromolecules* **2004**, *37*, 4351. (b) Stepp, B.; Nguyen, S. T. *Macromolecules* **2004**, *37*, 8222.

[8] (a) Tanaka, S.; Kumei, M. *J. Chem. Soc. Chem. Commun.* **1995**, 815. (b) Rebourt, E.; Pepin-Donat, B.; Dinh, E. *Polymer*, **1995**, *36*, 399. (c)Sixou, B.; Pepin-Donat, B.; Nechtschien. M. *Polymer* **1997**, *38*, 1581. (d) Chen, J.; Too, C. O.; Burrell, A. K.; Collis, G. E.; Officer, D. L.; Wallace, G. G. *Synth. Met.* **2003**, *137*, 1373.

[9] (a) Zotti, G.; Salmaso, R.; Gallazzi, M. C.; Marin, R. A. *Chem. Mater.* **1997**, *9*, 791. (b) Loganathan, K.; Cammisa, E. G.; Myron, B. D.; Pickup, P. G. *Chem. Mater.* **2003**, *15*, 1918.

[10] Davidson, K.; Ponsonby, A. M. *Synth. Met.* **1999**, *102*, 1512.

[11] Buey, J.; Swager, T. M. *Angew. Chem. Int. Ed.* **2000**, *39*, 608.

[12] (a) Grey, G. W.; Hird, M.; Lacey, D.; Toyne, K. J. *J. Chem. Soc. Perkin Trans. 2*, **1989**, 2041. (b) Tovar, J. D.; Rose, A.; Swager, T. M. *J. Am. Chem. Soc.* **2002**, *124*, 7762.

[13] Ishiyama, T.; Murata, M.; Miyaura, N. *J. Org. Chem.* **1995**, *60*, 7508.

[14] LeClerc, M.; Diaz, F. M.; Wegner, G. *Makromol. Chem.* **1989**, *190*, 3105.

[15] Ofer, D.; Crooks, R. M.; Wrighton, M. S. *J. Am. Chem. Soc.* **1990**, *112*, 7869.

[16] Roncali, J.; Blanchard, P.; Frere, P. *J. Mater. Chem.* **2005**, *15*, 1589

[17] Connelly, N. G.; Geiger, W. E. *Chem. Rev.* **1996**, *96*, 877.

[18] Groenendaal, L.; Jonas, F.; Freitag, D.; Pielartzik, H.; Reynolds, J. R. *Adv. Mater.* **2000**, *12*, 481.

[19]Patil, A.O; Heeger, A. J.; Wudl, F. *Chem. Rev.* **1988**, *88*, 183.

[20] Zhu, S. S.; Swager, T. M. *J. Am. Chem. Soc.* **1997,** *119*, 12568.

[21] Wilson, P.; Lacey, D.; Sharma, S.; Worthington, B. *Mol. Cryst. Liq. Cryst. Sci. Technol., Sect. A.* **2001**, *368*, 279.

[22] Campo, M. A.; Larock R. C. *J. Org. Chem.* **2002**, *67*, 5616.

Chapter 4:

Conducting Metallopolymers Based on Azaferrocene

Introduction

A central issue in the development of conducting metallopolymers is the nature of the interactions of the metal centers with the conducting organic polymer backbone and how the interactions between the associated metal centers affect the overall bulk conductive properties of the polymer.[1] Understanding these interactions is a continuing focus of our research in conducting metallopolymers for sensing applications.[2] In describing the metal to polymer interactions, conducting metallopolymers can be divided into groups based on an analogy to outer/inner sphere electron transfer in inorganic reactions between coordination complexes,[3] with the electron transfer being between the metal and the conducting organic polymer.[4] The basic distinction between the two groups is the degree of interaction between the metal and the organic π-systems: Indirect communication between the π-electrons of the conducting polymer and the metal is labeled as outer sphere. This group comprises conducting metallopolymers where the metal is linked to the polymer chain through a non π-conjugated linker. Direct communication between the π-electrons of the conducting polymer and the metal is labeled as inner sphere. This group comprises conducting metallopolymers with the metal bound to the polymer chain by a π-conjugated linker, the metal inserted into the polymer main chain, or the metal bound directly to the polymer chain. Wolf made similar distinctions between conducting metallopolymers but his analogy categorized conducting metallopolymers using Robin and Day's classification of mixed-valence complexes.[5] Pickup has grouped conducting metallopolymers by distinguishing between the types of interactions that occur between metal centers.[6] Our interest is focused on inner sphere type conducting metallopolymers since these polymers display significant redox conductivity.[4,7]

A type of inner sphere conducting metallopolymer that has not been fully explored are those in which the metal is bound to the delocalized π orbitals in a *fully* π-conjugated conducting

polymer. Chemical intuition would suggest a metal bound in a π fashion should provide excellent communication between the metal and extended π electron system of the polymers.[8,9] Although there are multiple conducting metallopolymers with a fully π-conjugated backbone wherein the metal is bound through σ bonds, there are few examples of transition metals bound in a π-fashion.[10] The majority of conducting metallopolymers with π-bound metals are based upon the 1,1'-substituted ferrocene structure.[1,11] With a 1,1'-substitution, the π-conjugated organic polymer segments are physically separated by the Fe center. This architecture produces polymers with a physically segmented structure and the accompanying localization of the electronic structure is a critical determinant of the polymer's electroactive properties.[12] In the more localized electronic structure, the charged migration between the strands can be thought of as redox (self-exchange) conduction. Although, this localization may not affect the short range metal to polymer interactions or the metal to metal interactions, it usually reduces the overall conductivity of the materials. There are few examples of the conjugated polymers containing ferrocene units where the ferrocene sections are linked to the polymer backbone through one of the cyclopentadiene rings (Cp).[13] The principle reason for this limitation is the relative synthetic difficulty in attaching multiple groups to only one Cp ring of a ferrocene.[14]

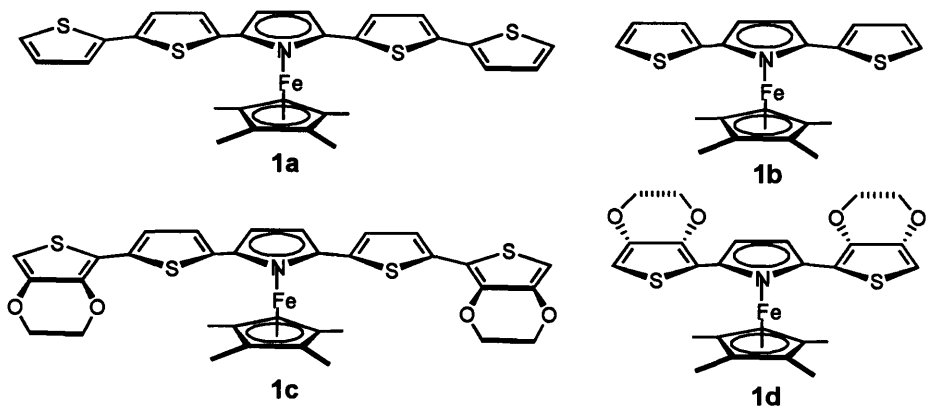

Scheme 1.

Azaferrocene is isoelectronic with ferrocene and involves the substitution of one of the Cp rings of ferrocene with a pyrrolide ligand.[15] The reactivity of the parent pyrrole provides easy access to azaferrocene derivatives with thiophene substituents on the α positions, as shown in Scheme 1.[16] The polymerization of the azaferrocene derivatives through the coupling of the terminal thiophenes provides a fully conjugated polymer with a metal bound to the polymer backbone in a π-fashion.

Azaferrocenes have not been widely investigated as an element in conducting polymers. The only previously investigated poly(azaferrocene) was produced by an innovative precursor approach wherein a $CpFe(CO)_2$ was first coordinated η^1 to an imine nitrogen within a polypyrrole.[17] Decarbonylation resulted in a reorganization to give the η^5-azaferrocene containing polypyrrole. In our present study, we begin with azaferrocene that can be polymerized to give an azaferrocene-polythiophene hybrid materials.

Even without a structural segmentation of the carbon-based π system, electronic localization can occur. The binding of the metal to the conducting polymer strand can induce localization of the π-electrons of the polymer. This localization is caused by the binding of a metal to a monomer unit of the polymer, which can localize of the molecular orbitals by effectively stabilizing (lowering the energy) of the interacting π-electrons of the monomer. This feature, which we term "energetic localization", was studied by Mann and co-workers in their examination of ruthenium and osmium oligothiophene complexes and the oxidation potential of the organic fragment.[18] Our hypothesis is that although similar energetic localization may occur by the binding of the metal, this effect would not be as significant as that caused by the direct physical disruption of the π-conjugation as in the case of 1,1'-substituted ferrocenes.

Maximized polymer to metal interactions are an important element in the design of the efficient metal-organic conducting polymers. However, we also seek to maximize the metal to

metal interactions to create materials with the optimal bulk electronic/magnetic properties. Plenio and co-workers investigated ferroceneacetylene based oligomers and polymers, and the results suggested that the 1,3-substitution on the ferrocene provided strong metal to metal electronic interactions.[13] In describing the metal to metal interactions observed in conducting metallopolymers, Pickup and co-workers have made a useful distinction between the types of interactions that can exist between the metal centers. These interactions were described as superexchange interactions, direct charge hopping (similar to outer sphere inorganic electron transfer), and mediated charge transfer. For the superexchange interaction, the classical studies on mixed-valance metal complexes provide a useful model for the description of these interactions.[19] In these mixed-valance complexes, the relative strength of the interaction between the metal centers can be described by a comproportionation constant, K_{com}. Most often the K_{com} increases with a decrease in the length of a conjugated linker.[20] This increased interaction should affect the electroactivity of the polymer and perhaps increase in the superexchange conduction process. To explore this idea, the length the thiophene linkage (the conjugated linker) was systematically varied to study the effect of the metal to metal interaction on the electroactivity and conductivity of the resulting polymer.

The electronic transport (conductivity) will be dependant on the metal-polymer electron exchange and rates. We have previously utilized redox matching, wherein the oxidation potentials of the metal and the polymer are matched as closely as possible, to enhance these rates and consequently the electroactivity and conductivity.[2b,2c] Pickup and coworkers have investigated the role of superexchange and used several different methods to interrogate conducting metallopolymers.[21] Their research focused on conducting polymers in which the organic elements were not electroactive over the potential ranges exhibited by the metal centered redox couples. Hence, the role of the superexchange conduction mechanism on a conducting

metallopolymer containing electroactive redox matched organic segments and metal centers remains an important question. The competitive, cooperative, or independent nature of the metal to metal interactions and how this influences the bulk conductive properties of a material must also be understood for the applications of these materials. Hence, both the length and the oxidation potential of the conjugated linkers between the azaferrocene units were varied to observe how both the mediated and superexchange mechanisms affect the overall polymer electroactivity.

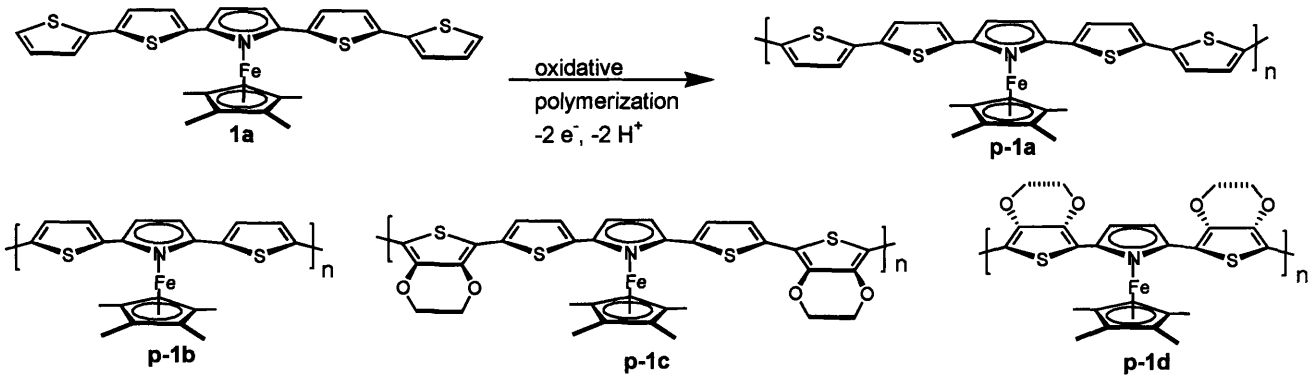

Scheme 2. Oxidative polymerization of **1a** and polymer structures.

We describe herein the synthesis and characterization of a series of polythiophene derivatives containing azaferrcoene which give polymers **p-1a**, **p-1b**, **p-1c** and **p-1d** with a fully π-conjugated backbone as shown in Scheme 2. The monomers were anodically polymerized and the resulting polymers were characterized by using cyclic voltammetry (CV), in situ conductivity and spectroelectrochemistry. Our results suggest that the superexchange mechanism alters the electroactivity of these systems.

Results and Discussion

Synthesis

The starting pyrrole compounds needed for the target azaferrocenes were synthesized by Stille cross-coupling reactions of the appropriate thiophene units with 2,5-dibromo-1-(carboxylic acid *tert*-butyl ester)–pyrrole, as shown in Scheme 3.[16,22] The BOC groups in **2a-d** were removed by treatment with sodium methoxide in THF, and the de-protected pyrroles were then reacted *in situ* with the half sandwich complex of Cp^*FeCl to produce the appropriate azaferrocenes.

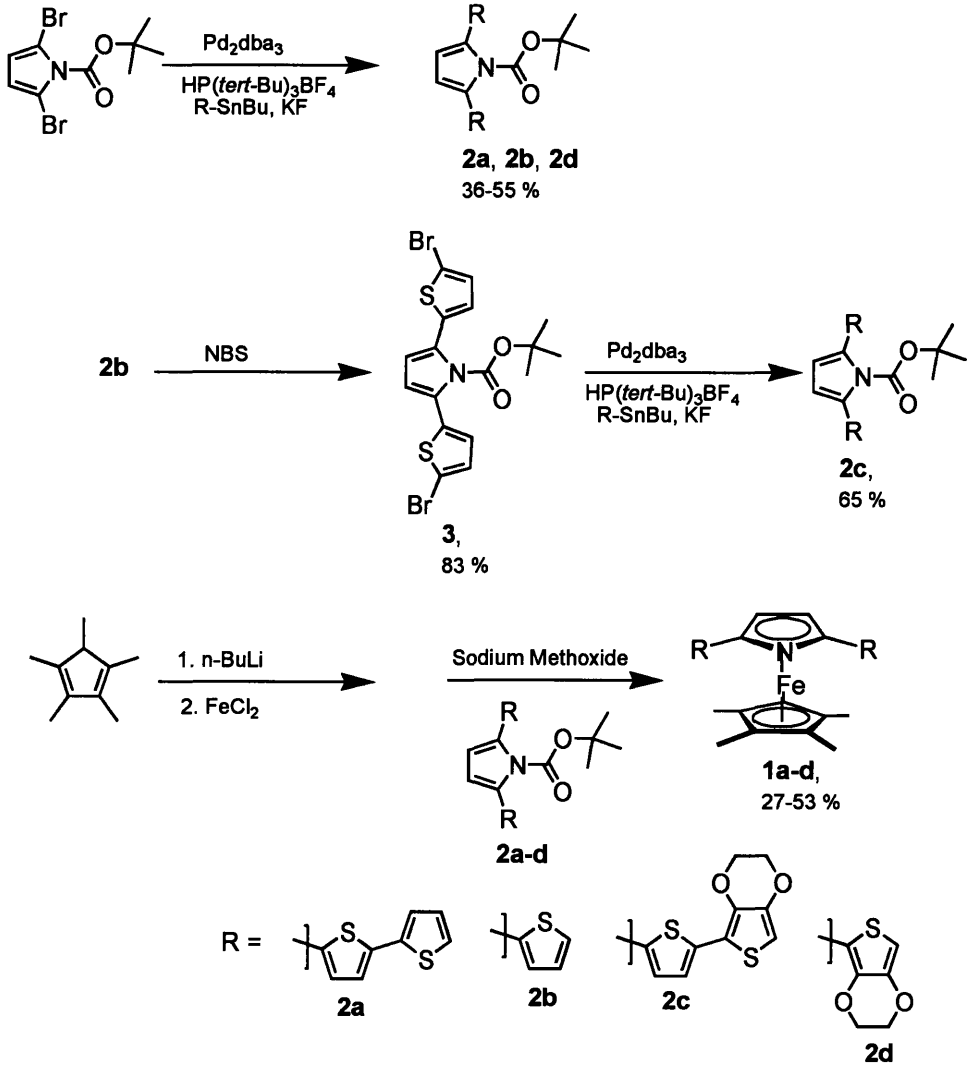

Scheme 3. Synthesis of the azaferrocene complexes.

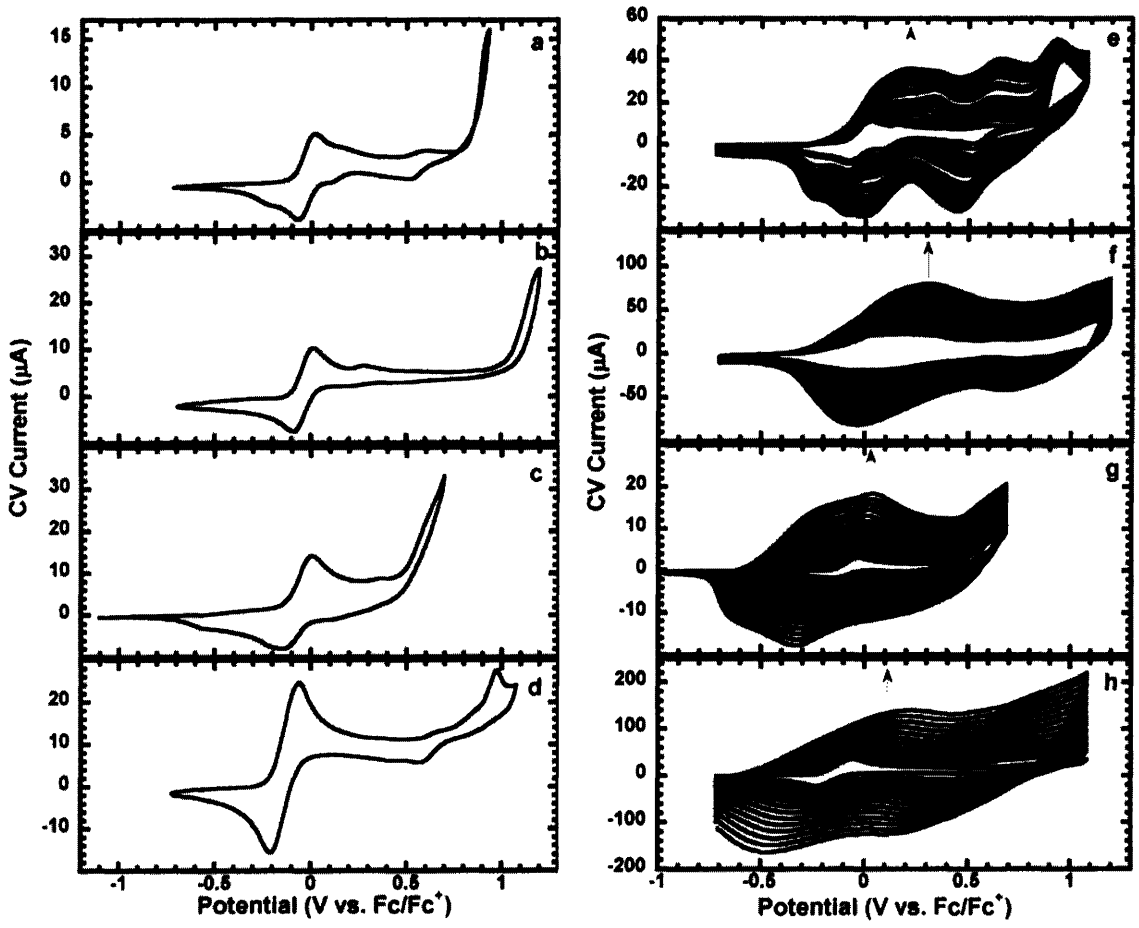

Figure 1. The initial cyclic voltammogram scans and the polymerizations of complexes **1a** (**a** and **e**), **1b** (**b** and **f**), **1c** (**c** and **g**) and **1d** (**d** and **h**) at 100 mV/s in 0.1 M $(n\text{-}Bu)_4NPF_6$ in CH_2Cl_2 with an interdigitated 5 μm Pt microelectrode as the working electrodes.

Monomers **1a-d** were subjected to anodic polymerization conditions in an electrolyte solution of 0.1 M $(n\text{-}Bu)_4NPF_6$ in CH_2Cl_2 to give polymers **p-1a**, **p-1b**, **p-1c**, and **p-1d** as shown in Scheme 2. As shown in Figure 1, for this polymerization, the potential was cycled between a potential where a chemically irreversible oxidation (polymerization) occurred and then back to a potential wherein the material is fully reduced. The azaferrocene electrochemistry is prominent in the first cycle but is subsequently overlapped by the large electroactivity of the conducting

polymer that deposits on the electrode with each cycle. The observed reversible $Fe^{II/III}$ redox potential is in accord with previous electrochemical work on azaferrocene complexes.[23] A summary of the results is listed in Table 1.

Table 1. Electrochemical and UV-vis data of complexes **1a-d** and the corresponding polymers.

Complex	Monomer[a] $E_{1/2}$ (V)	Monomer[a] E_{pa} (V)	Monomer[b] λ_{max} (nm)	Polymer[c] E_{pa} (V)	Polymer[d] λ_{max} (nm)	σ_{max} (S cm^{-1})
1a	-0.0	0.02	360, 431 (sh)	0.17	435	0.0047
1b	-0.04	0.02	296, 391 (sh)	0.33	463	0.0052
1c	-0.07	0.00	366, 435 (sh)	0.00	572, 586	0.0092
1d	-0.14	-0.07	301 393 (sh)	-0.02	503, 537, 592	0.0095

[a]The values refer to the first wave in the CV of the monomer. [b]The UV-vis spectra were obtained in CH_2Cl_2 (sh = shoulder). [c]The values refer to the first wave of the CV of the polymer. [d]These values are for the neutral (undoped) polymer.

Energetic Localization vs. Structural Localization

As mentioned earlier, we are interested in assessing the effect of energetic versus structural localization on the polymer's electroactivity and conductivity. In **p-1a**, the oxidation potential of the organic fragments is higher than the metal centered electroactivity. The azaferrocene units are separated by relatively long conjugated linkers that contain four thiophene units. Both of these effects should decrease the interaction between the individual metal centers of the polymer. The cyclic voltammetry (CV) of **p-1a** displays two waves with half wave potentials ($E_{1/2}$'s) near approximately 0.10 and 0.49 V, as shown in Figure 2. Analysis of the

atomic composition of **p-1a** by X-ray photoelectron spectroscopy gave a ratio of 4.28 to 1 ratio of S to Fe for the atomic composition of the polymer.

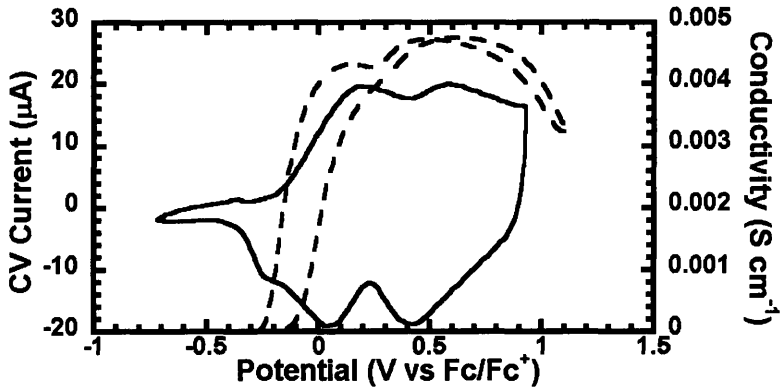

Figure 2. Cyclic voltammogram (solid line) at 100 mV/s and *in situ* conductivity (dashed line) of **p-1a** grown onto interdigitated 5 μm Pt microelectrodes at 10 mV/s with 40 mV offset potential between the working electrodes.

The wave at 0.1 V was assigned to the $Fe^{II/III}$ redox couple of complex since it was closest in potential to the wave assigned as the $Fe^{II/III}$ redox couple in the initial CV scan of the monomer. The $E_{1/2}$ of the second wave in the CV of **p-1a** was near previously reported $E_{1/2}$'s for quarterthiophenes oligomers so this wave was categorized as the oxidation of quarterthiophene section of the polymer.[24] This categorization was also based on the idea that the binding of the Fe to pyrrole unit would produce a break in the π-conjugation from pyrrole to the thiophenes, which is consistent with Mann's previous findings.[18] The CV of **p-1a** suggested that the polymer should have the conductive properties of a charge localized polymer and the *in situ* conductivity of **p-1a** was to some extent consistent with this idea. The conductivity of the **p-1a** in the *in situ* conductivity experiment of **p-1a**, shown in Figure 2, increased significantly at potentials near the metal oxidation and then continued to increase till the potential of the electrochemical cell approached the oxidation of the quarterthiophene fragment.[25] After that point, the conductivity

went down. The confinement of the region of high conductivity to potential windows corresponding to the waves in the CV is consistent with a charge localized polymer. Charge localized polymers typically have much smaller areas of conductivity which are strictly confided to the potentials corresponding to the waves of the polymer CV.[26] Fully extended π-conjugated polymers with a significant amount of charge delocalization have much larger windows of conductivity and these windows typically extend well beyond the potentials of the initial waves of the polymer CV.[27] This result is consistent with the idea of energetic localization of the polymer.

A spectroelectrochemistry study of **p-1a**, shown in Figure 3, was performed to provide more information about the polymer's response to oxidation. In agreement with the *in situ* conductivity, a change in potential of the electrochemical cell from a potential where the polymer is neutral (-0.4 V, λ_{max} = 435 nm) to a potential near the $Fe^{II/III}$ redox couple (0.2 V) produces a new peak in the absorbance, λ_{max} = 662 nm, of the film absorption. Upon oxidation at a potential near the quarterthiophene fragment oxidation (0.8 V), a red shifted to a broad

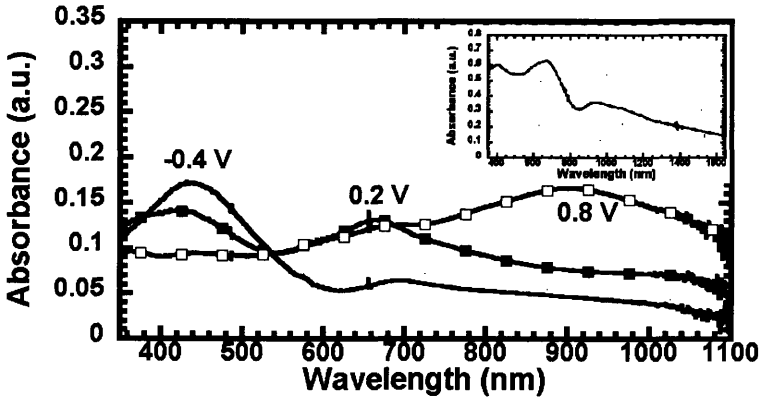

Figure 3. The UV-vis absorption of a film of **p-1a** on ITO at potentials of the electrochemical cell set at -0.4 (solid line), 0.2 (■) and 0.8 V (□) vs. Fc/Fc^+. Inset is the UV-vis/Near IR absorption of a film of **p-1a** with potential of the electrochemical cell set at 0.2 V.

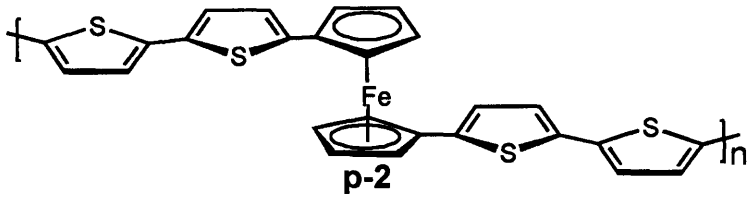

p-2

absorption emerges with a prominent feature centered at 900 nm in the absorbance of **p-1a**. The spectroelectrochemistry of an analogous polymer based on a 1,1' bithiophene substituted ferrocene, **p-2**, provides an interesting comparison.[12] The neutral absorbance of **p-2** has a λ_{max} at 445 nm and upon oxidation at potentials near the $Fe^{II/III}$ redox couple (0.8 V vs. SCE), the λ_{max} shifted to 495 nm and a weaker band appears at 1395 nm. The higher energy absorbance at 495 nm was assigned as the $\pi \rightarrow \pi^*$ of the quarterthiophene section with some possible contributions from a Cp to Fe^{III} ligand to metal charge transfer band. The shift in wavelength of the λ_{max}'s of the UV-vis spectrum of the polymer from the neutral state to the metal oxidized state was significantly different for **p-1a** (227 nm) than **p-2** (50 nm). This result suggests that the fully π-conjugated backbone in **p-1a** promotes delocalization of charge throughout the polymer and the structural localization of **p-2** is more significant than the energetic localization of **p-1a**. The lower energy absorbance (1395 nm) was assigned as a charge transfer band from the quaterthiophene section (LMCT band) to the Fe^{III}. A similar lower energy absorbance was not observed in **p-1a**. The absorption spectrum of **p-1a**, as shown in the inset of Figure 3, when oxidized at a potential corresponding to the $Fe^{II/III}$ redox couple displays a very broad absorption in the relevant region. However, it was assumed that a distribution of LMCT bands may have contributed to this absorption in the near IR region by **p-1a** at this oxidized state. Oxidation at higher potential (1.5 V vs. SCE) in **p-2**, which was assumed to be the oxidation of the quarterthiopene section, produced a UV-vis absorbance spectrum that had a broad absorption

with a feature centered near 900 nm. This result is similar to the spectroelectrochemical results of **p-1a** when the quarterthiophene section of **p-1a** was oxidized and suggested at this oxidized state **p-1a** and **p-2** had similar charge delocalizations.

Superexchange Mechanism

The comparison of **p-1b** to **p-1a** is useful in the study of how the superexchange mechanism affects the conductivity. As stated in the introduction, the decrease in the length of the oxidizable thiophene linker between the Fe sites in **p-1b** (bithiophene linker) versus **p-1a** (quarterthiophene linker) should lead to an increase in the metal to metal interactions. There is precedent for the improvement of the K_{com} for binuclear metallocene complexes as the length of an aryl conjugated linker between the metallocene units is decreased.[28]

As in **p-1a**, the CV of **p-1b** displayed two waves. The $E_{1/2}$ of the first wave in **p-1b** was

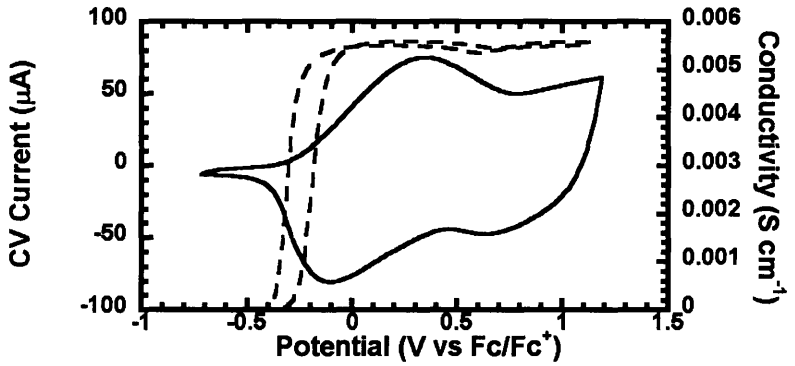

Figure 4. Cyclic voltammogram (solid line) at 100 mV/s and *in situ* conductivity (dashed line) of **p-1b**. The same *in situ* conductivity conditions for **p-1a** were used for **p-1b**.

at approximately the same potential as the half wave potential of the corresponding wave in **p-1a**. The exact point of the $E_{1/2}$ of the second wave of **p-1b** could not be precisely determined since the peak oxidation was beyond the edge of the solvent window. Hence, the $E_{1/2}$ for **p-1b**'s second wave, as shown in Figure 4, at a significantly higher potential than the half wave

potential of the second wave of **p-1a**. Using the same logic as the wave assignment in **p-1a**, the first wave in the CV of **p-1b** was assigned to $Fe^{II/III}$ redox couple and the higher oxidation was considered to be the oxidation of the bithiophene section. For the $Fe^{II/IIII}$ redox couple, the separation between the peak oxidation potential and the peak reduction potential of **p-1b** (0.46 V) was significantly larger than separation observed for in **p-1c** (0.12 V). For a completely reversible surface confined electrochemical event, the separation between the oxidation and reduction peaks of CV wave should be zero.[29] However, conducting polymers often show significant peak separation in their CV's. This separation is generally attributed to poor electrochemical kinetics (limited charge and ion mobility) caused by a thick polymer film on the electrode.[30] Yet, the differences in the thicknesses in the polymer films was only about 20 % (2000 Å for **p-1b** and 1600 Å for **p-1a**) so other causes for this disparity between the peak separation of first wave in the CV's of **p-1b** and **p-1a** can not be ruled out.

The *in situ* conductivity of **p-1b**, like **p-1a,** had an on-set of conductivity which was coincident with the on-set of oxidation of the $Fe^{II/III}$ redox couple wave, as shown in Figure 4. The on-set of conductivity was lower in potential for **p-1b** than in **p-1a** and parallels the lower potential for the $Fe^{II/III}$ redox wave in **p-1b** as compared to **p-1a**. The *in situ* conductivity of **p-1b** had a significantly smaller hysteresis than **p-1a**. The lack of a significant hysteresis in the *in situ* conductivity of **p-1b** can be attributed to a decrease in the structural changes of the polymer during the experiment.[31] The *in situ* conductivity of **p-1b** does display a small local minimum near the end of the $Fe^{II/III}$ redox wave. In contrast to **p-1a**, the *in situ* conductivity of **p-1b** does not show the decrease in conductivity at higher potentials. This outcome may be due to the fact that the organic oxidation wave is outside the potential window of the solvent (CH_2Cl_2).

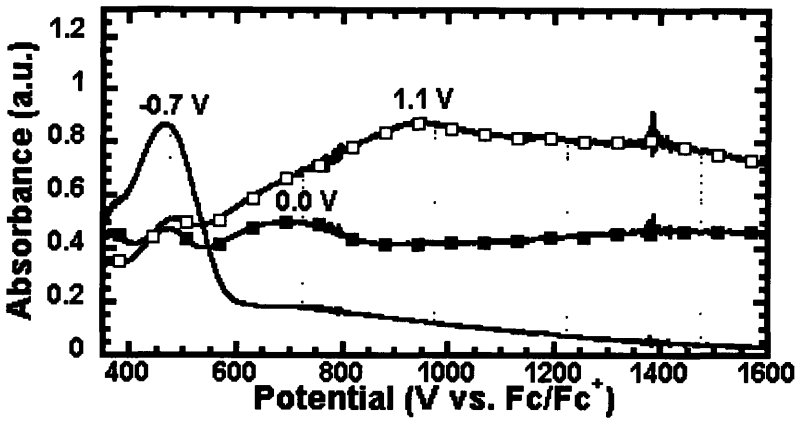

Figure 5. The UV-Vis absorption of a film of **p-1b** on ITO at potentials of the electrochemical cell set at -0.7 (solid line), 0.0 (■) and 1.1 V (□).

The spectroelectrochemistry of **p-1b** displays interesting phenomena when compared to the spectroelectrochemistry of **p-1a**, as shown in Figure 5. The λ_{max} in the UV-vis spectrum of the neutral form of **p-1b** is 463 nm, which is a 28 nm bathochromic shift from the λ_{max} of **p-1a**. As in the spectroelectrochemistry of **p-1a**, the UV-vis absorption spectrum of **p-1b** changed significantly at potentials near the $Fe^{II/III}$ redox couple wave and the UV-vis spectrum displayed a new λ_{max} at approximately 690 nm. The slight bathochromic shift of 28 nm in the neutral forms relative to the absorbance of **p-1a** is maintained with the oxidation of the metal sites in **p-1b**. Consistent with its lower potential on set of conductivity is that **p-1b** displayed this change in the UV-vis spectrum at a lower potential (0.0 V). With the oxidation of the Fe centers, the relative absorption of **p-1b** in the near IR was more pronounced than that of **p-1a**. In the fully oxidized state, the dominant UV-vis absorbance at 930 nm of **p-1b** displays a slight red shift in comparison to analogous feature in the UV-vis spectrum of **p-1a**. In total, all of these spectroelectrochemical properties suggest improved delocalization in **p-1b** relative to **p-1a**.

Redox Matching

Redox matching involves the systematic modification of the organic polymer to bring its redox potential to be commiserated with the metal centered redox potential, and we have previously shown this will improve both the electroactivity and conductivity of the polymer.[2c,32] Although the previously discussed azaferrocene polymers, **p-1a** and **p-1b**, display significant conductivity and electroactivity, we speculated that these properties could still be increased with redox matching. Given that the oxidation potentials of the organic fragments of these materials was higher than the $Fe^{II/III}$ redox couples, the oxidation potential of the organic fragments needed to be lowered to meet the matching condition. The substitution of a thiophene unit with a 3,4-ethylenedioxythiophene (EDOT) group was used to lower the oxidation potential of the organic section. An important issue is that the electron density donation from the electron rich EDOT unit can also lower the potential of $Fe^{II/III}$ redox couple. The initial scans of **1c** and **1d**, as shown in Figure 1, display this effect with their $Fe^{II/III}$ redox couples occurring at lower potentials than the redox couples of **1a** and **1b**. However, this donation effect of the EDOT on the $Fe^{II/III}$ redox couple was smaller than the effect of the EDOT group on the oxidation potential of the organic fragment. In the end, the overall effect of the substitution of the EDOT groups is to bring the potential of the $Fe^{II/III}$ redox couple and the potential of the oxidation of the organic fragment closer to each other.

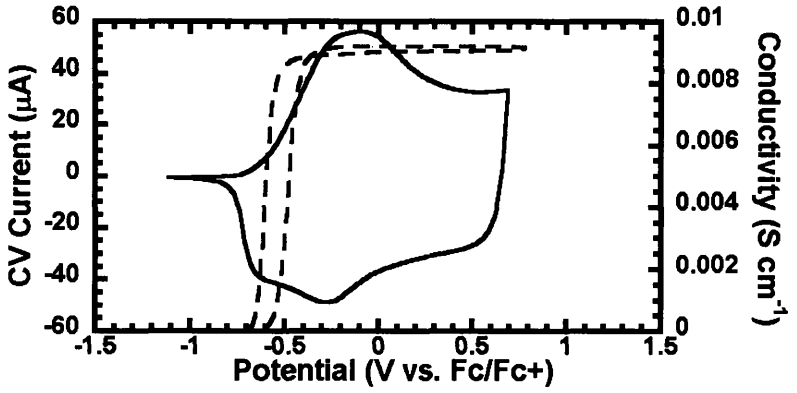

Figure 6. Cyclic voltammogram (solid line) at 100 mV/s and *in situ* conductivity (dashed line) of **p-1c** grown onto interdigitated 10 μm Pt microelectrodes at 10 mV/s with 40 mV offset potential between the working electrodes.

The effect of the addition of the EDOT groups is readily apparent in the CV of **p-1c**, as shown in Figure 6. The CV of **p-1c** had only one broad oxidation peak at -0.02 V and two unresolved reduction peaks at -0.31 and -0.66 V. This result is in stark contrast to its simple thiophene homolog **p-1a**, which had two clear oxidation waves. Based on comparisons with other polymers, the electroactivity around -0.02 V contained both the $Fe^{II/III}$ redox couple and thiophene centered electroactivity. The observation of two reduction waves is also consistent with this assertion. The *in situ* conductivity of **p-1c** had only one point of conductivity change and remained high well past the potential region of the wave in the CV. This type of conductivity profile, with large regions of uniformly high conductivity, resembles the conductivity profiles of fully π-conjugated polymers.[27] This result suggested that the redox matching of the metal and organic oxidations produces a polymer with a highly charge delocalized conductive state. The absolute conductivity of **p-1c** was only higher by a factor of two than that of the non-matched polymer (**p-1a**).

The absorption spectrum of **p-1c** in its neutral state (neutral λ_{max}= 572 nm with a slight shoulder at 586) is significantly red shifted from those of **p-1a** and **p-1b**, as shown in Figure 7. This effect is typical of EDOT substitution in polythiophene.[33] The changes in the UV-vis absorption spectrum of **p-1c** occurred over a smaller potential window (-0.5 to 0.1 V) than the potential window needed for the corresponding changes in the spectroelectrochemistry of **p-1a** (-0.4 to 0.8 V). This decrease of the potential window was consistent with the single broad oxidation which had only one broad oxidation wave observed for **p-1c**. At potentials from -0.3 to -0.1 V, a broad absorption at intermediate wavelengths, $\lambda_{max} \approx$ 780 nm, is observed and at higher potentials (-0.1 to 0.1 V) a featureless extremely broad absorption at longer wavelengths dominates the spectrum.

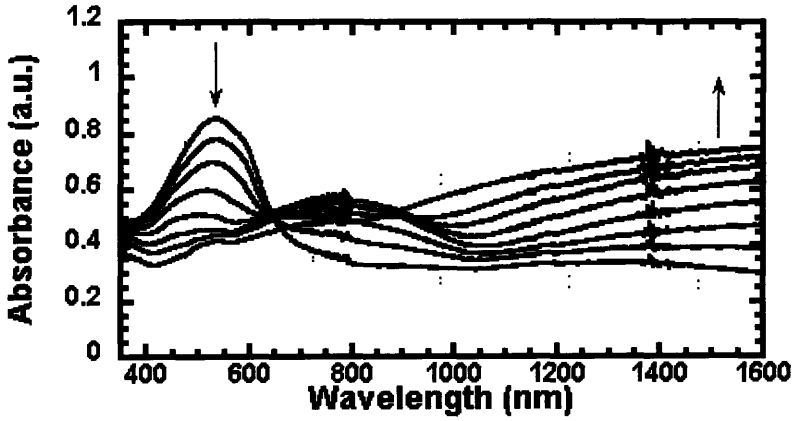

Figure 7. Spectroelectrochemistry of **p-1c** deposited onto ITO with potential changes from -0.5 to 0.1 V in 0.1 V intervals.

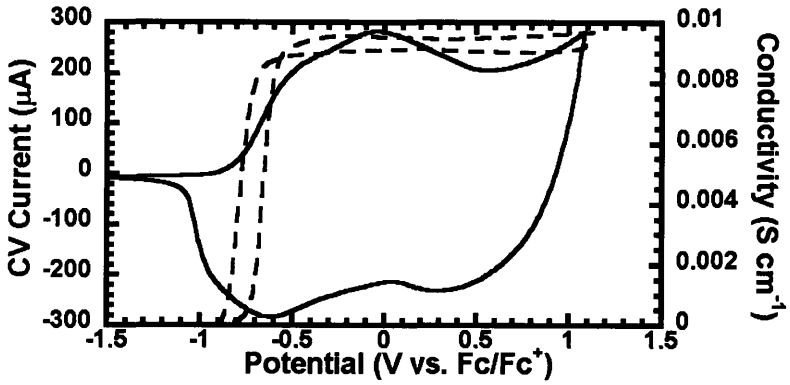

Figure 8. Cyclic voltammogram (solid line) at 100 mV/s and *in situ* conductivity (dashed line) of **p-1d.** The same *in situ* conductivity conditions for **p-1c** were used for **p-1d**.

The EDOT homolog of **p-1b** is **p-1d**. As expected, **p-1d**'s on set of electroactivity, as shown in Figure 8, is at a lower potential than **p-1b**. Similar to our comparisons of **p-1b** with **p-1a**, **p-1d** displays a larger separation between oxidation and reduction peaks than **p-1c** (0.58 for **p-1d** vs. ~ 0.29 V for **p-1c**). The *in situ* conductivity of **p-1d** had a similar profile to the *in situ* conductivity of **p-1c** in that the profile had only point of conductivity change and displayed a large window of high conductivity. In contrast to the *in situ* conductivity of **p-1b**, there was no local minimum in the conductivity profile of **p-1d**. The effects of the length of the thiophene groups are less pronounced than **p-1b** and **p-1a**, the difference in the absolute conductivities of **p-1d** and **p-1c** are not significant.

In accord with our comparisons of **p-1c** to **p-1a**, the spectroelectrochemistry of **p-1d** was red shifted relative to that of **p-1b**. The neutral absorption of **p-1d** displays a λ_{max} = 537 nm with shoulders at 503 and 590 nm, as shown in Figure 9 and intermediate wavelength absorptions (λ_{max} ≈770 nm) were observed at potentials corresponding to the $Fe^{II/III}$ redox couple, from -0.6 to -0.2 V. Similar to the spectroelectrochemistry of **p-1c**, a broad featureless absorption at longer wavelengths was observed as the polymer was oxidized at higher potentials (-0.2 to 0.2 V). In contrast to the differences observed in the spectroelectrochemistry of **p-1b** relative to **p-**

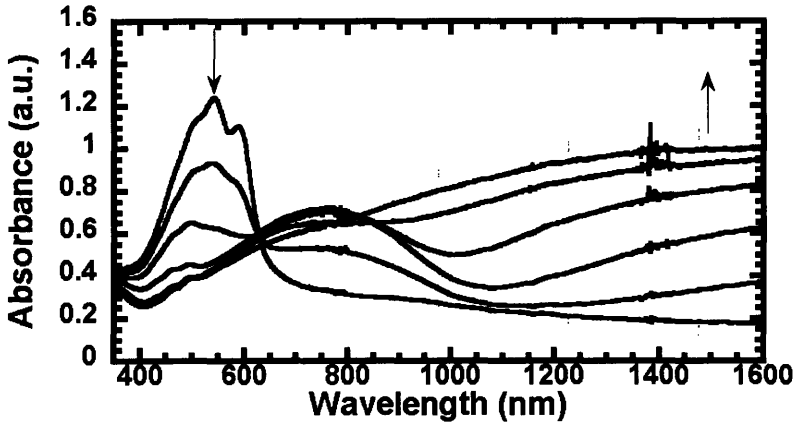

Figure 9. Spectroelectrochemistry of **p-1d** deposited onto ITO with potential changes from -0.8 to 0.2 V in 0.2 V intervals.

1a, there was no red shift of the neutral absorption λ_{max}'s of **p-1d** in comparison to **p-1c**. This result was consistent with the comparison the absolute conductivities of **p-1c** and **p-1d.** . It appears that in the case of the EDOT substitution that a difference in the length of the conjugated linker between the metal sites in each polymer does not produce an observable effect in the bulk charge delocalization However like the difference in the on set of conductivity for **p-1b** in comparison to the on set of **p-1a**, the on set of conductivity of **p-1d** did occur at a lower potential than **p-1c**'s. A direct comparison of the *in situ* conductivities of all the polymers, as shown in Figure 10, demonstrates the lowering of the on-set of conductivity by decreasing the length in the conjugated linker between metal sites. It is readily apparent that the on-set conductivity of a polymer with two thiophene units between the azaferrocene sites (**p-1b** and **p-1d**) occurs at lower potential than the on set conductivity of a polymer of the analogous polymer with four thiophene units between azaferrocene units (**p-1a** and **p-1c**). These results suggest that a superexchange mechanism may be the cause for the lowering of these on-sets. However, a model study and a Hush analysis is needed to quantify the amount of electronic and electrostatic

contributions to the interaction between the metal centers.[34] Such a study was beyond that the scope of this investigation.

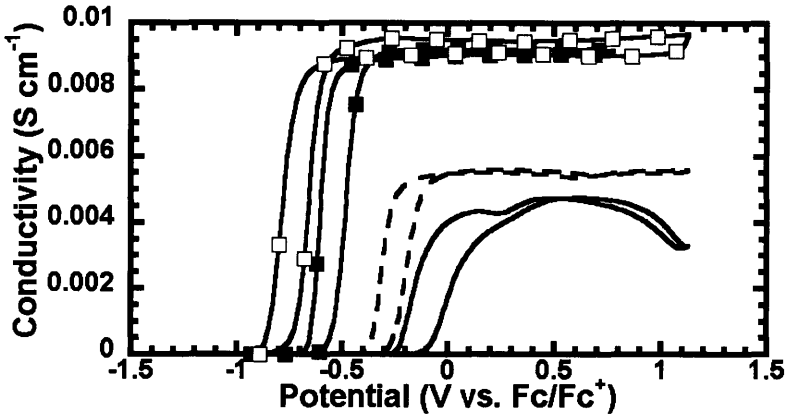

Figure 10. *In situ* conductivities of **p-1a** (solid line), **p-1b** (dashed line), **p-1c** (■)and **p-1d** (□).

Conclusions

A series of polythiophene derivatives containing azaferrocene were synthesized. The polymers displayed metal-based redox conductivity. This significant redox conductivity was attributed to the molecular architecture wherein the π-bound metal was attached to a fully π-conjugated polymer backbone. A change in the length of thiophene section between the azaferrocene units seemed to indicate a modification in redox conductivity mechanism perhaps involving a superexchange type mechanism.

Experimental Section

General Comments ^{1}H and ^{13}C NMR spectra were recorded on a Bruker 400 MHz spectrometer and are referenced to residual $CHDCl_2$ (5.32 ppm for ^{1}H and 54.00 ppm for ^{13}C). Melting points are uncorrected. High-resolution mass spectra (HRMS) were determined with a Bruker Daltonics APEX II 3 Tesla FT-ICR-MS. The 2-tributylstannyl-3,4-ethylenedioxythiophene, 5-tributylstannyl-[2,2'] bithiophene and the 2,5-dibromo-1-(carboxylic acid *tert*-butyl ester)-pyrrole were synthesized according to published procedures.[2b,16] All

commercial chemicals were purchased from Aldrich. Solvents were dried by passing through activated alumina and de-oxygenated by purging with Ar or purified by a SPS-400-5 solvent purification system (Innovative Technologies). Air sensitive manipulations were performed using standard Schlenk techniques. Electrochemical measurements were performed in a nitrogen glovebox with an Autolab II with PGSTAT 30 potentiostat (Eco Chemie). The electrolyte solution for all electrochemical measurements, 0.1 M $(n\text{-}Bu)_4NPF_6$ in dry CH_2Cl_2, was stored over 4 Å molecular sieves in a glovebox. The quasi-internal reference electrode was a Ag wire submersed in 0.01 M $AgNO_3$/ 0.1 M $(n\text{-}Bu)_4NPF_6$ in anhydrous acetonitrile and a Pt wire or gauze was used as a counter electrode. All potentials were referenced to the Fc/Fc^+ couple. The working electrodes were 5 or 10 μm Pt interdigitated microelectrodes (Abtech Scientific, Inc.) or indium tin oxide coated unpolished float glass slides (Delta Technologies). Absorption spectra were collected on an Agilent 8453 diode array spectrophotometer or a Carey 6000i UV-vis-NIR spectrophotometer. A Dektak 6M stylus profiler (Veeco) was used to measure the film thickness of the polymers grown onto interdigitated microelectrodes. X-ray photoelectron spectroscopy measurements were collected on a Kratos Axis Ultra Imaging X-ray photoelectron spectrometer.

2,5-bis-(5-[2,2'] bithiophene)-1-(carboxylic acid *tert*-butyl ester)-pyrrole (2a) To a 100 mL Schlenk tube was placed 0.267 g of 2,5-dibromo-1-(carboxylic acid *tert*-butyl ester)-pyrrole, 2.0 g 5-tributylstannyl-[2,2'] bithiophene, 2.2 g of KF, and 50 mL of toluene. The solution was de-oxygenated by purging with Ar for 30 minutes. To the solution was added 0.078 g of Pd_2dba_3 and 0.048 g of $HP(tert\text{-}Bu)_3BF_4$ and the solution was stirred for 48 hours. Water was added and the product was isolated by extraction with CH_2Cl_2. The organic layer was dried with $MgSO_4$ and the solvent was evaporated in vacuo. Column chromatography was performed with silica gel (the silica gel was pretreated with 10 % triethylamine in hexanes before the column was run) using 28 % CH_2Cl_2 in hexanes as an eluent. After evaporation of the solvent under reduced

pressure, 0.173 g (42 %) of the product was obtained as a bright yellow solid, mp 127.2 °C. ^{1}H NMR (CD_2Cl_2): δ 7.30 (dd *J*= 3.6, 1.1 Hz, 2 H), 7.27 (dd *J*= 4.7, 1.1 Hz, 2 H), 7.20 (d *J* = 3.7 Hz, 2 H), 7.10 (dd *J* = 4.7, 3.6 Hz, 2 H), 7.07 (d *J* =3.7 Hz, 2 H), 6.44 (s, 2 H), 1.42 (s, 9 H) ppm. ^{13}C NMR (CD_2Cl_2): δ 149.8, 137.7, 137.5, 133.7, 129.2, 128.4, 128.1, 125.0, 124.2, 123.9, 114.2, 85.5, 27.5 ppm. HRMS calcd for $C_{25}H_{21}NO_2S_4$ $[M]^+$: 495.0450. Found 495.0470.

2,5-bis-(5-[2,2'] bithiophene)-1',2',3',4',5'-pentamethylazaferrocene (1a) In a glove box, 0.116 g of **2a**, 0.20 g of sodium methoxide and 5 mL of THF were stirred together for 3 hours. During that time in a separate flask, 0.037 g 1,2,3,4,5-pentamethyl cyclopentadiene (Cp^*) and 0.35 mL of 2.2 M solution of n-BuLi were stirred together in 5 mL of THF for 1.5 hours. Subsequently, 0.094 g of $FeCl_2$ was added to the Cp^*Li solution and this solution stirred an additional 1.5 hours. The mixtures of **2a** and Cp^*FeCl were added together and stirred for 16 hours. After stirring, the solution was taken out of the glove box, filtered through a column of silica gel using ethyl acetate as an eluent. The solvent was removed in vacuo. Column chromatography was performed with silica gel (the silica gel was pretreated with 10 % triethylamine in hexanes before the column was run.) using a solution of 10 % ethyl acetate in hexanes as an eluent. After evaporation of the solvent under reduced pressure, 0.071 g (53 %) of the product was obtained as an orange solid, mp 147 °C. The product was stored in a glovebox. ^{1}H NMR (CD_2Cl_2): δ 7.30 (broad m; apparent s, 4 H), 7.19 (broad m; apparent d, 4 H), 7.08 (apparent s, 2 H) 4.66 (s, 2 H), 1.58 (s, 15 H) ppm. ^{13}C NMR (CD_2Cl_2): δ 139.2, 138.4, 135.9, 128.5, 124.7, 124.4, 123.7, 123.6, 99.4, 82.6, 72.4, 9.4 ppm. HRMS calcd for $C_{30}H_{28}FeNS_4$ $[M+H]^+$: 586.0459. Found 586.0480.

2,5-bis-[2-thiophene]-1-(carboxylic acid *tert*-butyl ester) -pyrrole (2b) To a 50 mL Schlenk flask was placed 0.297 g of 2,5-dibromo-1-(carboxylic acid *tert*-butyl ester)-pyrrole, 1.4 g of 2-tributylstannylthiophene, 1.7 g of KF, and 20 mL of toluene. The solution was de-oxygenated by

purging with Ar for 30 minutes. To the solution was added 0.080 g of Pd_2dba_3 and 0.040 g of HP(*tert*-Bu)$_3BF_4$ and the solution was then stirred for 40 hours. Water was added, and the product was isolated by extraction with ethyl acetate. The organic layer was dried with $MgSO_4$ and the solvent was evaporated in vacuo. The isolated product was purified by column chromatography with silica gel (the silica gel was pretreated with 10 % triethylamine in hexanes before the column was run to avoid oxidation) using 10 % CH_2Cl_2 in hexanes as an eluent. After removal of the solvent by evaporation, the product was obtained as a slightly yellow solid, 0.149 g (49 %), mp 90 °C. ^{1}H NMR (CD_2Cl_2): δ 7.39 (dd J = 5. 0, 1.4 Hz, 2 H), 7.11 (m, 4 H), 6.37 (s, 2 H), 1.31 (s, 9 H) ppm. ^{13}C NMR (CD_2Cl_2): δ 149.9, 134.9, 129.2, 127.6, 127.4, 126.1, 114.0, 85.2, 27.5 ppm. HRMS calcd for $C_{17}H_{17}NO_2S_2$ $[M]^+$: 331.0695 Found 331.0696.

2,5-bis-(2-thiophene)-1',2',3',4',5'-pentamethylazaferrocene (1b) In a glove box, 0.090 g of **2b**, 0.12 g of sodium methoxide and 5 mL of THF were stirred together for 3 hours. During that time in a separate flask, 0.025 g of Cp^* and 0.12 mL of 2.2 M solution of n-BuLi were stirred together in 5 mL of THF for 1.5 hours. Subsequently, 0.035 g of $FeCl_2$ was added to the Cp^*Li solution and this solution was stirred an additional 1.5 hours. The mixtures of **2b** and Cp^*FeCl were added together and stirred at r.t. for 28 hours. The solution was then taken out of the glove box, filtered through a column of silica gel using ethyl acetate as an eluent and the solvent was removed in vacuo. Column chromatography was performed with silica gel (the silica gel was pretreated with 10 % triethylamine in hexanes before the column was run.) using a mixture of 10 % ethyl acetate in hexanes as an eluent. After evaporation of the solvent under reduced pressure, 0.041 g (36 %) of the product was obtained as an orange solid, mp 133.3 °C. The product was stored in a glovebox. ^{1}H NMR (CD_2Cl_2): δ 7.30 (broad m, 4 H), 7.12 (apparent broad triplet, 2 H), 4.64 (s, 2 H), 1.52 (s, 15 H) ppm. ^{13}C NMR (CD_2Cl_2): δ 140.1, 128.1, 124.0, 123.1, 99.6, 82.3, 72.2, 9.3 ppm. HRMS calcd for $C_{22}H_{23}FeNS_2Na$ $[M+Na]^+$: 444.05190. Found 444.0528.

2,5-bis-[5-bromo-2-thiophene]-1-(carboxylic acid *tert*-butyl ester)–pyrrole (3) To a 100 mL round bottom flask was placed 0.146 g of **2b** which then dissolved in 25 mL of dimethylformamide. To this solution was added 0.165 g of N-bromosuccimide dissolved in 25 mL of dimethylformamide. The solution was stirred for 12 hours. Water was added to the mixture and the product was extracted with ethyl ether. The organic layer was dried with $MgSO_4$ and the solvent was removed in vacuo. Column chromatography was performed with a short column of silica gel using hexanes as an eluent. After evaporation of the solvent under reduced pressure, 0.178 g (83 %) of the product was obtained as a slightly yellow solid, mp 91 °C. ^{1}H NMR (CD_2Cl_2): δ 7.05 (d J = 3.8 Hz, 2 H), 6.87 (d J= 3.8 Hz, 4 H), 6.35 (s, 2 H), 1.34 (s, 9 H) ppm. ^{13}C NMR (CD_2Cl_2): δ 149.4, 136.6, 130.2, 128.7, 128.3, 114.9, 112.6, 85.7, 27.6 ppm. HRMS calcd for $C_{17}H_{15}Br_2NO_2S_2$ $[M]^+$: 486.8905. Found 486.8922.

2,5-bis-(5-(2-[3,4-ethylenedioxythiophene]thiophene)-1-(carboxylic acid *tert*-butyl ester) - pyrrole (2c) To a 50 mL Schlenk flask was added 0.178 g of 2, 5-bis-[5-bromo-2-thiophene]-1-(carboxylic acid *tert*-butyl ester)–pyrrole, 1.0 g of 2-tributylstannyl-3,4-ethylenedixoythiophene, 1.4 g of KF, and 20 mL of toluene. The solution was de-oxygenated by purging with Ar for 30 minutes. To the solution was added 0.080 g of Pd_2dba_3 and 0.040 g of HP(*tert*-Bu)$_3$BF$_4$ and the solution was then stirred for 20 hours. Water was added and the product was isolated by extraction with ethyl acetate. The organic layer was dried with $MgSO_4$ and the solvent was evaporated in vacuo. Column chromatography with silica gel (the silica gel was pretreated with 10 % triethylamine in hexanes before the column was run) was performed using a gradient of 20 to 40 % ethyl acetate in hexanes as an eluent. After evaporation of the solvent under reduced pressure, 0.145 g (65 %) of the product was obtained as a yellow solid, mp 169 °C (dec.). ^{1}H NMR (CD_2Cl_2): δ 7.19 (d J = 3.8 Hz, 2 H), 7.03 (broad d with an apparent J = 3.3 Hz, 2 H), 6.40 (s, 2 H), 6.28 (s, 2 H), 4.37 (m, 4 H), 4.28 (m, 4 H), 1.39 (s, 9 H) ppm. ^{13}C NMR (CD_2Cl_2): δ

150.1, 142.6, 138.3, 135.3, 132.9, 129.4, 127.3, 123.0, 113.9, 112.2, 97.4, 85.6, 65.6, 65.2, 27.6 ppm. HRMS calcd for $C_{29}H_{25}NO_6S_4Na$ $[M+Na]^+$: 634.0457. Found 634.0441.

2,5-bis-(5-(2-[3,4-ethylenedioxythiophene]thiophene)-1',2',3',4',5'-pentamethylazaferrocene (1c) In a glove box, 0.108 g of **2c**, 0.20 g of sodium methoxide and 5 mL of THF were stirred together for 3.5 hours. During that time, 0.028 g of Cp^* and 0.1 mL of 2.2 M solution of n-BuLi were stirred together in 5 mL of THF for 1.5 hours. Subsequently, 0.035 g of $FeCl_2$ was added to the Cp^*Li solution and this solution stirred an additional 1.5 hours. The mixtures of **2c** and Cp^*FeCl were added together and then stirred for an additional 20 hours. After stirring, the solution was taken out of the glove box and filtered through a column of silica gel using ethyl acetate as an eluent. The solvent was removed in vacuo. Column chromatography was performed using silica gel (the silica gel was treated with 10 % triethylamine in hexanes before the column was run) and a mixture of 30 % ethyl acetate in hexanes as an eluent. After evaporation of the solvent under reduced pressure, 0.034 g (27 %) of the product was obtained as an orange solid, mp 254 °C (dec.). The product was stored in a glovebox. ^1H NMR (CD_2Cl_2): δ 7.24 (broad d J= 3.6 Hz, 2 H), 7.19 (broad d J = 3.6 Hz, 2 H) 6.27 (s, 2 H), 4.65 (s, 2 H), 4.41 (m, 4 H), 4.32 (m, 4 H), 1.58 (s, 15 H) ppm. ^{13}C NMR (CD_2Cl_2): δ 142.7, 138.3, 137.9, 133.6, 123.7, 123.2, 113.1, 99.7, 96.7, 82.5, 72.2, 65.7, 65.3, 9.5 ppm. HRMS calcd for $C_{26}H_{28}FeNO_4S_2$ $[M+H]^+$: 702.0569. Found 702.0575.

2,5-bis-(2-[3,4-ethylenedioxythiophene])-1-(carboxylic acid *tert*-butyl ester) -pyrrole (2d)

To a 50 mL Schlenk flask was placed 0.343 g of 2,5-dibromo-1-(carboxylic acid *tert*-butyl ester)-pyrrole, 1.0 g of 2-tributylstannyl-3,4-ethylenedixoythiophene, 0.30 g of KF, and 20 mL of toluene. The solution was de-oxygenated by purging with Ar for 30 minutes. To the solution was added 0.048 g of Pd_2dba_3 and 0.020 g of $HP(tert\text{-}Bu)_3BF_4$ and the solution was then stirred for 48 hours. Water was then added and the product was extracted with CH_2Cl_2. The

organic layer was dried with $MgSO_4$ and the solvent was removed in vacuo. Column chromatography was performed with silica gel (the silica gel was pretreated with 10 % triethylamine in hexanes before the column was run) using 20 % ethyl acetate in hexanes as an eluent. After evaporation of the solvent under reduced pressure, 0.262 g (55 %) of the product was obtained as a slightly yellow solid, 155-158 °C (dec.). ^{1}H NMR (CD_2Cl_2): δ 6.38 (s, 2 H), 6.26 (s, 2 H), 4.22 (s, 8 H), 1.38 (s, 9 H) ppm. ^{13}C NMR (CD_2Cl_2): δ 149.2, 141.6, 139.3, 125.9, 114.6, 108.9, 98.8, 83.9, 65.2, 65.0, 27.5 ppm. HRMS calcd for $C_{21}H_{21}NO_6S_2Na$ $[M+Na]^+$: 470.0702. Found 470.0702.

2,5-bis-(3,4-ethylenedioxythiophene)-1',2',3',4',5'-pentamethylazaferrocene (1d) In a glove box, 0.194 g of **2d**, 0.30 g of sodium methoxide and 5 mL of THF were stirred together for 3 hours. During that time in a separate flask, 0.085 g of Cp^* and 0.35 mL of 2.2 M solution of n-BuLi were stirred together in 5 mL of THF for 1.5 hours. Subsequently, 0.085 g of $FeCl_2$ was added to the Cp^*Li solution and this solution stirred an additional 1.5 hours. The mixtures of **2d** and Cp^*FeCl were added together and stirred for 28 hours. After stirring, the solution was taken out of the glove box, filtered through a short column of silica gel using ethyl acetate as an eluent and the solvent was then removed in vacuo. Column chromatography was performed with silica gel (the silica gel was pretreated with 10 % triethylamine in hexanes before the column was run) using a mixture of 1:1 ethyl acetate and hexanes as an eluent. After evaporation of the solvent under reduced pressure, 0.117 g (50 %) of the product was obtained as an orange solid, 250° (dec.) C. The product was stored in a glovebox. ^{1}H NMR (CD_2Cl_2): δ 6.28 (s, 2 H), 4.86 (s, 2 H), 4.40 (m, 4 H), 4.29 (m, 4 H), 1.58 (s, 15 H) ppm. ^{13}C NMR (CD_2Cl_2): δ 142.5, 138.2, 114.0, 97.3, 97.1, 81.8, 73.3, 65.4, 65.3, 9.3 ppm. HRMS calcd for $C_{26}H_{28}FeNO_4S_2$ $[M+H]^+$: 538.0814. Found 538.0805.

References

[1] (a) Manners, I. *Synthetic Metal-Containing Polymers*; Wiley-VCH: Weinheim, Germany, 2004. (b) Kingsborough, R. P.; Swager, T. M. *Prog. Inorg. Chem.* **1999**, *48*, 123.

[2] (a) Zhu, S. S.; Swager T. M. *Adv. Mater.* **1996**, *8*, 497. (b) Zhu, S. S.; Swager, T. M. *J. Am. Chem. Soc.* **1997**, *119*, 12568. (c) Kingsborough, R. P.; Swager, T. M. *Adv. Mater.* **1998**, *11*, 1100. (d) Kingsborough, R. P.; Swager, T. M. *J. Am. Chem. Soc.* **1999**, *121*, 8825. (e) Kingsborough, R. P.; Swager, T. M. *Chem. Mater.* **2000**, *12*, 872. (f) Kingsborough, R. P.; Swager, T. M. *Angew. Chem. Int. Ed.* **2000**, *39*, 2897. (g) Vigalok, A.; Zhu, Z.; Swager, T. M. *J. Am. Chem. Soc.* **2001**, *123*, 7917. (h) Vigalok, A.; Swager, T. M. *Adv. Mater.* **2002**, *14*, 368. (i) Shioya, T.; Swager, T. M. *Chem. Commun.* **2002**, 1364. (j) Kwan, P. H.; Swager, T. M. *Chem. Commun.* **2005**, 5211.

[3] (a) Atwood, J. D. *Inorganic and Organometallic Reaction Mechanisms*; Wiley: New York, 1997. (b) Rodgers, G. E. *Introduction to Coordination, Solid State, and Descriptive Inorganic Chemistry*; McGraw-Hill: New York, 1994.

[4] Holliday B. J.; Swager T. M. *Chem. Commun.* **2005**, 23.

[5] Wolf, M. O. *Adv. Mater.* **2001**, *13*, 545.

[6] (a) Pickup, P. G. *J. Mater. Chem.* **1999**, *9*, 1641. (b) Cameron, C. G.; Pittman, T. J.; Pickup, P. G. J. *Phys. Chem. B* **2001**, *105*, 8838.

[7] Zotti, G., Zecchin, S.; Schiavon, G.; Berlin, A.; Pagani, G.; Canavesi, A. *Chem. Mater.* **1995**, *7*, 2309

[8] Martin, R. E.; Diederich, F. *Angew. Chem. Int. Ed.* **1999**, *38*, 1350.

[9] Cornil, J.; Beljonne, D.; Calbert, J-P.; Brédas, J-L. *Adv. Mater.* **2001**, *13*, 1053.

[10] (a) Altmann, M.; Enkelmann, V.; Beer, F.; Bunz, U. H. F. *Angew. Chem. Int. Ed. Engl.* **1995**, *34*, 569. (b) Tomita, I.; Nishio, A.; Endo, T. *Macromolecules* **1995**, *28*, 3042. (c) Bunz, U. H. F. *Pure Appl. Chem.* **1996**, *68*, 309. (d) Morisaki, Y.; Chen, H.; Chujo, Y. *Polym. Bull.* **2002**, *48*, 243.

[11] (a) Wolf, M. O.; Zhu Y.; *Adv. Mater.* **2000**, *12*, 599. (b) Higgins, S. J.; Jones C. L.; Francis, S. M. *Synth. Met.* **1999**, *98*, 211. (c) Foucher D. A.; Tang, B.; Manners, I. *J. Am. Chem. Soc.*, **1992**, *114*, 6246; (d) Bureteau, M. A.; Tilly, T. D. *Organometallics* **1997,** *13*, 4367.

[12] Zhu Y.; Wolf M. O. *Chem. Mater.* **1999**, *11*, 2995.

[13] Plenio, H.; Hermann, J.; Sehring, A. *Chem. Eur. J.* **2000**, *6*, 1820.

[14] Plenio, H.; Hermann J.; Leukel, J. *Eur. J. Inorg. Chem.* **1998**, 2063.

[15] (a) Joshi, K.K.; Pauson, P. L.; Quazi, A. R.; Stubbs, W. H. *J. Organomet. Chem.* **1964**, *1*, 471. (b) King, R. B.; Bisnette, M. B. *Inorg. Chem.* **1964**, *3*, 796.

[16] Groenendaal, L.; Peerlings, H. W. I.; van Dongen, J. L. J.; Havinga, E. E.; Vekemans, J. A. J. M.; Meijer, E. W. *Macromolecules* **1995**, *28*, 116.

[17] Martin, K. F.; Hanks, T. W. *Organometallics* **1997**, *16*, 4857.

[18] Graf, D. D.; Mann, K. R. *Inorg. Chem.* **1997**, *36*, 150.

[19] (a) Robin M. B.; Day, P. *Adv. Inorg. Chem. Radiochem.* **1967**, *10*, 247. (b) Allen, G. C.; Hush, N S. *Prog. Inorg. Chem.* **1967**, *8*, 357 (c) Demadis, K. D.; Hartshorn, C. M.; Meyer, T. J. *Chem. Rev.* **2001**, *101*, 2655.

[20] Barlow, S.; O'Hare, D. *Chem. Rev.* **1997**, *97*, 637.

[21] (a) Cameron, C. G.; Pickup, P. G. *Chem. Commun.* **1997**, 303. (b) Cameron, C. G.; Pickup, P. G. *J. Am. Chem. Soc.* **1999**, *121*, 7710. (c) Cameron, C. G.; Pickup, P. G. *J. Am. Chem. Soc.* **1999**, *121*, 11773.

[22] Netherton, M.R.; Fu, G. C. *Org. Lett.* **2001**, 3, 4295.

[23] (a) Audebert, P; Miomandre, F.; Zakrzewski, J. *J. Electroanal. Chem.* **2002**, *530*, 63. (b) Nakashima, S.; Tanaka, M.; Okuda, T. *Inorg. Chem. Commun.* **2002**, *5*, 312.

[24] Guay, J.; Kasai, P.; Diaz, A.; Wu, R.; Tour, J. M.; Dao, L. H. *Chem. Mater.* **1992**, *4*, 1097.

[25] (a) Zotti, G.; Schiavon, G. *Synth. Met.* **1990**, *39*, 183. (b) Schiavon, G.; Sitran, S.; Zotti, G. *Synth. Met.* **1989**, *32*, 209.

[26] Yu, H.-h.; Xu, B.; Swager, T. M. *J. Am. Chem. Soc.* **2003**, *125*, 1142.

[27] Ofer, D.; Crooks, R. M.; Wrighton, M. S. *J. Am. Chem. Soc.* **1990**, *112*, 7869.

[28] Bunel, E. E.; Campos, P.; Ruz, J.; Valle, L.; Chadwick, I.; Santa Ana, M.; Gonzalez, G.; Manriquez, J. M. *Organometallics* **1988**, *7*, 474.

[29] Bard, A. J.; Faulker, L. R. *Electrochemical Methods: Fundamentals and Applications* 2nd Edition, Wily & Sons: USA, 2001.

[30] *Handbook of Conducting Polymers*, Skotheim, T. A.,. Elsenbaumer, R. L, Reynolds, J. R. Eds. Marcel Dekker, New York, 1998.

[31] Chung, T.-C.; Kaufman, J. H.; Heeger, A. J.; Wudl, F. *Phys. Rev. B* **1984**, *30*, 702.

[32] Zhu, Y.; Wolf, M. O. *J. Am. Chem. Soc.* **2000**, *122*, 10121.

[33] (a) Groenendaal, L.; Jonas, F.; Freitag, D.; Pielartzik, H.; Reynolds, J. R. *Adv. Mater.* **2000**, *12*, 481. (b) Roncali, J.; Blanchard, P.; Frere, P. *J. Mater. Chem.* **2005**, *15*, 1589.

[34] Sutton, J. E.; Sutton, P. M.; Taube, H. *Inorg. Chem.* **1979**, *18*, 1017.

Chapter 5:

Polymerization of Thiophene Containing Cyclobutadiene Co Cyclopentadiene Complexes

Portions of this chapter have been accepted as a paper to Synthetic Metals

Introduction

Conducting polymers with metals incorporated into the polymer structure, known as conducting metallopolymers, are potentially useful materials in such applications as molecular actuators, electrocatalysts, sensors and NLO active materials.[1] The Swager research group has worked extensively on these types of materials and demonstrated their utility.[2] As an extension of this interest we have engaged in the synthesis of new conducting metallopolymers that can further increase our knowledge of how these materials function and interact. In this regard, a new conducting metallopolymer was designed with the incorporation of cyclobutadiene cobalt cyclopentadiene (CbCoCp) complexes. CbCoCp complexes have been utilized in liquid crystals, as the ridged structural feature for a molecular motor, macrocycle linkages and as groups to facilitate through space charge delocalization.[3]

The most important reason why CbCoCp was selected for this study is that the conjugation and charge migration of these polymers involves an interesting unit, namely the metal coordinated Cb. The free unbound Cb molecule is a highly unstable antiaromatic system.[4] The metal coordinated Cb, however, is extremely stable and displays some of the properties typical of aromatic systems.[5] We viewed that this pseudo aromaticity of the metal coordinated Cb system may instill interesting and useful properties into a conducting polymer. Charge migration through the Cb segment is of particular interest since it involves not only the pure carbon orbitals of the Cb ligand but also the π-bound metal orbitals acting as a single delocalized molecular structure. Conducting polymers with π-bound metals incorporated into their structure, e.g. ferrocene polymers, have previously been synthesized.[6] These polymers are in contrast to

the majority of conducting metallopolymers with segmented structures that have clearly delineated metal and conjugated polymer portions.[2d,7] The latter polymers have well defined molecular orbital structures that can lead to independent polymer and metal charge migration.

Complexes of CbCoCp have previously been incorporated by Bunz and coworkers into conjugated polymers as polyphenyleneethylene derivatives or 1, 3-diethynynl Cb homopolymers.[8] These materials were mostly studied for their liquid crystalline properties although the polybutadiyne Cb derivatives have been investigated for the delocalization through the Cb unit.[9] An oligomeric model study demonstrated a bathochromic shift in the UV-vis absorption as the number of monomer units increased.[10] This result supports the idea that some delocalization through the CbCoCp system is possible. Charge migration through the Cb system, however, was not investigated. Charge migration through a conjugated system is related to delocalization but also requires other properties such as the ability to stabilize cations and anions. Thus, the electrochemical characterization of the conjugated polymers containing CbCoCp poses a necessary step into understanding these polymers.

Another appeal of the CbCoCp system is that the $Co^{I/II}$ redox couple is present in the same region as typical conducting polymers.[11] This allows for the examination of a central theme in metal containing conducting polymers, namely how the metal redox properties affect the overall characteristics of the conducting polymer.[7] The consideration of the metal-polymer orbital interactions and the effect of these interactions on charge migration is critical for the design and application of conducting metallopolymers.

In the design of the polymers, it was assumed that the ethyne units would not allow facile charge migration since polyphenyleneethynylenes and its derivatives behave poorly under standard electrochemical conditions.[12] However, if instead thiophene units are selected as the conducting linkage then electrochemical characterization is possible.[13] Furthermore, a thiophene based monomer allows for versatile monomer syntheses and gives access to an oxidative polymerization route in the polymer synthesis. This chapter describes the synthesis, cyclic voltammetry, conductivity and UV-vis measurements of polythiophene analogues derived from the polymerization of thiophene containing CbCoCp complexes. It was discovered that the relative position of the thiophene fragment oxidation to the $Co^{I/II}$ redox couple determined the stability of the CbCoCp complex to the polymerization conditions.

Results and Discussion

General Synthetic Strategy

The synthesis of the CbCoCp complexes was accomplished by the dimerization of the appropriate alkynes with cyclopentadiene cobalt dicarbonyl ($CpCo(CO)_2$) or a derivative of the complex.[14] The desired ethynes were synthesized by a Songashira coupling reaction of aryl halides.[15] The complexes were characterized by NMR, mass spectrometry and single crystal X-ray diffraction. The electrochemical synthesis of the polymers was achieved by anodic electrochemical polymerization utilizing repeated cyclic voltammetry (CV) scans that deposited an insoluble polymer of unknown molecular weight onto the working electrode.

EDOT-Containing Complex

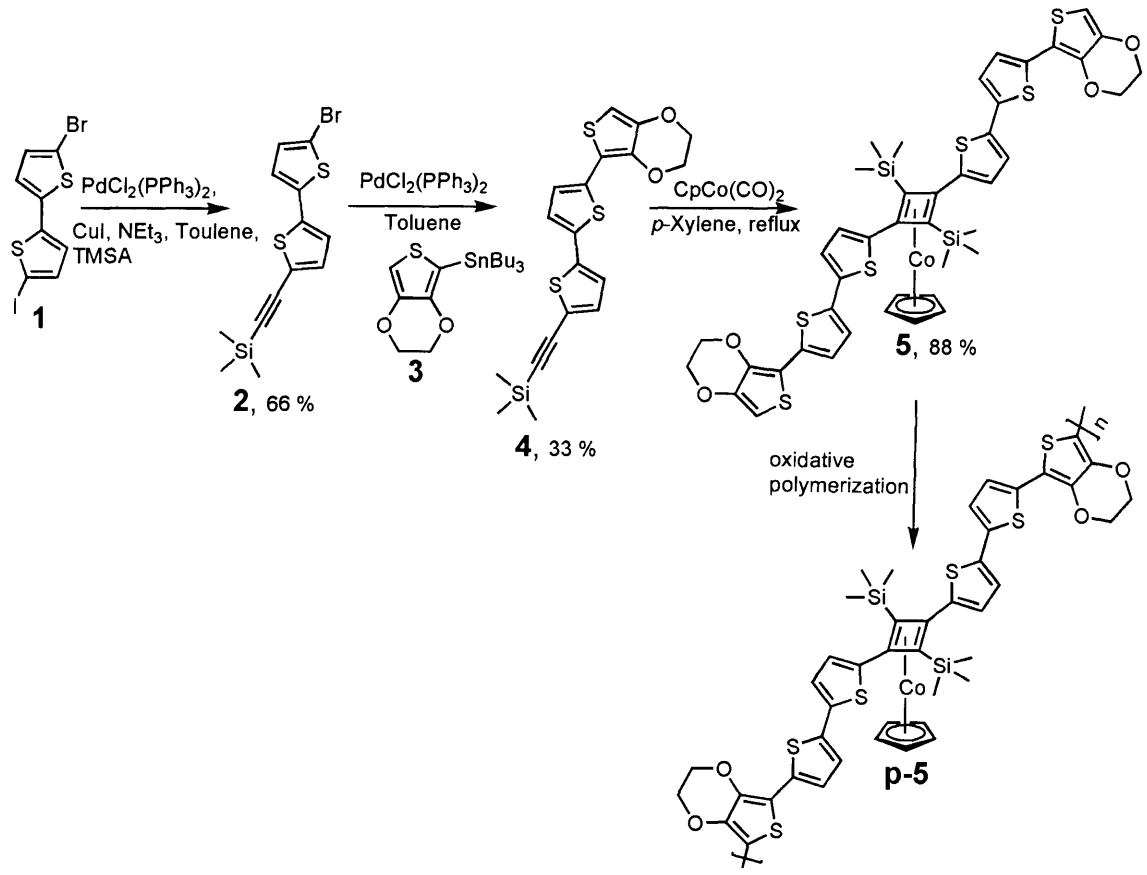

Scheme 1.

Scheme 1 illustrates the synthesis of a complex containing a 3,4-ethylenedioxythiophene (EDOT) unit. Complex **5** was the only complex synthesized that could be electrochemically polymerized while keeping the CbCoCp complexes of the polymer intact. The oxidation potential of the thiophene fragment in complex **5** is lower than the $Co^{I/II}$ redox couple by virtue of the EDOT unit connected to the end of a bithiophene fragment. Without the EDOT group, the oxidation potential of the pure bithiophene fragment is above the $Co^{I/II}$ redox. A series of these CbCoCp complexes

with bithiophene as the polymerizable unit was synthesized, and the characterization of the resulting polymers from these complexes will be discussed *vide infra.*

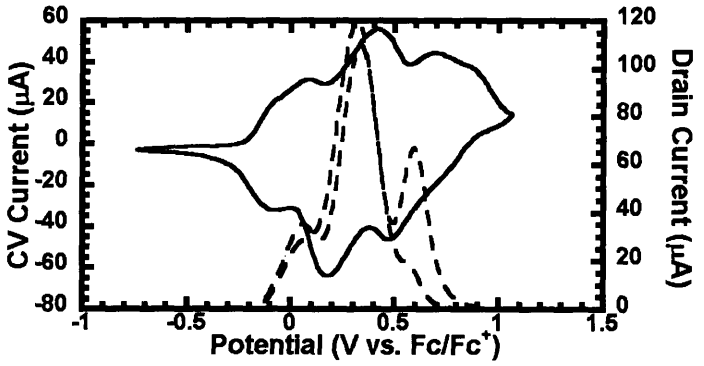

Figure 1. Cyclic voltammogram (solid line) at 100 mV/s and *in situ* conductivity (dashed line) of **p-5** grown onto interdigitated 5 μm Pt microelectrodes at 5 mV/s with 40 mV offset potential between the working electrodes.

The CV's and *in situ* conductivity of **p-5** are shown in Figure 1. The CV of **p-5** had three waves with half wave potentials ($E_{1/2}$'s) of -0.03, 0.34 and 0.58 V. The peak at 0.34 V was assigned as the metal wave. This assignment was based on two factors. First, the approximate potential value of the peak is near the expected value for this type of CbCoCp complex. The basis for this expectation is the fact that CbCoCp complex with four aryl groups on the Cb has an $E_{1/2}$ of approximately 0.5 V for the $Co^{I/II}$ redox couple and a CbCoCp complex with four alkyl groups on the Cb has an $E_{1/2}$ of approximately 0.1 V for the $Co^{I/II}$ redox couple.[11,16] Assuming that a trimethylsilyl (TMS) group has the same inductive donating ability as an alkyl group, the $E_{1/2}$ for $Co^{I/II}$ redox couple for complex **5** should be in near 0.3 V. Secondly, the prominent shape of the wave at 0.34 V resembled the metal wave seen previously in ferrocene oligomer work.[17] The peaks at -0.03 and 0.58 V were assigned as the oxidations of the organic fragment.

The use of Pt interdigitated microelectrodes as the working electrode in the electrochemical cell allowed the *in situ* conductivity to be measured.[18] The *in situ* conductivity of **p-5** displayed an onset of conductivity at -0.1 V, and the conductivity of the material displayed maxima at the potentials near the $E_{1/2}$'s of each wave. From this result, it can be interpreted that the oxidation of the Co centers enhanced the conductivity of the polymer. In these measurements, the drain current is directly proportional to the conductivity of the polymer and the measurement of the polymer film thickness permitted the maximum absolute conductivity of **p-5** to be measured (uncorrected for the resistance of the leads), at 4.1 x 10^{-3} S cm^{-1}.[19] The overall results suggested that the incorporation of the CbCoCp structure, at the very least, does not inhibit charge migration.

To further characterize the resulting polymer, a polymer film was grown on indium tin oxide (ITO) coated glass slide and spectroelectrochemistry was performed on the resulting film. The spectroelectrochemistry of **p-5** suggested that the metal coordinated

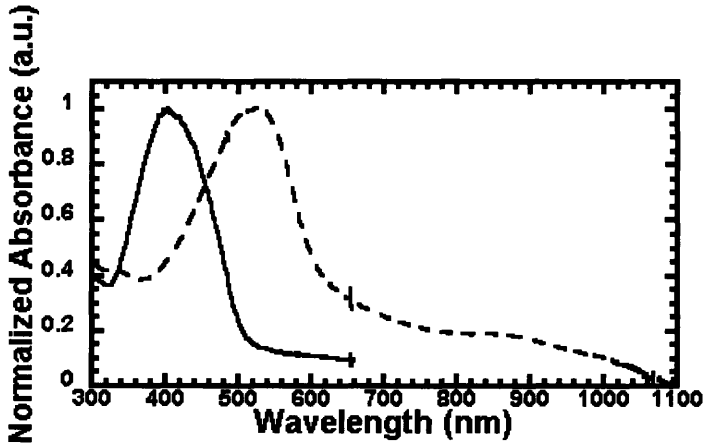

Figure 2. UV-vis absorption of complex **5** (bold line) and **p-5** (dashed line) coating an ITO slide

Cb has moderate charge migration ability. The monomer **5** in the solid state had a λ_{max} of 403 nm and the neutral polymer **p-5** had a λ_{max} of 518 nm, which corresponded to a red shift of 115 nm as seen in Figure 2.

Figure 3 shows that the oxidation of the polymer up to 0.4 V produced a broad absorption from approximately 660 nm to 850 nm. This result was consistent with the results of the *in situ* conductivity of the polymer which suggested that the metal center oxidation enhances the conductivity of the polymer. It can be seen that the oxidation of **p-5** at potentials of 0.4 V and higher gave rise to a band that tailed into the maximum observable wavelengths for the UV-vis instrument (1100 nm). The intensity of this long wavelength absorption band grew larger as the potential of the electrochemical cell was increased.

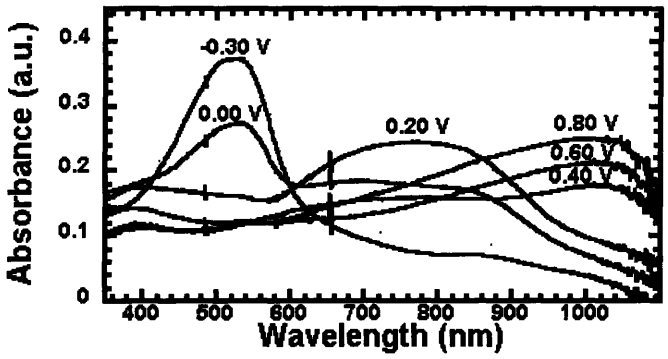

Figure 3. Changes in the UV-vis absorption at different potentials for a film of **p-5** grown onto ITO.

As mentioned earlier, the polymers that result from the bithiophene based monomers have significantly different behavior than **p-5**. The synthesis of a series of bithiophene complexes is shown in Scheme 2. The resulting polymer from complex **7**

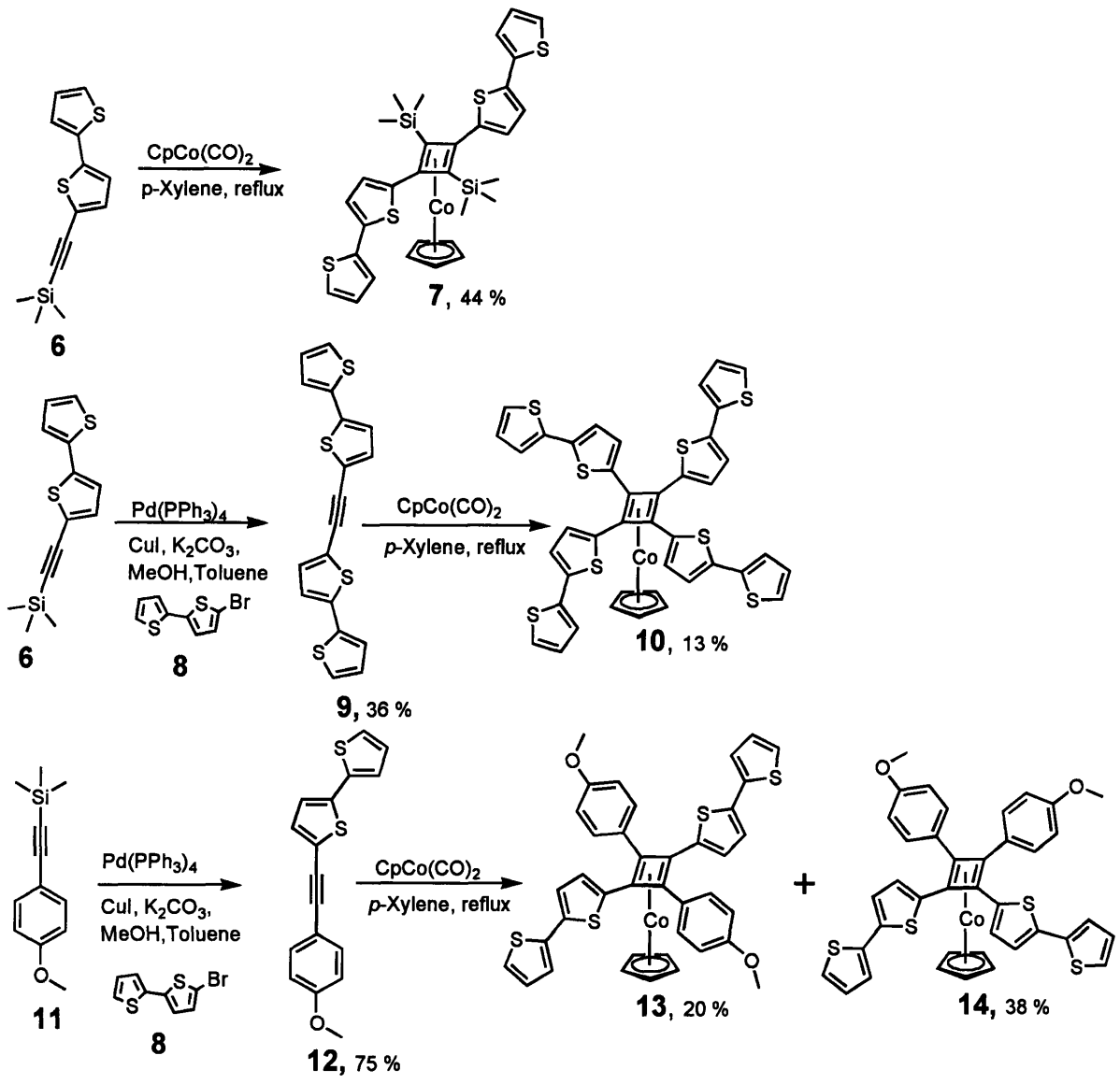

Scheme 2.

that provides the most direct comparison to **p-5**. The CV of **p-7** had two waves: a smaller wave at approximately -0.4 V and a larger broad wave at 0.5 V, as shown in Figure 4. The *in situ* conductivity of **p-7** had an onset of conductivity at approximately 0.65 V and the drain current did not plateau even to the edge of the solvent window.[20]

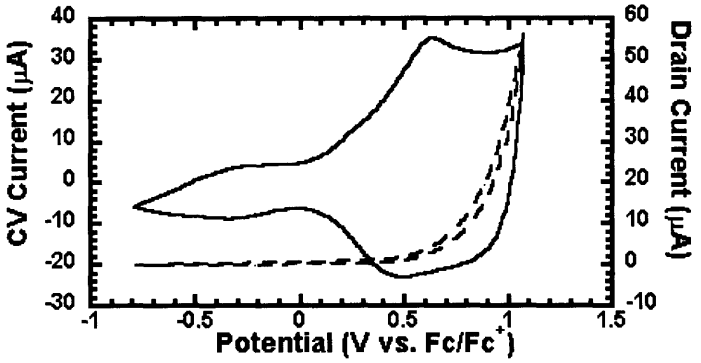

Figure 4. Cyclic voltammogram (solid line) at 100 mV/s and *in situ* conductivity (dashed line) of **p-7** grown onto interdigitated 5 μm Pt microelectrodes. The same *in situ* conductivity conditions for **p-5** were used for **p-7**.

Conducting polymers display finite windows of conduction, and the fact that **p-7** did not display a plateau or reduction suggested that the bands responsible for conduction were not depleted at these potentials.[21] The wave at -0.4 V did not seem to alter the conductivity of the polymer. The absolute conductivity of **p-7** was 1.4 x 10^{-3} S cm^{-1}.

The polymer from the tetrabithiophene complex, **p-10**, has similar electrochemical properties as **p-7**, as shown in Figure 5. This result was unusual since **p-10** should be a highly cross-linked polymer and this cross-linking may affect the three

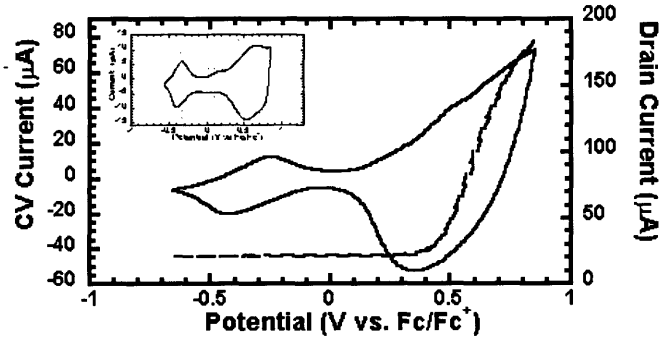

Figure 5. Cyclic voltammogram (solid line) at 100 mV/s and *in situ* conductivity (dashed line) of **p-10** grown onto interdigitated 5 μm Pt microelectrodes . Inset is the CV of **p-10** on a 2 mm^2 Pt button.

dimensional conduction network of the polymer.[22] Though unlike **p-7**, the CV profile of **p-10** seemed to depend on the type of electrode used for the polymerization, as shown in the inset of Figure 5. The absolute conductivity of **p-10** was 7.3 x 10^{-4} S cm^{-1}.

In order to probe how the relative position of the bithiophene segments affected the electrochemistry of the resulting polymers, two anisole derivatives, **13** and **14** were

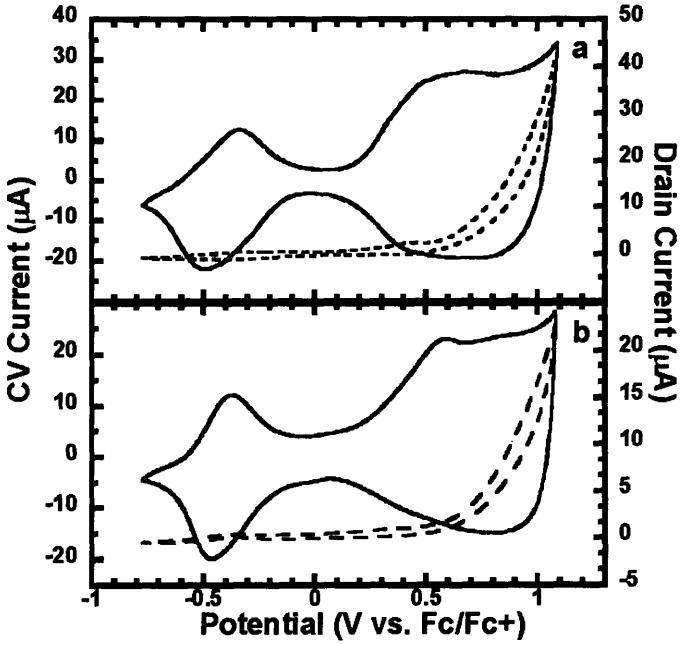

Figure 6. (a) Cyclic voltammogram (solid line) at 100 mV/s and *in situ* conductivity (dashed line) of **p-14**. (b) Cyclic voltammogram (solid line) at 100 mV/s and *in situ* conductivity (dashed line) of **p-13**.

synthesized. Anisole was chosen since the TMS substitution produced only the trans isomer in significant yields and the cis isomer could not be isolated. The methoxy groups also increased the polarity difference between the two isomers and thus facilitating the chromatographic separation of the two isomers. The cyclic voltammograms of both isomers were very similar to that of **p-7** and **p-10**, as shown in Figure 6. The CV's of both **p-13** and **p-14** exhibited waves in similar regions to the two waves that were present

in **p-7** and the on sets of conductivity for **p-13** and **p-14** appeared at approximately 0.1 V higher than for **p-7** and **p-10**. The *in situ* conductivities of **p-13** and **p-14** also displayed a larger hysteresis than either **p-7** or **p-10** and this result suggested greater structural reorganization in the oxidized, doped state. A minor difference between **p-13** and **p-14** was that **p-13** displayed a very slight drain current (conductivity) in a potential range near -0.4 V while the *in situ* conductivity of **p-14** displayed only the background Faradaic current at those potentials. It is not certain whether the different conjugation pathways of these polymers or their different morphologies were the source of these differences. This is a central problem of conducting polymers and requires macroscopic orientation to elucidate the causes of bulk properties.[23] The absolute conductivities of **p-13** and **p-14** were in the same range as **p-10**.

The spectroelectrochemistry of **p-10** is shown in Figure 7. The inherent absorption of the ITO coated glass substrate obscured most of the UV-vis spectra of the neutral polymer below 350 nm, allowing observation of only a large shoulder extending from 350 nm to 800 nm. As the polymer film was oxidized, the shoulder in the 350-500 nm region decreased in intensity and a new peak grew in at 735 nm.

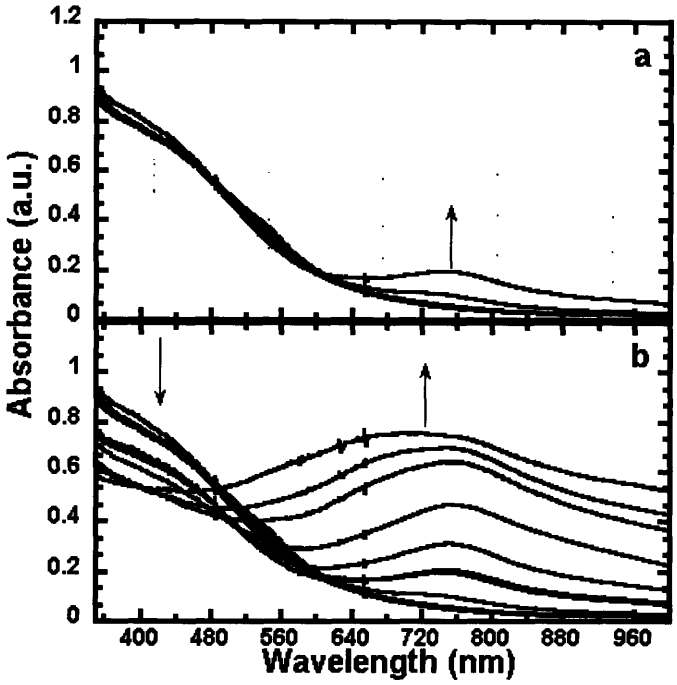

Figure 7. (a) Changes in the UV-vis absorption of a film of **p-10** grown onto ITO when the potential of the electrochemical cell was changed from -1.00 V to -0.20 V in 0.20 V intervals. (b) Changes in the UV-vis absorption of a film of **p-10** grown onto ITO when the potential of the electrochemical cell was changed from -1.00 V to 1.00 V in 0.20 V intervals.

This response occurred in potential regions (-0.85 to -0.25 V) of the first wave as well as the second wave (0.00 to 1.05 V) of the CV of the polymer film. However, at the higher potentials of the second wave, the changes in the UV-vis spectrum were more dramatic. The tailing of the peak at 735 nm to longer wavelengths is typical of conducting polymers and bands in the NIR region are often attributed to delocalized charges.[24] This result agreed with *in situ* conductivity results in that the changes in the conductivity of the polymer film occurred in this region. Polymers **p-7**, **p-13** and **p-14** had similar spectroelectrochemistry to **p-10**. The polymers displayed new long wavelength absorptions at potentials near -0.5 V, and much larger absorption changes were observed

at potentials above 0.20 V. For the anisole polymers, there was a difference between isomers. The absorption maximum for oxidized cis isomer polymer, **p-14**, was at 656 nm while the absorption of the oxidized **p-13** was at 729 nm, as show in Figure 8. As with the *in situ* conductivity, the origin of this difference can not be fully elucidated at present, it does suggest greater delocalization in **p-13** (trans isomer).

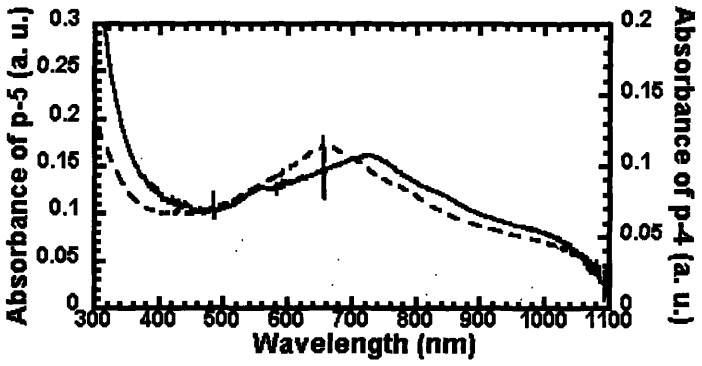

Figure 8. UV-vis absorption of the oxidized **p-13** (solid line) and **p-14** (dashed line) grown onto ITO.

Overall, only minor differences were observed for the electrochemistry of the polymers **p-7**, **p-10**, **p-13** and **p-14**. These results suggest that effects such as cross-linking or regiochemical issues do not significantly influence the electrochemistry of the resulting polymers. The results of the electrochemistry also lead to the conclusion that the composition of **p-7**, **p-10**, **p-13** and **p-14** is significantly different than **p-5**. This conclusion produced two important questions; what is the composition of **p-7** and similar polymers and why is it different from **p-5**?

Studies of the Polymer Composition

As an initial attempt to understand the composition of the polymers like **p-7**, X-ray photoelectron spectroscopy (XPS) was carried out on polymer films grown on ITO or polished steel. The XPS confirmed the presence of cobalt in all of the polymers. As another method to understand the composition of these polymers, monomers **21** and **22** were synthesized in an attempt to produce soluble versions of the polymers, as shown in Scheme 3.

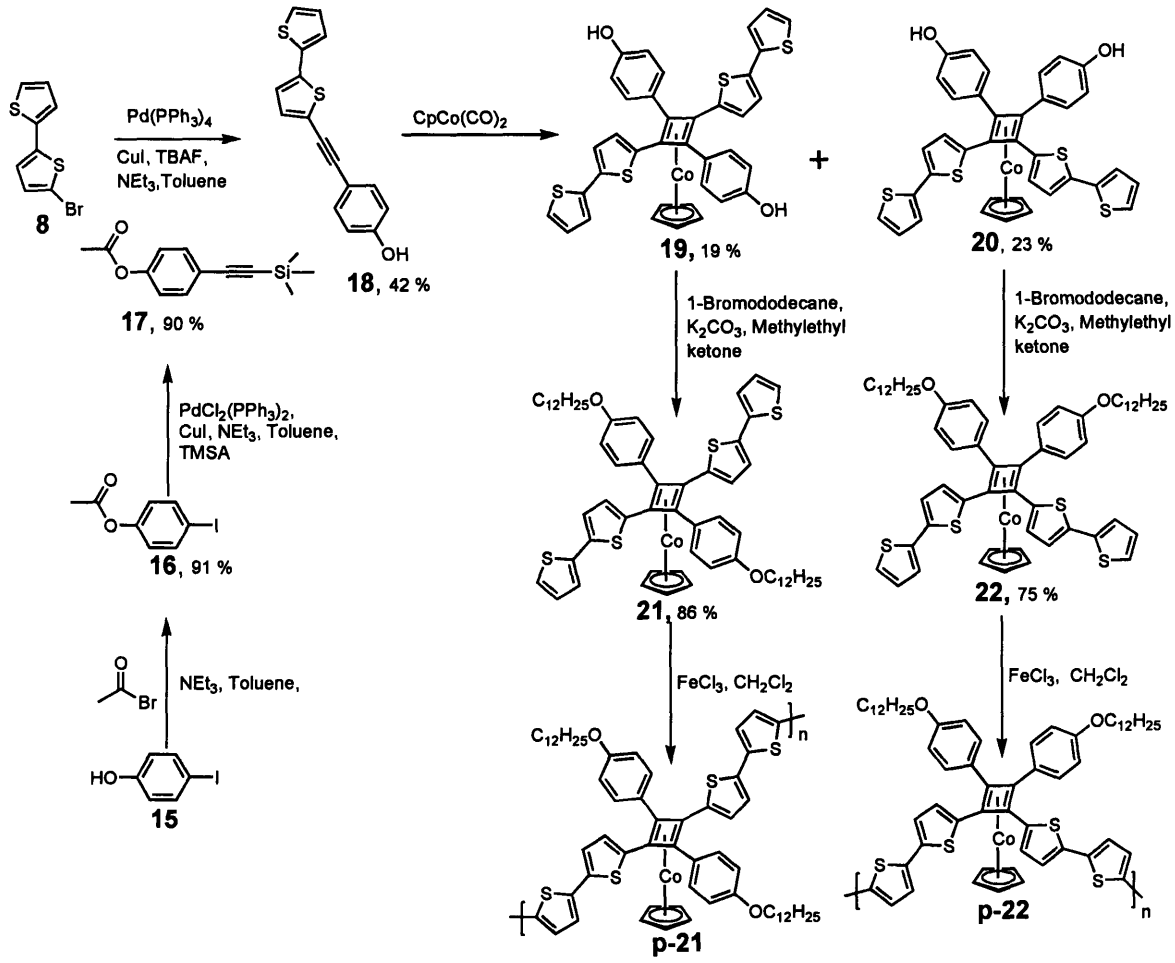

Scheme 3.

The polymerization was performed by $FeCl_3$ oxidation in dry CH_2Cl_2 to produce soluble oligomers with M_n = 6570 g/mol, PDI =1.56 for **p-21** and M_n = 3830 g/mol, PDI = 2.04 for **p-22** according to gel permeation chromatography (GPC) analysis. While ^1H demonstrated that the CoCp fragments were in place, a suitable ^{13}C could not be obtained for the polymers to investigate the presence of the Cb ring. One method to explore the composition of **p-7** and similar polymers is to change the Cp ligand to the1,2,3,4,5-pentamethyl derivative (Cp^*), as exemplified by complex **23** in Scheme 4.

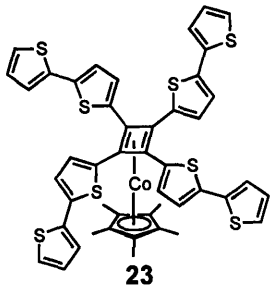

23

Scheme 4.

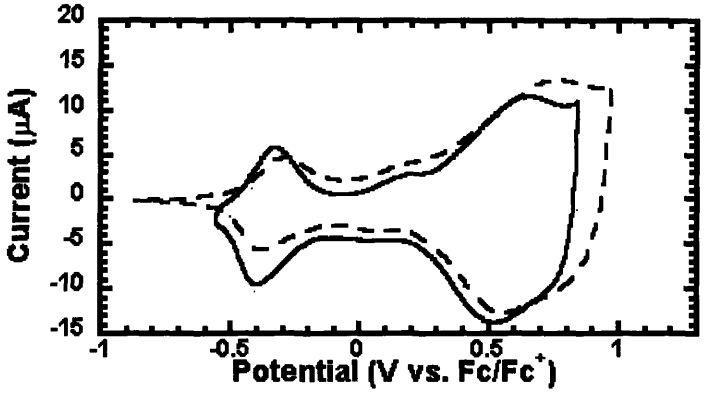

Figure 9. Cyclic voltammogram (solid line) of **p-10** and **p-23** (dashed line) at 100 mV/s on 2 mm^2 Pt button.

The Cp^* ligand has a well known inductive effect that lowers the metal oxidation of a sandwich complex.[25] The CV results of **p-23**, as shown in Figure 9, were not significantly different from that of **p-10**. This fact suggested that in **p-7** and similar polymers, a side reaction occurred. One possible side reaction that could have occurred in these polymers is a ligand (e.g.; thiophene) promoted insertion of the Co metal center into the Cb ring, as shown in Scheme 5. A Co insertion into Cb ring has been observed but it is usually thermally promoted.[26] The potential $Co^{III/IV}$ redox couple of the cobaltacyclopentadiene species is approximately -0.4 V and all the polymers derived from the bithiophene monomers had a wave at this potential.[27] Polymers of a similar molecular structure have been synthesized and these polymers have CV's similar to the polymers derived from the bithiophene monomers.[28] If the metal insertion does occur, the effect of the change in the Cp ligand on the oxidation potential of metal center shift would be significantly decreased. This effect is caused by the different orbital overlaps in a metallocyclopentadiene or similar complex versus a metal sandwich complex.[29]

However, another factor to consider is if the CoCp fragment was completely removed from polymer. This factor was considered by the oxidation of the complex **25**

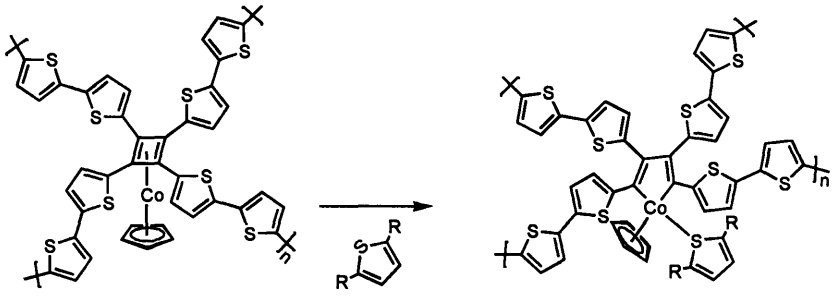

Scheme 5.

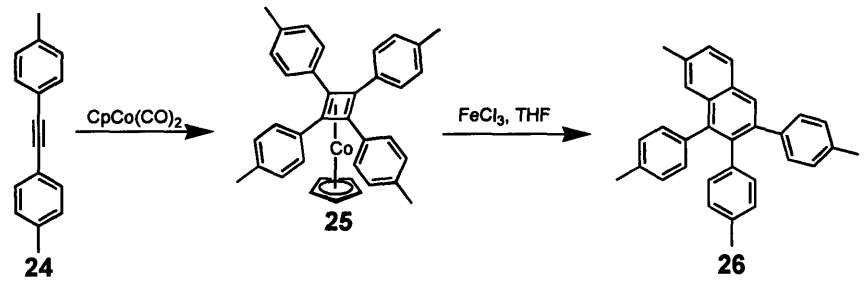

Scheme 6.

in the presence of a ligand like THF to see what possible products would occur, as shown in Scheme 6. The result was a rearrangement of the Cb ring that created a naphthalene structure. If this reaction did occur then it should place an aryl group in the main chain of a polythiophene. Typically, polythiophene derivatives with aryl groups substituted in the main polymer chain tend act as at least partially π-delocalized polymers.[30] The polymers like **p-7** did not seem to act as fully π-delocalized polymers and these types of aryl substituted polythiophene derivatives tend not to have any electroactivity in region near -0.4 V. However, the electroactivity in region near -0.4 V could be due to an impurity, such as completely disproportionated Co^{2+} centers, so this possibility can not be completely ruled out.

Model Study

To understand why the CbCoCp complexes in polymers like **p-7** appear to decompose, it is important to understand the metal to metal interaction within the polymer. There are three types of metal to metal interaction: charge hopping, mediated and superexchange. Charge hopping is similar to outer sphere inorganic electron transfer.[31] The mediated interaction is a two-step process with involving metal to polymer electron exchange then polymer to metal electron exchange.[32] To maximize this

interaction, the oxidation waves of the metal and the polymer should be as closely matched as possible. The superexchange interaction involves interactions similar to those observed in mixed-valence metal complexes and the methods to describe mixed valence interactions can be applied to the conducting polymer systems. [33] To assess the metal to metal communication in **p-7** and similar polymers, model compounds **29** and **30** were synthesized, as shown in Scheme 7. The CV's of both compounds were quasireversible.

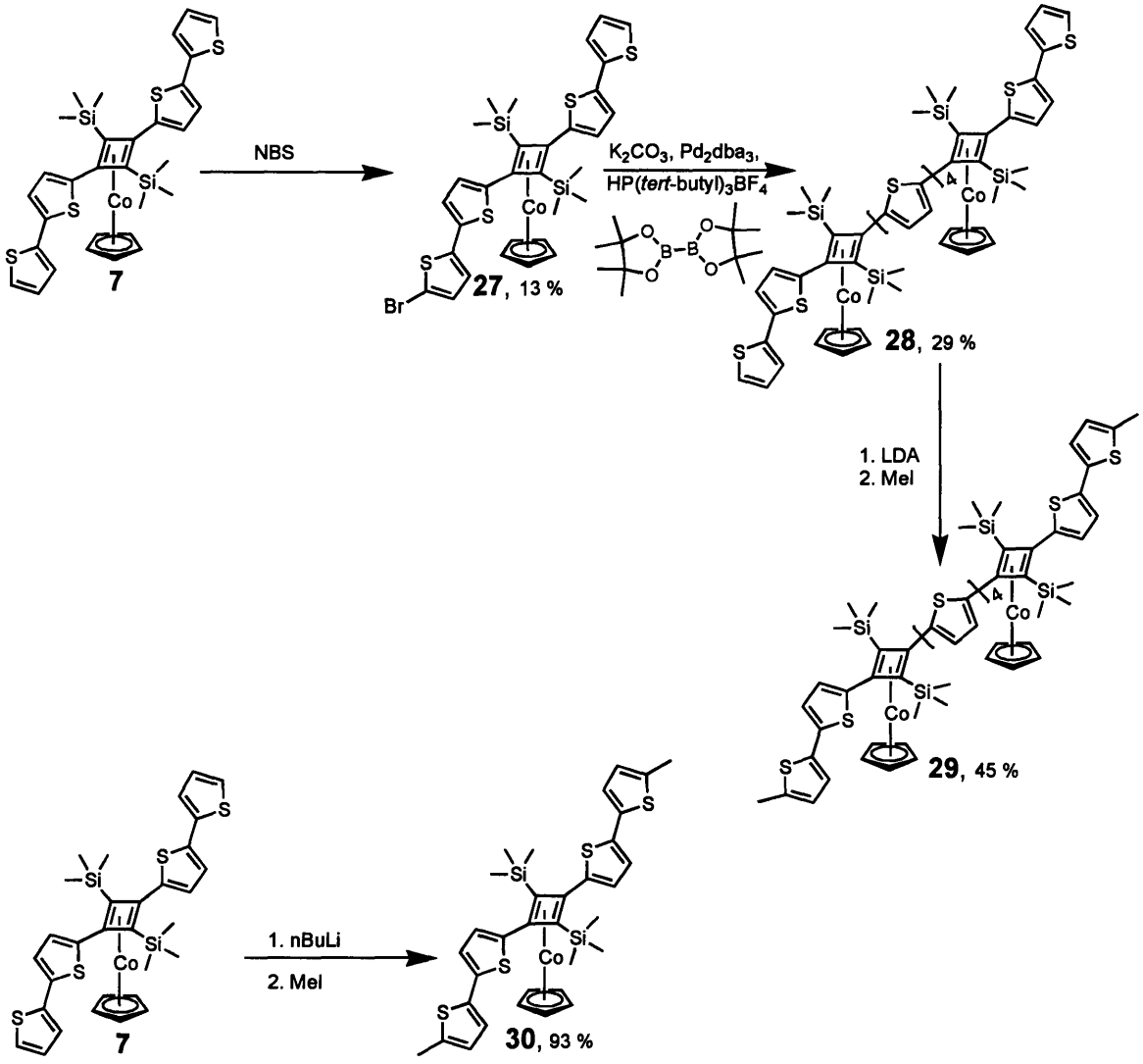

Scheme 7.

The results of this model study were clearly displayed in differential pulse voltammetry (DPV) of the model compounds as seen in Figure 10. The DPV displayed two peaks for complex **30** and three peaks for complex **29**. Both **29** and **30** display peaks near 0.30 V and 0.50 V. Complex **29** also displayed an additional peak at 0.9 V. The peaks near 0.3 V were assigned to the $Co^{I/II}$ redox couple using the same arguments as the wave assignment in **p-5**. Since only a single redox event for Co metal centers of complex **29** was observed, it was concluded that there was not significant electronic communication between the metal centers through the thiophene fragment.[34] This result suggested that a superexchange type interaction was not likely. The DPV of complex **29** also demonstrated that the thiophene fragment oxidation was clearly separate from the $Co^{I/II}$ redox couple which decreased the probability of mediated type interactions. Without a superexchange or mediated mechanism for the communication between the metal centers, the only possible interaction is the charge hopping mechanism. Since charge hopping is an inefficient mechanism for metal to metal communication, the oxidized metal centers would remain in isolated sites within the polymer. This isolation could be the cause of the side reactions. In comparison, the metal to metal interactions of **p-5** are significantly enhanced by having the thiophene fragment oxidation below that of the $Co^{I/II}$ redox couple. When the Co sites are oxidized in **p-5**, the polymer is already in a conductive state which should greatly facilitate the metal to metal interactions.

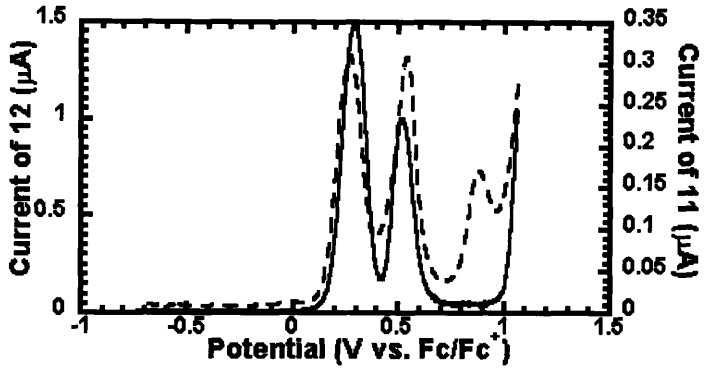

Figure 10. Differential pulse voltammetry of complex **29** (dashed line) and complex **30** (solid line) with a pulse height of 10 mV and scan rate of 2 mV/s on a 2 mm^2 Pt button.

The significant improvement in the electroactive properties (e.g.; conductivity) from **p-5** to **p-7** and similar polymers could be, in part, attributed to a more fully conjugated polymer with the Cb unit in the polymer main chain rather than the metal inserted into the polymer main chain. However, the fact that monomer **5** has a terthiophene fragment versus a bithiophene for monomer **7** may also account for the increase conjugation length from **p-7** to **p-5**. Since these polymers should have significantly different molecular structures, a comparison between the polymers has a limited value but it appears that the metal coordinated Cb has a moderate ability to allow charge migration.

Conclusions

A series of CbCoCp complexes containing thiophene units was synthesized and polymerized electrochemically. The viability of an oxidative polymerization with these CbCoCp complexes was determined by the relative position of the oxidation potential for the thiophene fragment. According to the electrochemical characterization, if the

oxidation potential of the thiophene fragment was below the $Co^{I/II}$ redox couple then the CbCoCp complex remained intact. If the oxidation potential of the thiophene fragment was above the $Co^{I/II}$ redox couple then it appeared that there was some decomposition of the CbCoCp complexes during the polymerization.

Experimental Section

General Comments

^1H and ^{13}C NMR spectra were recorded on a Bruker 400 MHz spectrometer and are referenced to residual $CHCl_3$ (7.27 ppm for ^1H and 77.23 ppm for ^{13}C) or $CHDCl_2$ (5.32 ppm for ^1H and 54.00 ppm for ^{13}C). Melting points are uncorrected. High-resolution mass spectra (HRMS) were determined on a Bruker Daltonics APEX II 3 Tesla FT-ICR-MS. The Pd catalysts and $CpCo(CO)_2$ were purchased from Strem. All other chemicals were purchased from Aldrich. The solvents were dried by passing through activated alumina and de-oxygenated by purging with Ar or by using a SPS-400-5 solvent purification system (Innovative Technologies). All air sensitive manipulations were performed using standard Schlenk techniques. Electrochemical measurements were performed in a nitrogen glovebox with an Autolab II with PGSTAT 30 potentiostat (Eco Chemie). The electrolyte solution for all electrochemical measurements, 0.1 M $(n\text{-}Bu)_4NPF_6$ in dry CH_2Cl_2, was stored over 4 Å molecular sieves in a glovebox. The quasi-internal reference electrode was a Ag wire submersed in 0.01 M $AgNO_3$/ 0.1 M $(n\text{-}Bu)_4NPF_6$ in anhydrous acetonitrile and a Pt wire or gauze was used as a counter electrode. All potentials were referenced to the Fc/Fc^+ couple. A 2 mm^2 Pt button (Bioanalytical), 5 μm Pt interdigitated microelectrodes (Abtech Scientific, Inc.) or indium tin oxide coated unpolished float glass slide (Delta Technologies) were used as the

working electrodes. Absorption spectra were collected on an Agilent 8453 diode array spectrophotometer. The GPC analysis was performed using a PLgel 5 μm Mixed -C column (300 x 7.5 mm) and a diode detector at 254 nm with a flow rate of 1 mL/min. in THF. The molecular weights were reported relative to polystyrene standards purchased from Polysciences Inc. A Dektak 6M stylus profiler (Veeco) was used to measure the film thickness of the polymers grown onto interdigitated microelectrodes. XPS measurements were collected on a Kratos Axis Ultra Imaging X-ray photoelectron spectrometer. Compounds **1**,[35] **3**,[2a] **24**,[36] and $[C_5(CH_3)_5]Co(CO)_2$[37] were synthesized according to published procedures. A Discovery model (CEM) microwave reactor was used for reactions involving heating by microwaves.

5'-Bromo-[2,2']bithiophene-5-ylethynl-trimethylsilane (2) To a 100 mL Schlenk flask was added 0.540 g of **1**, 15 mL of toluene, and 15 mL triethylamine. The solution was then de-oxygenated by purging with Ar for 15 min. To the solution was added 0.030 g of $PdCl_2(PPh_3)_2$, 0.12 g of trimethylsilyl acetylene (TMSA), and 0.150 g of CuI. The solution was stirred at room temperature for 20 hours. After stirring, the solution was flushed through silica gel pad with ethyl acetate. The solvent was evaporated in vacuo. Column chromatography was performed with silica gel using a gradient of 100 % hexanes to 10 % CH_2Cl_2 in hexanes. After evaporation under reduced pressure of the solvent, 0.328 g (66 %) of the product was obtained as a white solid, mp 88-90 °C. ^{1}H NMR ($CDCl_3$): 1H NMR (CDCl3): δ 7.13 (d J = 3.8 Hz, 1 H), 6.98 (d J = 3.9 Hz, 1 H), 6.95 (d J = 3.8 Hz, 1H), 6.92 (d J = 3.9 Hz, 1 H), 0.50 (s, 9 H) ppm. ^{13}C NMR ($CDCl_3$): δ 138.5, 138.1, 133.9, 131.2, 124.7, 123.9, 122.7, 112.2, 100.9, 97.6, 0.30 ppm. HRMS calcd for $C_{13}H_{13}BrS_2Si$ [M+]: 339.9406. Found 339.9403.

[5'-(3,4-ethylenedixoythiophene)-[2,2']bithiophene-5-ylethynyl]-trimethyl-silane (4) To a 10 mL microwave tube was placed 0.448 g of **2**, 1.31 g of **3**, 5 mL of dry toluene, and 0.050g of $PdCl_2(PPh_3)_2$ and then using a microwave reactor was heated to 130 °C for 30 min. After heating, the solution was washed with a 20 % aqueous KF solution. The organic solution was dried with $MgSO_4$ and the solvent was removed in vacuo. Column chromatography was performed with silica gel using 20 % CH_2Cl_2 in hexanes as an eluent. After evaporation of the solvent under reduced pressure, 0.177 g (33 %) of the product was obtained as a yellow-orange oil. ^{1}H NMR ($CDCl_3$): δ 7.15 (d J =3.8 Hz, 1 H), 7.11 (d J = 3.9 Hz, 1 H), 7.09 (d J = 3.8 Hz, 1H), 7.01 (d J = 3.9 Hz, 1 H), 6.27 (s, 1 H), 4.35 (m, 2 H), 4.25 (m, 2 H), 0.31 (s, 9 H) ppm. ^{13}C NMR ($CDCl_3$): δ 142.3, 139.4, 138.3, 135.0_4, 134.9_9, 134.0, 124.8, 123.7, 123.2, 121.8, 112.3, 100.5, 98.0, 97.9, 65.5, 65.0, 0.3_5 ppm. HRMS calcd for $C_{19}H_{18}O_2S_3Si$ $[M+Na]^+$: 425.0130. Found 425.0130

[η^4-1,3-(bis-[5'-(3,4-ethylenedioxythiophene)-[2,2']bithiophene])-2,4-(trimethylsilane)-cyclobutadieyl] [η^5-cyclopentadienyl]cobalt(I) (5) In a glovebox, 0.160 g of **4**, 0.061g of $CpCo(CO)_2$, 20 mL of *p*-xylene were placed into a 50 mL Schlenk flask. The flask was brought out of the glovebox, placed on a Schlenk line with a reflux condenser. The solution was then heated to reflux for 17 hours, cooled to room temperature and then the contents were filtered through an alumina plug with ethyl acetate. The solvent was removed in vacuo and column chromatography was performed with 30 % CH_2Cl_2 in hexanes as an eluent. After removal of solvent in vacuo, 0.162 g (88 %) of **5** was isolated as a red solid, mp 194-195 °C. The cis isomer could not be purified. ^{1}H NMR ($CDCl_3$): δ 7.13 (d J = 3.5 Hz, 2 H), 7.07 (d J = 3.5 Hz, 2 H), 6.93 (d J = 3.3 Hz, 2 H), 6.77 (d J = 3.3 Hz, 2 H), 6.26 (s, 2 H), 4.99(s, 5 H), 4.40 (m, 4 H), 4.29

(m, 4 H) 0.25 (s, 18 H) ppm. ^{13}C NMR ($CDCl_3$): δ 142.1, 141.2, 137.8, 136.4, 135.9, 133.6, 127.8, 123.6, 123.3, 123.2, 112.4, 97.2, 81.6, 80.6, 71.4, 65.3, 64.8 1.1 ppm. HRMS calcd for $C_{43}H_{41}Co\ O_4S_6Si_2$ $[M]^+$: 928.0194. Found 928.0204.

[2,2']Bithiophene-5-ylethynl-trimethylsilane (6) To a 100 mL Schlenk flask was added 2.51 g of **8**, 3.60 g of TMSA, 20 mL of toluene, and 40 mL triethylamine. The solution was then de-oxygenated by purging with Ar for 10 min. To the solution was added 0.200 g of $PdCl_2(PPh_3)_2$ and 0.260 g of CuI. The solution was heated to 80 °C for 12 hours. After heating, the solution was flushed through silica gel pad with ethyl acetate. The solvent was evaporated in vacuo. Column chromatography was performed with silica gel using hexanes as an eluent. After evaporation under reduced pressure of the solvent, 2.42 g (90 %) of the product was obtained as a pale yellow solid, mp 40.5-41.5 °C. ^1H NMR ($CDCl_3$): δ 7.25 (dd J = 2.7, 1.1 Hz, 1 H), 7.19 (dd J = 3.6, 1.1 Hz, 1 H), 7.15 (d J = 3.8 Hz, 1H), 7.03 (m, 2 H), 0.28 (s, 9 H) ppm. ^{13}C NMR ($CDCl_3$): δ 139.3, 137.1, 133.9, 128.4, 125.4, 124.7, 123.7, 122.2, 100.3, 97.8, 0.2_7 ppm. HRMS calcd for $C_{13}H_{14}S_2Si$ $[M]^+$: 262.0301. Found 262.0309.

[η^4-1,3-(bis-[2,2']bithiophene)-2,4-(trimethylsilane)-cyclobutadieyl] [η^5-cyclopentadienyl]cobalt(I) (7) In a glovebox, 2.42 g of **6**, 0.940 g of $CpCo(CO)_2$, 25 mL of *p*-xylene were placed into a 50 mL Schlenk flask. The flask was brought out of the glovebox, placed on a Schlenk line with a reflux condenser. The solution was then heated to reflux for 12 hours, cooled to room temperature and then the contents were filtered through an alumina plug with toluene. The solvent was removed in vacuo and column chromatography was performed with 10 % CH_2Cl_2 in hexanes as an eluent. After removal of solvent in vacuo, 1.30 g (44 %) of **7** was isolated as a yellow-brown solid, mp

175-176 °C. The cis isomer could not be purified. ^{1}H NMR ($CDCl_3$): δ 7.23 (dd J = 5.4, 1.0 Hz, 2 H), 7.19 (dd J = 3.7, 1.0 Hz, 2 H), 7.04 (dd J = 5.4, 3.6 Hz, 2 H), 6.97 (d J = 3.7 Hz, 2 H), 6.80 (d J = 3.7 Hz, 2 H), 5.01(s, 5 H), 0.27 (s, 18 H) ppm. ^{13}C NMR ($CDCl_3$): δ 141.3, 137.8, 136.4, 128.0, 127.7, 124.2, 123.6, 123.3, 81.6, 80.5, 71.5, 1.0 ppm. HRMS calcd for $C_{31}H_{33}CoS_4Si_2$ $[M]^+$: 648.0330. Found 648.0316.

Di-(5-[2,2']bithiophene)-acetylene (9) To a 100 mL Schlenk flask was added 1.18 g of **6**, 0.917 g of **8**, 25 mL of toluene, and 15 mL of methanol. The solution was de-oxygenated by purging with Ar for 20 min. To the solution was added 0.100 g of $Pd(PPh_3)_4$, 0.105 g of CuI and 6.07 g of K_2CO_3. The solution was heated to 80 °C for 12 hours. After heating, the solution was flushed through a silica gel pad with ethyl acetate. The solvent was removed in vacuo. Column chromatography was performed using a gradient of pure hexanes to 5% ethyl acetate in hexanes as an eluent. After evaporation of the solvent under reduced pressure, 0.482g (36 %) of the product was obtained as a bright yellow solid, mp 125-127 °C. Over time, the compound will decompose so it was stored under inert atmosphere. ^{1}H NMR ($CDCl_3$): δ 7.25 (dd J = 5.1, 1.2 Hz, 2 H), 7.20 (dd J = 3.6, 1.2 Hz, 2 H), 7.18 (d J = 3.9 Hz, 2 H), 7.07 (d J = 3.9 Hz, 2 H), 7.03 (dd J = 5.1, 3.6 Hz, 2 H) ppm. ^{13}C NMR ($CDCl_3$): δ 139.4, 136.7, 133.1, 128.1, 125.2, 124.4, 123.7, 121.4, 87.5 ppm. HRMS calcd for $C_{18}H_{10}S_4$ $[M]^+$: 353.9660. Found 353.9664.

[η^4-tetra[2,2']bithiophenecyclobutadienyl][η^5-cyclopentadienyl]cobalt(I) (10) In a glovebox, 0.28 g of **9**, 0.07g of $CpCo(CO)_2$, 10 mL of *p*-xylene were placed into a 25 mL Schlenk flask. The flask was brought out of the glovebox, placed on a Schlenk line and a reflux condenser was fitted to the flask. The solution was then heated to reflux for 24 hours, cooled to room temperature and then the contents were filtered through an alumina

plug with toluene. The toluene was removed in vacuo and silica gel column chromatography was performed with 5 % ethyl acetate in hexanes as an eluent. After evaporation under reduced pressure of the solvent, 51 mg (13 %) of **10** was isolated as a red-brown solid, mp 277.5 °C. ^{1}H NMR ($CDCl_3$): δ 7.25 (d J = 3.6 Hz, 4 H), 7.21 (m, 8 H), 7.04 (m, 8 H), 4.87 (s, 5 H) ppm. ^{13}C NMR ($CDCl_3$): δ 137.8, 137.6, 136.9, 128.4, 128.3, 124.8, 124.4, 124.0, 84.2, 69.9 ppm. HRMS calcd for $C_{41}H_{25}S_8CoNa$ $[M+Na]^+$: 854.8951. Found 854.9170.

5-(4-Methoxyphenylethynyl)-[2,2']Bithiophene (12) To a 100 mL Schlenk flask was added 2.49 g of **8**, 2.84 g of 4-methoxyphenylethynyl-trimethyl silane (**11**), 20 mL of toluene, and 50 mL methanol. The solution was then de-oxygenated by purging with Ar for 30 min. To the solution was added 8.0 g of K_2CO_3, 0.20 g of $PdCl_2(PPh_3)_2$ and 0.25 g of CuI. The solution was heated to 70 °C for 48 hours. After heating, water was added and the product was extracted with ethyl acetate, 2 x 20 mL. The organic layer was washed with 1 x 50 mL of concentrated NH_4Cl. The organic layer was dried with $MgSO_4$ and the solvent was removed in vacuo. Silica gel column chromatography was performed with 500 mL hexanes then a gradient of 5 to10 % ethyl acetate in hexanes. Removal of the solvent in vacuo gave 2.28 g (75 %) of the product as a light yellow solid, mp 93.8 °C. ^{1}H NMR ($CDCl_3$): δ 7.48 (d J = 8.6 Hz, 2 H), 7.32 (d J = 4.5 Hz, 1 H), 7.19 (d J = 3.5 Hz, 1H), 7.15 (d 3.7 Hz, 1 H), 7.06 (d J = 3.7 Hz, 1H), 7.02 (dd J = 4.5, 3.6 Hz, 1H), 6.91 (d J = 8.6 Hz, 2H), 3.84 (s, 3H) ppm. ^{13}C NMR ($CDCl_3$): δ 160.3, 138.9, 137.3, 133.4, 132.8, 128.4, 125.3, 124.6, 124.0, 122.9, 115.4, 114.6, 94.7, 81.9, 55.7 ppm. HRMS calcd for $C_{17}H_{12}S_2O$ $[M+H]^+$: 297.0402. Found 297.0401.

[η^4-1,3-(bis[2,2']bithiophene)-2,4-(4-Methoxyphenyl)-cyclobutadieyl] [η^5-cyclopentadienyl]cobalt(I) (13) and [η^4-1,2-(bis[2,2']bithiophene)-3,4-(4-Methoxyphenyl)-cyclobutadieyl] [η^5-cyclopentadienyl]cobalt(I) (14) In a glovebox, 0.944 g of **12**, 0.42 g of $CpCo(CO)_2$, and30 mL of *p*-xylene were placed into a 50 mL Schlenk flask. The flask was brought out of the glovebox, placed on a Schlenk line and a reflux condenser was fitted to the flask. The solution was then heated to reflux for 24 hours, cooled to room temperature and then the contents were filtered through an alumina plug eluting first with hexanes then with ethyl acetate. The solvent was removed in vacuo and column chromatography was performed with 20 % CH_2Cl_2 in hexanes as an eluent. Removal of the solvent in vacuo produced 268 mg (20 %) of **13** as a red-brown solid, mp 253 °C. ^{1}H NMR ($CDCl_3$): δ 7.63 (d *J* = 8.9 Hz, 4 H), 7.23 (dd *J* = 5.1, 1.1 Hz, 2 H), 7.10 (dd *J* = 3.6, 1.1 Hz, 2 H), 7.02 (dd *J* = 5.1, 3.6 Hz, 2 H), 6.99 (d 3.7 Hz, 2 H), 6.95 (d *J* = 3.7 Hz, 2 H), 6.88 (d *J* = 8.9 Hz, 4 H), 4.76 (s. 5 H), 3.88 (s, 6 H) ppm. ^{13}C NMR ($CDCl_3$): δ 158.9, 138.9, 138.0, 136.8, 130.4, 128.3, 127.5, 127.4, 124.5, 124.3, 123.7, 114.2, 84.5, 76.6, 68.4, 55.7 ppm. HRMS calcd for$C_{39}H_{29}S_4O_2Co$ $[M]^+$: 716.0377 Found 716.0396. A second fraction was collected with 40 % CH_2Cl_2 in hexanes as an eluent. After evaporation of the solvent under reduced pressure, 507 mg (38 %) of **14** was isolated as a red-brown solid, 93-96 °C. ^{1}H NMR ($CDCl_3$): δ 7.51 (d *J* = 8.6 Hz, 4 H), 7.22 (dd *J* = 5.1, 1.0 Hz, 2 H), 7.18 (dd *J* = 3.6, 1.0 Hz, 2 H) 7.05 (d *J* = 5.3 Hz, 2 H), 7.01 (m, 4 H), 6.83 (d *J* = 8.6 Hz, 4 H), 4.75 (s. 5 H), 3.84 (s, 6 H) ppm. ^{13}C NMR ($CDCl_3$): δ 158.6, 138.4, 137.9, 136.8, 130.1, 128.1, 127.6, 127.4, 124.3, 124.1, 123.6, 113.9, 83.5, 76.4, 68.2, 55.4 ppm. HRMS calcd for $C_{39}H_{29}S_4O_2Co$ $[M]^+$: 716.0377. Found 716.0384.

Acetic acid- 4-iodophenyl ester (16) To a 200 mL Schlenk flask were added 4.13 g of 4-iodophenol, **15**. The phenol was dissolved in 20 mL of dry triethylamine and 50 mL of dry toluene. The solution was cooled to 0 °C. To the solution was added 6 mL of acetyl bromide via syringe. The solution was then stirred for 12 hours after which 30 mL of methanol added via syringe into the flask to quench any excess acetyl bromide. Water was then added to the mixture and the product was extracted with CH_2Cl_2. The solution was dried with $MgSO_4$ and the solvent was removed in vacuo. Column chromatography was performed with silica gel using 40 % CH_2Cl_2 in hexanes as an eluent. After evaporation of the solvent under reduced pressure, 4.56 g (91 %) of **16** was isolated as a pungent oil. ^{1}H NMR ($CDCl_3$): δ 7.70 (d J = 8.8 Hz, 2 H), 6.88 (d J = 8.8 Hz, 2 H), 2.31 (s, 3 H) ppm. ^{13}C NMR ($CDCl_3$): δ 169.5, 150.9, 138.9, 124.5, 90.3, 21.6 ppm. HRMS calcd. for $C_8H_7IO_2Na$ $[M+Na]^+$: 284.9390 Found 284.9383.

Acetic Acid-4-trimethylsilanylethynyl-phenyl ester (17) To a 100 mL Schlenk flask were added 1.42 g of **16**, 3.50 g of TMSA, 20 mL of toluene, and 30 mL triethylamine. The solution was then de-oxygenated by purging with Ar for 20 min after which 0.10 g of $PdCl_2(PPh_3)_2$ and 0.150 g of CuI were then added to the solution. The solution was heated to 85 °C for 20 hours. After heating, the solution was passed through a silica gel pad with ethyl acetate. The solvent was removed in vacuo. Column chromatography was performed with silica gel using 40 % CH_2Cl_2 in hexanes as an eluent. After evaporation under reduced pressure of the solvent, 1.13 g (90 %) of the product was obtained as an off-white solid, mp 74.7 °C. ^{1}H NMR ($CDCl_3$): δ 7.49 (d J = 8.6 Hz, 2 H), 7.05 (d J = 8.6 Hz, 2 H), 2.31 (s, 3 H), 0.27 (s, 9 H) ppm. ^{13}C NMR ($CDCl_3$): δ 169.5.3, 151.0, 133.5,

122.0, 121.2, 104.6, 94.7, 21.5, 0.36 ppm. HRMS calcd for $C_{13}H_{14}S_2Si$ $[M+H]^+$: 233.0992. Found 233.0996.

4-[2,2']Bithiophenyl-5-ethynyl-phenol (18) To a Schlenk flask was added 0.90 g of **8**, 1.08 g of **17**, 15 mL of toluene, and 30 mL triethylamine. The solution was de-oxygenated by purging with Ar for 20 min after which 0.100 g of $Pd(PPh_3)_4$, 0.100 g of CuI and 2.5 g of TBAF were then added to the solution. The solution was heated to 85 °C for 20 hours. After heating, the solution was flushed through a silica gel pad with ethyl acetate. The solvent was removed in vacuo. Column chromatography was performed using a mixture of 1:1 CH_2Cl_2 to hexanes as an eluent. After removal of the solvent in vacuo, 0.432g (42 %) of the product was obtained as a pale yellow solid, mp 118-121 °C. The compound was stored under inert atmosphere. ^1H NMR ($CDCl_3$): δ 7.44 (d J = 8.8 Hz, 2 H), 7.26 (dd J = 5.4, 1.1 Hz, 1 H), 7.21 (dd J = 3.6 , 1.1 Hz, 1 H), 7.16 (d J = 3.8 Hz, 1 H), 7.08 (d J = 3.8 Hz, 1 H), 7.04 (dd J = 5.4, 3.6 Hz, 1 H), 6.84 (d J = 8.8 Hz, 2 H), 4.97 (s, 1 H) ppm. ^{13}C NMR ($CDCl_3$): δ 156.2, 138.9, 137.2, 133.6, 132.7, 128.4, 125.3, 124.5, 123.9, 122.7, 116.0, 115.6, 94.3, 81.7 ppm. HRMS calcd for $C_{18}H_{10}S_4$ $[M]^+$: 282.0168 Found 282.0165.

[η^4-1,3-(bis[2,2']bithiophene)-2,4-(4-hydroxyphenyl)-cyclobutadieyl] [η^5-cyclopentadienyl]cobalt(I) (19) and [η^4-1,2-(bis[2,2']bithiophene)-3,4-(4-hydroxyphenyl)-cyclobutadieyl] [η^5-cyclopentadienyl]cobalt(I) (20) In a glovebox, 1.21 g of **18**, 0.80g of $CpCo(CO)_2$, 35 mL of *p*-xylene were placed into a 100 mL Schlenk flask. The flask was brought out of the glovebox, placed on a Schlenk line with a reflux condenser. The solution was then heated to reflux for 24 hours, cooled to room temperature and then the contents were filtered through an alumina plug with methanol.

The solvent was removed in vacuo and column chromatography was performed with CH_2Cl_2 as an eluent. After removal of solvent in vacuo, 281 mg (19 %) of **19** was isolated as a brown solid, mp 190-193 °C. ^{1}H NMR ($CDCl_3$): δ 7.55 (d J = 8.4 Hz, 4 H), 7.22 (dd J = 4.8, 1.1, Hz, 2 H), 7.15 (dd J = 3.8, 1.1 Hz, 2 H), 7.01 (dd J = 4.8, 3.8 Hz, 2 H), 6.96 (d J = 3.7 Hz, 2 H), 6.92 (d J = 3.7 Hz, 2 H), 6.78 (d J = 8.4 Hz, 4 H), 4.77 (s. 2 H), 4.74 (s, 5 H) ppm. ^{13}C NMR ($CDCl_3$): δ 154.8, 138.8, 138.0, 136.8, 130.6, 128.3, 127.7, 127.4, 124.5, 124.2, 123.7, 115.6, 83.7, 76.4, 68.3 ppm. HRMS calcd for $C_{37}H_{25}S_4O_2Co$ [M-H]$^-$: 687.00 Found 686.99. A second fraction was collected with 40 % CH_2Cl_2 in acetonitrile as an eluent. After removal of the solvent in vacuo, 507 mg (38 %) of **20** was isolated as a brown solid, mp 123-125 °C. ^{1}H NMR ($CDCl_3$): δ 7.46 (d J = 8.5 Hz, 4 H), 7.23 (dd J = 5.1, 1.1 Hz, 2 H), 7.19 (dd J = 3.6, 1.1 Hz, 2 H) 7.03 (m, 6 H), 6.76 (d J = 8.5 Hz, 4 H), 5.07 (s, 2 H), 4.75 (s, 5 H) ppm. ^{13}C NMR ($CDCl_3$): δ 154.7, 138.4, 138.0, 137.0, 130.5, 128.4, 128.0, 127.6, 124.6, 124.3, 123.8, 115.6, 83.7, 76.4, 68.3 ppm. HRMS calcd for$C_{37}H_{25}S_4O_2Co$ [M-H]$^-$: 687.00. Found 686.99

[η^4-1,3-(bis[2,2']bithiophene)-2,4-(4-dodecyloxyphenyl)-cyclobutadieyl] [η^5-cyclopentadienyl]cobalt(I) (21) To a 50 mL Schlenk flask was added 0.246 g of **19**, 0.5 g of 1-bromododecane, 0.6 g of K_2CO_3, and 30 mL of methylethyl ketone. The solution was de-oxygenated by purging with Ar for 5 min then placed on a Schlenk line with a reflux condenser. The solution was heated to reflux for 12 hours. Water was added to the solution and the product was extracted with ethyl acetate, 2 x 20 mL. The organic layer was dried with $MgSO_4$ and the solvent was removed in vacuo. Column chromatography was performed with 30 % CH_2Cl_2 in hexanes as an eluent. After evaporation under reduced pressure of the solvent, 0.314 g (86 %) of the product was

isolated as a red-brown oil. ^{1}H NMR ($CDCl_3$): δ 7.61 (d J =8.8 Hz, 4 H), 7.23 (dd J = 5.1, 1.1 Hz, 2 H), 7.17 (dd J = 3.6, 1.1 Hz, 2 H), 7.03 (dd J = 5.1, 3.6 Hz, 2 H), 6.99 (d J = 3.7 Hz, 2 H), 6.95 (d J = 3.7 Hz, 2 H), 6.87 (d J =8.8 Hz, 4 H), 4.76 (s, 5 H), 4.00 (t J = 6.5 Hz, 4 H), 1.84 (tt J = 6.5, 7.9 Hz, apparent quintet, 4 H), 1.51 (m, 4 H), 1.31 (m, 32 H), 0.92 (t J = 6.7 Hz, 6 H) ppm. ^{13}C NMR ($CDCl_3$): δ 158.5, 139.0, 138.1, 136.7, 130.4, 128.3, 127.3, 127.2, 124.5, 124.2, 123.6, 114.6, 83.7, 76.6, 68.4, 68.3, 32.4, 30.1_2, 30.0_9, 30.0_5, 29.9, 29.8_8, 29.8_0, 29.7_8, 26.6, 23.1, 14.6 ppm. HRMS calcd for $C_{61}H_{73}CoO_2S_4$ $[M]^+$: 1024.38 Found 1024.36.

[η^4-1,2-(bis[2,2']bithiophene)-3,4-(4-dodecyloxyphenyl)-cyclobutadieyl] [η^5-cyclopentadienyl]cobalt(I) (22) The same experimental procedure was used as in the synthesis of **21** starting with 0.148 g of **20** and 0.165 g (75 %) of **21** was obtained as a red-brown oil. ^{1}H NMR ($CDCl_3$): δ 7.52 (d J = 8.8 Hz, 4 H), 7.23 (dd J = 5.2, 1.1 Hz, 2 H), 7.21 (dd J = 3.6, 1.1 Hz, 2 H), 7.07 (d 3.7 Hz, 2 H), 7.03 (m, 4 H), 6.84 (d J = 8.8 Hz, 4 H), 4.76 (s, 5 H), 4.00 (t J= 6.5 Hz, 4 H), 1.84 (tt J = 6.5, 7.9 Hz, apparent quintet, 4 H), 1.51 (m, 4 H), 1.32 (m, 32 H), 0.93 (t J =6.6 Hz, 6 H) ppm. ^{13}C NMR ($CDCl_3$): δ 158.4, 138.7, 138.1, 136.9, 130.3, 128.3, 127.6, 127.5, 124.5, 124.3, 123.7, 114.6, 83.7, 76.7, 68.4, 68.2, 32.3, 30.1_3, 30.1_0, 30.0_7, 29.8_9, 29.8_1, 26.6, 23.2, 14.6 ppm. HRMS calcd for $C_{61}H_{73}CoO_2S_4$ $[M]^+$: 1024.38 Found 1024.38.

General Procedure for the Synthesis of soluble polymers, p-21 and p-22 The appropriate monomer was placed into a 7 dram scintillation vial and placed in a glove box. The monomer was dissolved in CH_2Cl_2 and three equivalents of $FeCl_3$ were added. The solution was stirred in the glovebox for 24 hours. While still in the glovebox, 5 mL of dry methanol was added to the solution. The vial was taken out of the glovebox and

the contents were poured into a separatory funnel. Then 20 mL of $CHCl_3$ was added to the solution and the solution was washed 2 x 30 mL of con. NH_4OH. The solution was concentrated by solvent evaporation under reduced pressure and the concentrated solution poured into methanol to precipitate the polymer. The polymer was collected by centrifuge and dried in vacuo. **p-21** M_n =6570, M_w =10300 , PDI = 1.56, ^{1}H NMR ($CDCl_3$): δ 7.50, 7.21, 7.03, 4.80, 3.90, 1.70, 1.40, 0.90 ppm. **p-22** M_n =3830, M_w =7810 , PDI = 2.04 ^{1}H NMR ($CDCl_3$): δ 7.35, 7.21-6.90, 3.90, 3.50, 1.90, 1.40, 0.90 ppm.

[η^4-tetra[2,2']bithiophenecyclobutadienyl][η^5-(1,2,3,4,5)-pentamethylcyclopentadienyl]cobalt(I) (23) In a glovebox, 0.167 g of **9**, 0.070g of $Cp^*Co(CO)_2$, 20 mL of *p*-xylene were placed into a 25 mL Schlenk flask. The flask was brought out of the glovebox, placed on a Schlenk line and a reflux condenser was fitted to the flask. The solution was then heated to reflux for 24 hours, cooled to room temperature and then the contents were filtered through an alumina plug with toluene. The toluene was removed in vacuo and silica gel column chromatography was performed with 5 % ethyl acetate in hexanes as an eluent. After evaporation under reduced pressure of the solvent, the complex was recrystallized from $HCCl_3$ and hexanes and 22 mg (10 %) of **23** was isolated as a red solid, mp 164-166 C. ^{1}H NMR ($CDCl_3$): δ 7.23 (dd *J* = 5.4, 1.0 Hz, 4 H), 7.20 (dd *J* = 3.7, 1.05 Hz, 4 H), 7.18 (d *J* = 3.8 Hz, 4 H), 7.11(d *J* = 3.8 Hz, 4 H), 7.03 (dd *J* = 5.4, 3.6 Hz, 4 H), 1.60 (s, 15 H) ppm. ^{13}C NMR ($CDCl_3$): δ 137.9, 136.6, 135.9, 128.1, 127.0, 124.2, 123.5, 90.5, 67.8, 8.7 ppm. HRMS calcd for $C_{46}H_{35}S_8Co$ $[M]^+$: 901.9836. Found 901.9799.

[η^4-tetra-(4-methyl-benzene)cyclobutadienyl][η^5-cyclopentadienyl]cobalt(I) (25) In a glovebox, 1.00 g of **24**, 0.53 g of $CpCo(CO)_2$, 50 mL of p-xylene were placed into a 100 mL Schlenk flask. The flask was brought out of the glovebox, placed on a Schlenk line and a reflux condenser was fitted to the flask. The solution was then heated to reflux for 12 hours, cooled to room temperature and then the contents were filtered through an alumina plug with toluene. The toluene was removed in vacuo and silica gel column chromatography was performed with 20 % CH_2Cl_2 in hexanes as an eluent. After evaporation under reduced pressure of the solvent, 0.669 g (26 %) of **25** was isolated as a yellow solid. The physical and spectroscopic properties match those previously reported.[38]

7-Methyl-1,2,3-tri-*p*-tolyl-naphthalene (26) In a glovebox, 0.1651 g of **25** was placed in a 7 dram scintillation vial and dissolved in a 1:1 mixture of CH_2Cl_2 and THF. Three equivalents of $FeCl_3$ were added to the solution which was then stirred in the glovebox for 2 hours. . The vial was then brought of the glovebox and the solution was treated NH_2NH_2. Water was added to the solution and the products were extracted from the solution with CH_2Cl_2. The solvent was removed in vacuo and silica gel column chromatography was performed with 20 % CH_2Cl_2 in hexanes as an eluent. After evaporation under reduced pressure of the solvent, 0.023 g (36 %) of **26** was isolated as a white solid. The physical and spectroscopic properties match those previously reported.[39]

[η^4-1-(5-bromo-[2,2']bithiophene)-3-([2,2']bithiophene)-2,4-(trimethylsilane)-cyclobutadieyl] [η^5-cyclopentadienyl]cobalt(I) (27) To a round bottom flask was added 0.499 g of **7** with 20 mL of N, N' dimethylformamide. The flask was cooled to 0 °C and 0.15 g of N-bromosuccimide was added. The solution was stirred for 2.5 hours

then 40 mL of water was added to the flask. The product was extracted with diethyl ether. Dried with $MgSO_4$ and solvent was removed in vacuo. The residue was purified by column chromatography with 4 % CH_2Cl_2 in hexanes as an eluent. After removal of the solvent in vacuo, 75.6 mg (13 %) of **27** was obtained, mp 146.0-147.5 °C. ^{1}H NMR (CD_2Cl_2): δ 7.27 (dd *J* = 5.1, 1.1 Hz, 1 H), 7.19 (dd *J* = 3.6 , 1.1 Hz, 1 H), 7.05 (dd 5.1, 3.6 Hz, 1 H), 7.02 (d *J* = 3.9 Hz, 1 H), 6.98 (d *J*= 3.0 Hz, 1 H), 6.94 (m, 2 H), 6.82 (m, 2 H), 5.01 (s, 5 H), 0.26 (s, 18 H) ppm. ^{13}C NMR (CD_2Cl_2): δ 142.5, 141.6, 139.7, 138.0, 136.8, 135.5, 131.4, 128.4, 128.3, 124.6, 124.3, 123.9, 123.7_3, 123.6_8, 110.8, 81.9, 81.8, 81.0, 71.9, 1.0 ppm. HRMS calcd for $C_{31}H_{32}BrCoS_4Si_2$ $[M+H]^+$: 726.9514 Found 726.9524.

5,5'''-bis(1-[η^4-3-([2,2']bithiophene)-2,4-(trimethylsilane)-cyclobutadieyl] [η^5-cyclopentadienyl]cobalt(I)) [2,2',5',2'',5'',2'''']quarterthiophene (28) In a 10 mL Schlenk flask was added 0.0577 g of **27**, 0.044 g of bis(pinacolato)diboron, 0.40 g of K_2CO_3, 1 mL of THF, 0.5 mL of ethanol, and 0.25 mL of water. The solution was de-oxygenated by purging with Ar for 30 minutes after which 0.040 g of Pd_2dba_3 and 0.020 g of HP(*tert*-Bu)$_3BF_4$ were added. The reaction mixture was stirred for 24 hours at room temperature. After stirring, the reaction mixture was filtered through silica gel with ethyl acetate. The solvents were removed in vacuo. Column chromatography was performed with silica gel using a gradient of 10 % to 20 % CH_2Cl_2 in hexanes as an eluent. After evaporation under reduced pressure of the solvent, the product was isolated 0.0145 g (29 %) mp, 242-244 °C. ^{1}H NMR (CD_2Cl_2): δ 7.27 (d *J* = 5.1 Hz, 2 H), 7.20 (d *J* = 2.9 Hz, 2 H), 7.13 (m, 4 H), 7.10 (dd, *J* = 4.0, 5.1 Hz, 2 H), 7.00. (m, 4 H), 6.84 (m, 4 H) 4.98 (s, 10 H), 0.2_4 (s, 36 H) ppm. ^{13}C NMR (CD_2Cl_2): δ 142.2, 141.6, 138.0, 136.9, 136.7,

136.2, 136.0, 128.4, 128.3, 124.8, 124.6, 124.3, 124.0, 123.9, 123.6, 81.9, 81.0, 80.6, 71.8, 1.0 ppm. HRMS calcd for $C_{62}H_{64}Co_2S_8Si_4$ $[M+H]^+$: 1295.0588 Found 1295.0557.

5,5'''-bis(1-[η^4-3-(5-methyl-[2,2']bithiophene)-2,4-(trimethylsilane)-cyclobutadieyl] [η^5-cyclopentadienyl]cobalt(I)) [2,2',5',2'',5'',2''']quarterthiophene (29) To a 10 mL Schlenk flask was added 0.0054 g of **28** with 10 mL of dry THF. The solution was cooled to -78 °C then 0.2 mL of 2 M solution of lithium diisopropylamide in THF was added to the solution. The solution was stirred for 2 hours before 0.4 mL of methyl iodide was added. After stirring overnight, the solvent removed. Silica gel column chromatography was performed on the residue using 10 % CH_2Cl_2 in hexanes as an eluent. After evaporation under reduced pressure of the solvent, the product was isolated 0.0025 g (45 %), mp, 224-226 °C. ^{1}H NMR (CD_2Cl_2): δ 7.11 (m, 4 H), 6.98 (m, 4 H), 6.89 (d J = 3.6 HZ, 2 H), 6.84 (d J = 3.6 Hz, 2 H), 6.80 (d J = 3.7 Hz, 2 H), 6.71 (dd J = 3.6, 1.1 Hz, 2 H) 5.01 (s, 10 H) 0.2_3 (s, 36 H) ppm. ^{13}C NMR (CD_2Cl_2): δ 142.1, 140.9, 139.6, 137.2, 135.7, 128.3, 128.1, 126.5, 124.8, 124.3, 124.0, 123.5, 123.2, 123.1, 81.9, 81.8, 80.6, 71.8, 15.6, 0.9_7 ppm. HRMS calcd for $C_{36}H_{22}S_6$ $[M]^+$: 1323.0901 Found 1323.0937.

[η^4-1,3-(bis-5-methyl-[2,2']bithiophene)-2,4-(trimethylsilane)-cyclobutadieyl] [η^5-cyclopentadienyl]cobalt(I) (30) To a 10 mL oven dried Schlenk flask was added 0.116 g of **7** with 2 mL of dry THF. The solution was cooled to -78 °C and 0.25 mL of a 2.2 M solution of n-butyl lithium was syringed into flask. The resulting solution was stirred for 1 hour at -78 °C after which, 0.25 mL of methyl iodide was added. The solution was then stirred overnight. Solvent was removed and column chromatography was performed on the residue with 10 % CH_2Cl_2 in hexanes as an eluent. After removal of solvent in vacuo,

0.114 g (93 %) of **30** was isolated as a yellow-brown solid, mp 162.5-163.3 °C. ^{1}H NMR ($CDCl_3$): δ 6.95 (d J = 3.4 Hz, 2 H), 6.85 (d J = 3.6 Hz, 2 H), 6.75 (m, 2 H), 6.67 (d J = 3.6 Hz, 2 H), 4.97 (s, 5 H), 2.49 (s, 6 H), 0.24 (s, 18 H) ppm. ^{13}C NMR ($CDCl_3$): δ 140.7, 139.0, 136.9, 135.6, 127.7, 126.2, 123.2, 122.9, 81.5, 80.7, 71.3, 15.7, 1.1 ppm. HRMS calcd for $C_{33}H_{37}CoS_4Si_2$ $[M+H]^+$: 677.0721 Found 677.0737.

References

[1] (a) Pickup, P. G. *J. Mater. Chem.* **1999**, *9*, 1641. (b) Wolf, M. O. *Adv. Mater.* **2001**, *13,* 545. (c) Kingsborough, R. P.; Swager, T. M. *Prog. Inorg. Chem.* **1999**, *48,* 123.

[2] (a) Zhu, S. S.; Swager, T. M. *J. Am. Chem. Soc.* **1997**, *119,* 12568. (b) Kingsborough, R. P.; Swager, T. M. *J. Am. Chem. Soc.* **1999,** *121*, 8825. (c) Buey, J.; Swager, T. M. *Angew. Chem. Int. Ed.* **2000**, *39*, 608. (d) Kingsborough, R. P.; Swager, T. M. *Chem. Mater.* **2000**, *12*, 872. (e) Vigalok, A.; Zhu, Z.; Swager, T. M. *J. Am. Chem. Soc.* **2001,** *123*, 7917; (f) Shioya, T.; Swager, T. M. *Chem. Commun.* **2002,** 1364.

[3] (a) Altmann, M.; Bunz, U. H. F. *Angew. Chem., Int. Ed. Engl.* **1995,** *34*, 569. (b) Zheng, X.; Mulcahy, M. E.; Horinek, D.; Galeotti, F.; Magnera, T. F.; Michl, J. *J. Am. Chem. Soc.* **2004**, *126*, 4540. (c) Virtue, G. A.; Coynr, N. E.; Hamilton, D. G. *J. Org. Chem.* **2002**, *67*, 6856. (d) Stoll, M. E.; Lovelace, S. R.; Geiger, W. E.; Schimanke, H.; Hyla-Kryspin, I.; Gleiter, R. *J. Am. Chem. Soc.* **1999**, *121*, 9343.

[4] Mair, G. *Angew. Chem. Int. Ed. Engl.* **1988**, *27*, 309.

[5] Fiztpatrick, J. D.; Watts, L.; Emerson, G. F.; Petit, R. *J. Am. Chem. Soc.* **1965**, *87* 3254.

[6] (a) Wolf, M. O.; Zhu, Y. *Adv. Mater.* **2000**, *12*, 599. (b) Zhu, Y.; Wolf, M. O. *Chem. Mater.* **1999**, *11*, 2995. (c) Higgins, S. J.; Jones, C. L.; Francis, S. M. *Synth. Met.* **1999**, *98*, 211. (d) Foucher, D. A.; Tang, B.; Manners, I. *J. Am. Chem. Soc.* **1992**, *114*, 6246; (e) Bureteau, M. A.; Tilly, T. D. *Organometallics* **1997**, *13*, 4367.

[7] Holliday, B. J.; Swager, T. M. *Chem. Commun.* **2005**, 23.

[8] (a) Rozhanskii, I. L.; Tomita, I.; Endo, T. *Macromolecules* **1997**, *30*, 1222. (b) Altmann, M.; Enkelmann, V.; Lieser, G.; Bunz, U. H .F *Adv. Mater.* **1995**, 7, 726.

[9] (a) Altmann, M.; Bunz, U. H. F. *Marcomol. Rapid Commun.* **1994**, *15*, 785. (b) Steffen, W.; Bernhard, K.; Altmann, M.; Scherf, U.; Stitzer, K.; zur Loye, H.; Bunz, U. H. F. *Chem. Eur. J.* **2001**, *7*, 117.

[10] Altmann, M.; Enkelmann, V.; Beer, F.; Bunz, U. H. F. *Organometallics* **1996**, *15*, 394.

[11] Koelle, U. *Inorg. Chim. Acta.* **1981**, *47*, 13.

[12] Ofer, D.; Swager, T. M.; Wrighton, M. S. *Chem. Mater.* **1995**, *7*, 418.

[13] *Handbook of Conducting Polymers* Skotheim, T. A., Elsenbaumer, R. L., Reynolds, J. R. Eds.; Marcel Dekker: New York, 1998

[14] (a) Rausch: M. D.; Genetti, R. A. *J. Am. Chem. Soc.* **1967**, *89*, 5502. (b) Clearfield, A.; Gopal, R.; Rausch, M. D.; Tokas, E. F.; Higbie, F. A. Bernal, I. *J. Organomet. Chem.* **1977**, *135*, 229.

[15] Songashira, K.; Tohda, Y.; Hagihara, N. *Tetraherdon Lett.* **1975**, *50*, 4467.

[16] Roers, R.; Rominger, F.; Gleiter, R. *Tetrahedron Lett.* **1998**, *39*, 6695.

[17] Zhu, Y.; Wolf, M. O. *J. Am. Chem. Soc.* **2000**, *122*, 10121.

[18] White, H. S.; Kittlesen, G. P.; Wrighton, M. S. *J. Am. Chem. Soc.* **1984**, *106*, 5375.

[19] (a) Zotti, G.; Schiavon, G. *Synth. Met.* **1990,** *39,* 183. (b) Schiavon, G.; Sitran, S.; Zotti, G. *Synth. Met.* **1989**, *32*, 209.

[20] Bard, A. J.; Faulker, L. R.; *Electrochemical Methods: Fundamentals and Applications* 2nd Edition, Wiley & Sons, USA, 2001.

[21] Ofer, D.; Crooks, R. M.; Wrighton, M. S. *J. Am. Chem. Soc.* **1990**, *112*, 7869.

[22] Jang, S.; Sotzing, G. A.; Marquez, M. *Macromolecules* **2004**, *37*, 4351. (b) Stepp, B.; Nguyen, S. T. *Macromolecules* **2004**, *37*, 8222.

[23] Tolbert, L. T. *Acc. Chem. Res.* **1992**, *25*, 561.

[24] (a) Patil, A. O.; Heeger, A. J.; Wudl, F. *Chem. Rev.* **1988**, *88*, 183; (b) Chen, X.; Inganäs, O. *J. Phys. Chem.* **1996**, *100*, 15202.

[25] Schaller, R. J.; Haberhauer, G.; Gleiter, R.; Rominger, F. *Eur. J. Inorg. Chem.* **2002**, 2296.

[26] Gleiter, R.; Werz, D. B. *Organometallics* **2005**, *24*, 4316.

[27] Kelly, R. S.; Geiger, W. E. *Organometallics* **1987**, *6*, 1432.

[28] (a) Matsuoka, I.; Aramki, K.; Nishihara, H. *J. Chem. Soc. Dalton Trans.* **1998**, 147. (b) Matsuoka, I.; Yoshikawa, H; Kurihara, M.; Nishihara, H.; *Synth. Met.* **1999**, *102*, 1519.

[29] Miller, E. J.; Landon, S. J.; Brill, T. B. *Organometallics* **1985**, *4*, 533.

[30] Reynolds, J. R.; Ruiz, J. P.; Child, A. D.; Nayak, K.; Marynick, D. S. *Macromolecules* **1991**, *24*, 678.

[31] (a) Atwood, J. D. *Inorganic and Organometallic Reaction Mechanisms,* Wiley, New York, 1997.

[32] Cameron, C. G.; Pittman, T. J.; Pickup, P. G. *J. Phys. Chem. B* **2001**, *105*, 8838.

[33] (a) Robin, M. B.; Day, P. *Adv. Inorg. Chem. Radiochem.* **1967**, *10*, 247; (b) Allen, G. C.; Hush, N. S. *Prog. Inorg. Chem.* **1967**, *8*, 357; (c) Demadis, K. D.; Hartshorn, T. J. Meyer, C. M. *Chem. Rev.* **2001**, *101*, 2655.

[34] Paul, F.; Lapinte, C. *Coord. Chem. Rev.* **1998**, *178-180*, 431.

[35] Boas, U.; Dhanabalan, A.; Greve, G.; Meijer, E. W. *Synlett.* **2001**, *5*, 634.

[36] Mio, M. J.; Kopel, L. C.; Braun, J. B.;. Gadzikwa, T. L.; Hull, K. L.; Brisbois, R. G.; Markworth, C. J.; Grieco P. A. *Org. Lett.* **2002**, *4*, 3199.

[37] Byers, L. R.; Dahl, L. F. *Inorg. Chem.* **1980**, *19*, 277.

[38] Wang, H.; Tsai, F.; Nakajima, K.; Takahashi, T. *Chem. Lett.* **2002**, 578.

[39] Huang, L.; Aulwurm, U. R.; Heinemann, F. W.; Kisch, H. *Eur. J. Inorg. Chem.* **1998** 1951.

Curriculum Vitae
Paul D. Byrne

Education

Massachusetts Institute of Technology — Cambridge, MA
Ph.D. in Organic Chemistry — March, 2006
Thesis: "Synthesis and Characterization of Conducting Polymers with New Architectural Motifs"
University of Vermont — Burlington, VT
B.S. (summa cum laude), Chemistry — 2000

Research Interests

- Electroactive materials.
- Solid state characterization of electroactive materials and utilizing this characterization for the development of these materials toward applications such as sensory and actuation devices.
- Utilizing organometallic complexes for materials applications.

Research Experience

2000-present — Massachusetts Institute of Technology
Institute for Solider Nanotechnology
Advisor: Professor Timothy M. Swager
Research Assistant

- Designed and developed synthetic routes to a wide variety of thiophene based monomers. These monomers were then utilized to produce a series of conducting polymers with new linkages in the main chain of the polymer. These linkages included cyclobutadiene cobalt cyclopentadiene complexes, azaferrocene complexes and 2, 2'-substituted biphenyl compounds.
- Characterized these conducting polymers using a variety of electrochemical techniques including cyclic voltammetry, differential pulse voltammetry, square wave voltammetry, *in situ* conductivity, UV-vis spectroelectrochemistry, *in situ* electron paramagnetic resonance spectroscopy. Utilized these techniques to assess the viability of these materials for potential application as actuation and sensory materials. The characterizations of a majority of these polymers were performed under an inert atmosphere.
- Utilized the molecular structure of the 2, 2'-substituted biphenyl based polymers to study the through space π-interactions between thiophene fragments. Utilized the organometallic polymers to study the interactions between transition metals and conducting polymers.

1998-2000 — University of Vermont
Advisor: Christopher Landry
Undergraduate Research Assistant

- Studied the use of mesoporous silicates as a solid support for ruthenium epoxide catalysts. Synthesized small peptides (3-4 units) by solid state synthetic techniques. These peptides were then utilized as ligands for the ruthenium catalysts. Characterized the mesoporous silicates by BET surface area and BJH absorption/desorption pore volume distribution measurements.

Teaching Experience

Spring and Fall 2001 MIT Department of Chemistry Laboratory Assistant

- Supervised and instructed chemical laboratory techniques to undergraduate students.

Fall 2000 MIT Department of Chemistry Teaching Assistant

- Led a recitation class for an undergraduate general chemistry lecture.

Professional Affiliations

American Chemical Society
Materials Research Society

Scientific Presentations

"Electroactive Polymers Containing Cyclobutadiene Cp Cobalt Complexes" Paul Byrne and Timothy M. Swager, 228th National ACS Meeting (Philadelphia, PA) (August, 2004)

"Electroactive Polymers Containing Cyclobutadiene Cp Cobalt Complexes" Paul Byrne and Timothy M. Swager, 6th International Symposium on Fictional π-Electron Systems (Ithaca, NY) (June, 2004).

"Synthesis and Electrochemical Properties of Bithiophene-containing Cyclobutadiene Cp Cobalt Complexes" Paul Byrne, Dongwhan Lee and Timothy M. Swager 2003 Materials Research Society Fall Meeting and Exhibit. (Boston, MA) (December, 2003)

Publications

"Conducting Polymers Containing Cyclobutadiene Co Cyclopentadiene Complexes" Paul D. Byrne, Dongwhan Lee, Peter Müller, Timothy M. Swager. (Accepted, Synthetic Metals.)

Acknowledgements

The first person I need to thank is Tim. I will always be grateful for all his help, guidance, generosity and his general attitude. However, the main thing I'm grateful for is his patience, especially after two broken hands. I just wished I had delivered more for his patience.

I have to thank my first bay-mates, J.D. and Holger. J. D. was an ideal bay-mate and Holger only seemed a little annoyed when I keep asking if something he was synthesizing, looking at or holding was a liquid crystal. I need to thank Aimee for being a great teammate. I will remember Bruce (Hsiao-Hua) for his advice on everything from E-chem to backyard soccer. I need to thank Araki for teaching me everything I needed to know about glove-box maintenance. Kenichi was the master of gels and perseverance. Karen, Phoebe and Alex were transcendent desk-mates. I will always associate THK with the some extremely funny times. I need to thank Dongwhan for everything he did for me while at MIT and afterwards. Eugenevy was a unique talent with great comic timing. I must thank Nate for all his help and showing the truth about PGSTAT 30's. I want to thank John for the listening to the many subgroup issues I would bug him with. I need to thank Sam for many stimulating conservations from the 49ers to how characterize an oligomeric series. I want Gigi for all her general help but especially the HPLC help. I also need to thank Paul for all his general help but I still consider him the evil Paul. I want thank Kouschik all his help but I definitely need to thank him for one long conservation on mixed-valence complexes. I want to thank Anne for her advice on getting out. I'll miss occasionally seeing Jessica as I walk into the lab. I greatly appreciated the e-chem and synthesis talks with Changsik. I always enjoyed Jean's ingrained understanding of the importance of beer. I need to thank Zhihua because I probably took some stuff from him and didn't tell him. I need Scott for pointing out that a minivan is never cool, no matter what music you play. I want to thank Michael for all his help with e-chem and I hope he's still not angry with me for head-butting him. I will remember Youngmi for her unique way to get stuff done. I want to thank Juan for all the important conservations we had. I need to thank Craig for just being himself and I want to thank Sandra as well for being herself. I need to thank Becky for all the help in the lab and for inviting me to some very fascinating parties. I want to thank Hyun A for her time at ISN, it made the move over easier. I really do need to thank Brad for everything he did for me. He helped with the chemistry, wine, how to race cars and the motivation. I really need to thank Jocelyn for a lot of stuff but in particular her through research methods and her through relaxation methods. I want to thank Ivory for a lot stuff too, but mostly I want to thank him for the conservations and useful advice on just about everything. I blame Lokman for anything bad that happens at the ISN. I need to thank the new ISN crew, Yong, Hongwei and Mark. I have to thank Inja for every big and small thing that she did. I want to wish good luck to Fei and Eric in their graduate careers. I want to thank Dave, Jenny and Liz for the great hockey experience. I need thank one of the best roommates I've had, Touch. Dave, Mark and Lili were always extremely helpful. The ISN staff, Abeer, Steve, Marco, Joanne, Josh and Kathy gave me considerable help as well. I need to thank Peter for his great work. I need to thank the 7-11 guys, I would probably starved without them. I need thank Andrew for being a good friend. I need to thank the ISN for many reasons.

I need thank Mom for her unconditional love. I need thank Dad and Mary for their support. I need to thank Matt, Erynne, Brendyn and Adowyn and for letting me enjoy their house on Cornell St. I need to thank Vince, Christy and Alex for their brief but highly enjoyable visit. I need to thank Andy, Pamela and Sam. I especially need to thank Andy and Pamela for what felt like an all too brief period in which we lived in Mass. together, they helped me in unbelievable ways. I have thank Mark for the unique Thanksgiving in Somerville. I need to thank Todd for his no holds barred opinions. If I accomplish anything, I feel it is only because of my big lovable family.

Appendix 1:

Electrochemical Measurements

Cyclic Voltammetry

Cyclic voltammetry (CV) is a powerful analytical technique that can be applied to a wide variety of electroactive analytes. The waveform for CV is a simple linear increase to a desired potential then a linear decrease from that potential, see Figure 1.

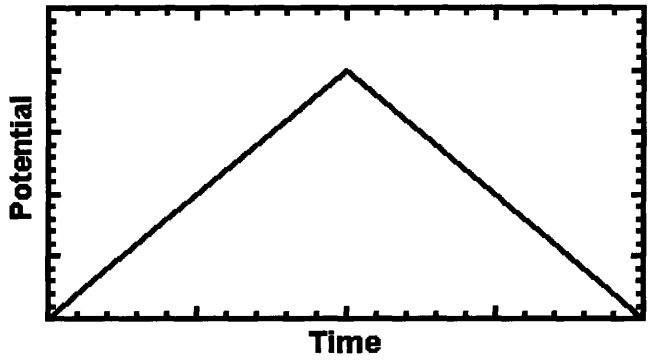

Figure 1. Input for a cyclic voltammetry experiment.

The peak current, i_p, for an electrochemical process in solution is determined by the Randles-Sevcik equation: $i_p = (2.69*10^5)\, An^{3/2}C_aD_a^{1/2}\upsilon^{1/2}$. Where A is the area, n is the

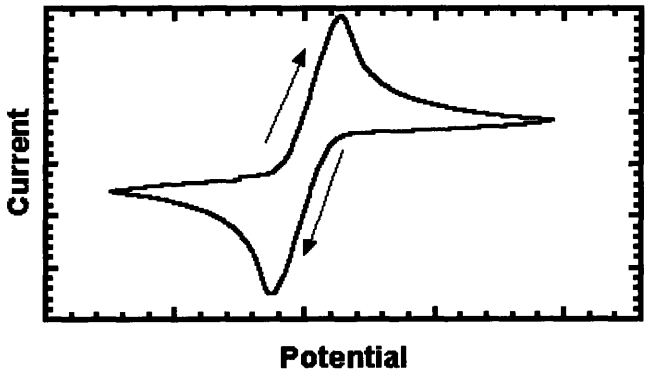

Figure 2. Cyclic voltamogram of ferrocene at 100 mV/s.

number of concentration of the analyte, D_a is the diffusion constant of the analyte and υ is the scan electrons, C_a is the rate. The important feature here is that i_p is proportional to $\upsilon^{1/2}$. In the case of a surface bound electrochemical process, the equation for the peak current is: $i_p = (n^2F^2C_a\upsilon V)/(4RT)$. In this case the peak current is now proportional to υ.

An important consideration in CV is the separation of the oxidation peak, and the reduction peak for an electrochemical process.[1] This separation is how the electrochemical reversibility of the process is defined. In solution the peak separation for a completely reversible reaction is 59 mV and in the solid state the separation is 0 mV.

Faradaic and Nonfaradaic Currents

The currents observed in a typical CV experiment can be divided into two types, faradaic and nonfaradaic currents. A faradaic current involve processes that obey Faraday's law. Therefore the amount of a chemical reaction at an electrode surface is proportional to the current observed. The nonfaradaic current resembles a charging and discharging of a capacitor since this is essentially what is taking place. The application of a potential charges the electrode surface making the electrode surface act as a one side of capacitor. This charging and discharging of the electrode surface produces a capacitive current. A simplistic way to understand the differences between the faradaic and nonfaradaic currents is to think if a charge moves from the electrode surface that is a faradaic current. If the charges stays at the electrode surface, that is a nonfardic current.[2]

***In situ* Conductivity**

This technique involves a special type of working electrode, an interdigitated micorelectrode, IDE. An IDE are two set of electrode fingers, made up of Pt, Au or ITO, interspaced between each other by a fix distance (2-20 μm). Typically, a polymer is electrochemically polymerized across these electrodes but the polymer may also be drop-cast or spin cast onto the electrode. A potential gradient (drain potential, V_d) is then set between the two electrodes to create a field effect transistor. The overall potential

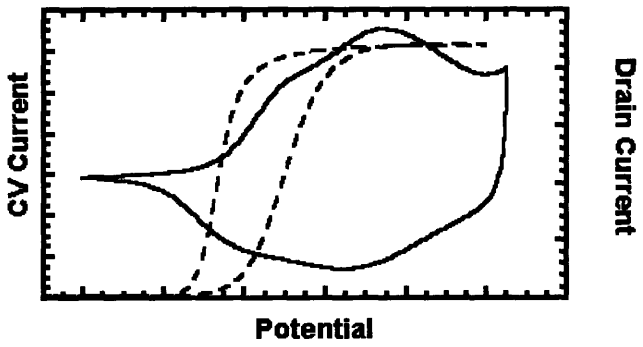

Figure 3. The cyclic voltamogram and *in situ* conductivity of polythiophene.

of the cell is then varied (gate potential, V_g) oxidizing or reducing the polymer. With the oxidation or reduction of the polymer, there is concurrent change in the conductivity, σ_{con}, of polymer. With the potential gradient between the electrodes, a current should occur (drain current, i_d) with this change in the conductivity. This current will be directly proportional to the conductivity of the polymer at a particular gate potential. The conductivity is described by this equation: $\sigma = A(i_d/V_d)*(W)/(n*L*T)$ where n is the number of "fingers" of each electrode, W is the width of the electrode array, L is the spacing between the electrodes and T is the thickness of the electrode. A is a correction factor used to adjust for internal resistance of the leads and the roughness of the film. This technique provides precise information on the relative conductivity of a polymer versus potential. An Eco-Chemie PGstat 30 model bipotentiostat may be used to perform this experiment. However, this model comes in two bipotentiostat modes. The bipotentiostat mode (B mode) locks the second working electrode at a fixed potential and this mode is unsuitable for *in situ* conductivity experiments. The array mode (A mode) will cycle the second working electrode at fixed potential difference relative to the first working electrode. This mode is suitable for *in situ* conductivity experiments.

Pulse Voltammetry

Differential pulse voltammetry (DPV) is a voltammetric method based on the measuring the differential current after two time periods, t_1 and t_2. The t_1 is a preelectrolysis period to establish a thick diffusion layer and a short pulse period to measure to the change current to an incremental change in potential. This method is very

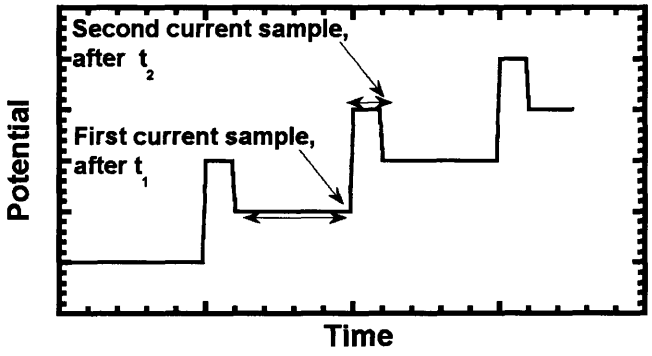

Figure 4. Input for a differential pulse voltammetry experiment.

sensitive and the differential form of the output give better resolution than CV. This pulsed method allows reduces the amount of nonfaradaic current measured. The Δi_{max} is determined by this equation; $\Delta i_{max} = ((nFAC_aD_a^{1/2})/(\pi^{1/2}t_p^{1/2})*((1-\sigma)/(1+\sigma)))$ where t_p is the pulse duration and $\sigma = e^{((nF(Ep))/(RT2)}$. The potential at Δi_{max} (E_{max}) is determined by this equation; $E_{max} = E_{1/2} - E_p/2$ where E_p is the pulse amplitude. One drawback to DPV is a preelectrolysis step that is needed. This preelectrolysis step takes about 0.5 to 4 sec and adds a considerable amount of experimental time to the method.

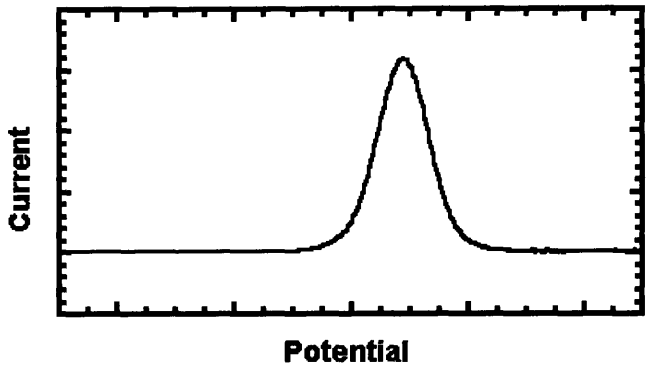

Figure 5. The differential pulse voltammetry of ferrocene. Scan rate of 0.0042 V/s with a step potential of 0.0021 V, amplitude of 0.010 V.

Square wave voltammetry (SWV) is a modified pulse method that does not suffer from long experimental times. The lack of preelectroylsis step makes the experimental time of SWV similar to that of CV. The waveform is one in which potential is cycled

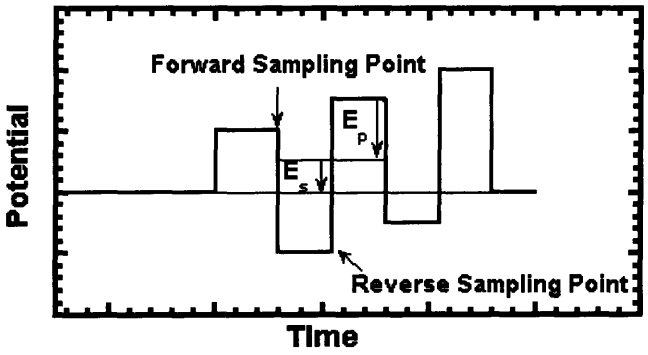

Figure 6. The input for a square wave voltammetry experiment.

between a forward potential (higher potential) and a reverse potential (lower potential) with a slight increase in potential over each cycle (staircase). A more succinct description is that the waveform of consists of a bipolar square superimposed on to a staircase.[3] The potentials used will be determined by $E_{forward} = E_p + nE_s$ and $E_{reverse} = -E_p + nE_s$ where E_s is the staircase potential and n is the number cycles starting from 0. The SWV experiment produces three outputs, the forward current measured at forward

potential, the reverse current measured at reverse potential and the finally the difference current of the forward and the reverse currents. The forward and reverse potential outputs resemble the output of a CV. The difference output resembles that of a DPV scan. The differences output is the most reported output. The difference current reaches a max at ca. $E_{1/2}$ and has maximum value defined by $\Delta i_{max} = ((nFAC_aD_a^{1/2})/(\pi^{1/2}t_p^{1/2}) * \Delta\psi_{max}$ where t_p is the pulse height and $\Delta\psi_{max}$ is dimensionless peak current defined by the by n, E_p and E_s. This equation is a direct analogue of the Δi_{max} of DPV.

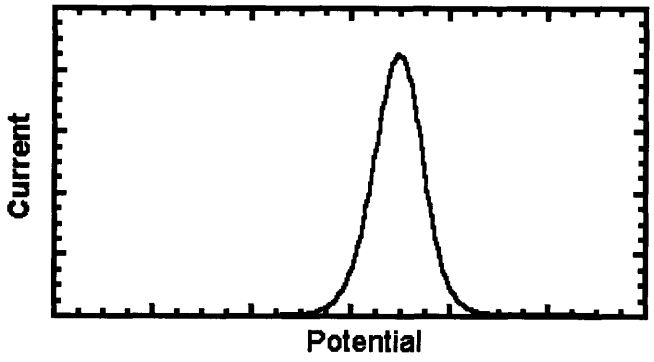

Figure 7. The square wave voltamogram of ferrocene. Scan rate of 0.148 V/s with a step potential of 0.005 V, amplitude of 0.025 V and a frequency of 30 Hz.

X-Ray Photoelectron Spectroscopy (XPS)

XPS is the ejection of electrons from a surface by irradiation by monochromatic X-rays. The energy of the photon needed to eject an electron from a surface is defined by this equation: $h\upsilon = E_b+E_k+E_r+\varphi_{sp}$. The two most important terms are the binding energy of the electron, E_b, and the kinetic energy of the electron, E_k. The E_b value is a discrete value and is defined by the atomic level occupied by the electron. So if the recoil energy, E_r, and the spectrometer work function, φ_{sp}, are corrected for, then the E_k values obtained should be discrete. This information can be related back to the type of atom and

corresponding atomic level the electron was ejected from. While the basics principles of XPS suggest that it is a powerful qualitative tool, it suffers from peak broadening and overlap. Curve resolution is used to correct for this problem but modeling the components of the surface must be done to for this technique to be done correctly. XPS can also be used for quantitative information and can describe the atomic composition of a surface with an accuracy of 1-10 %. XPS analysis is confined to the surface of an analyte in that the only atoms within 20 Å to the top of the surface are measured.

References

[1] *Handbook of Conducting Polymers* Skotheim, T. A., Elsenbaumer, R. L., Reynolds, J. R. Eds.; Marcel Dekker: New York, 1998

[2] Skoog, D. A.; Holler, F. J.; Nieman, T. A. *Principles of Instrumental Analysis* 5th edition, Saunders College Publishing: U.S.A, 1998.

[3] Bard, A. J.; Faulker, L. R. *Electrochemical Methods: Fundamentals and Applications* 2nd Edition, Wiley & Sons: USA, 2001.

Appendix 2:

X-ray Diffraction Crystal Structures

Chapter 2: Compound **6**

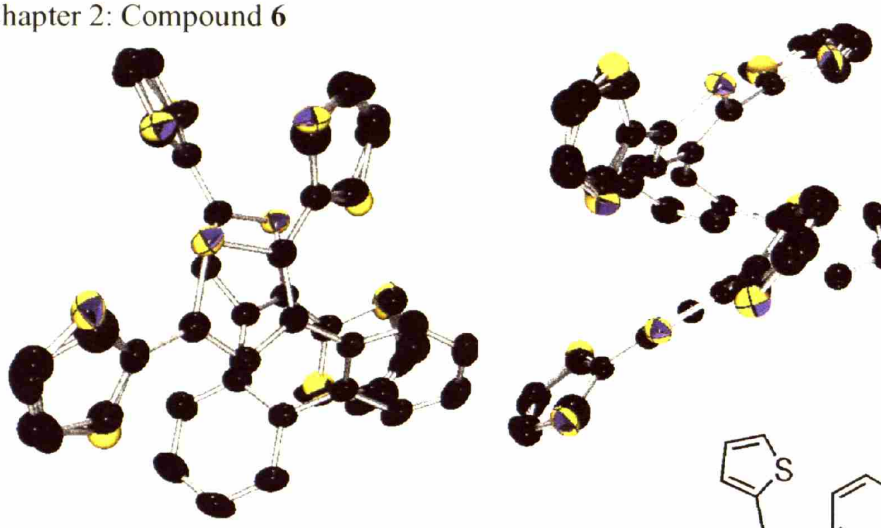

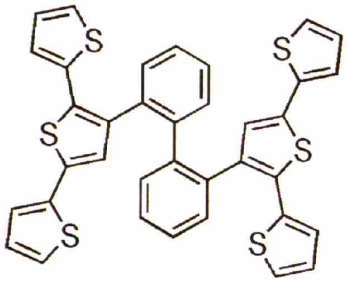

Chemical formula	$C_{36}H_{22}S_6$
Formula weight	646.90
Crystal size [mm^3]	0.20 x 0.15 x 0.08
Crystal system	Triclinic
Space group	P-1
Unit cell [Å and °] a	10.7643(2)
b	12.1305(3)
c	13.0027(3)
α	86.1130(10)
β	79.7480(10)
γ	66.8840(10)
Volume [$Å^3$]	1536.59(6)
Z	2
Density (calc) [Mg/m^3]	1.398
Theta range [°]	1.83 to 27.88
Temperature [K]	233(2)
Refelections collected	24106
Independent Reflecions	7316
R_{int}	0.0264
Completeness of data [%]	99.8
Absorption correction	semi empirical
Max. / min. transmission	0.9633 and 0.9117
Data/Restraints/Parameters	7316/ 797 / 527
Goodness-of-fit on F^2	1.032
Final *R* indices * [I>2σ(I)]	*R*1 = 0.0381 *wR*2 = 0.0948
Final *R* indices * (all data)	*R*1 = 0.0506 *wR*2 = 0.1029
Largest diff. peak and hole	0.273/ -0.254

Chapter 2: Compound **9**

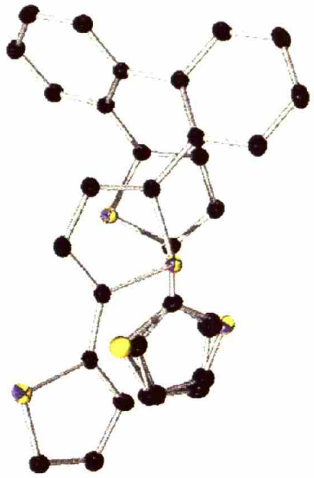

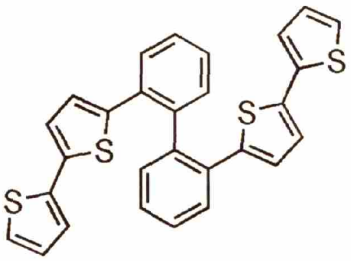

Chemical formula	$C_{28}\ H_{18}\ S_4$
Formula weight	482.66
Crystal size [mm^3]	0.25 x 0.15 x 0.08
Crystal system	Triclinic
Space group	P-1
Unit cell [Å and °] a	8.9671(3)
b	10.5901(4)
c	24.5596(8)
α	82.6200(10)
β	88.5580(10)
γ	87.6910(10)
Volume [$Å^3$]	2310.57(14)
Z	4
Density (calc) [Mg/m^3]	1.388
Theta range [°]	1.67 to 29.13
Temperature [K]	100(2)
Refelections collected	50559
Independent Reflecions	12407
R_{int}	0.0219
Completeness of data [%]	99.8
Absorption correction	semi empirical
Max. / min. transmission	0.9667 and 0.9010
Data/Restraints/Parameters	12407/ 396 / 676
Goodness-of-fit on F^2	1.025
Final *R* indices * [I>2σ(I)]	*R*1 = 0.0316 *wR*2 = 0.0840
Final *R* indices * (all data)	*R*1 = 0.0348 *wR*2 = 0.0867
Largest diff. peak and hole	0.552/ -0.360

Chapter 4: Compound **1a**

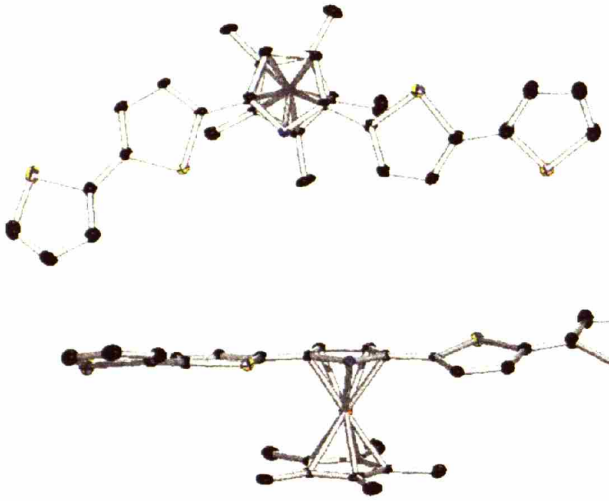

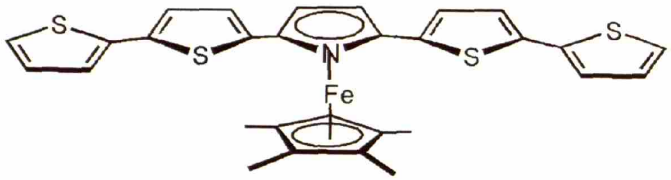

Chemical formula	$C_{30.5}H_{28}ClFeNS_4$
Formula weight	628.08
Crystal size [mm^3]	0.50 x 0.45 x 0.01
Crystal system	monoclinic
Space group	Pc
Unit cell [Å and °] a	18.0259(17)
b	14.9021(13)
c	10.5521(8)
α	90.00
β	97.917(3)
γ	90.00
Volume [$Å^3$]	2807.5(4)
Z	4
Density (calc) [Mg/m^3]	1.486
Theta range [°]	2.38 to 29.81
Temperature [K]	100(2)
Refelections collected	10158
Independent Reflecions	10158
R_{int}	0.0314
Completeness of data [%]	96.9
Absorption correction	semi empirical
Max. / min. transmission	0.9905 and 0.6474
Data/Restraints/Parameters	10158/ 1148 / 761
Goodness-of-fit on F^2	1.016
Final *R* indices * [I>2σ(I)]	*R*1 = 0.0539 *wR*2 = 0.1136
Final *R* indices * (all data)	*R*1 = 0.0703 *wR*2 = 0.1188
Largest diff. peak and hole	0.854/ -0.874

Chapter 5: Compound **5**

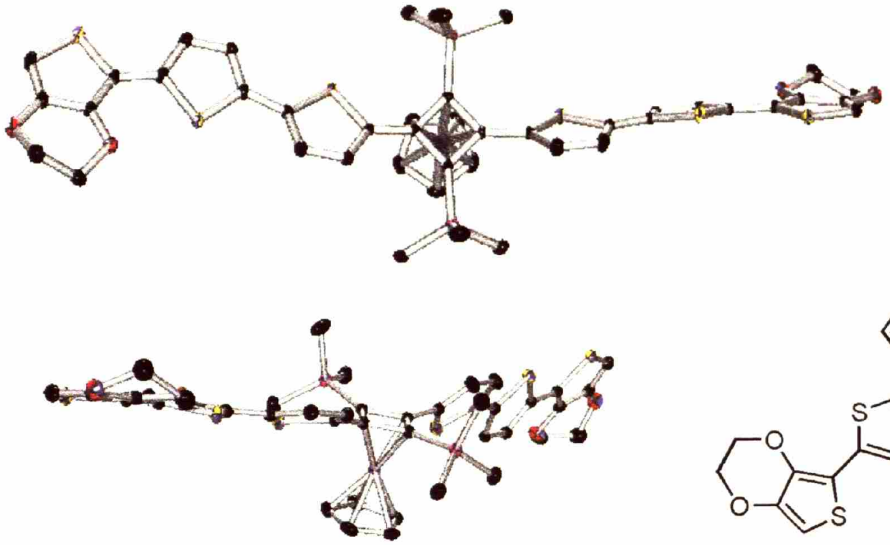

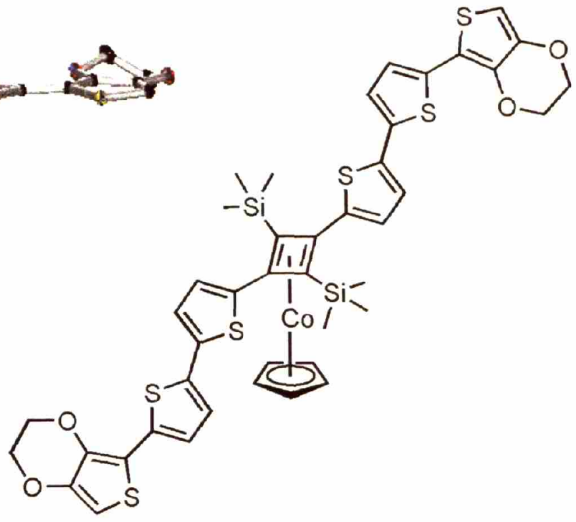

Chemical formula	$C_{43}H_{41}CoO_4S_6Si_2$
Formula weight	929.23
Crystal size [mm^3]	0.20 x 0.15 x 0.10
Crystal system	Triclinic
Space group	P-1
Unit cell [Å and °] a	10.4858(4)
b	14.7353(5)
c	14.9329(8)
α	77.4880(10)
β	69.7540(10)
γ	97.8340(10)
Volume [$Å^3$]	2111.59(13)
Z	2
Density (calc) [Mg/m^3]	1.461
Theta range [°]	1.82 to 26.01
Temperature [K]	100
Refelections collected	29899
Independent Reflecions	8295
R_{int}	0.0306
Completeness of data [%]	100
Absorption correction	semi empirical
Max. / min. transmission	0.9241 and 0.8560
Data/Restraints/Parameters	8295 /0 / 511
Goodness-of-fit on F^2	1.038
Final *R* indices * [I>2σ(I)]	*R*1 = 0.0345 *wR*2 = 0.0867
Final *R* indices * (all data)	*R*1 = 0.0399 *wR*2 = 0.0908
Largest diff. peak and hole	0.609 / -0.251

Chapter 5: Compound **7**

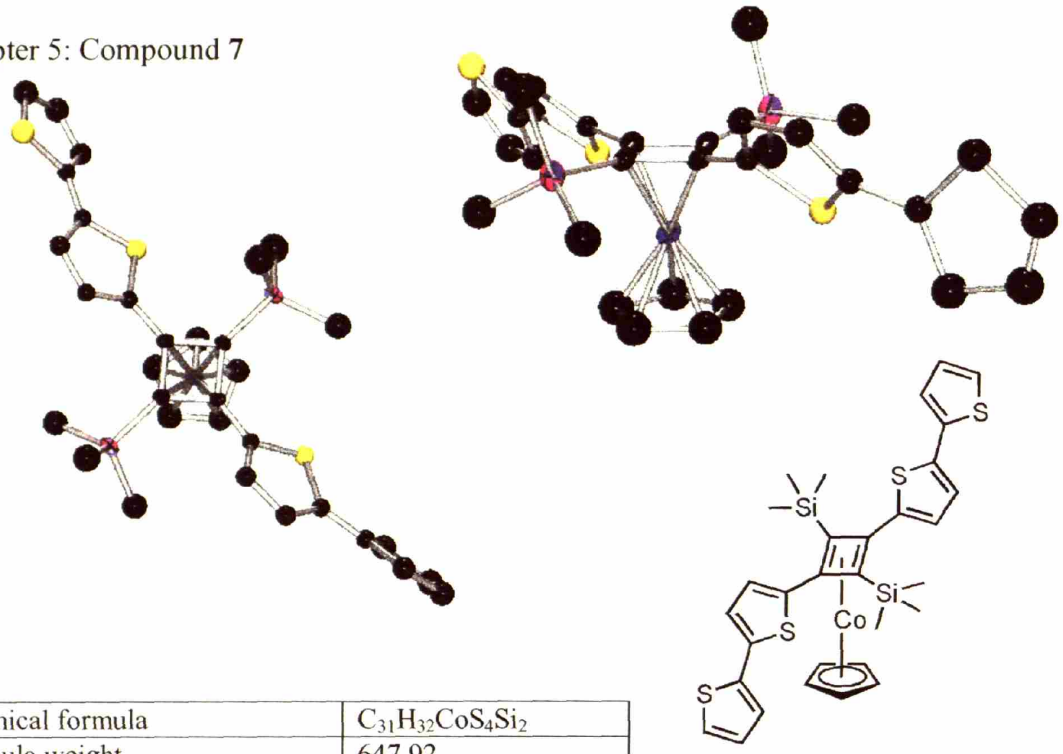

Chemical formula	$C_{31}H_{32}CoS_4Si_2$
Formula weight	647.92
Crystal size [mm^3]	0.30 x 0.25 x 0.01
Crystal system	Monoclinic
Space group	P-2_1/c
Unit cell [Å and °] a	17.614(2)
b	9.2037(11)
c	19.638(2)
α	90
β	90.618(2)
γ	90
Volume [$Å^3$]	3183.5(7)
Z	4
Density (calc) [Mg/m^3]	1.352
Theta range [°]	2.07 to 28.26
Temperature [K]	193
Refelections collected	16189
Independent Reflecions	7329
R_{int}	0.0737
Completeness of data [%]	92.9
Absorption correction	semi empirical
Max. / min. transmission	1.0000 and 0.8064
Data/Restraints/Parameters	7329 /0 / 341
Goodness-of-fit on F^2	1.018
Final *R* indices * [I>2σ(I)]	*R*1 = 0.0750 *wR*2 = 0.1567
Final *R* indices * (all data)	*R*1 = 0.1457 *wR*2 = 0.1810
Largest diff. peak and hole	0.773 / -0.651

Chapter 5: Compound **10**

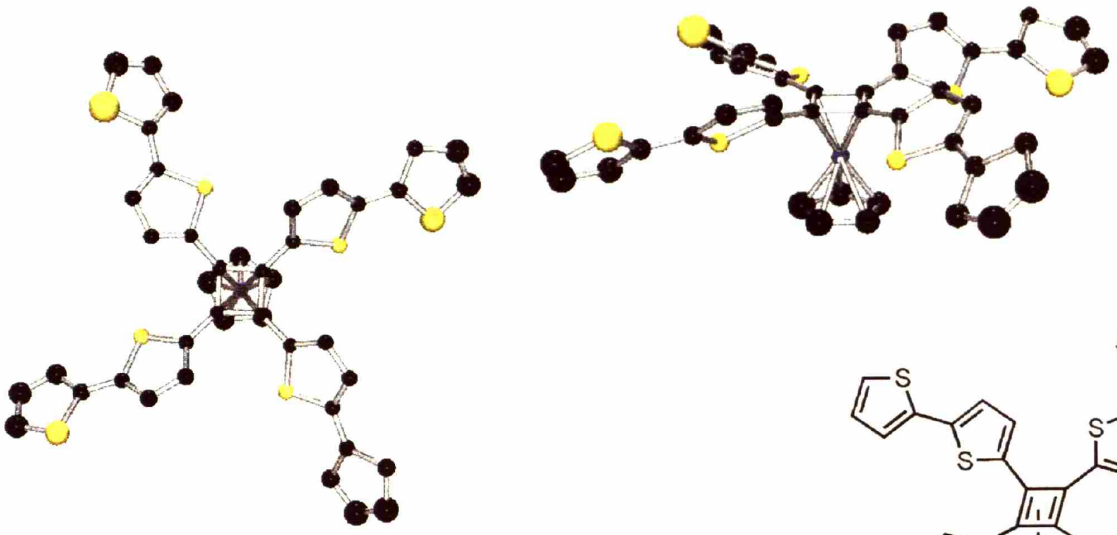

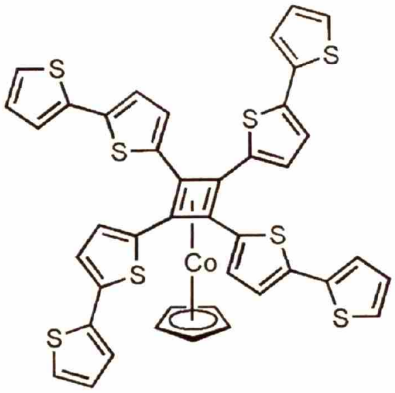

Chemical formula	$C_{41}H_{24}CoS_8$
Formula weight	832.01
Crystal size [mm^3]	0.30 x 0.20 x 0.10
Crystal system	Monoclinic
Space group	$P2_1/c$
Unit cell [Å and °] a	11.8672(7)
b	21.9640(14)
c	13.9578(8)
α	90
β	93.2710(10)
γ	90
Volume [$Å^3$]	3632.2(4)
Z	4
Density (calc) [Mg/m^3]	1.521
Theta range [°]	2.36 to 26.64
Temperature [K]	189
Refelections collected	20089
Independent Reflecions	8142
R_{int}	0.0475
Completeness of data [%]	90.1
Absorption correction	semi empirical
Max. / min. transmission	1.0000 and 0.7867
Data/Restraints/Parameters	8142 / 0 / 442
Goodness-of-fit on F^2	1.119
Final *R* indices * [I>2σ(I)]	*R*1 = 0.0873 *wR*2 = 0.1850
Final *R* indices * (all data)	*R*1 = 0.1234 *wR*2 = 0.2003
Largest diff. peak and hole	0.991 / -0.772

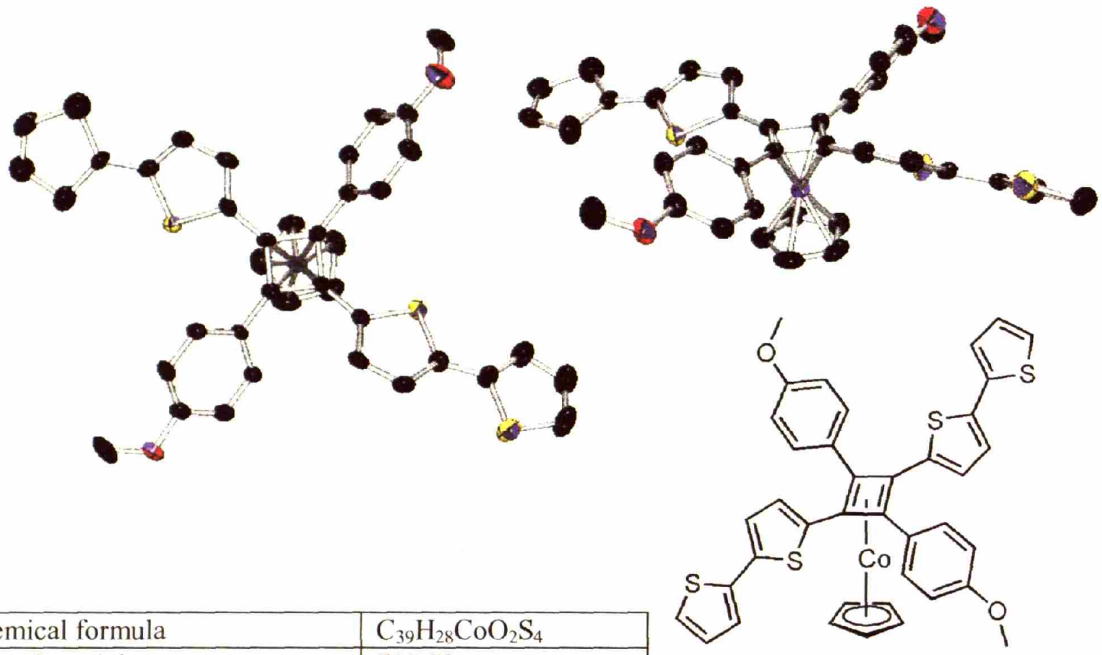

Chemical formula	$C_{39}H_{28}CoO_2S_4$
Formula weight	715.78
Crystal size [mm^3]	0.15 x 0.15 x 0.15
Crystal system	Triclinic
Space group	P-1
Unit cell [Å and °] a	12.1113(18)
b	12.7100(19)
c	13.165(2)
α	62.222(2)
β	82.336(2)
γ	67.978
Volume [$Å^3$]	1660.1(4)
Z	2
Density (calc) [Mg/m^3]	1.434
Theta range [°]	2.20 to 24.79
Temperature [K]	193
Refelections collected	9207
Independent Reflecions	6946
R_{int}	0.0418
Completeness of data [%]	84.3
Absorption correction	semi empirical
Max. / min. transmission	1.0000 and 0.8002
Data/Restraints/Parameters	6946 / 0 / 423
Goodness-of-fit on F^2	1.034
Final *R* indices * [I>2σ(I)]	*R*1 = 0.0993 *wR*2 = 0.1855
Final *R* indices * (all data)	*R*1 = 0.1693 *wR*2 = 0.2134
Largest diff. peak and hole	0.524 / -0.632

Chapter 5: Compound **14**

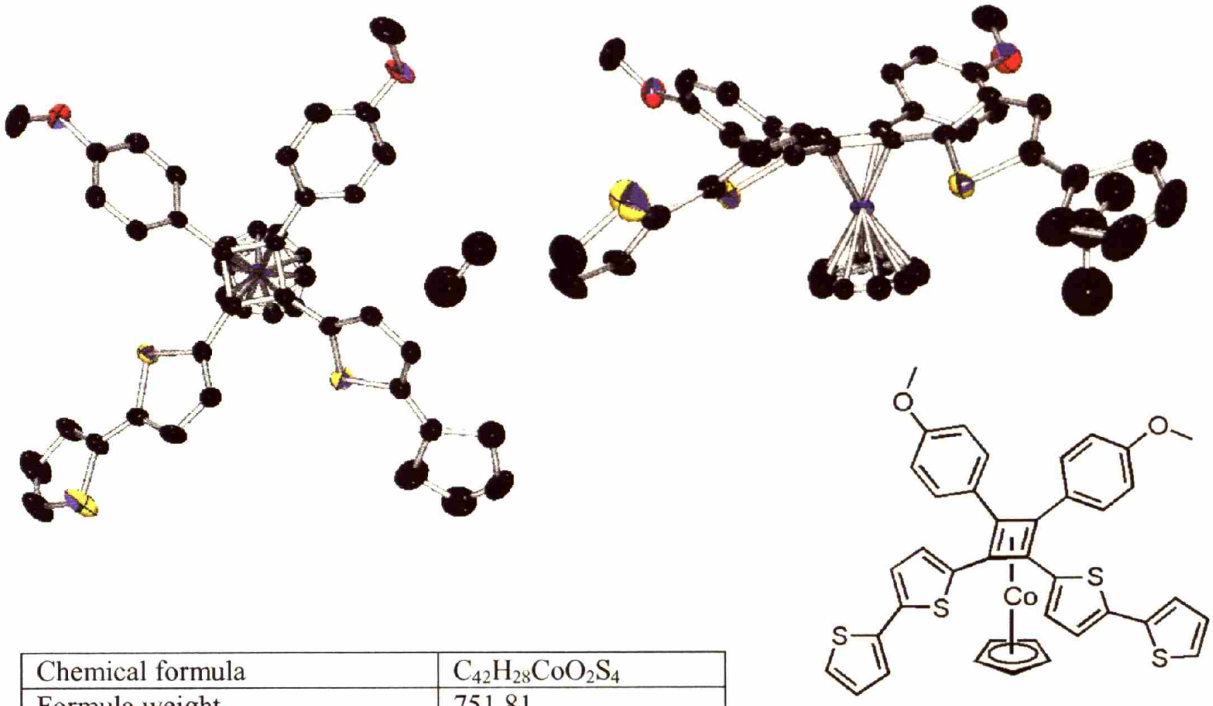

Chemical formula	$C_{42}H_{28}CoO_2S_4$
Formula weight	751.81
Crystal size [mm^3]	0.20 x 0.15 x 0.05
Crystal system	Triclinic
Space group	P-1
Unit cell [Å and °] a	12.5498(19)
b	13.2638(19)
c	13.672(2)
α	110.494(2)
β	92.624(2)
γ	116.831(2)
Volume [$Å^3$]	1844.9(5)
Z	2
Density (calc) [Mg/m^3]	1.290
Theta range [°]	2.17 to 28.28
Temperature [K]	193
Refelections collected	10159
Independent Reflecions	7718
R_{int}	0.0381
Completeness of data [%]	84.2
Absorption correction	semi empirical
Max. / min. transmission	1.0000 and 0.7976
Data/Restraints/Parameters	7718 / 0 / 439
Goodness-of-fit on F^2	1.096
Final *R* indices * [I>2σ(I)]	*R*1 = 0.0942 *wR*2 = 0.2064
Final *R* indices * (all data)	*R*1 = 0.1475 *wR*2 = 0.2293
Largest diff. peak and hole	0.750 / -0.667

Chapter 5: Compound **19**

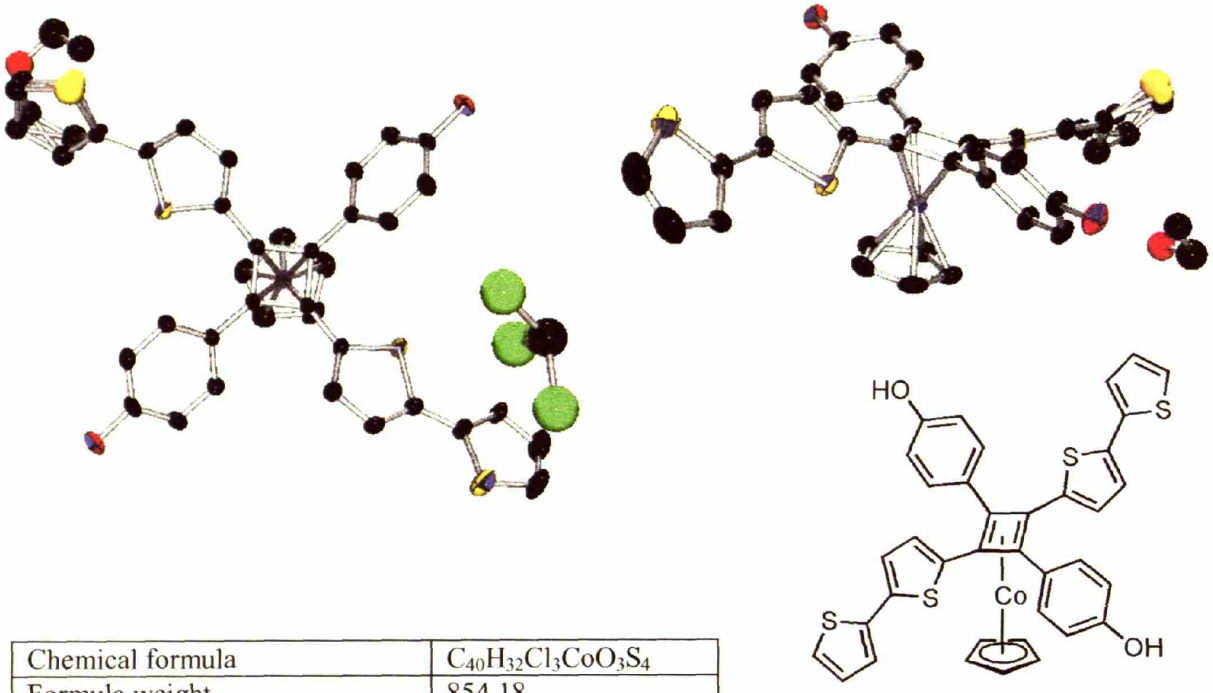

Chemical formula	$C_{40}H_{32}Cl_3CoO_3S_4$
Formula weight	854.18
Crystal size [mm^3]	0.15 x 0.10 x 0.10
Crystal system	Triclinic
Space group	P-1
Unit cell [Å and °] a	12.074(5)
b	12.875(5)
c	14.631(4)
α	111.866(16)
β	92.580(14)
γ	111.885(10)
Volume [$Å^3$]	1913.7(12)
Z	2
Density (calc) [Mg/m^3]	1.488
Theta range [°]	1.86 to 28.29
Temperature [K]	193
Refelections collected	36645
Independent Reflecions	9466
R_{int}	0.0344
Completeness of data [%]	99.4
Absorption correction	semi empirical
Max. / min. transmission	0.9141 and 0.8750
Data/Restraints/Parameters	9466 / 183 / 507
Goodness-of-fit on F^2	1.055
Final *R* indices * [I>2σ(I)]	*R*1 = 0.0598 *wR*2 = 0.1685
Final *R* indices * (all data)	*R*1 = 0.0727 *wR*2 = 0.1789
Largest diff. peak and hole	0.949 / -0.985

Chapter 5: Compound **20**

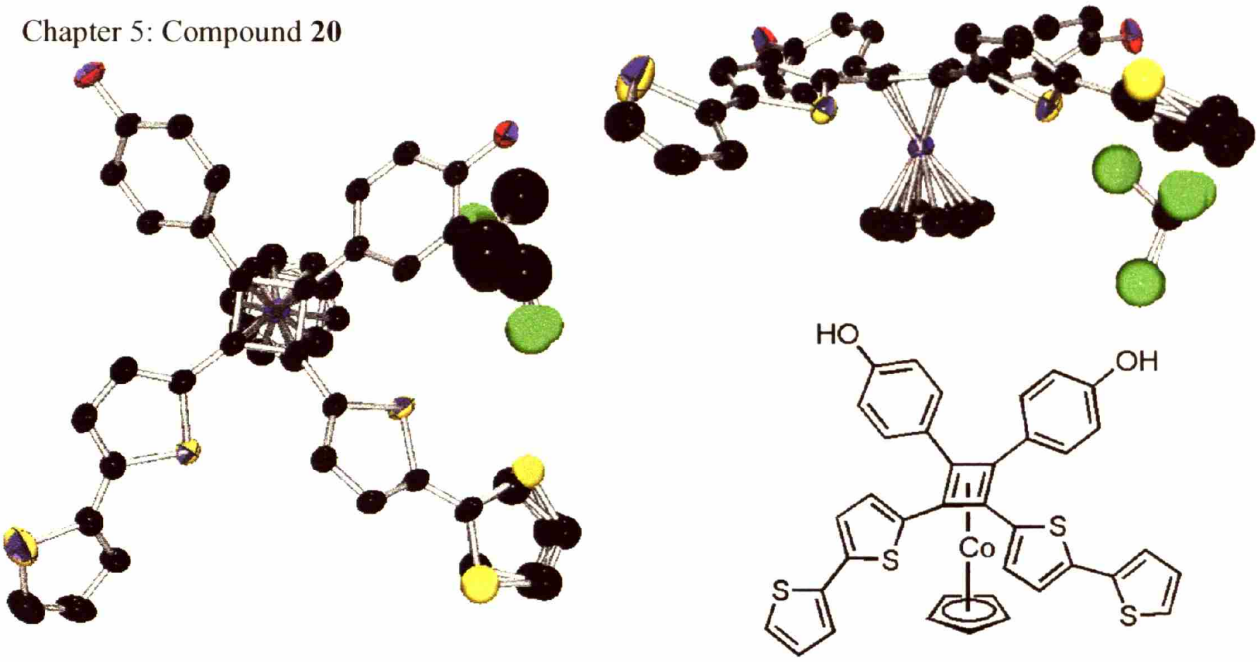

Chemical formula	$C_{41}H_{33}Cl_3CoO_2S_4$
Formula weight	854.19
Crystal size [mm^3]	0.33 x 0.30 x 0.25
Crystal system	Monoclinic
Space group	C2/c
Unit cell [Å and °] a	22.574(16)
b	15.046(6)
c	23.012(16)
α	90
β	96.20(2)
γ	90
Volume [$Å^3$]	7770
Z	8
Density (calc) [Mg/m^3]	1.476
Theta range [°]	1.63 to 26.05
Temperature [K]	193
Refelections collected	70335
Independent Reflecions	7677
R_{int}	0.0314
Completeness of data [%]	99.9
Absorption correction	semi empirical
Max. / min. transmission	0.8060 and 0.7552
Data/Restraints/Parameters	7677 / 812 / 578
Goodness-of-fit on F^2	1.098
Final *R* indices * [I>2σ(I)]	*R*1 = 0.0515 *wR*2 = 0.1501
Final *R* indices * (all data)	*R*1 = 0.0601 *wR*2 = 0.1602
Largest diff. peak and hole	1.437 / -0.641

Chapter 5: Compound **23**

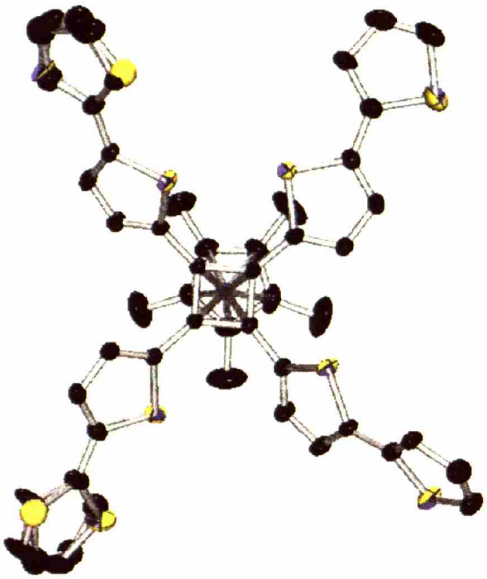

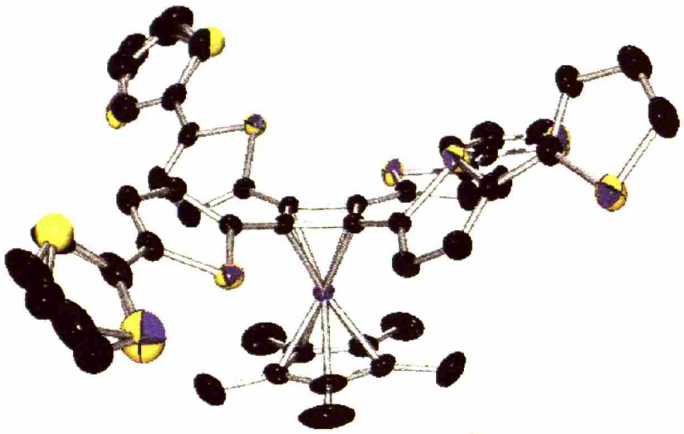

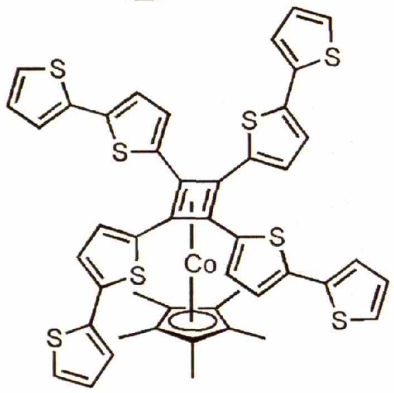

Chemical formula	$C_{46}H_{35}CoS_8$
Formula weight	903.15
Crystal size [mm^3]	0.33 x 0.23 x 0.20
Crystal system	Monoclinic
Space group	P-2_1/c
Unit cell [Å and °] a	15.7088(5)
b	17.9489(7)
c	16.3684(5)
α	90
β	116.8186
γ	90
Volume [$Å^3$]	4118.8(2)
Z	4
Density (calc) [Mg/m^3]	1.456
Theta range [°]	2.66 to 28.92
Temperature [K]	193
Refelections collected	24173
Independent Reflecions	8751
R_{int}	0.0340
Completeness of data [%]	100
Absorption correction	semi empirical
Max. / min. transmission	0.8474 and 0.7653
Data/Restraints/Parameters	8751 /947/ 575
Goodness-of-fit on F^2	1.084
Final *R* indices * [I>2σ(I)]	*R*1 = 0.0487 *wR*2 = 0.1090
Final *R* indices * (all data)	*R*1 = 0.0660 *wR*2 = 0.1156
Largest diff. peak and hole	0.579 / -0.839

Chapter 5: Compound **26**

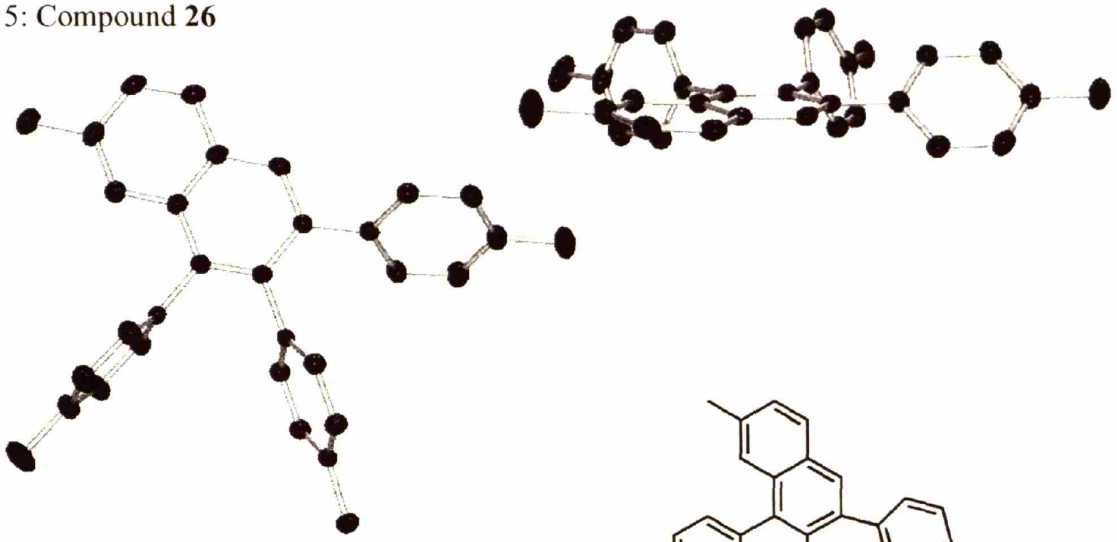

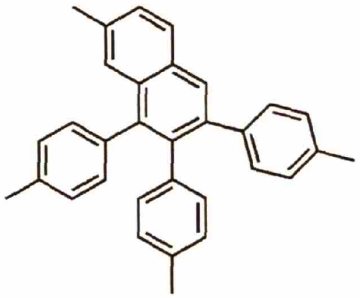

Chemical formula	$C_{32}H_{28}$
Formula weight	412.54
Crystal size [mm^3]	0.35 x 0.25 x 0.15
Crystal system	Triclinic
Space group	P-1
Unit cell [Å and °] a	10.4868(3)
b	13.8303(4)
c	17.2951(5)
α	105.8520(10)
β	97.4680(10)
γ	94.8180(10)
Volume [$Å^3$]	2373.69(12)
Z	4
Density (calc) [Mg/m^3]	1.154
Theta range [°]	1.24 to 27.48
Temperature [K]	100
Refelections collected	45861
Independent Reflecions	10899
R_{int}	0.0298
Completeness of data [%]	99.9
Absorption correction	semi empirical
Max. / min. transmission	0.9903 and 0.9776
Data/Restraints/Parameters	10899 / 0 / 585
Goodness-of-fit on F^2	1.038
Final *R* indices * [I>2σ(I)]	*R*1 = 0.0457 *wR*2 = 0.1200
Final *R* indices * (all data)	*R*1 = 0.0589 *wR*2 = 0.1318
Largest diff. peak and hole	0.377 / -0.250

Appendix 3:

Chapter 2 NMR

Compound **2**

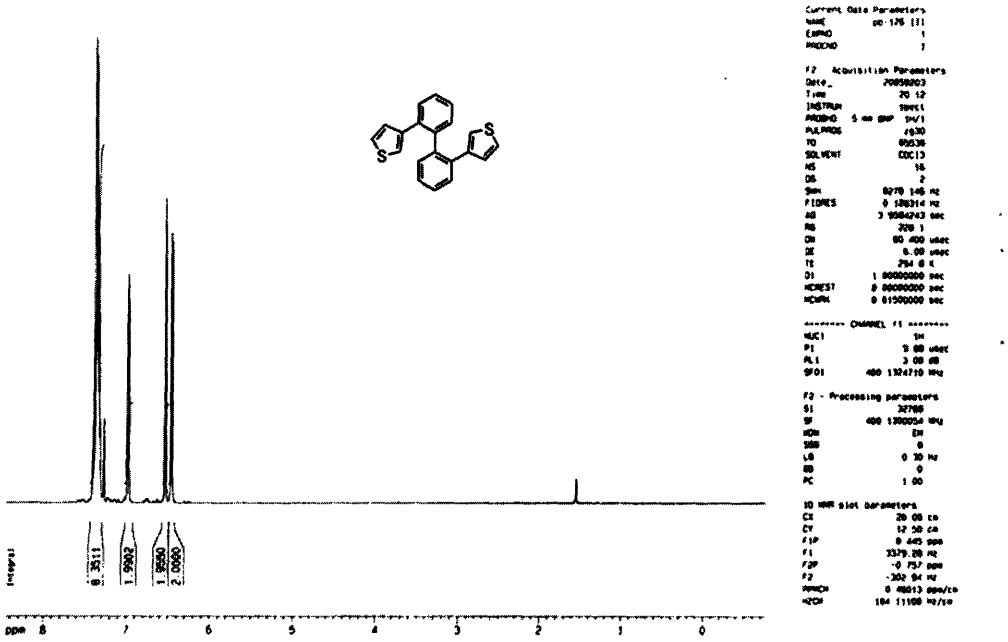

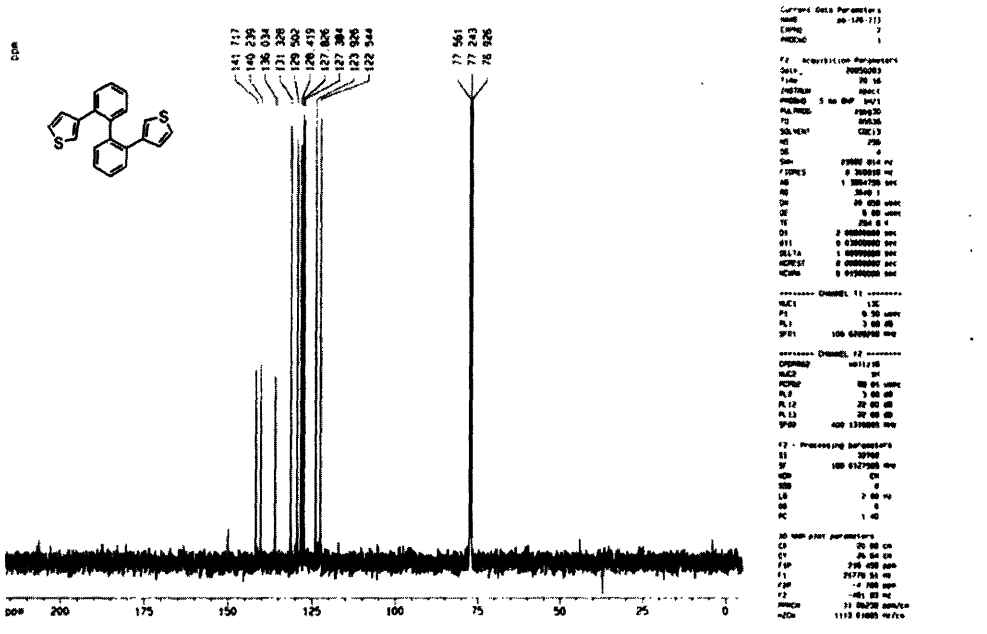

Compound **3**

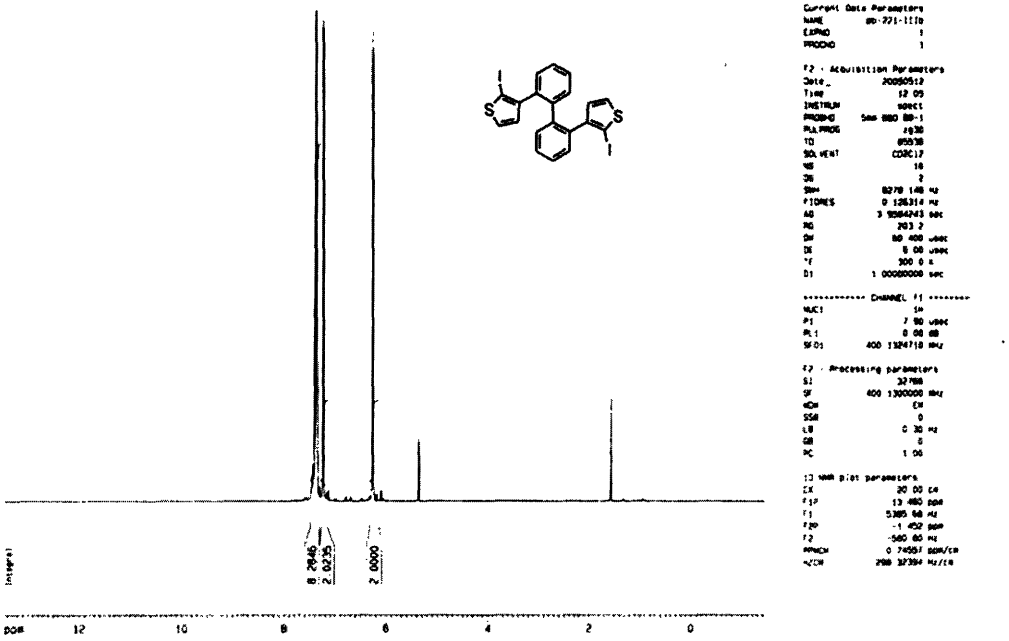

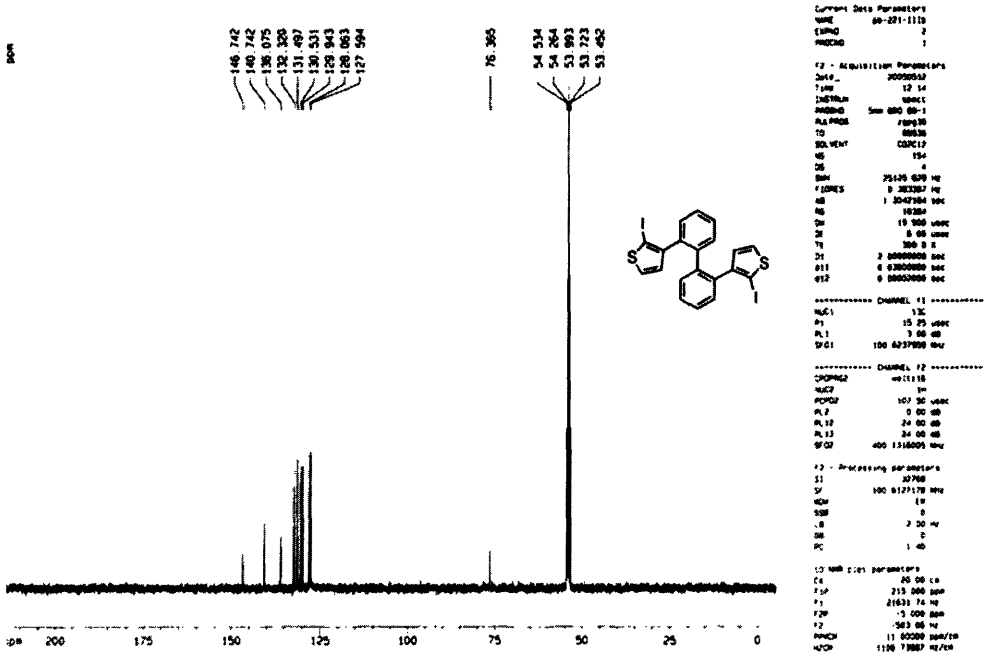

Compound **4**

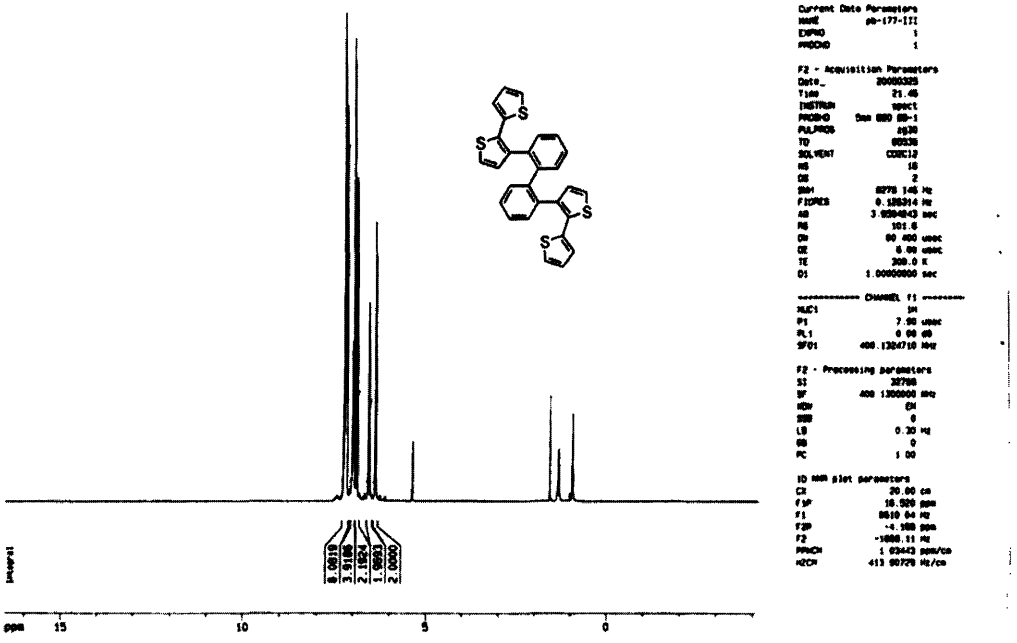

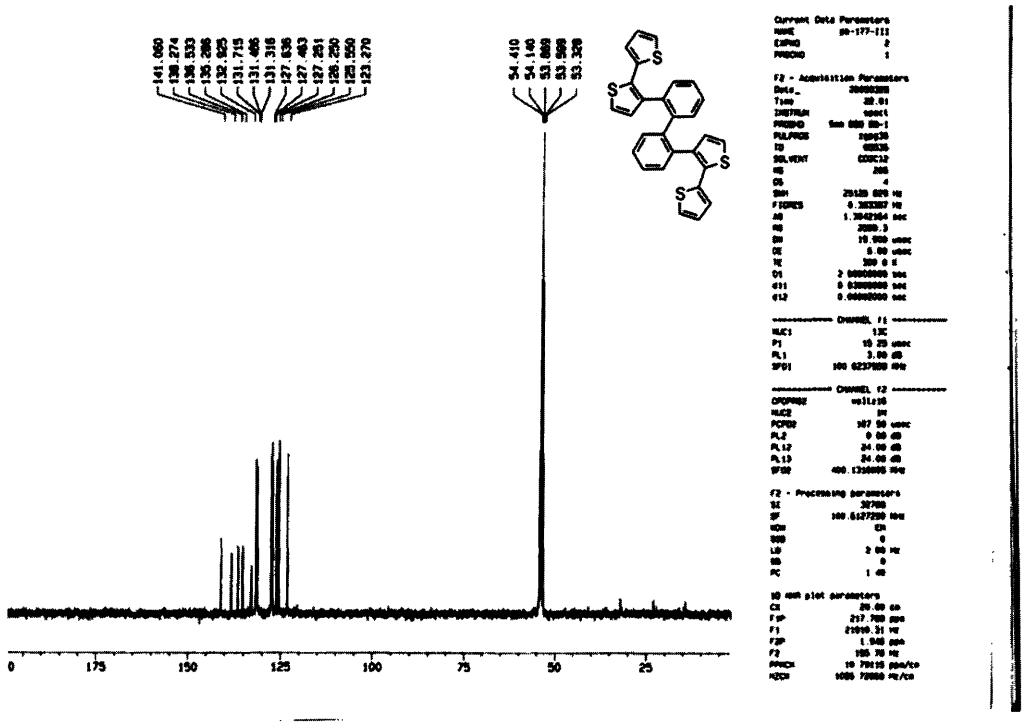

Compound **5**

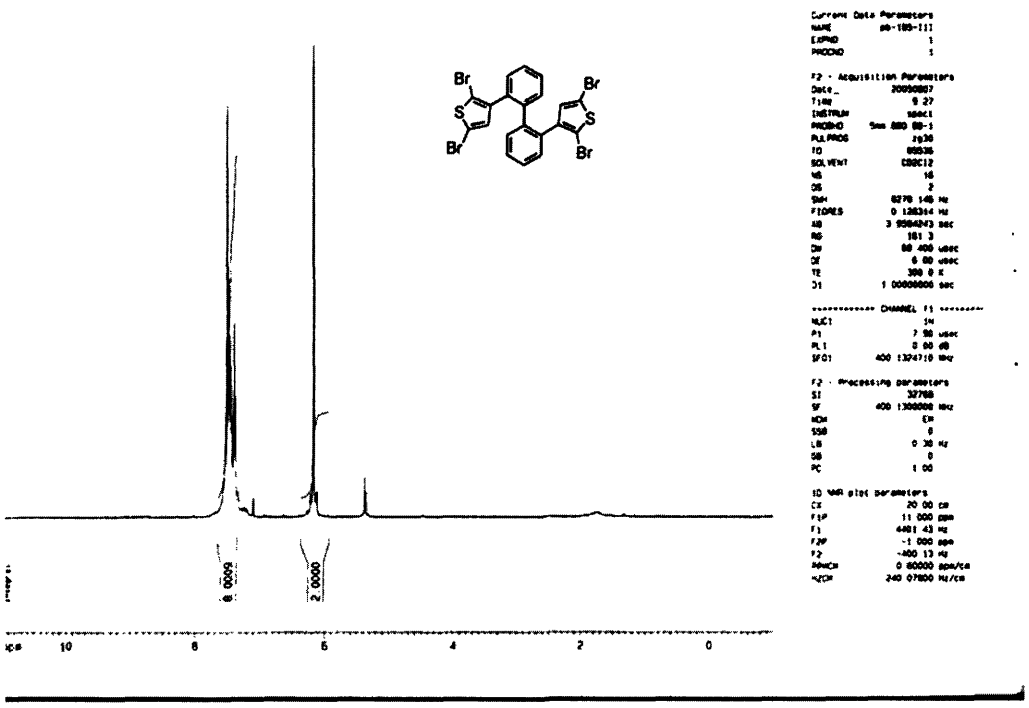

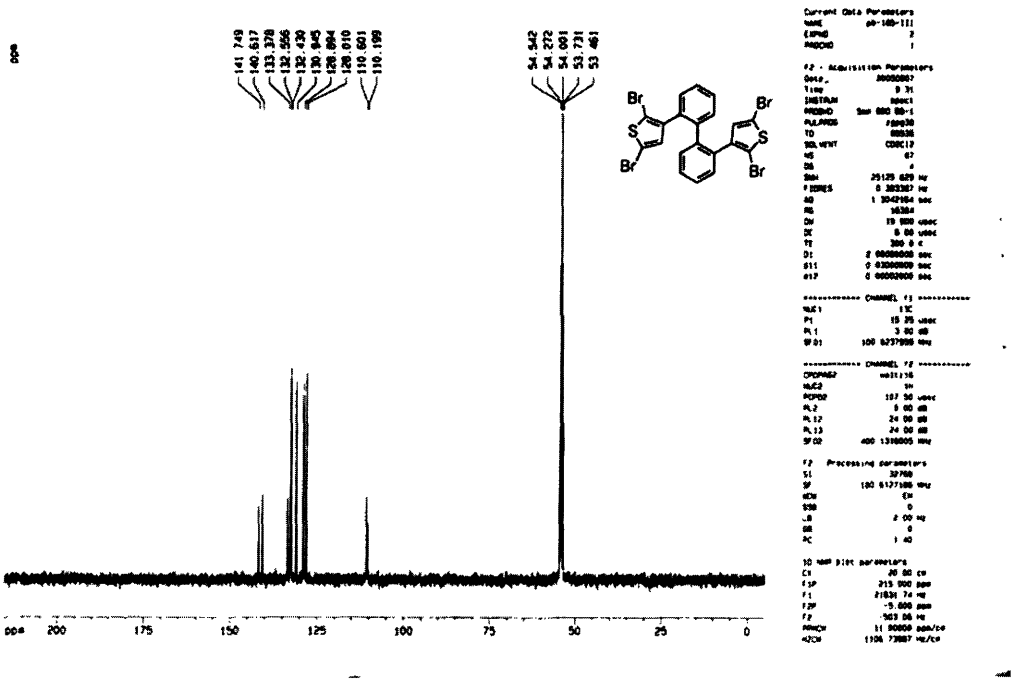

Compound **6**

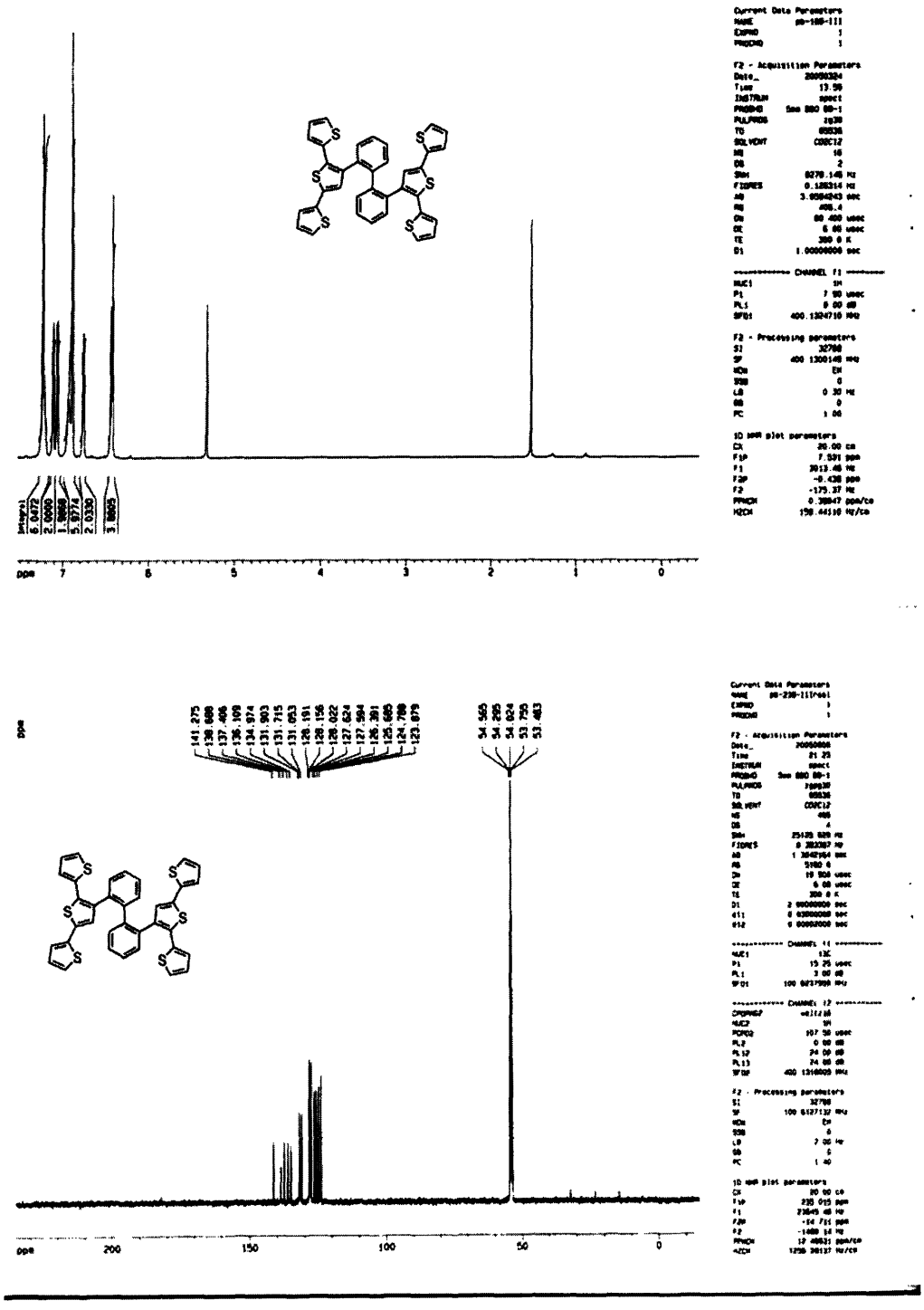

Compound **7**

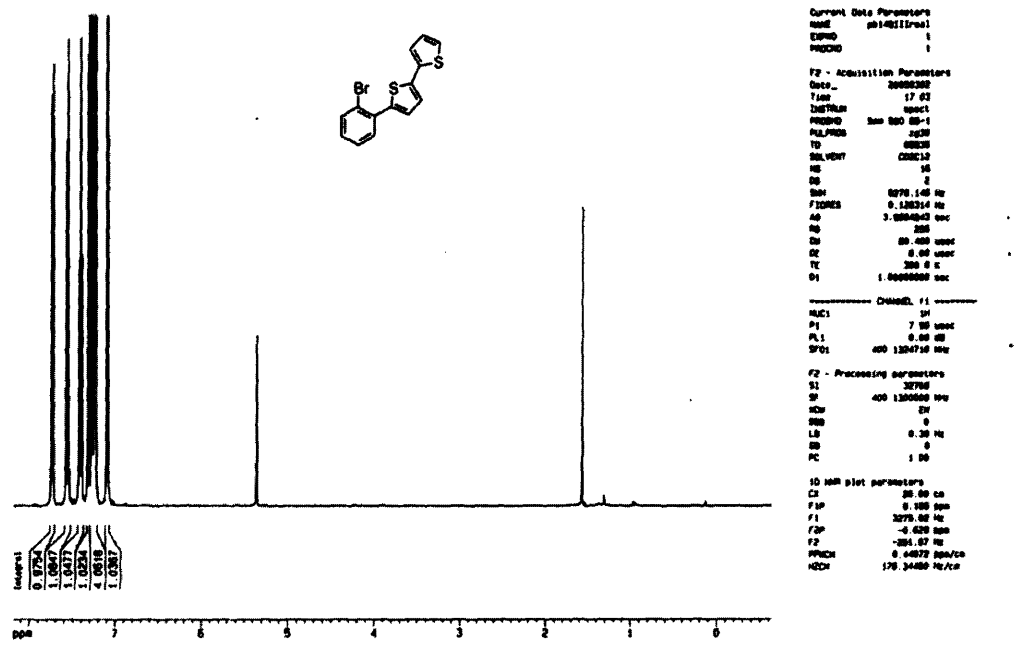

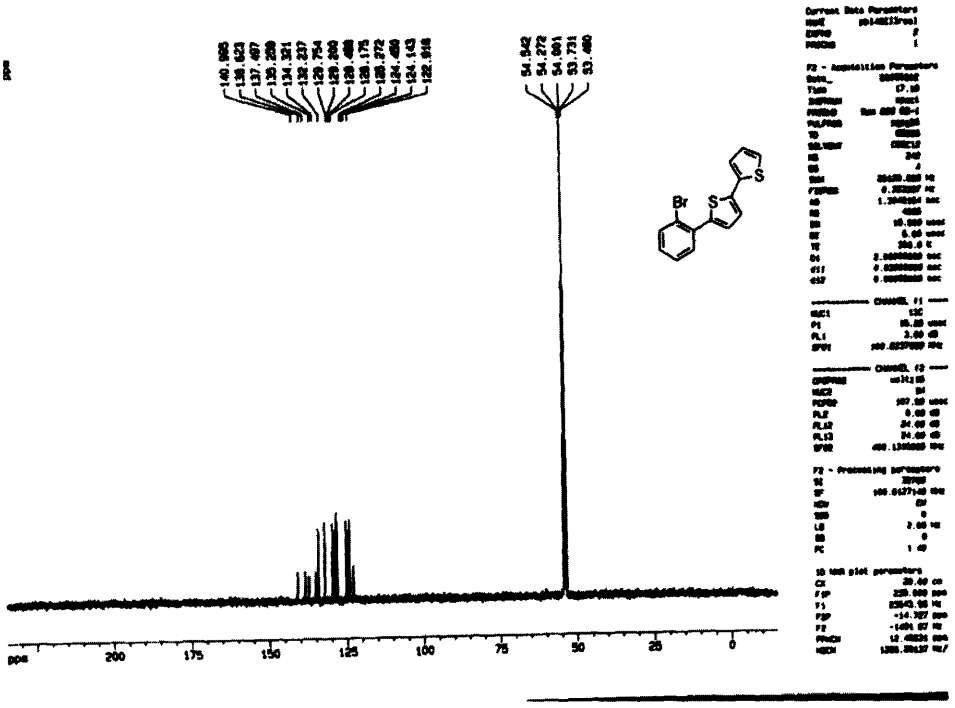

Compound **8**

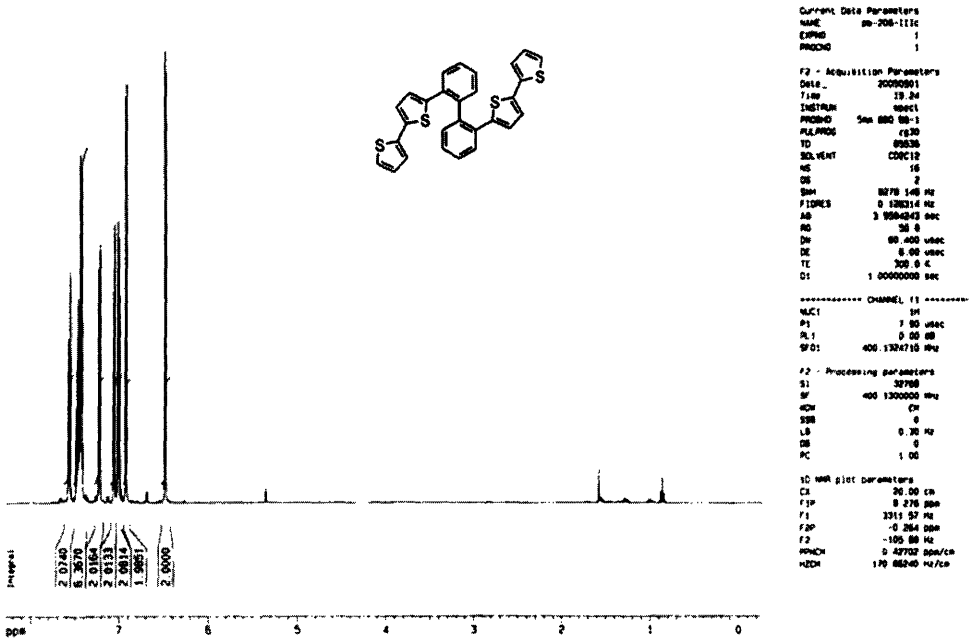

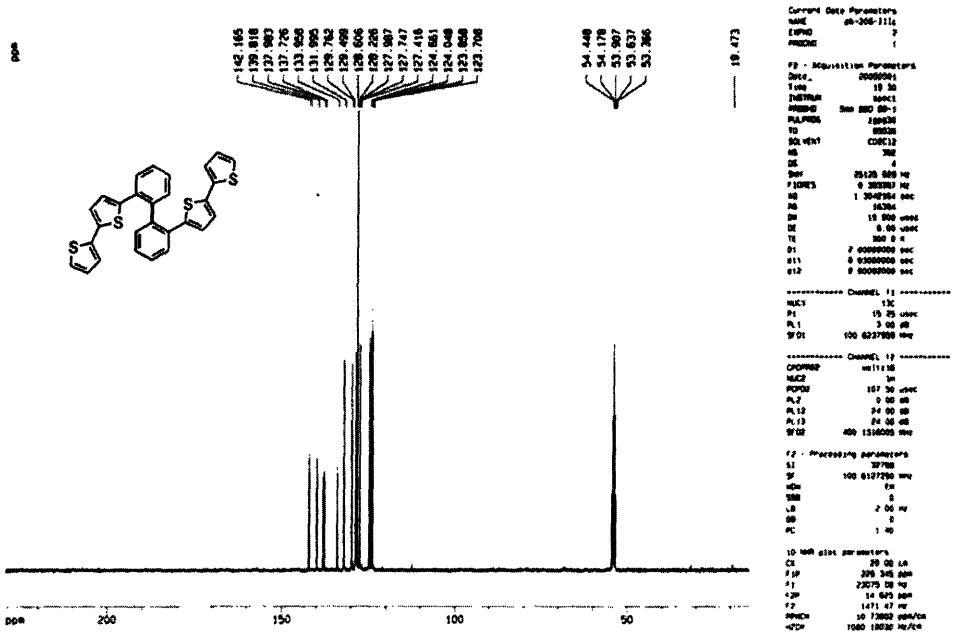

Compound **10**

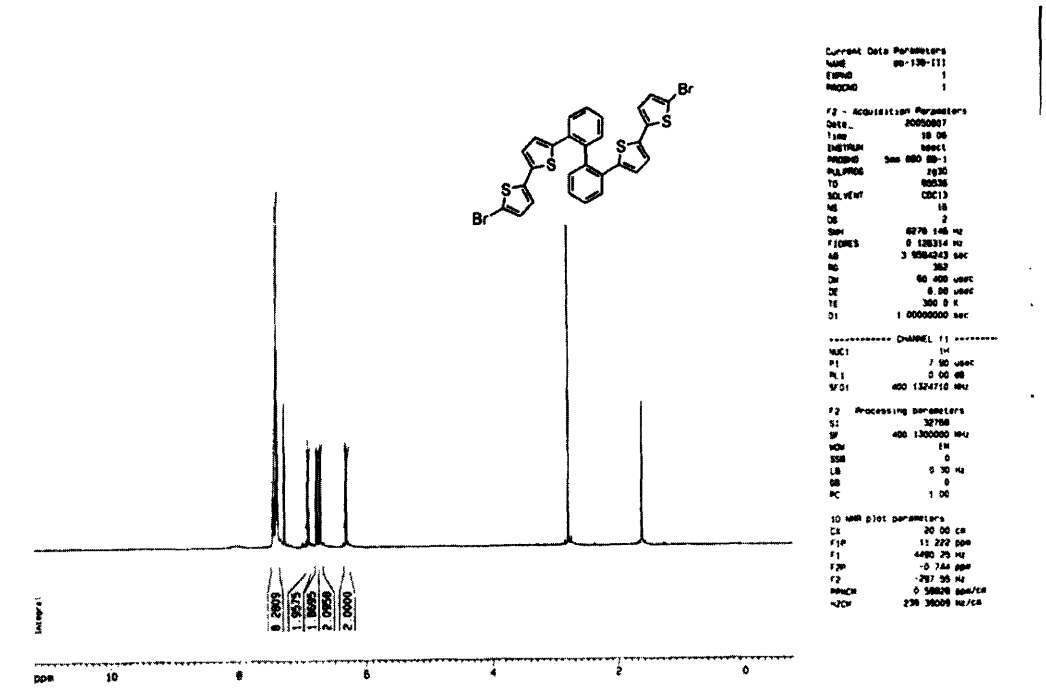

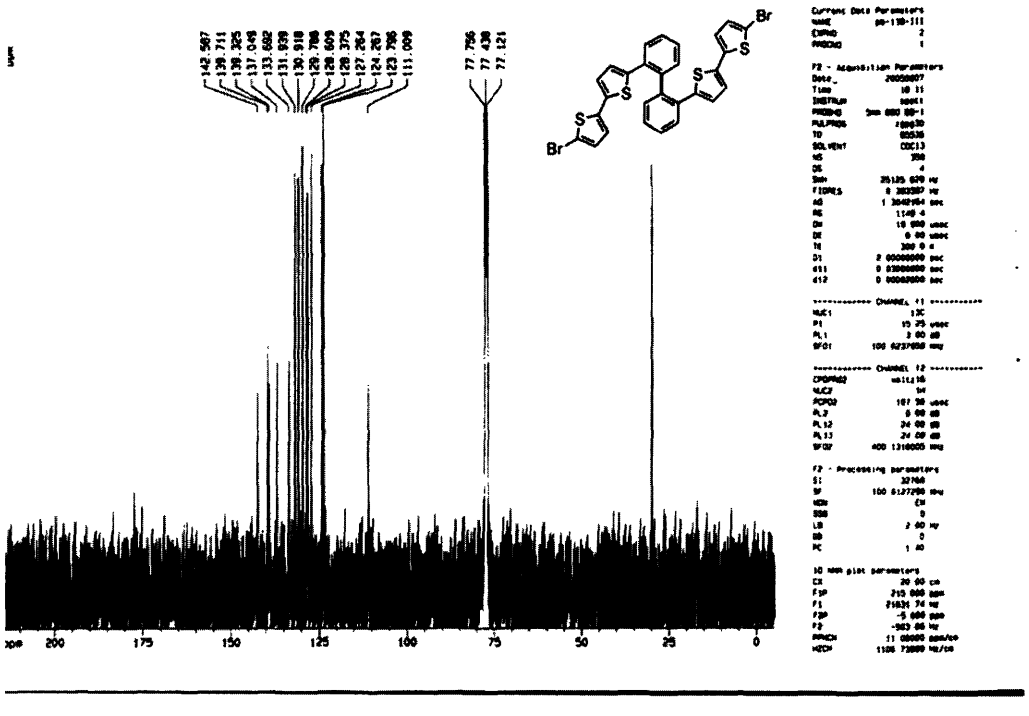

Compound **11**

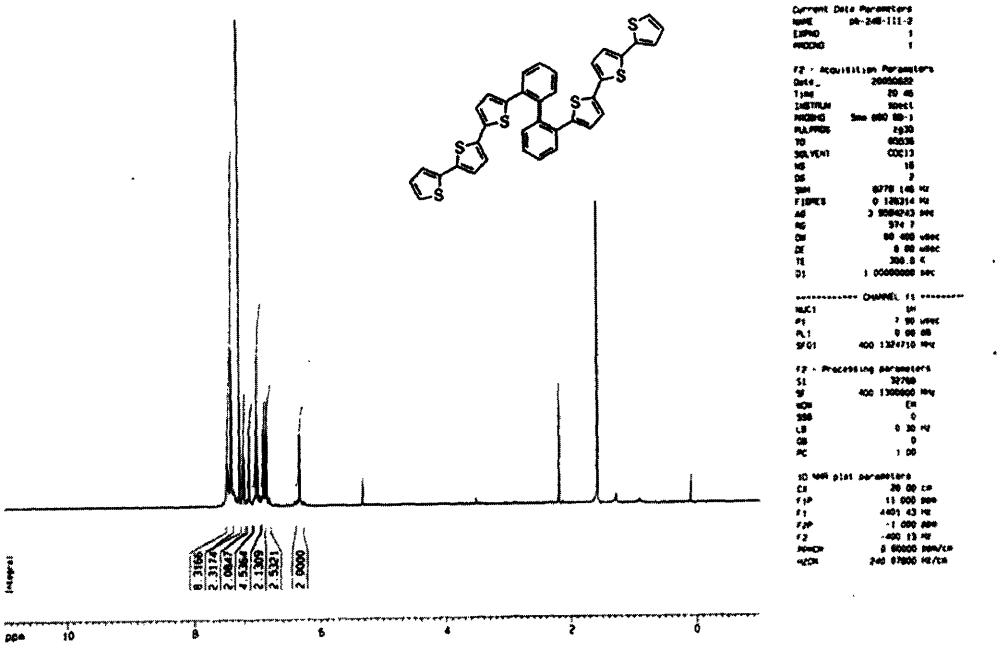

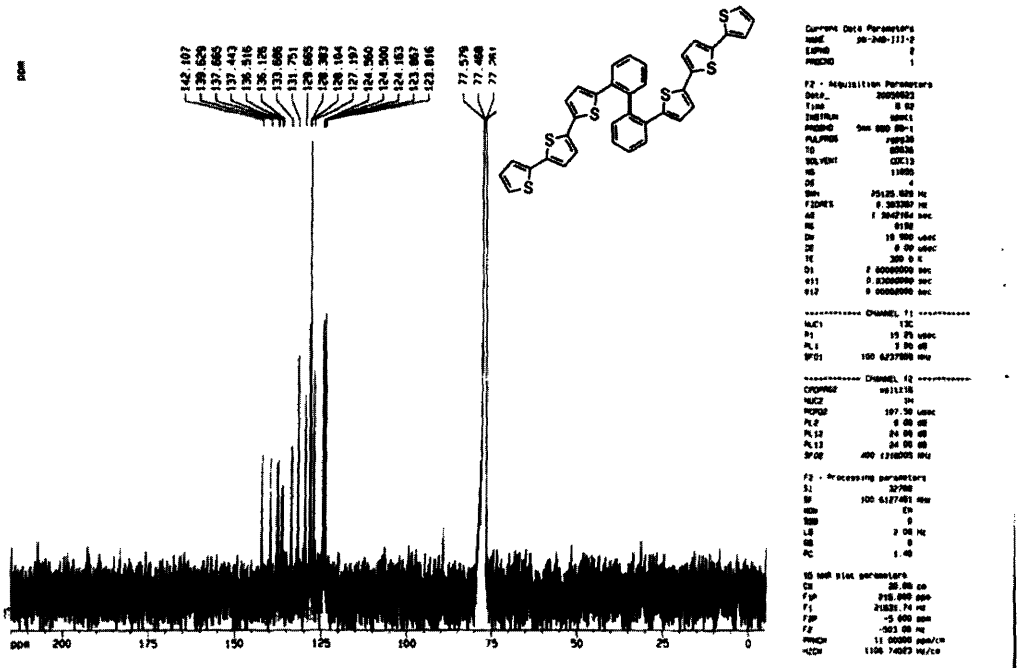

Compound **12**

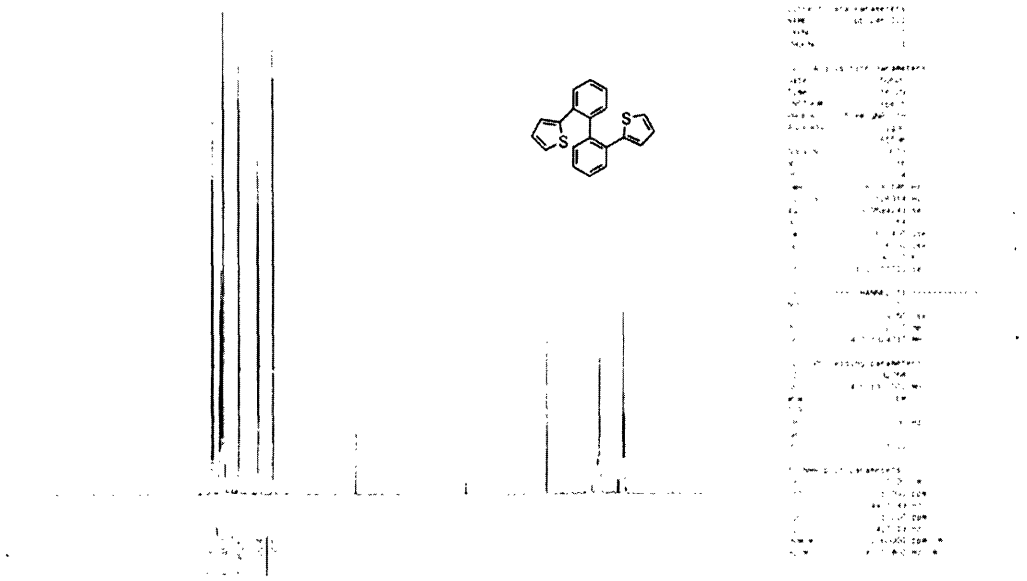

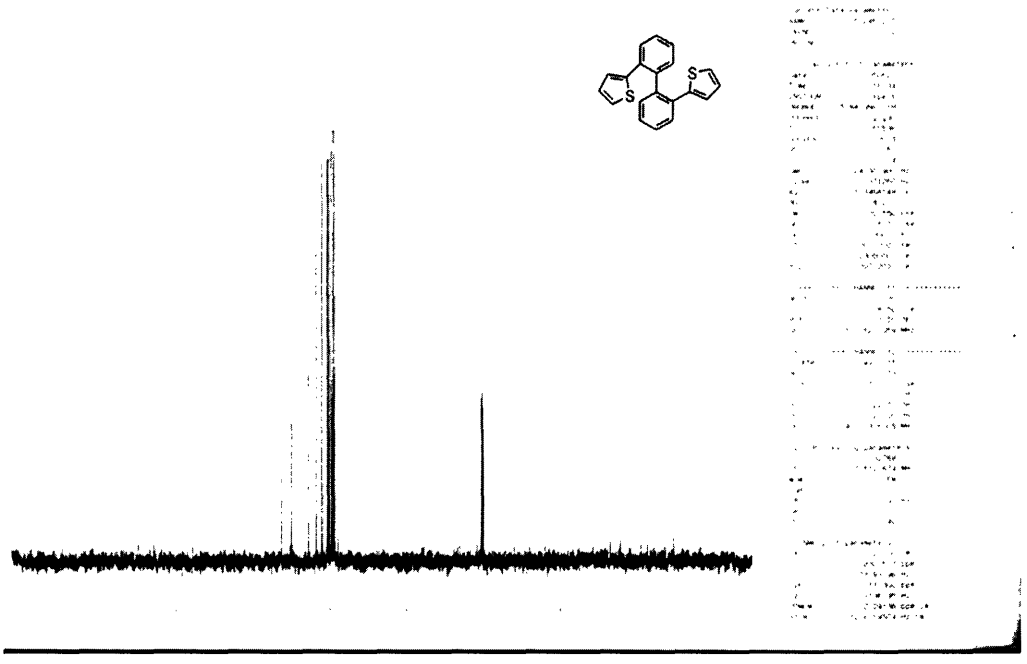

Compound **13**

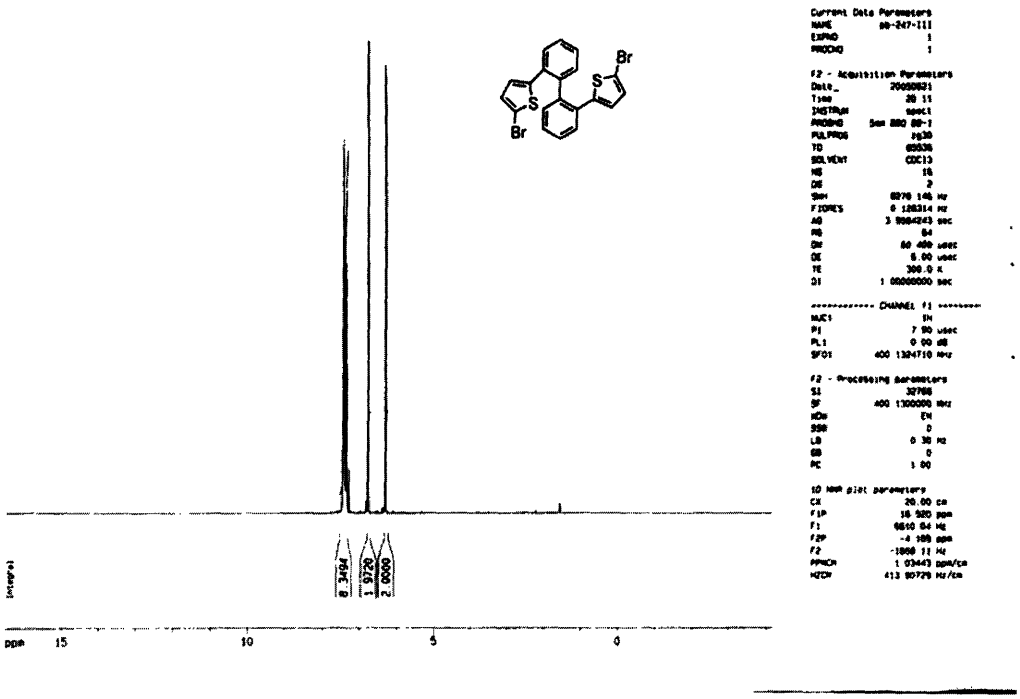
Br
S
Br
8.3494
1.9220
2.0000
ppm
15
10
5
0

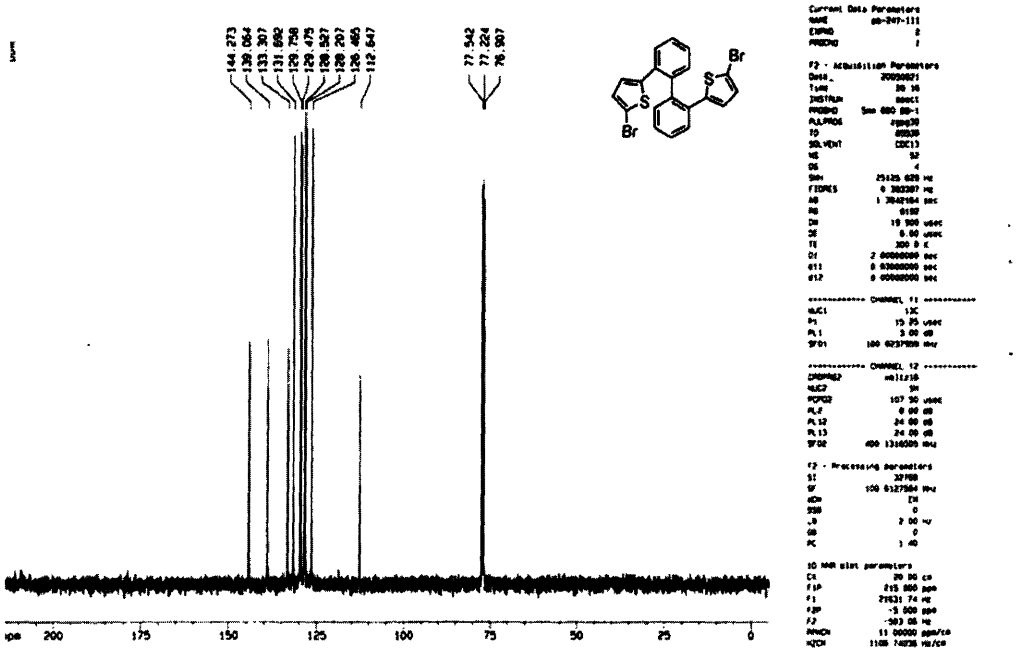
144.273
139.064
133.307
131.892
129.758
129.475
128.587
128.267
126.465
112.847
77.542
77.224
76.907
Br
S
Br
ppm
200
175
150
125
100
75
50
25
0

Compound **14**

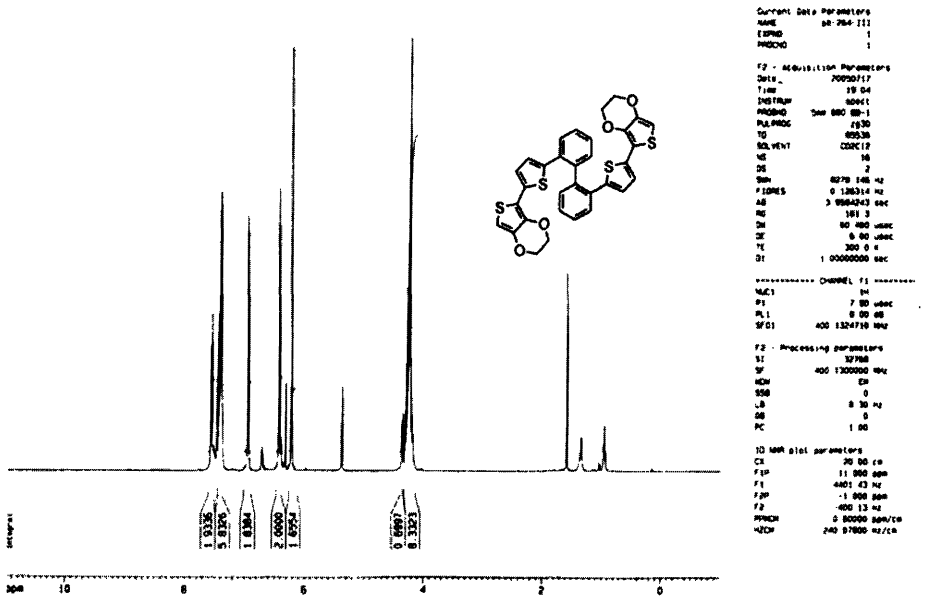

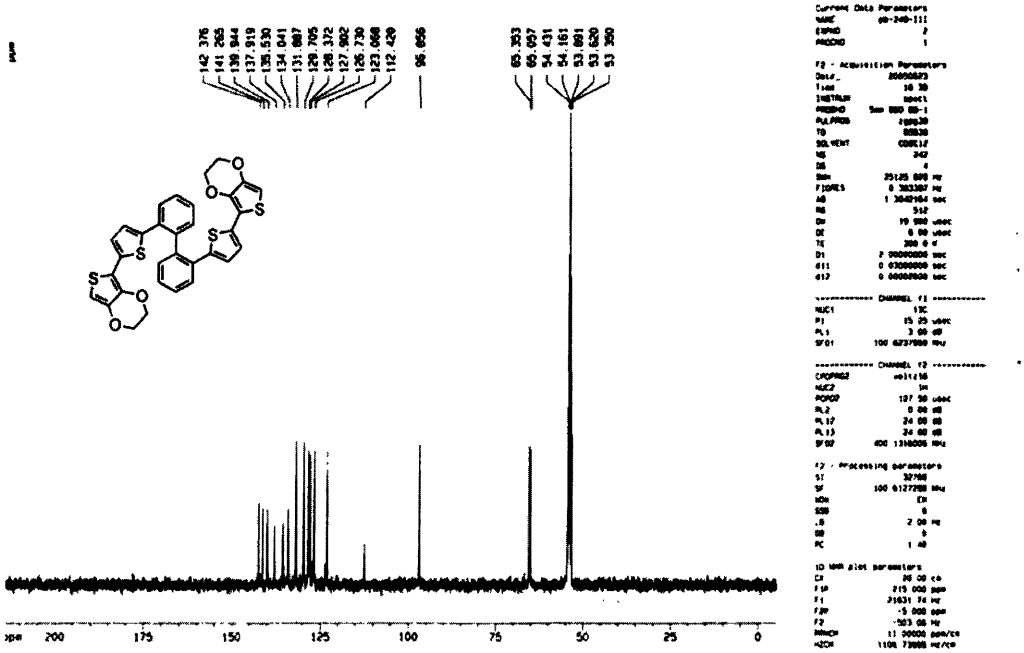

Compound **15**

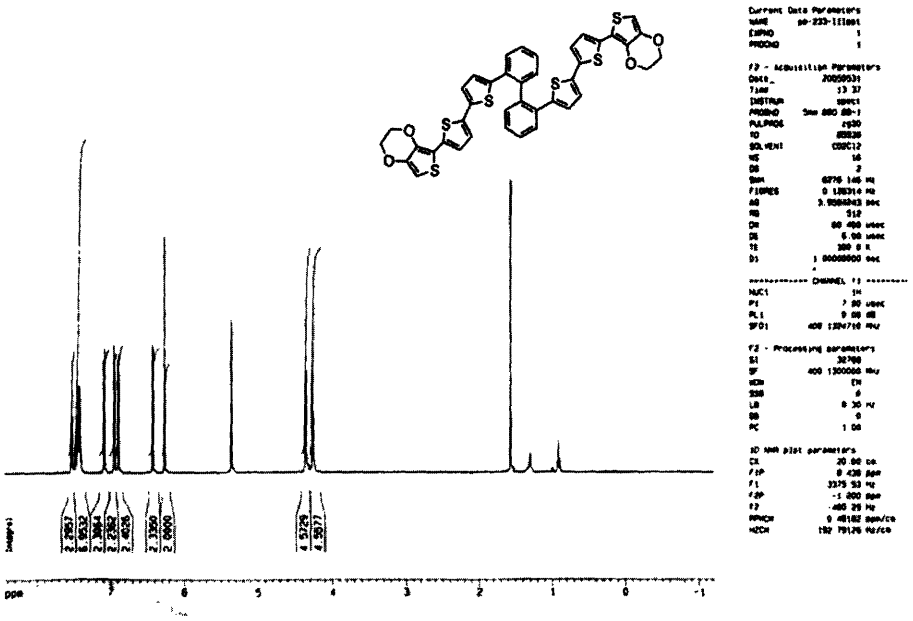

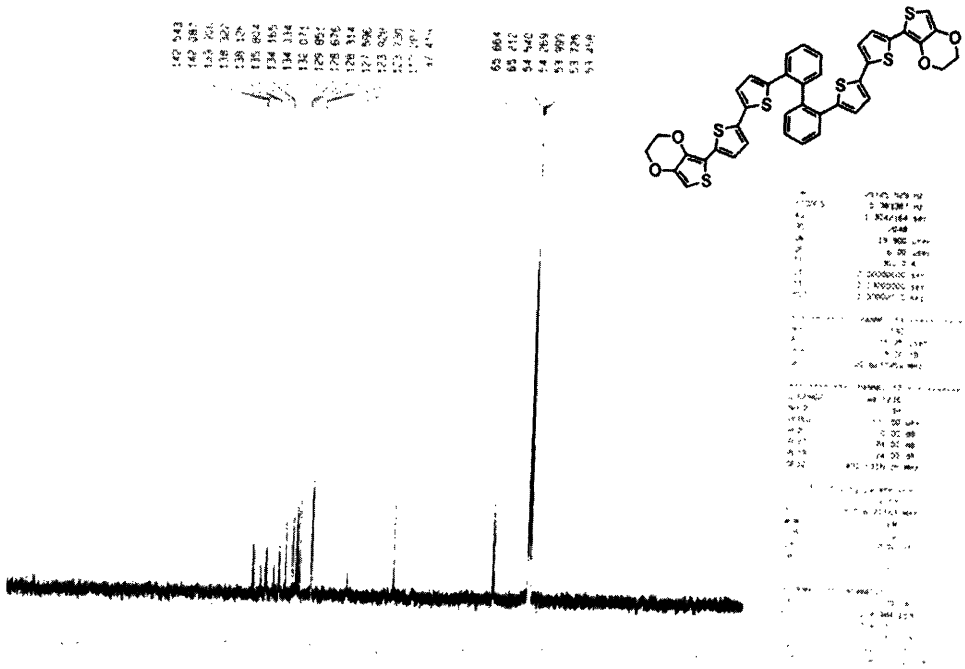

Compound **16**

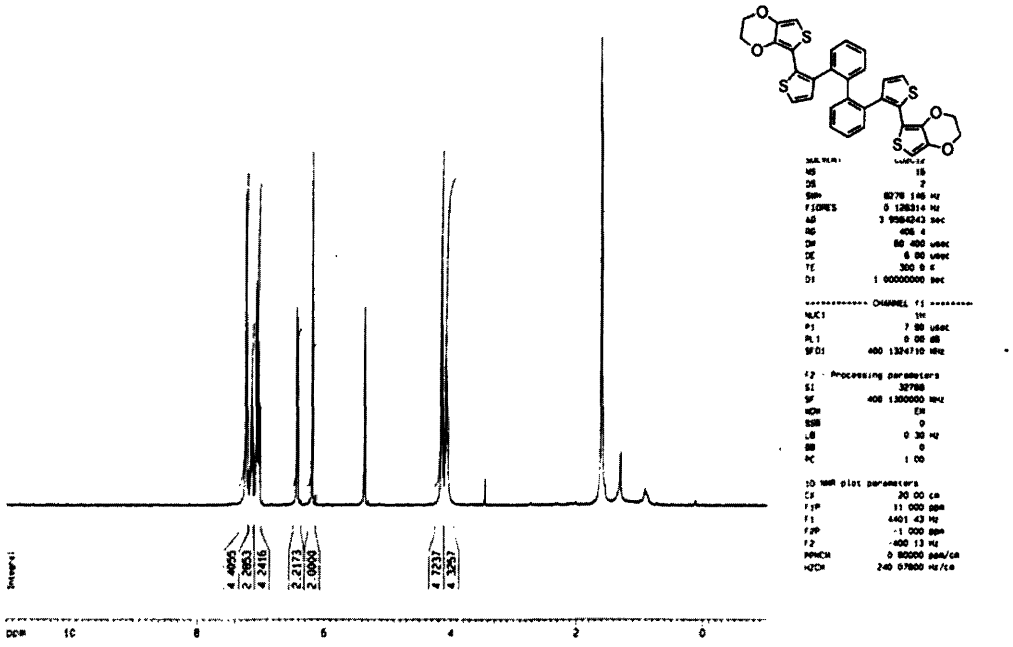

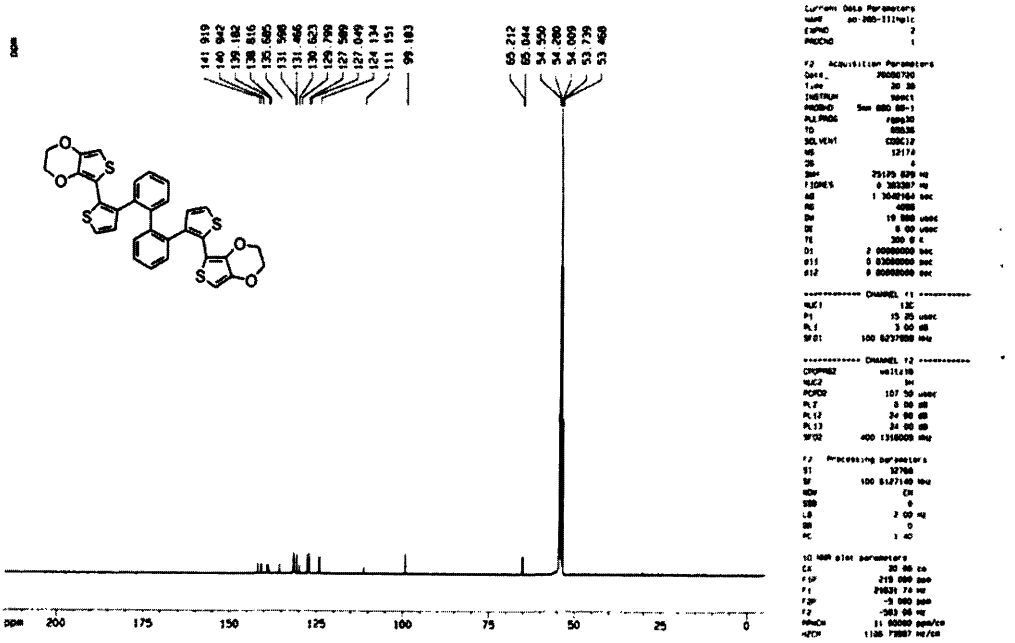

Compound **17**

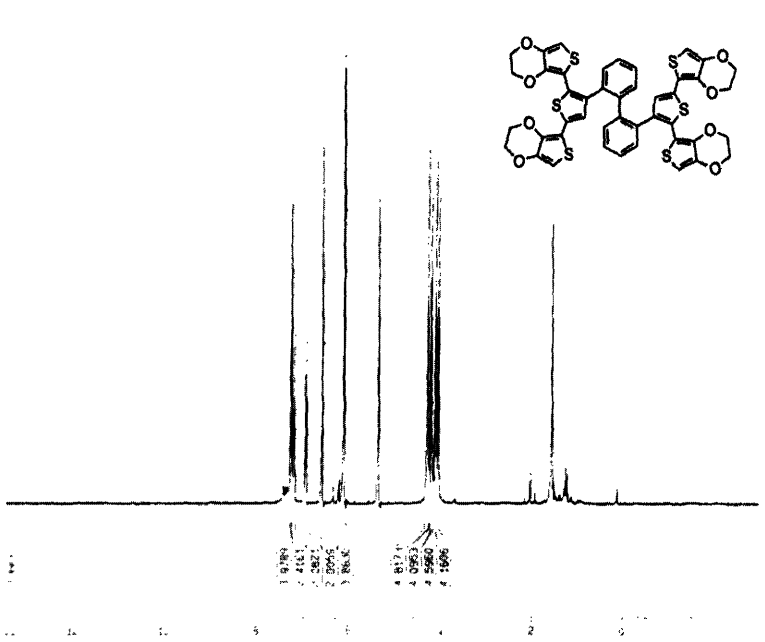

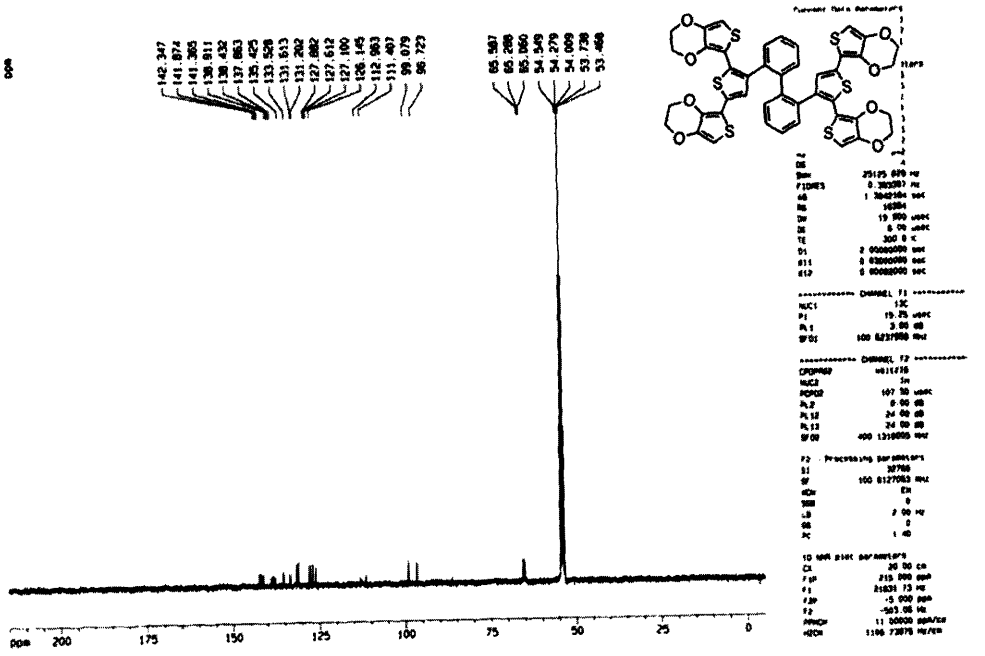

Compound **18**

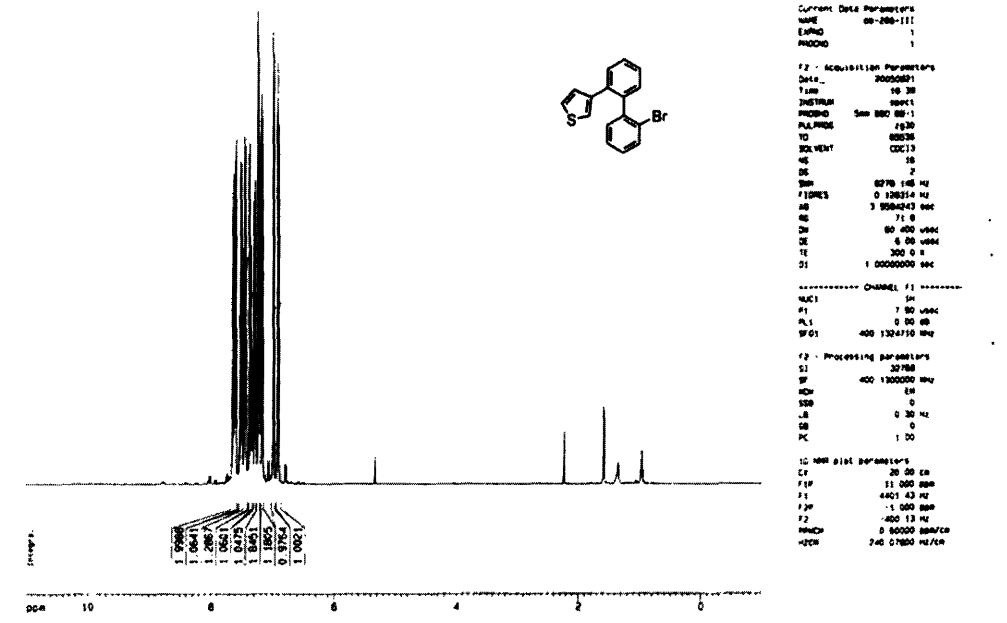

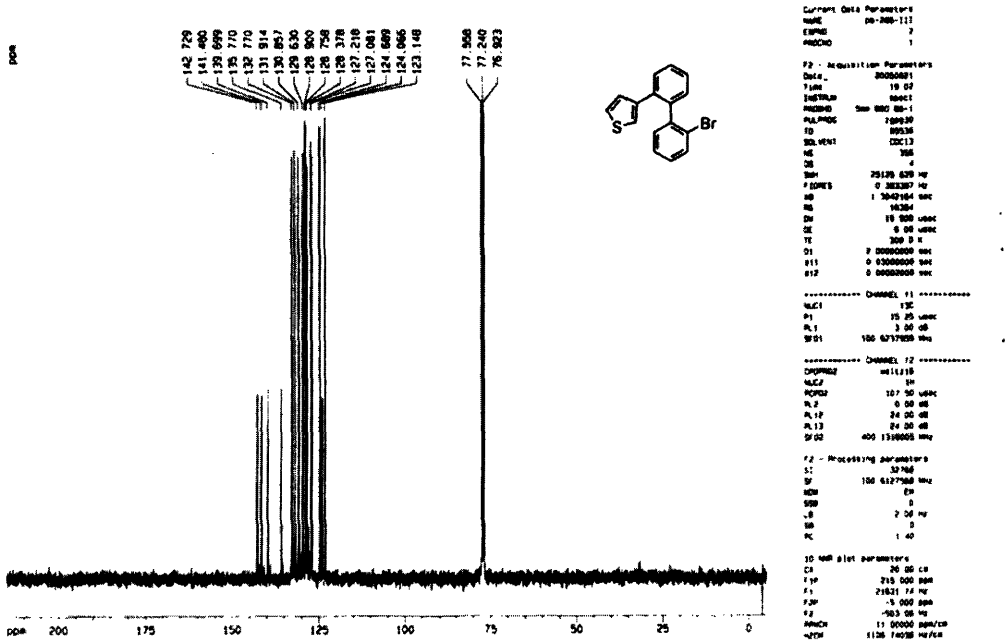

Compound **19**

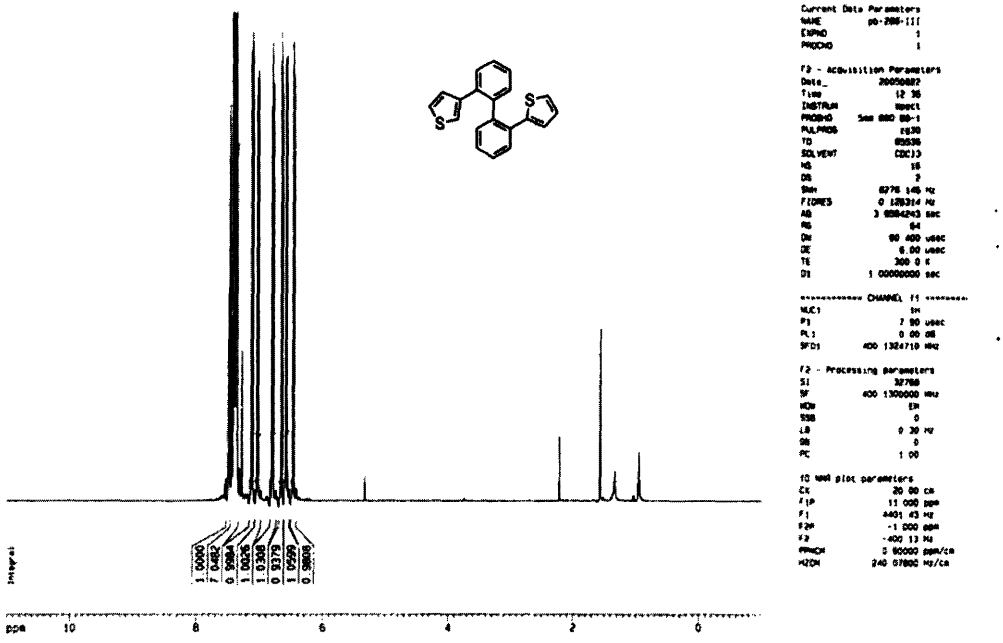

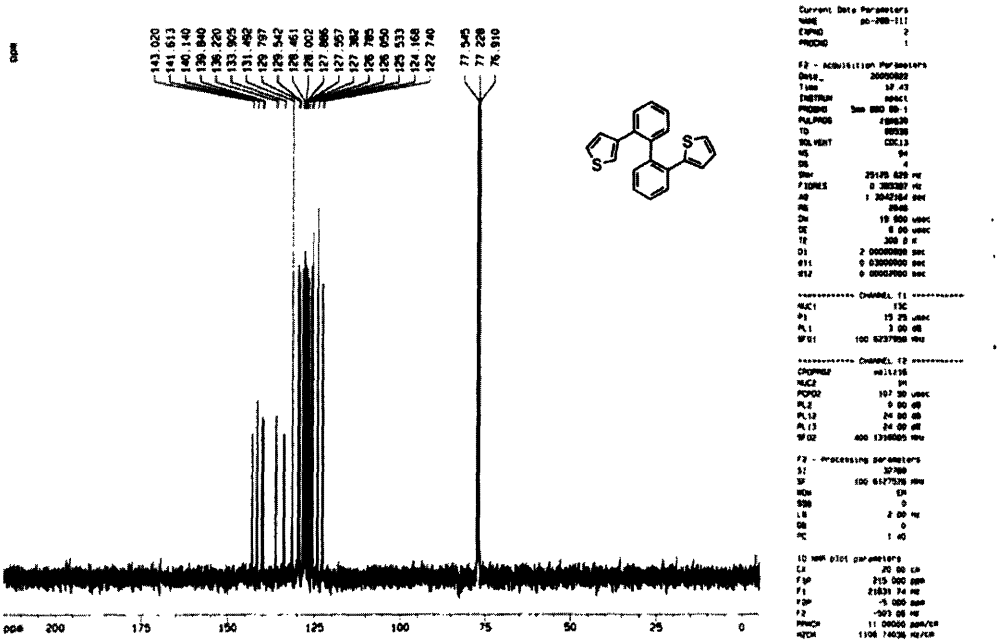

Compound **20**

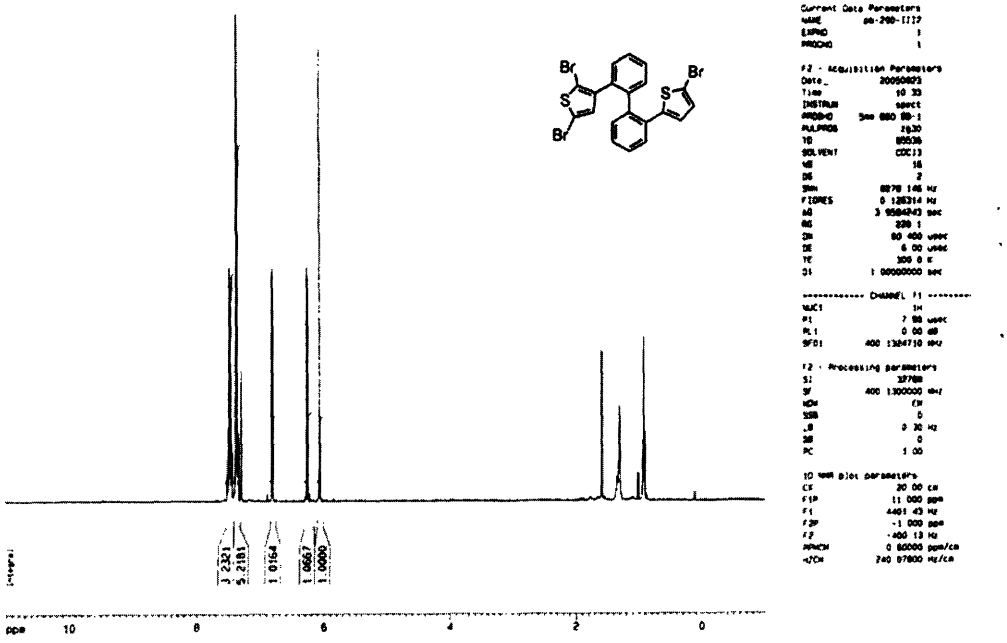

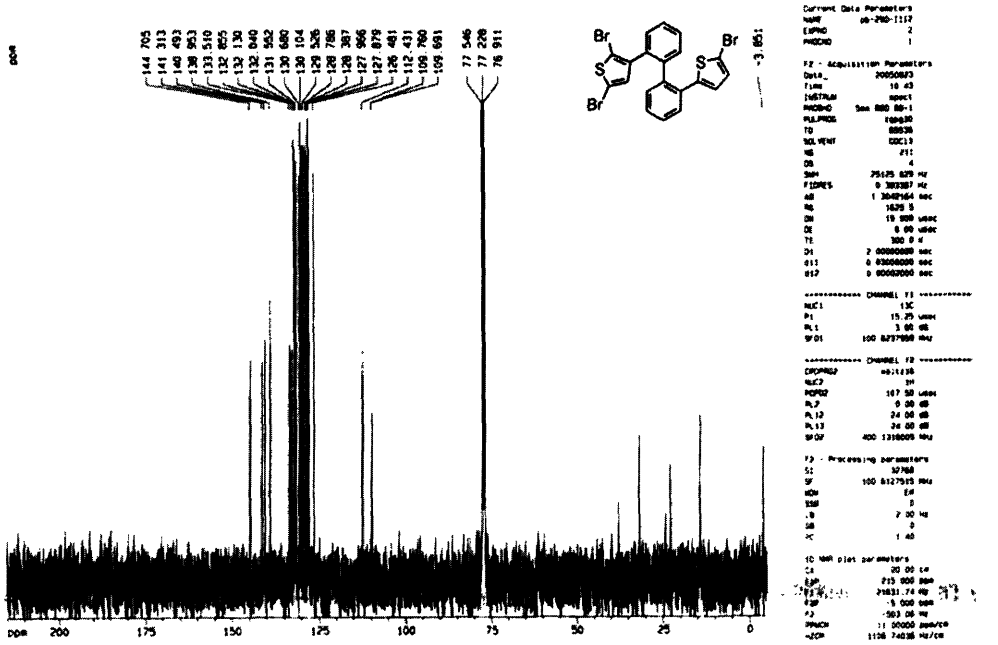

Compound **21**

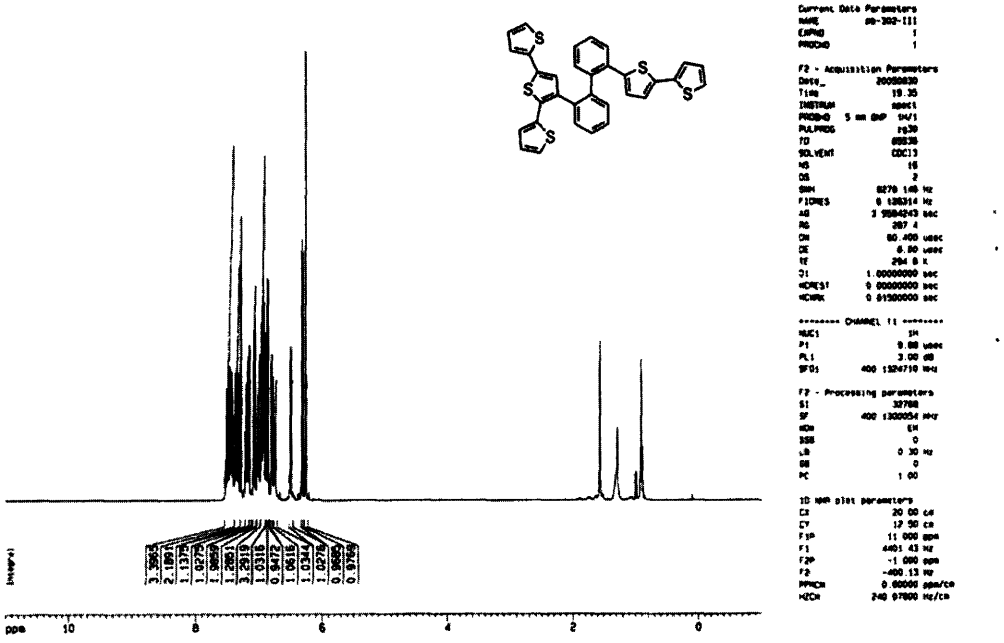

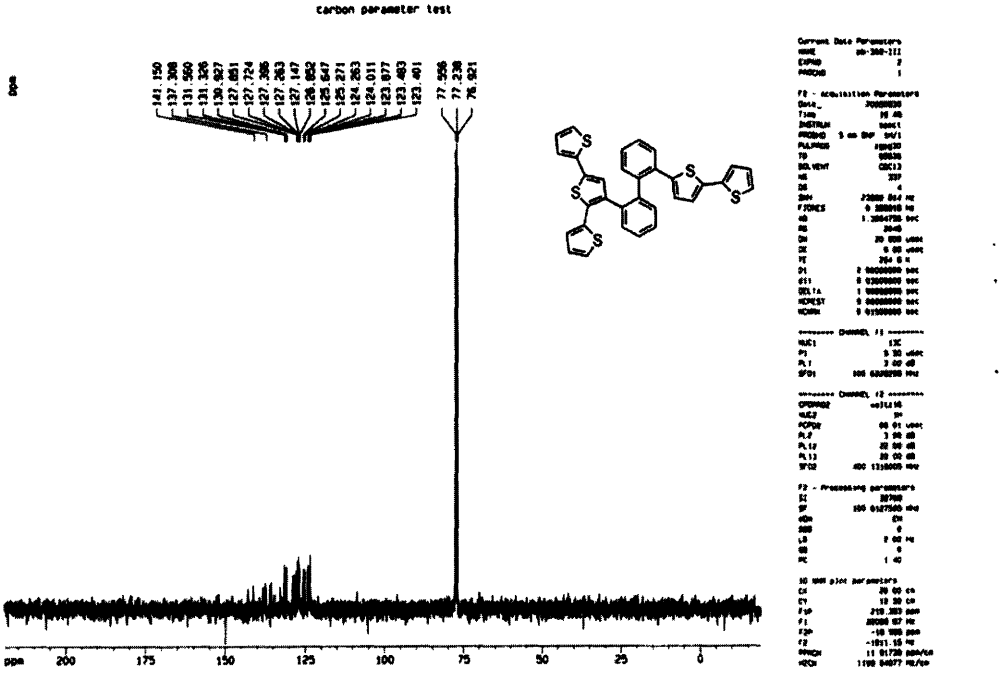

Compound **22**

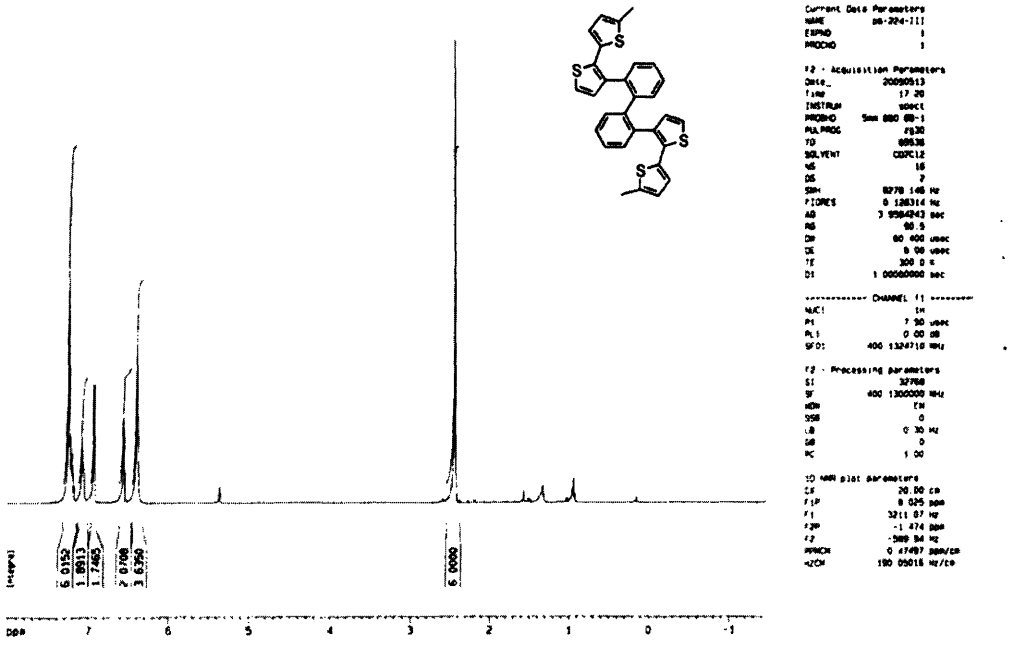

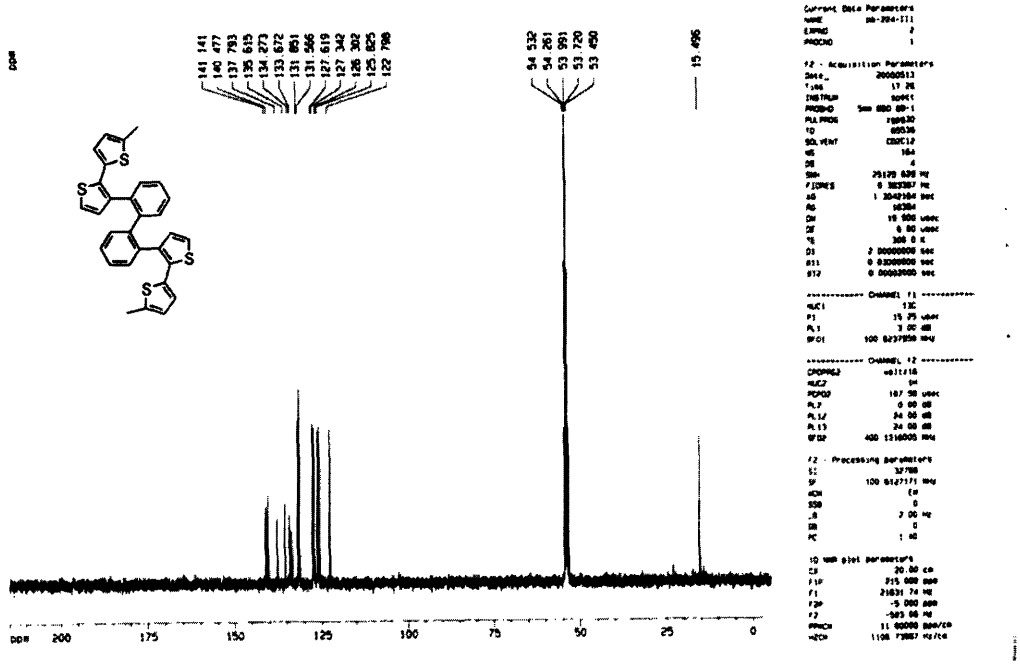

Compound **m-4**

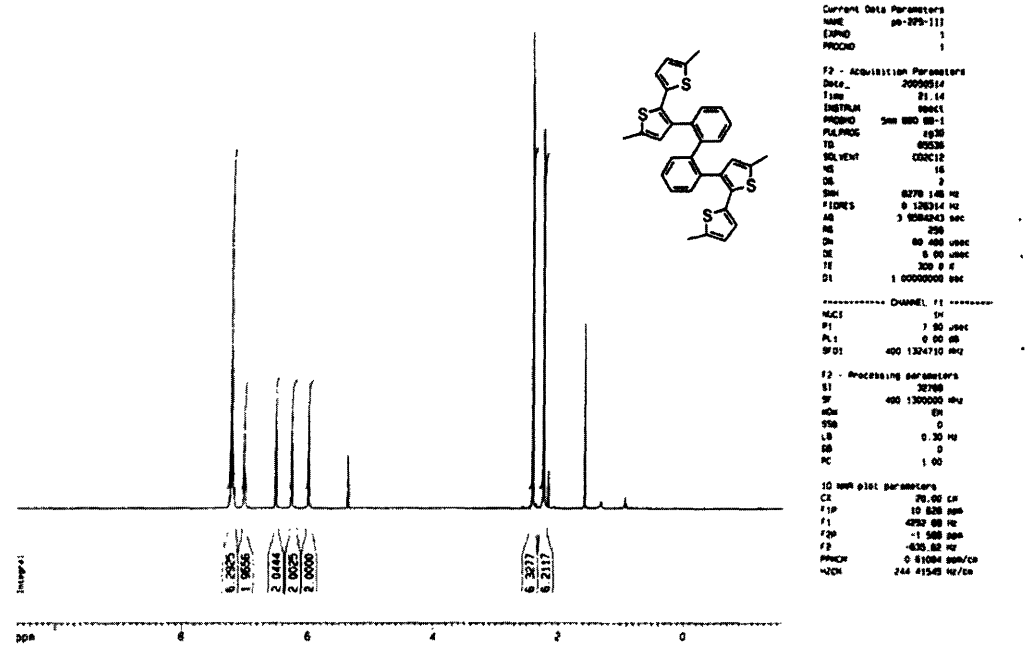

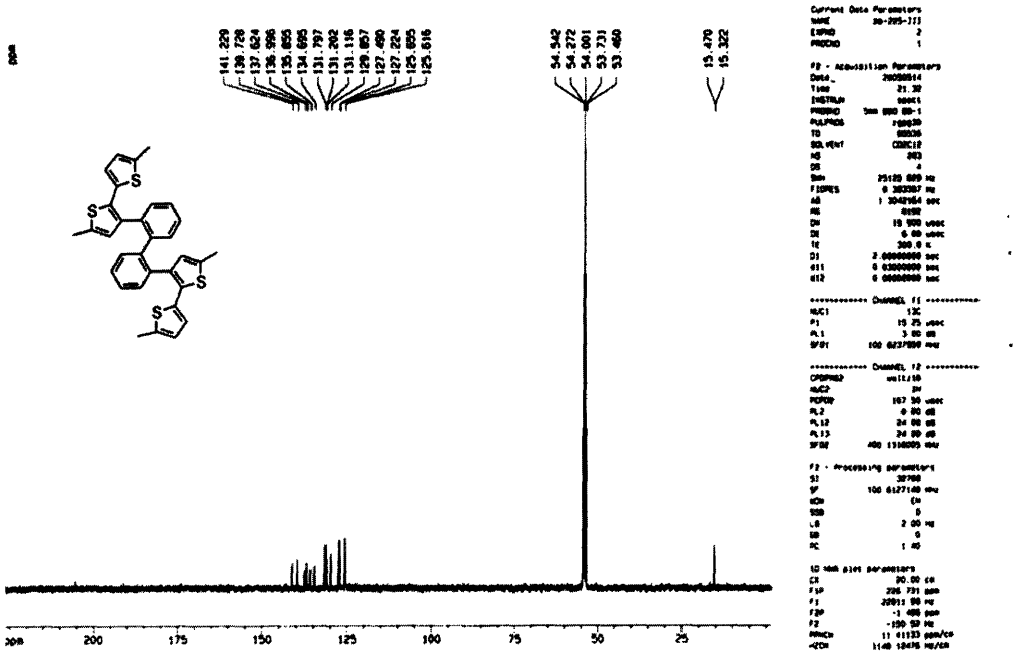

Compound **m-6**

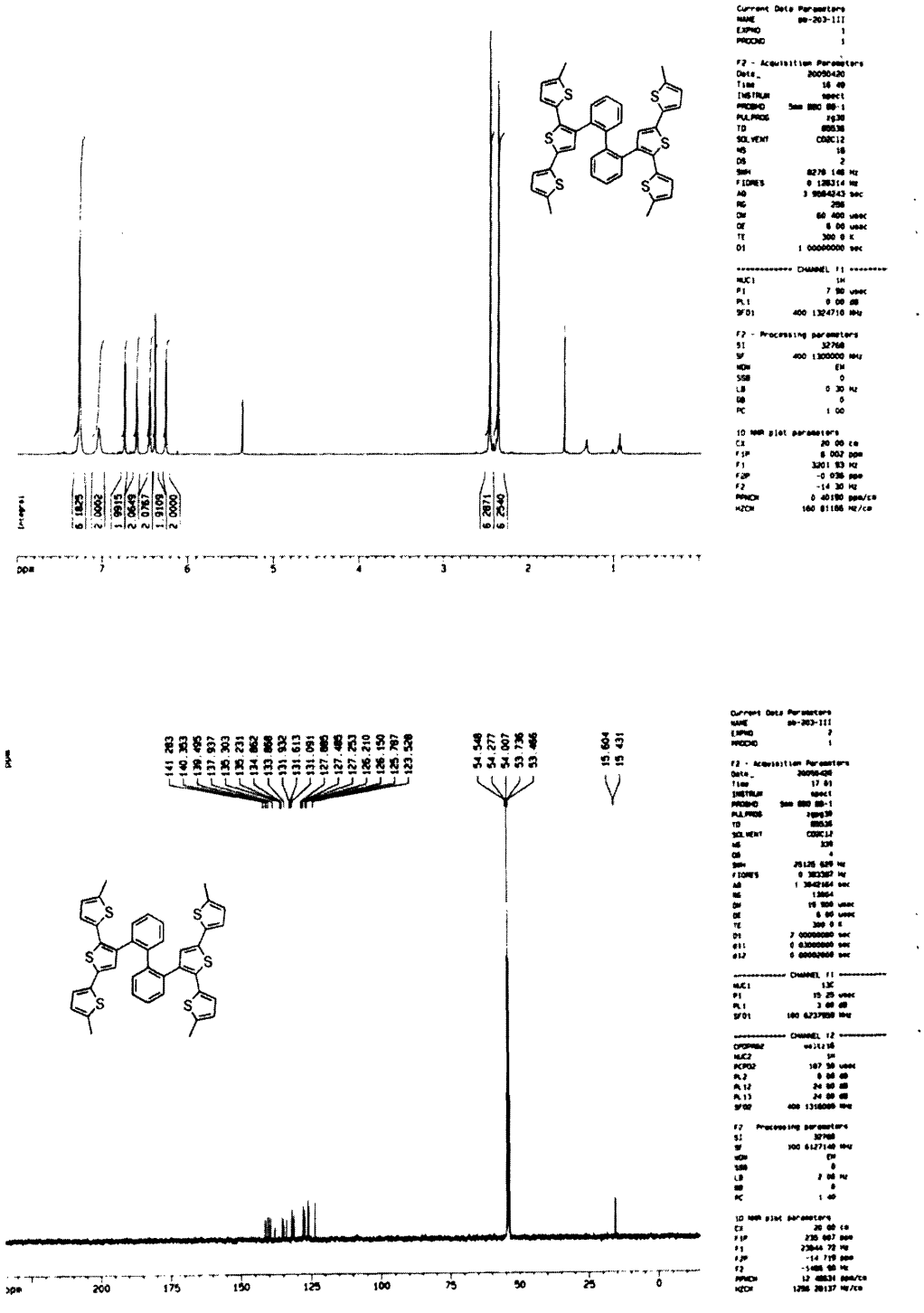

Compound **m-9**

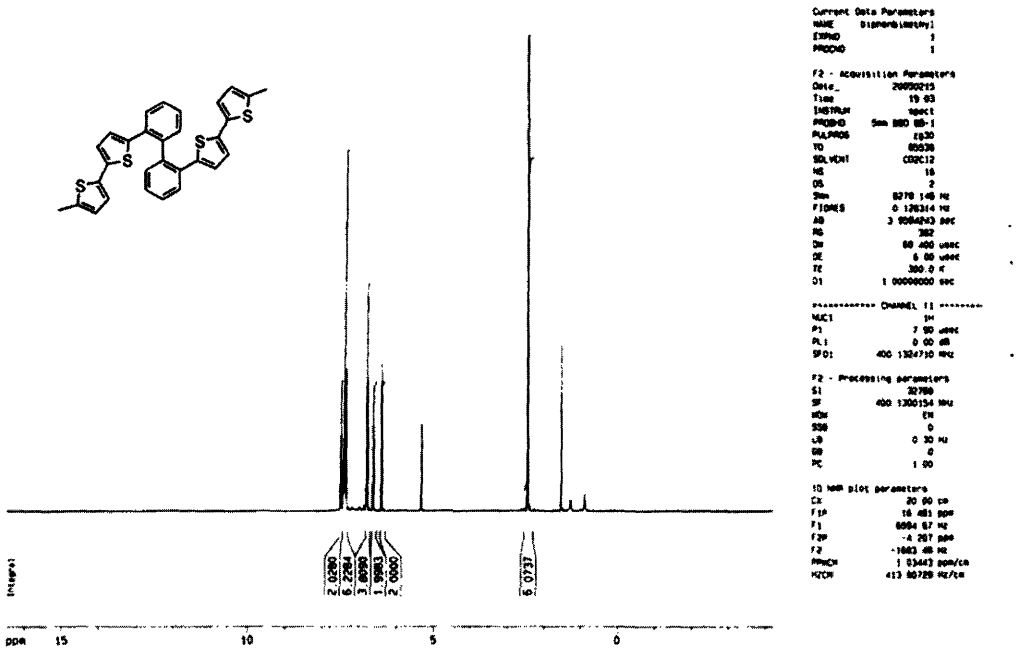

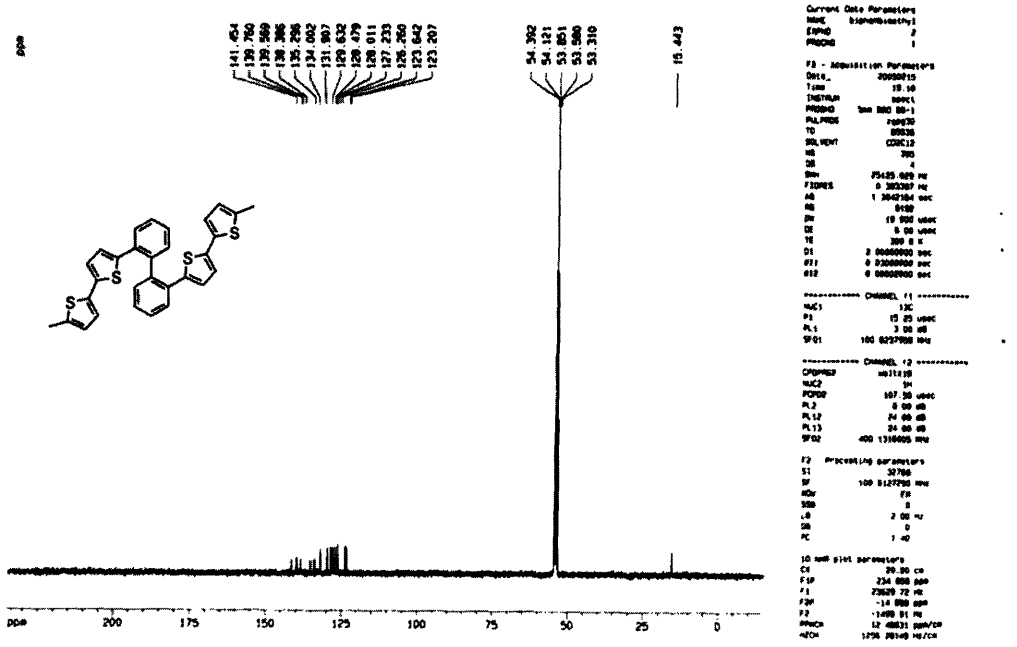

Compound **m-11**

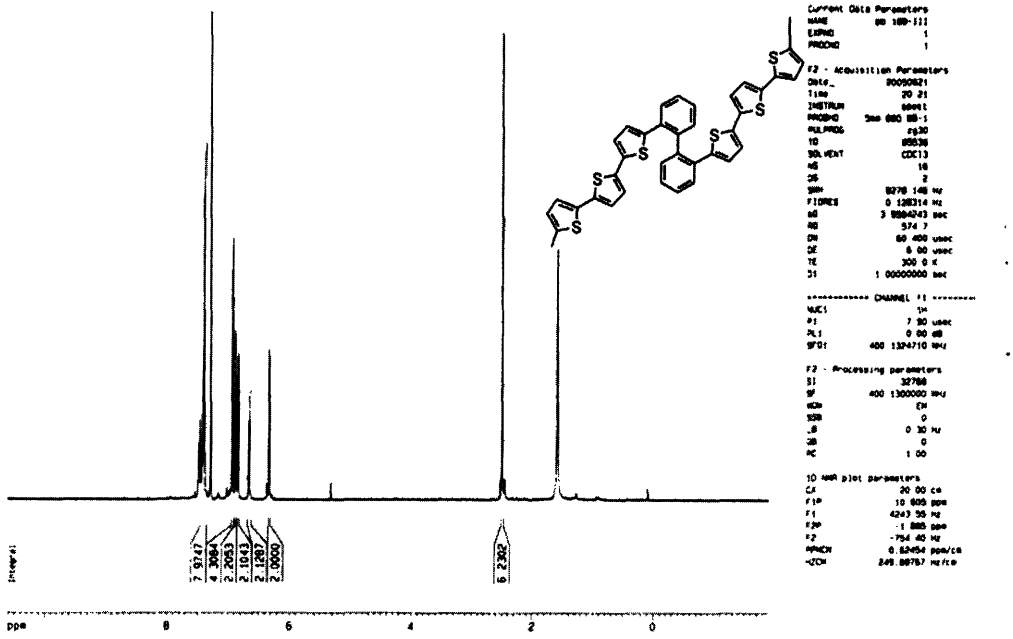

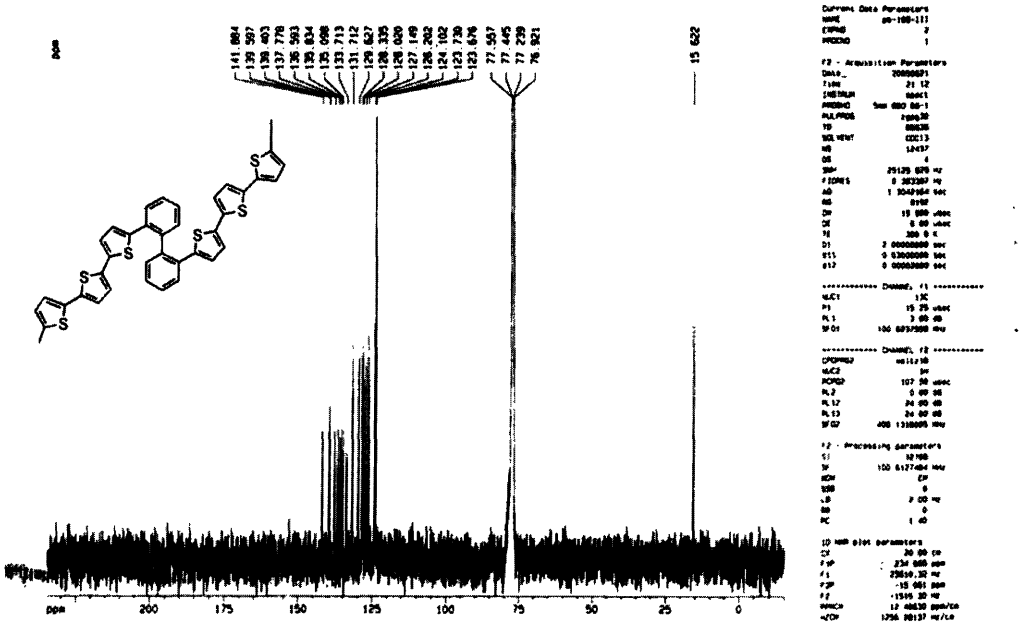

Compound **23**

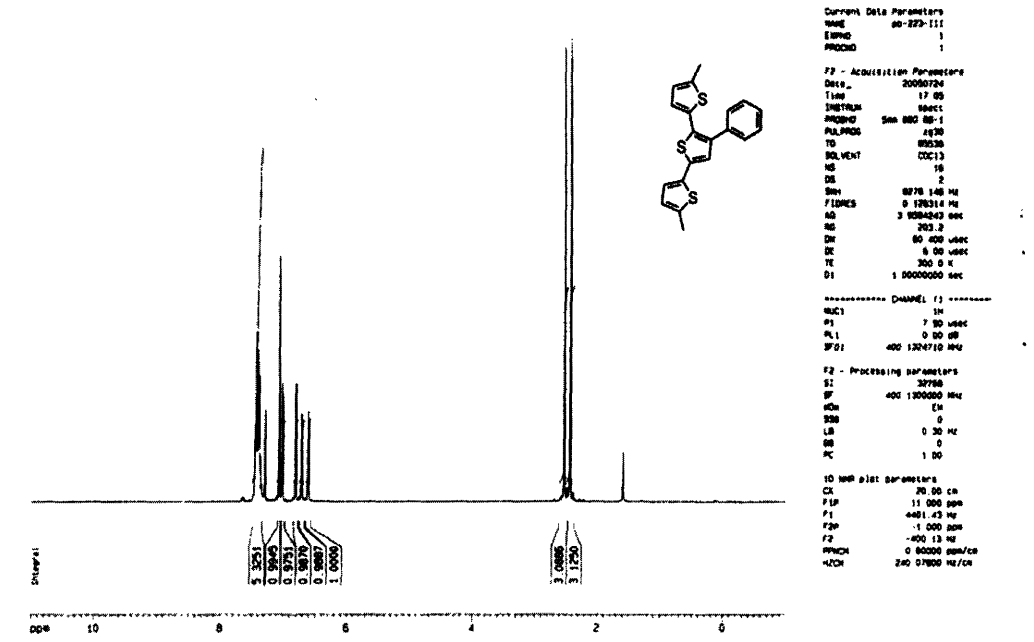

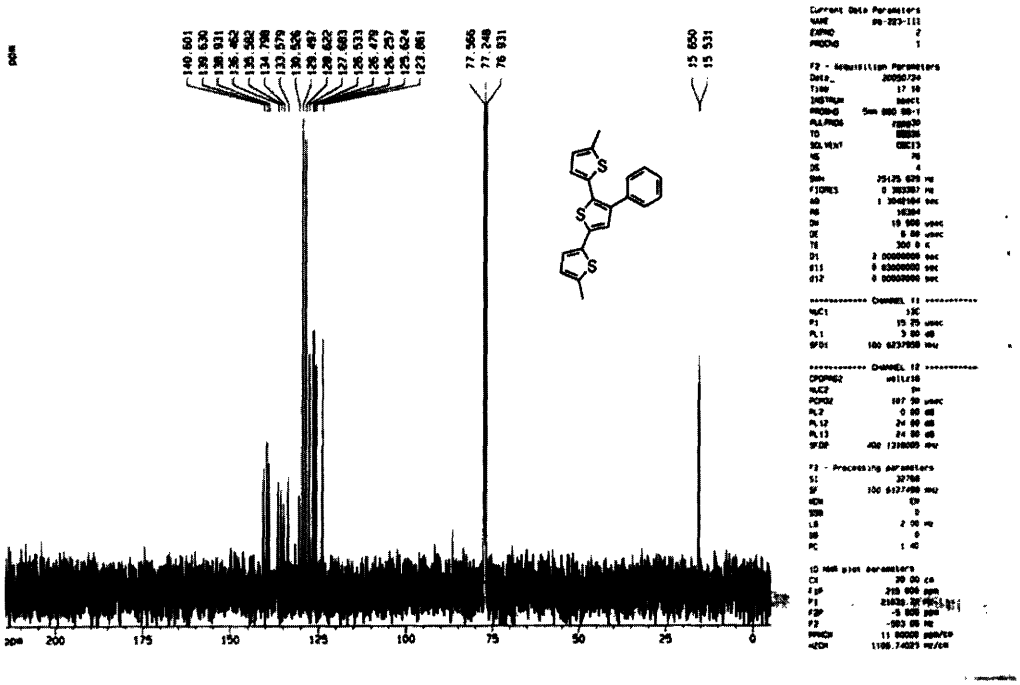

Compound **24**

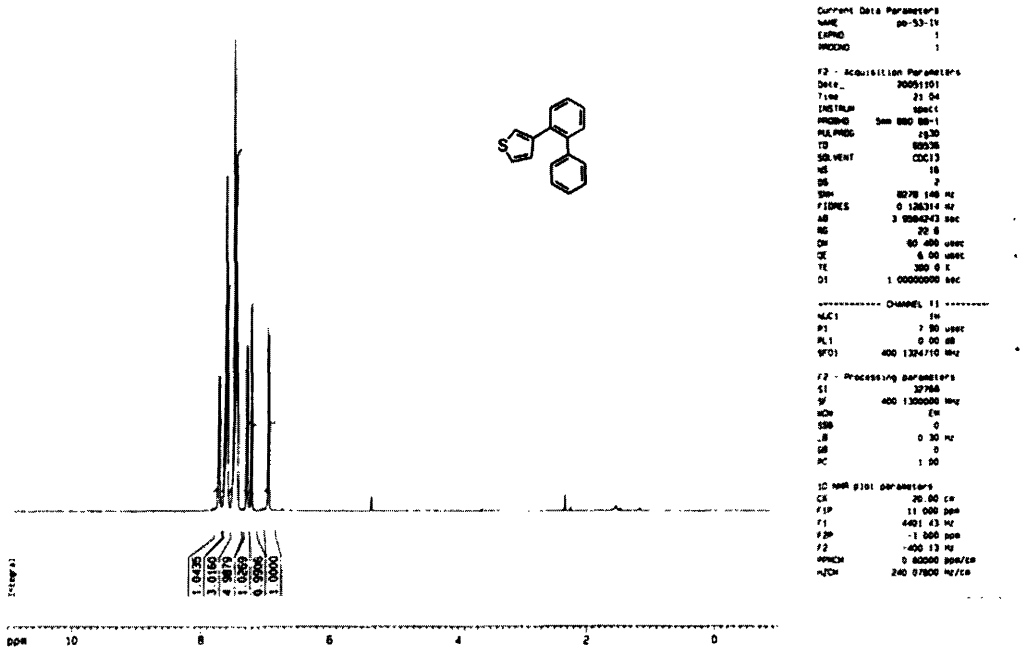

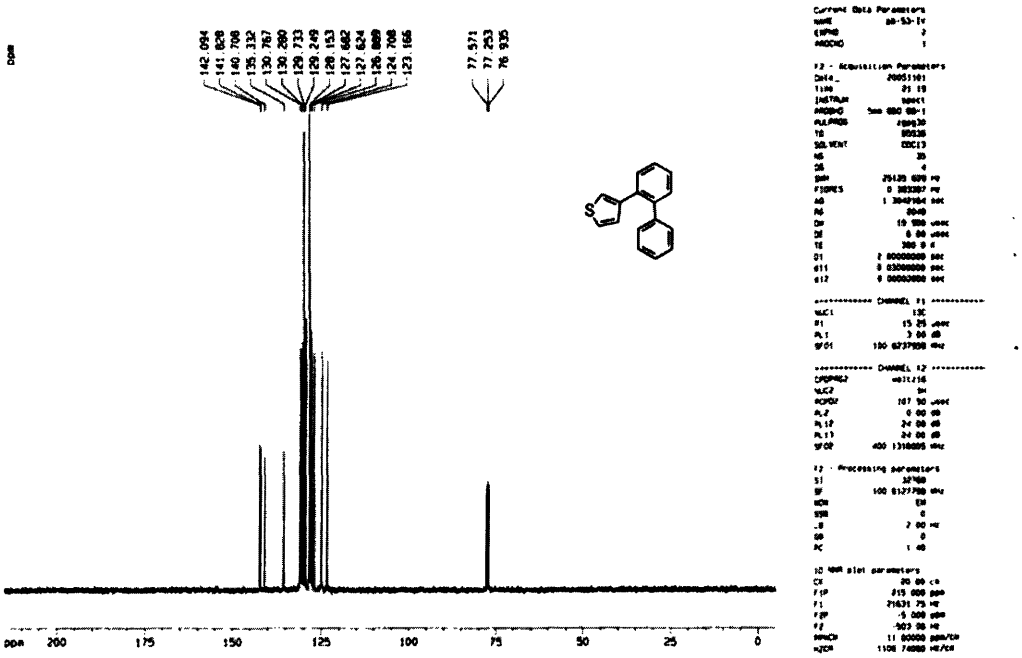

Compound **25**

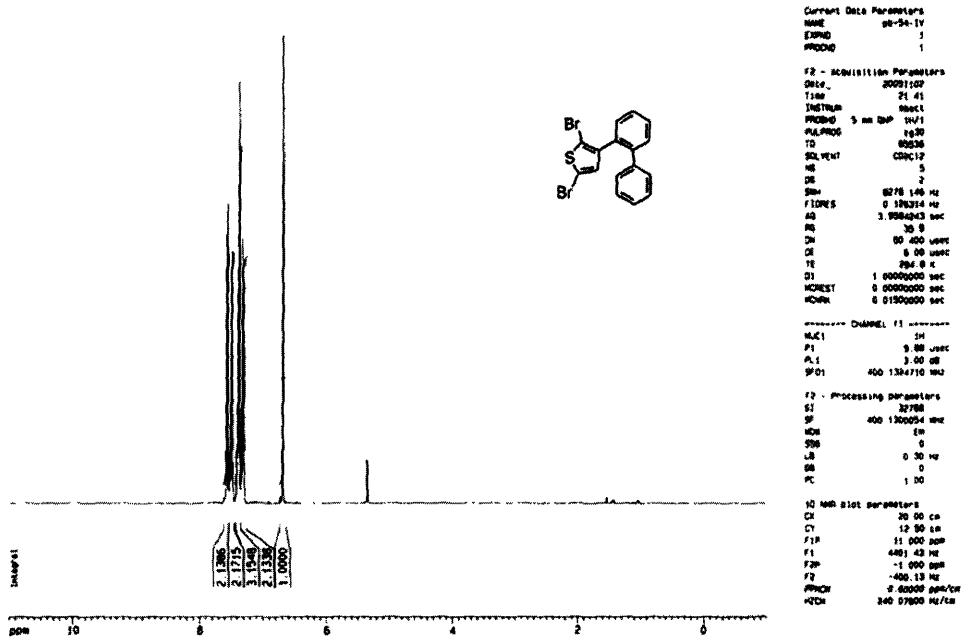

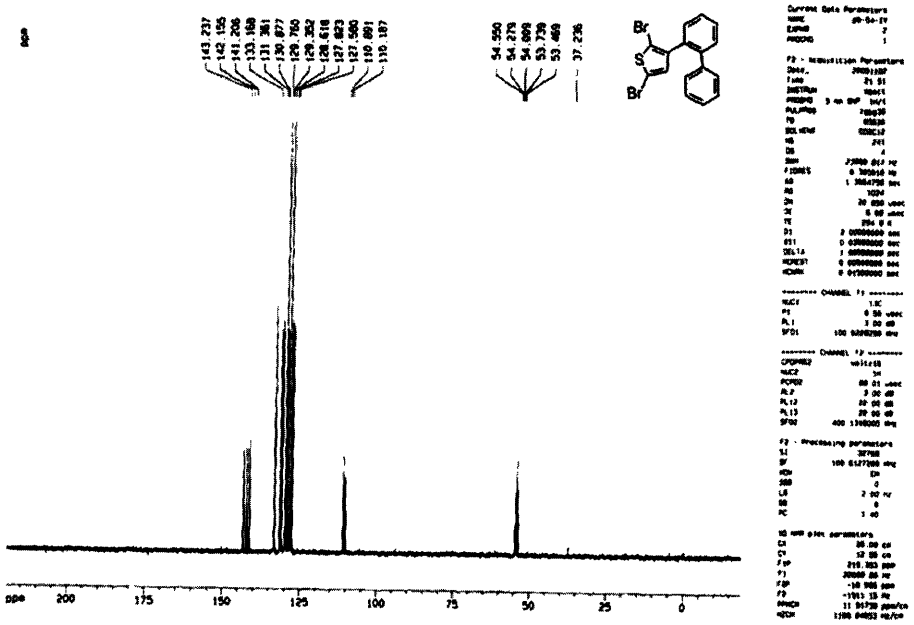

Compound **26**

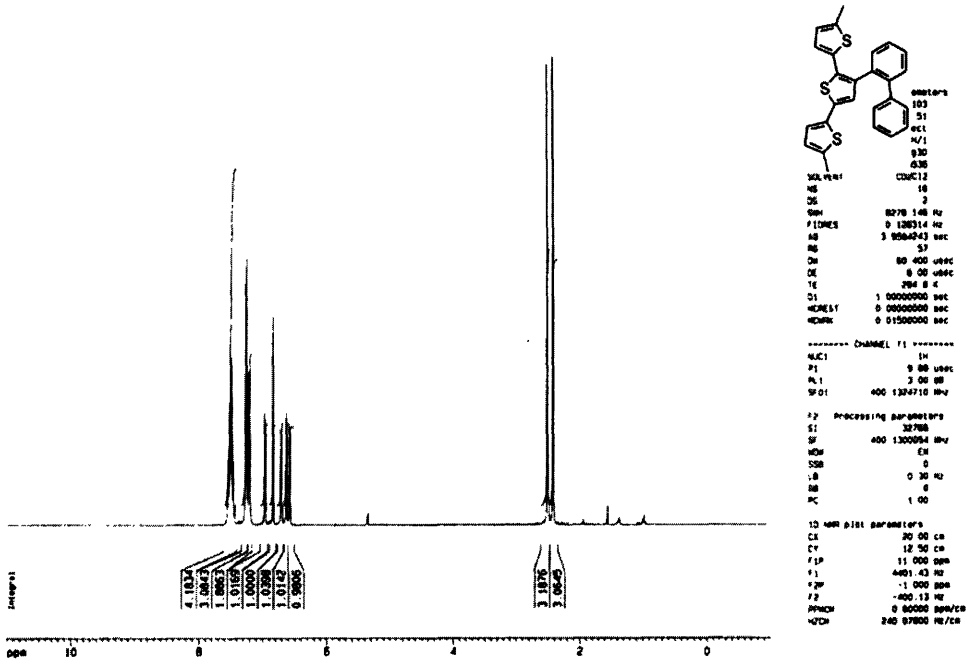

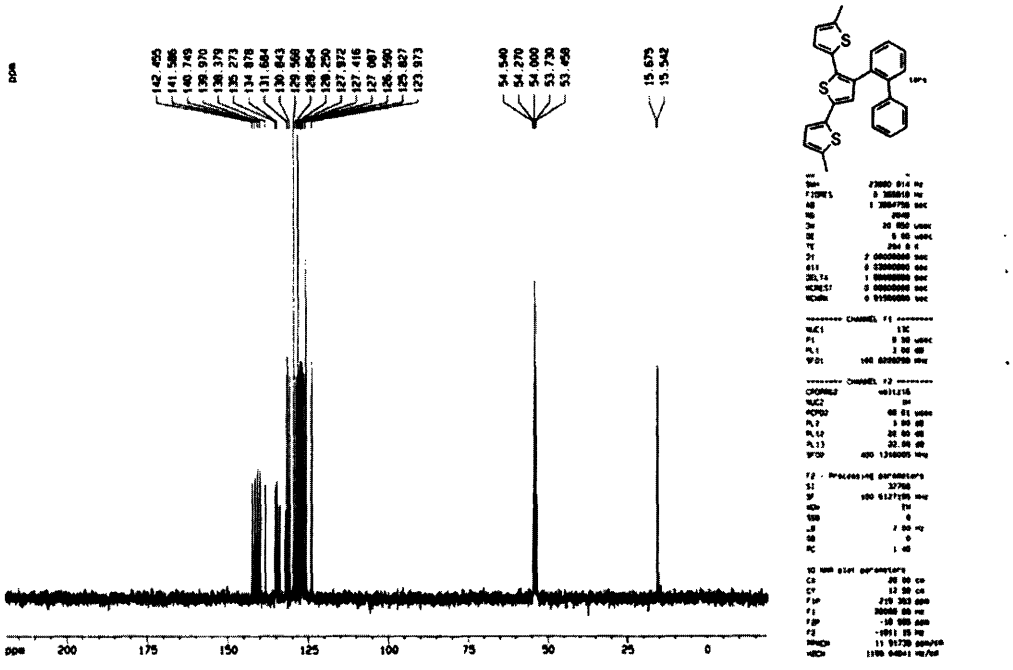

Compound **m-21**

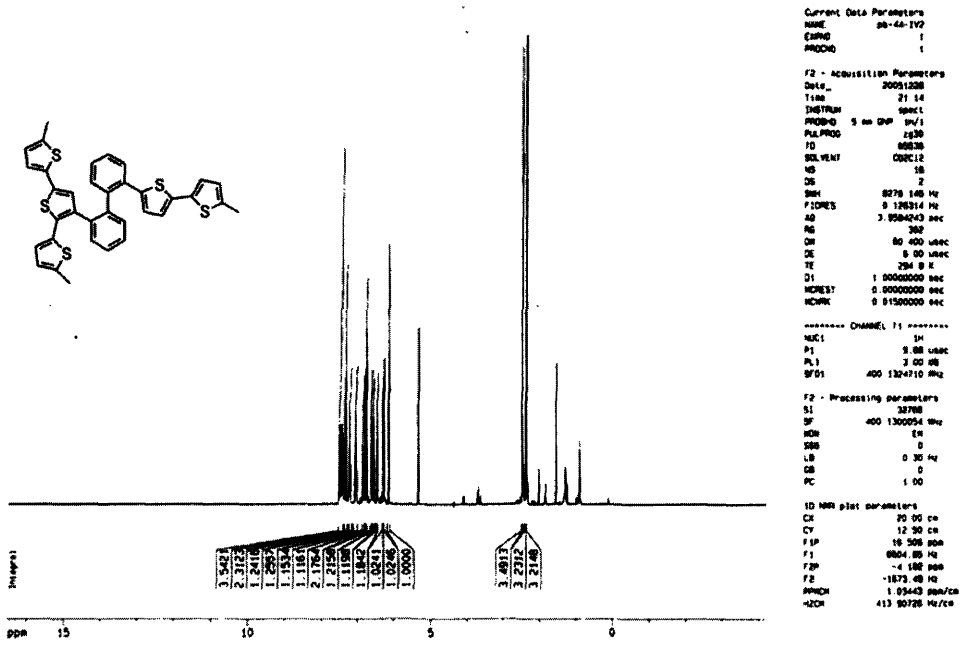

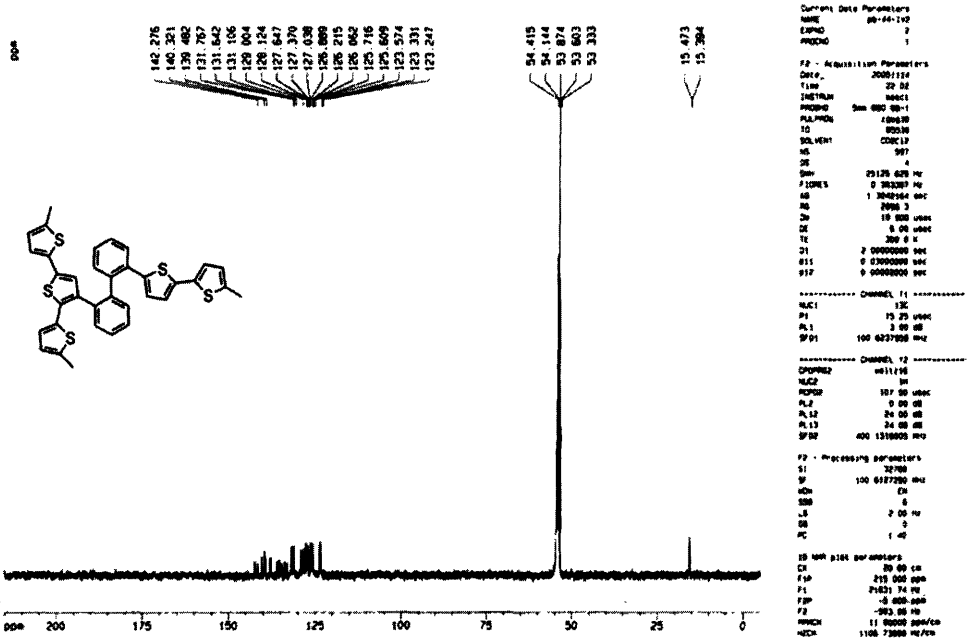

Appendix 4:
Chapter 3 NMR

Compound **2**

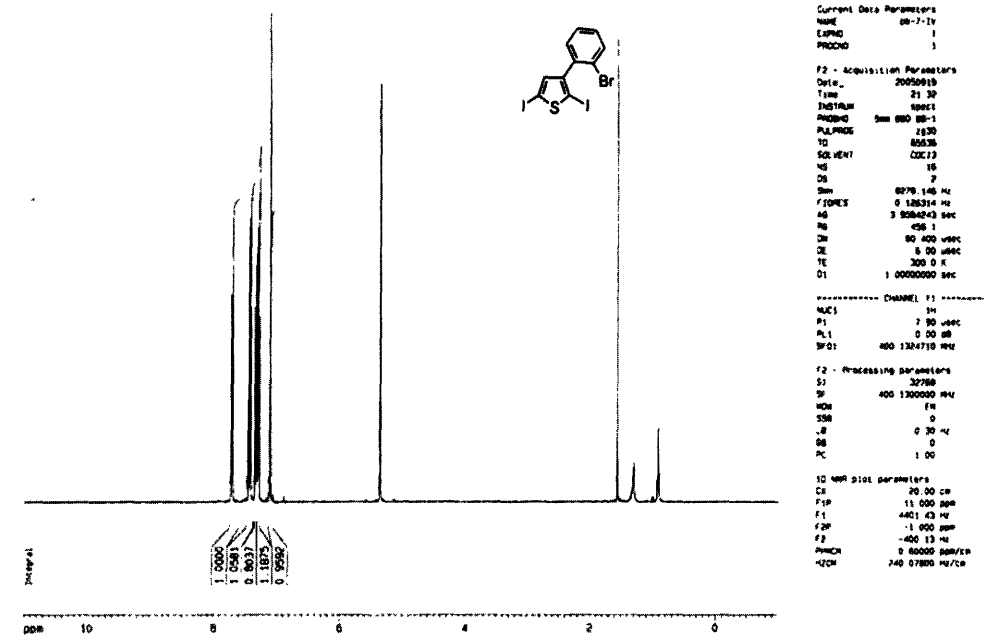

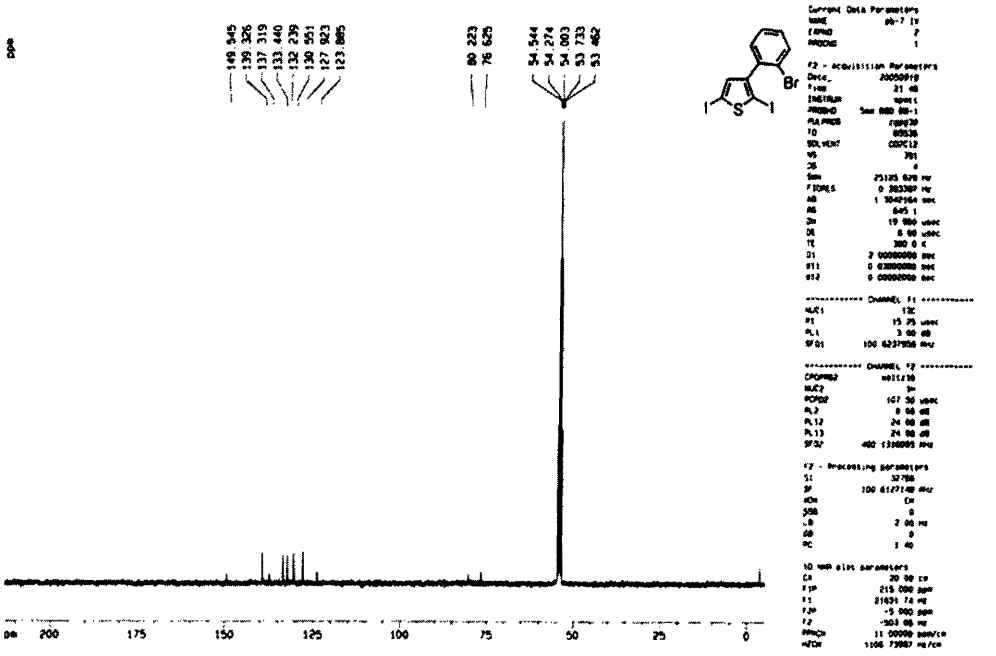

Compound **3a**

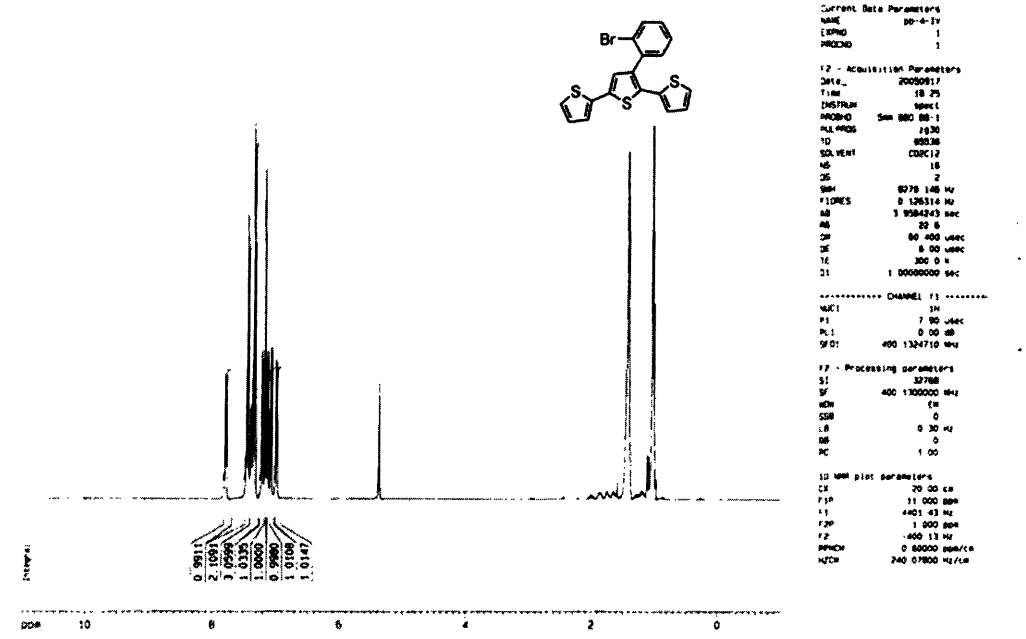

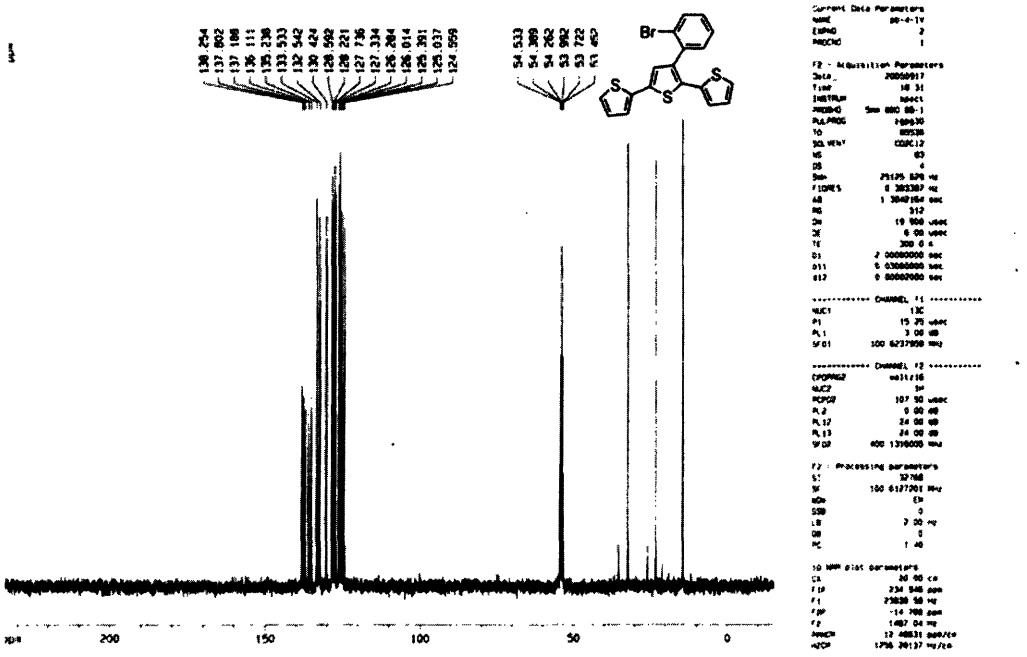

Compound **3b**

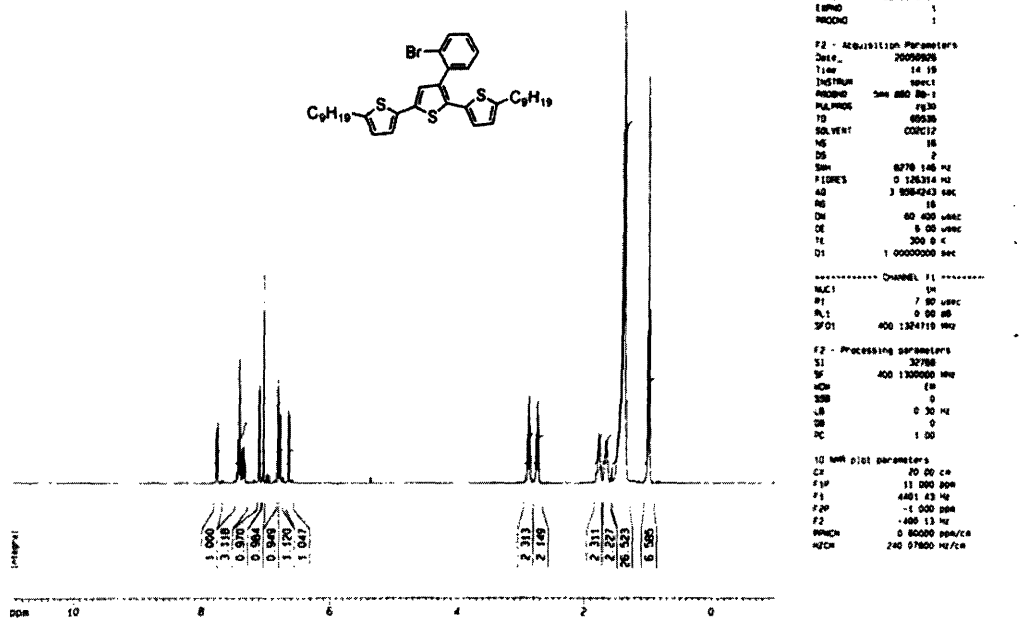
Br
C_9H_{19}
C_9H_{19}
ppm 10 8 6 4 2 0

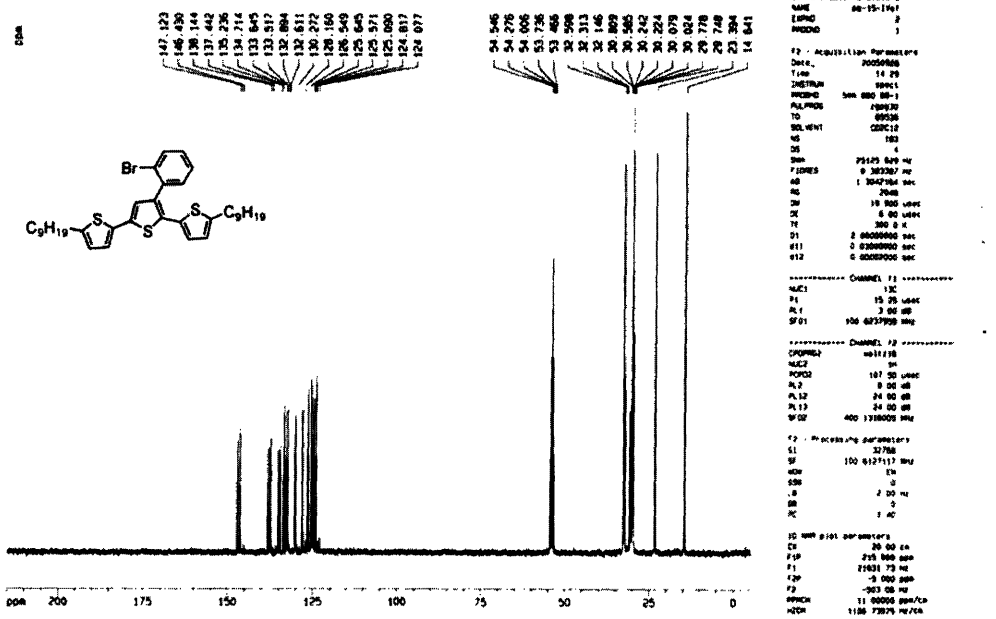
Br
C_9H_{19}
C_9H_{19}
ppm 200 175 150 125 100 75 50 25 0

Compound **3c**

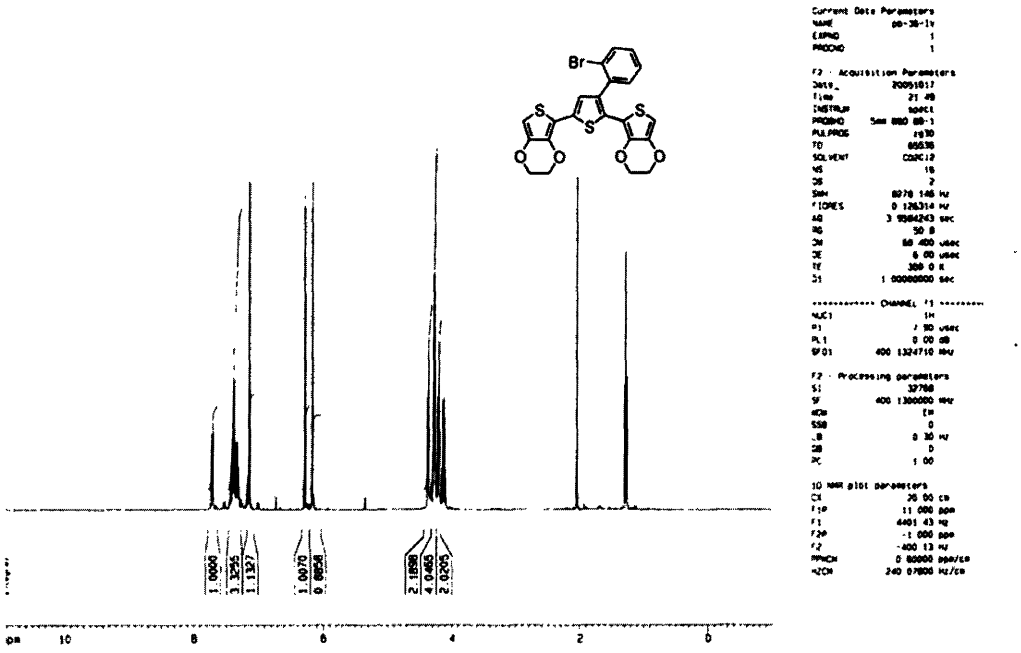

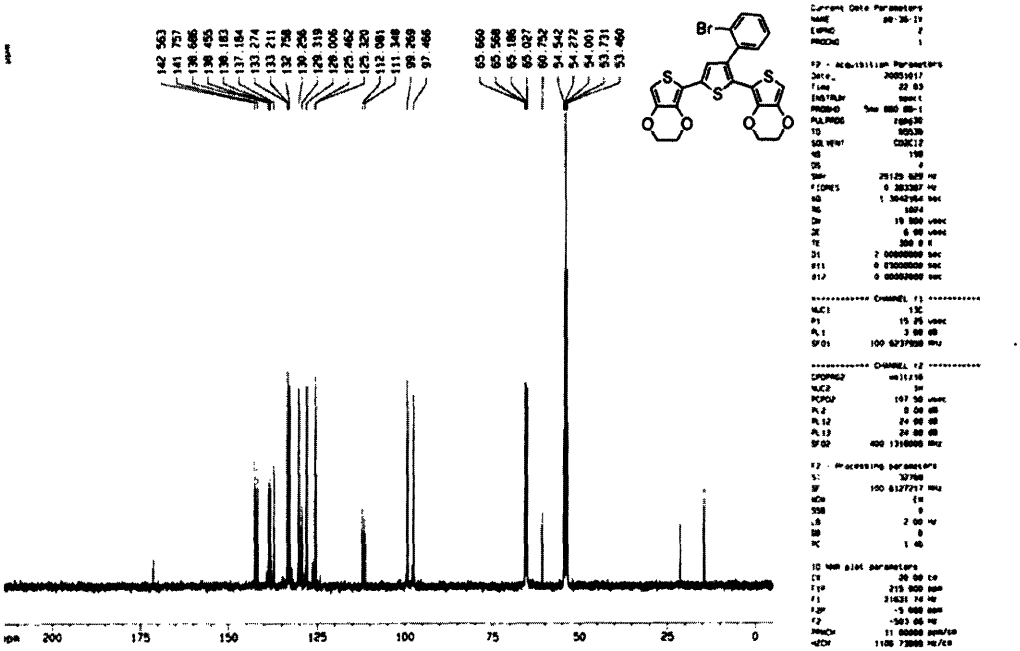

Compound **4a**

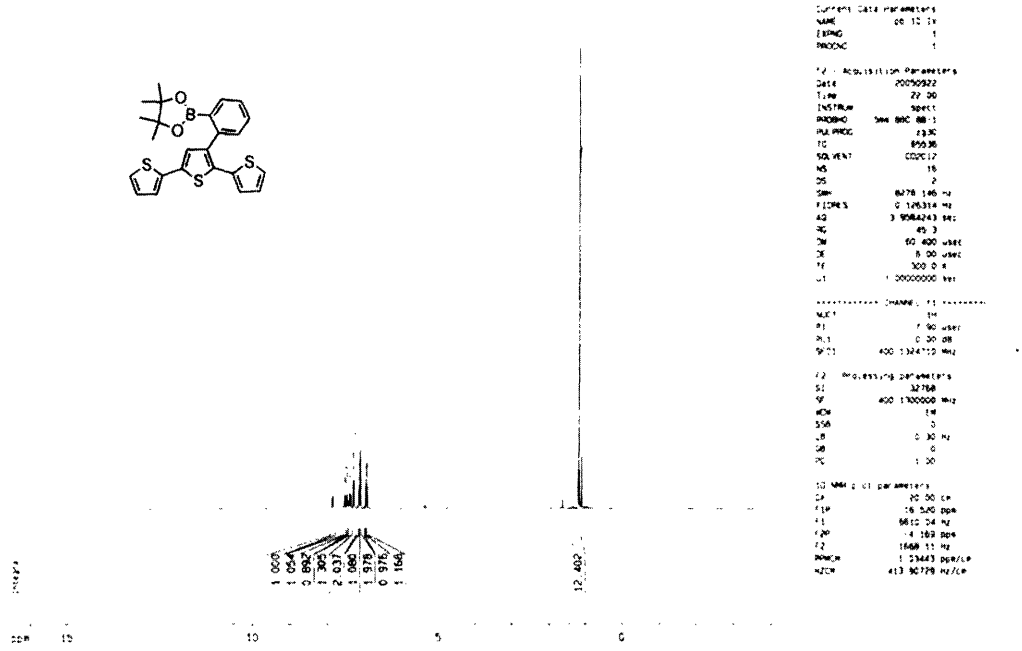

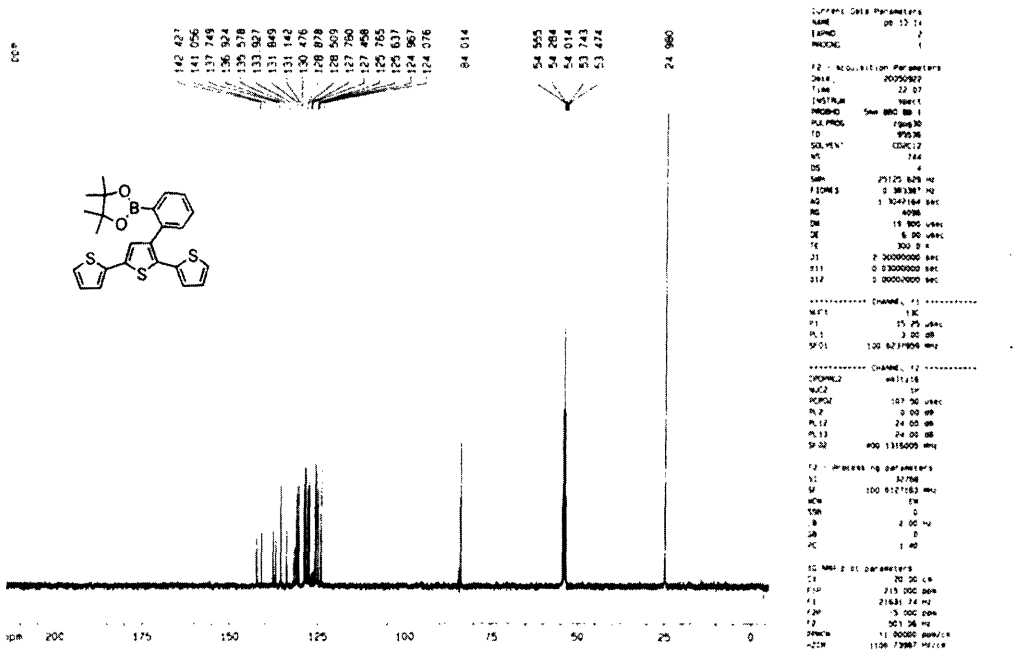

Compound **4b**

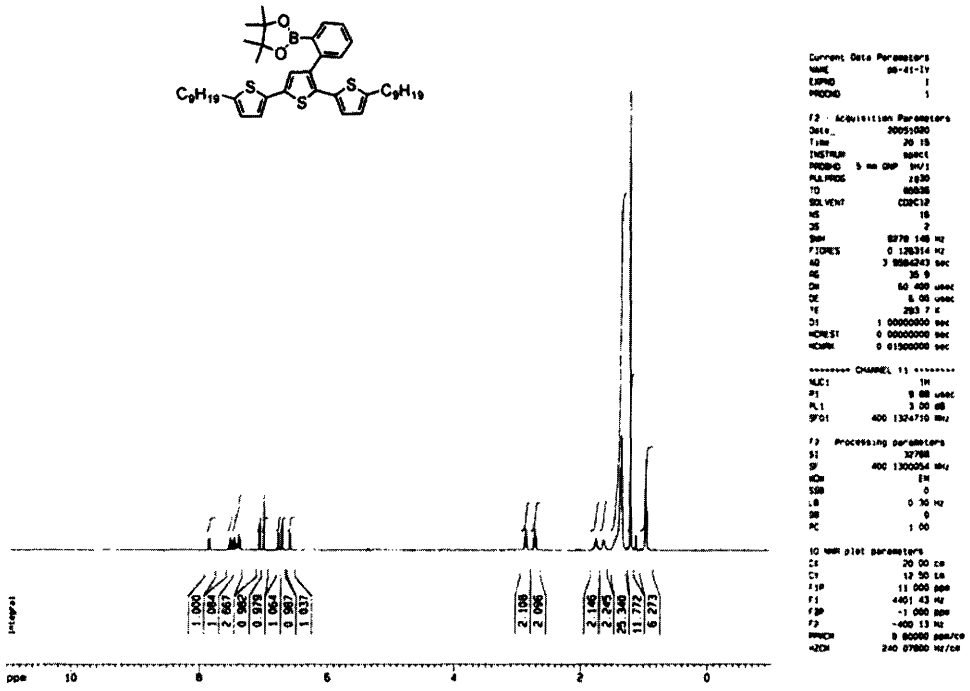

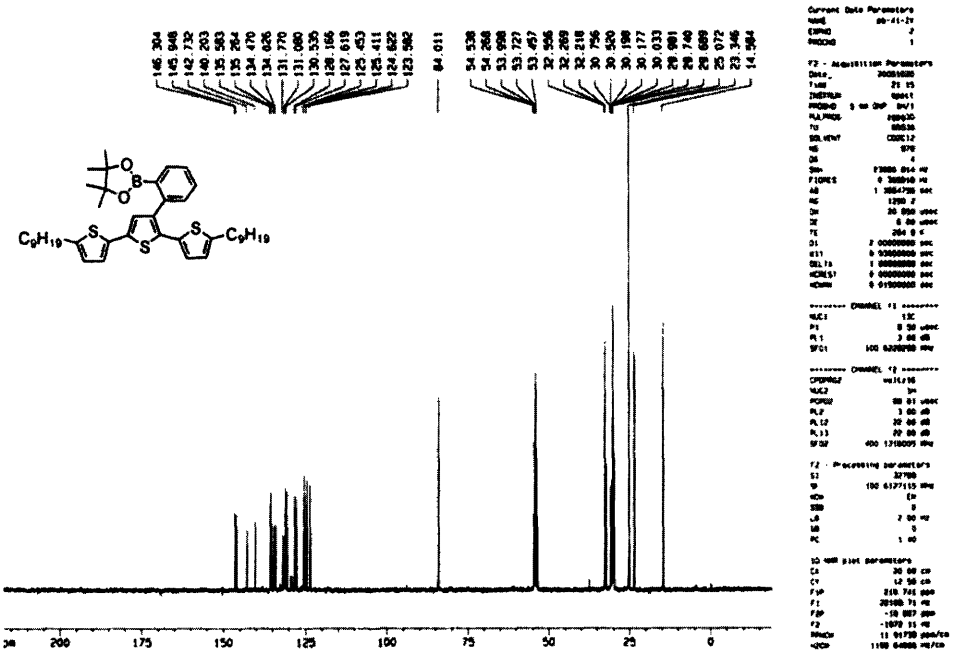

Compound **6**

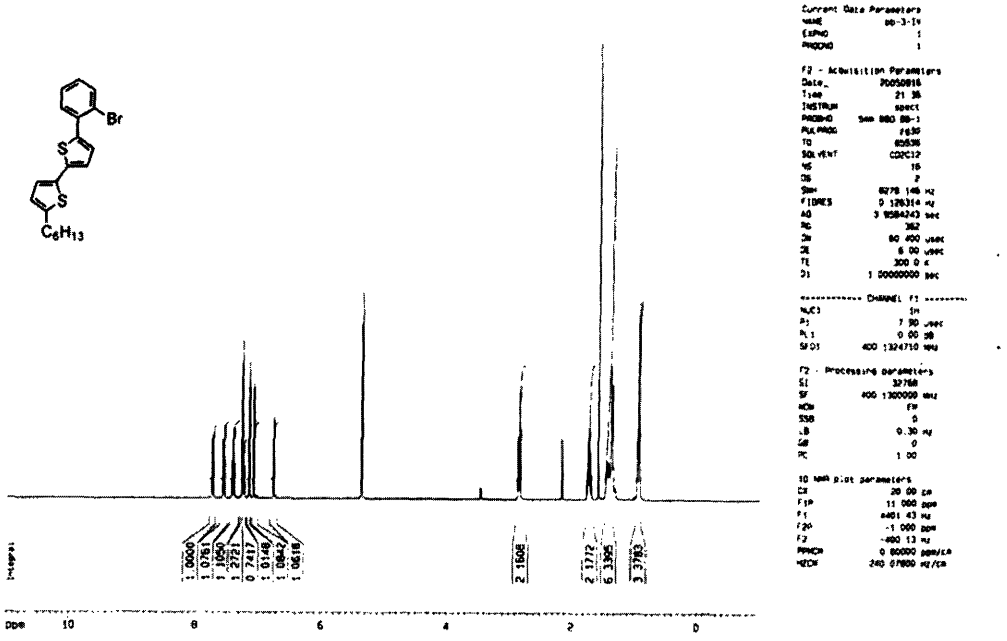

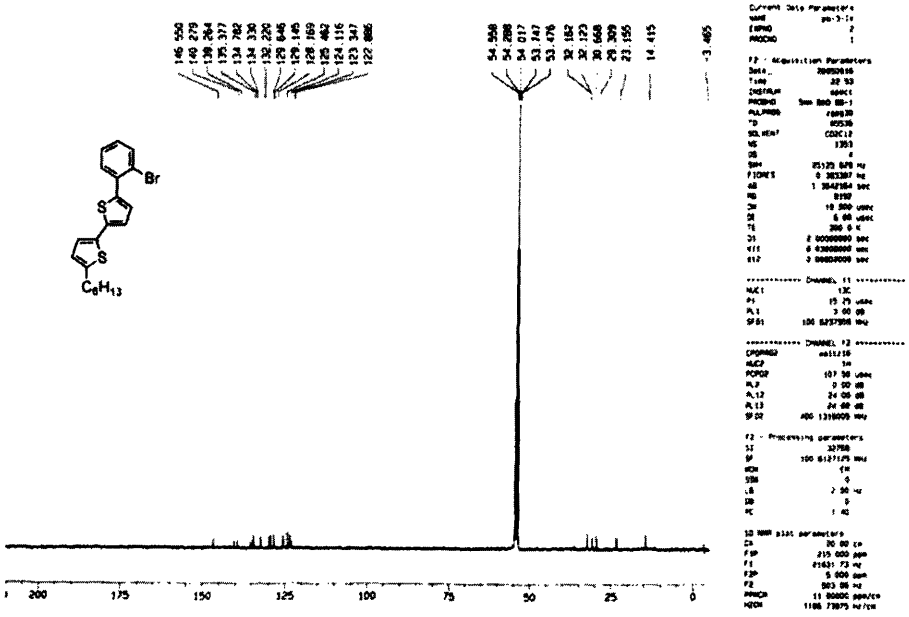

Compound 7

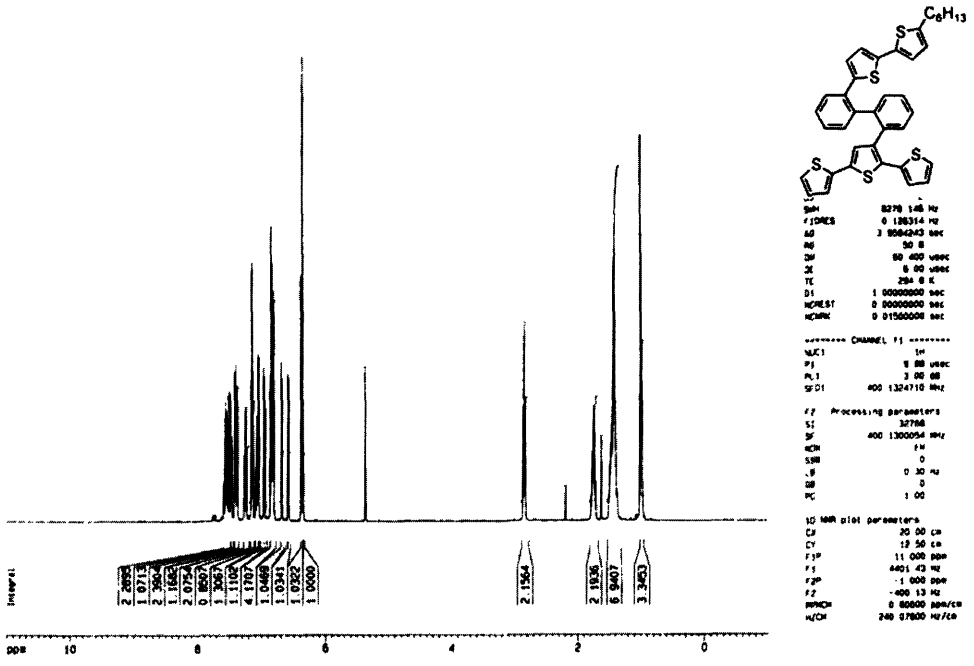

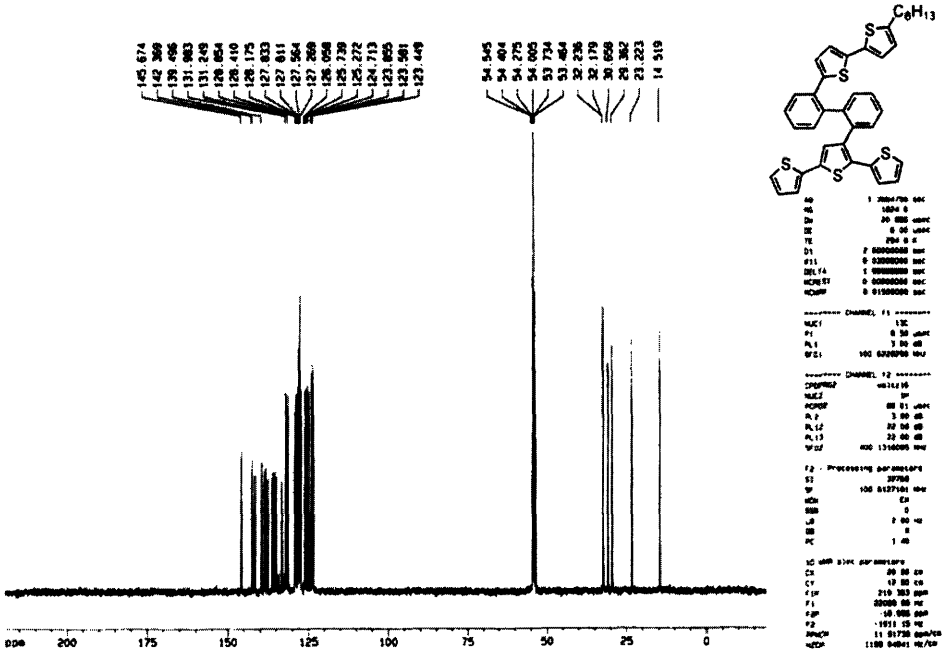

Compound **8**

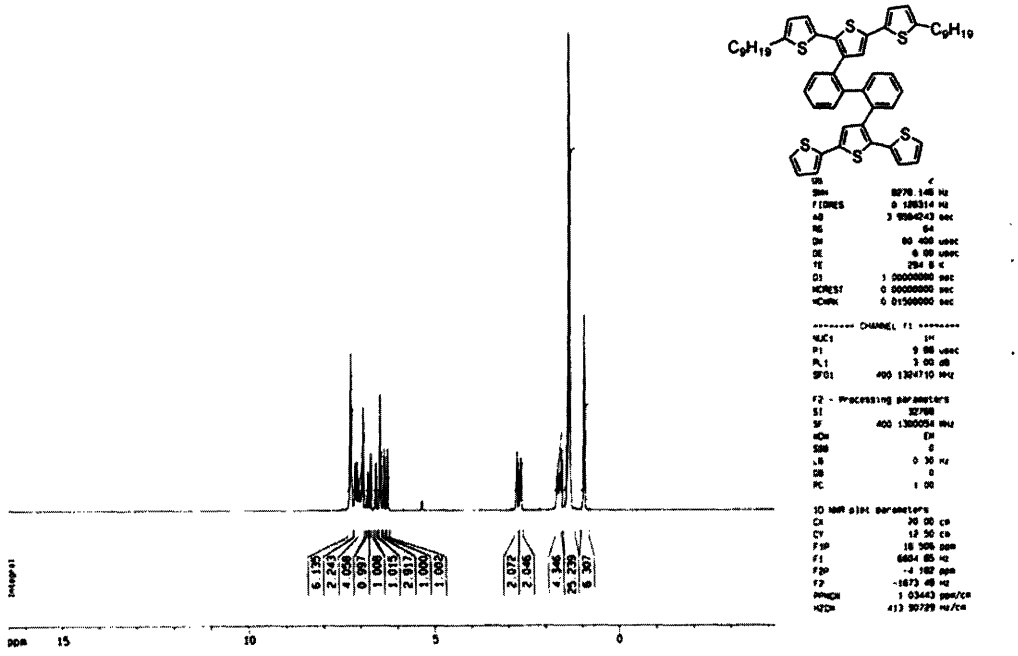

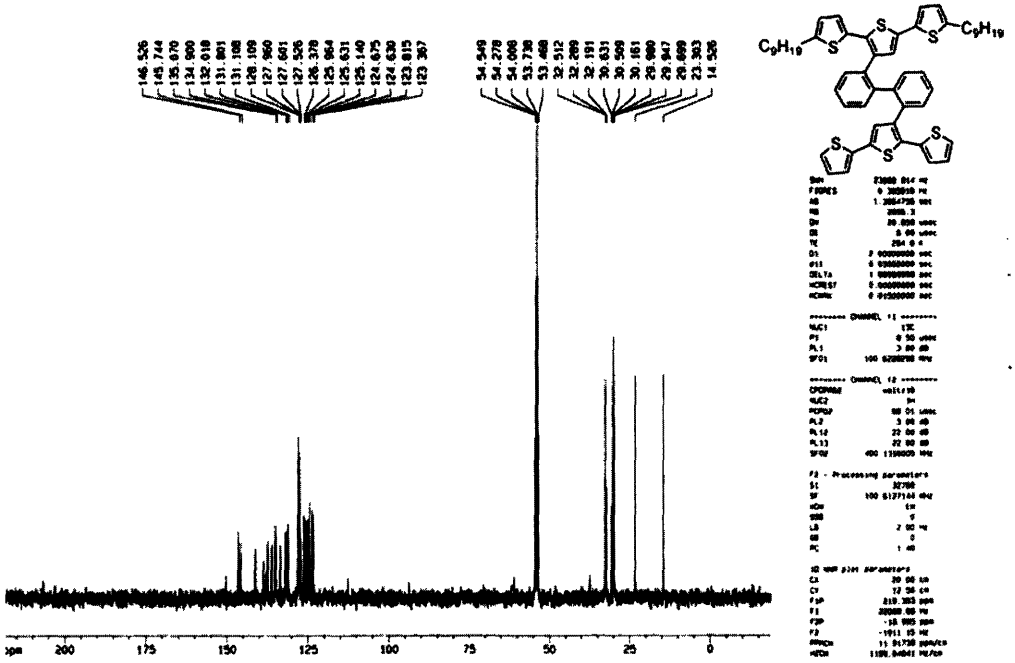

Compound **9**

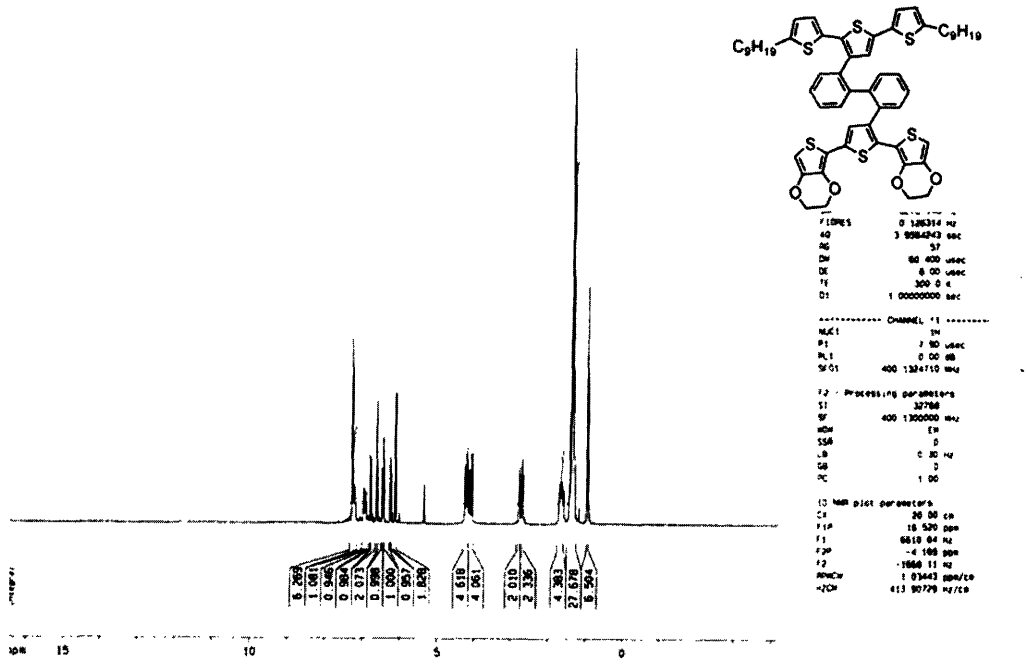

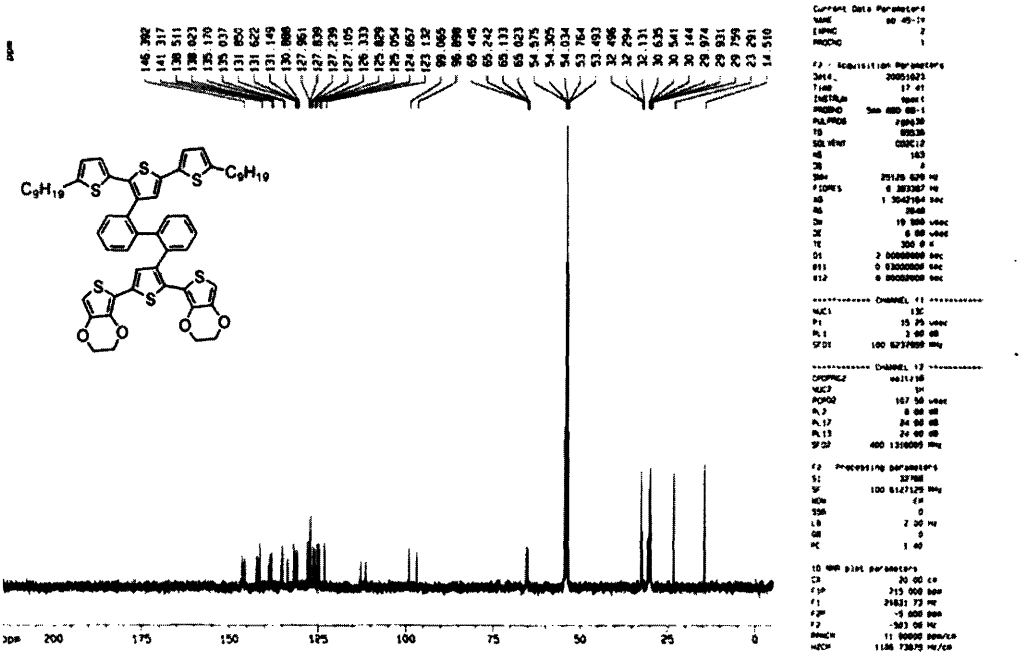

Compound **10**

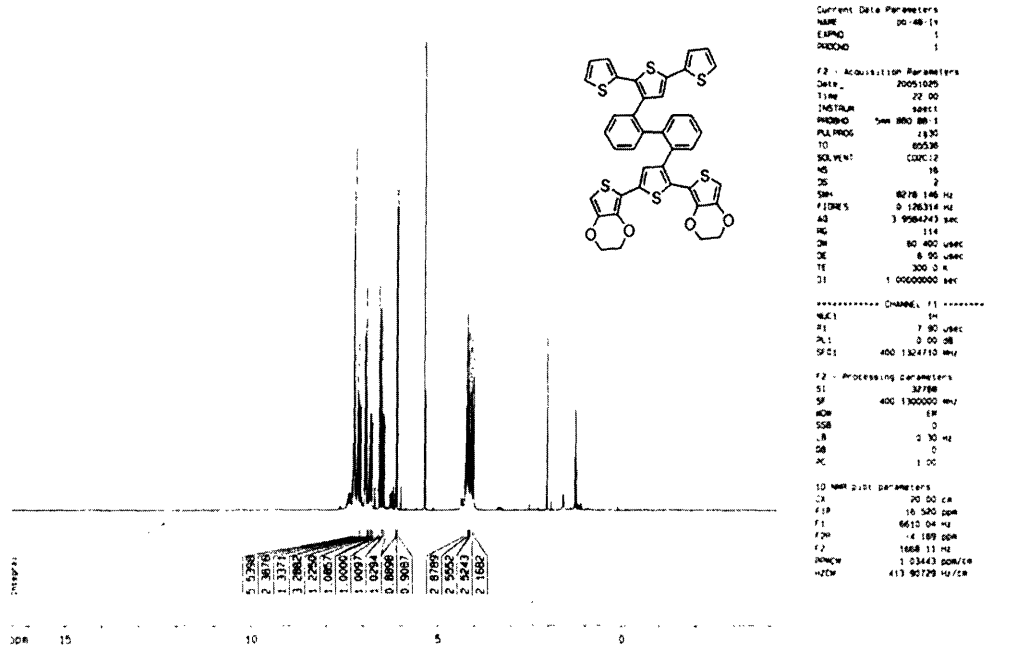

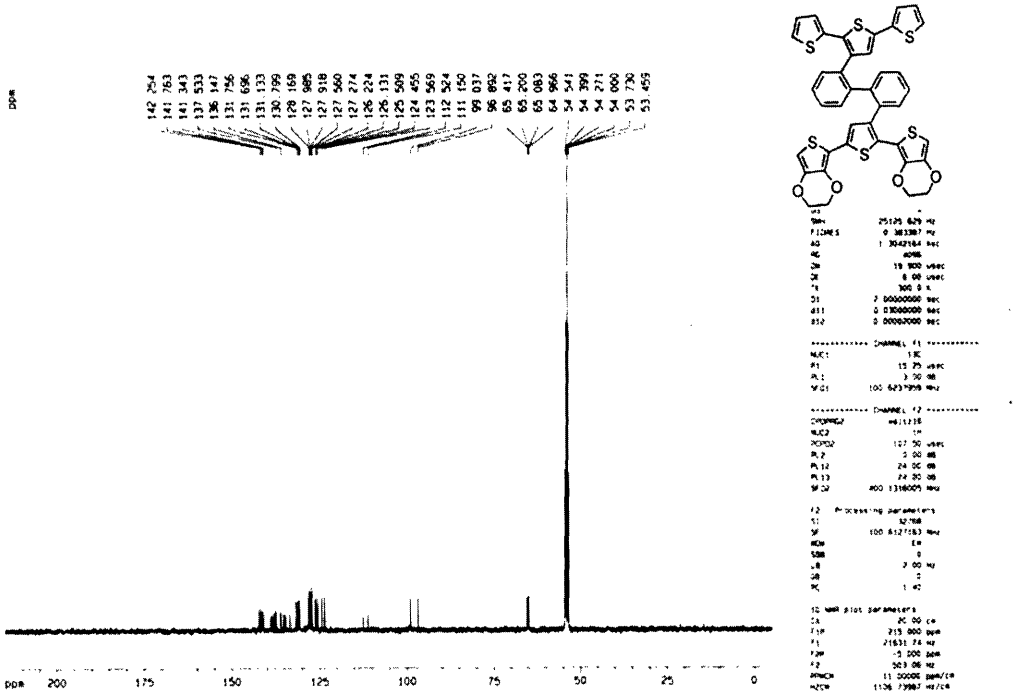

Appendix 5:
Chapter 4 NMR

Compound **1a**

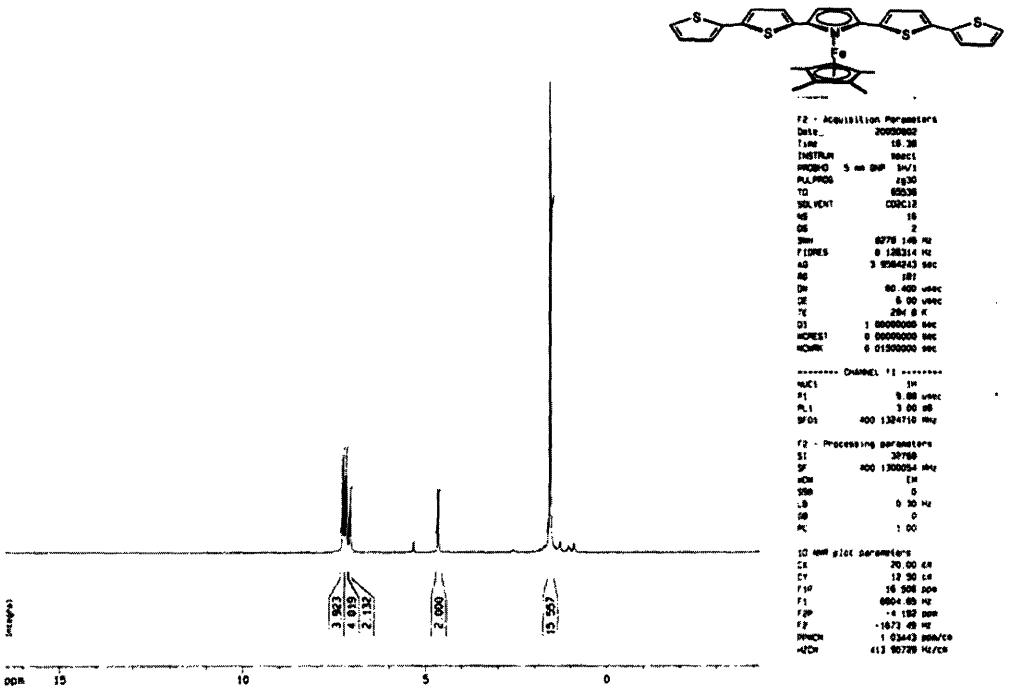

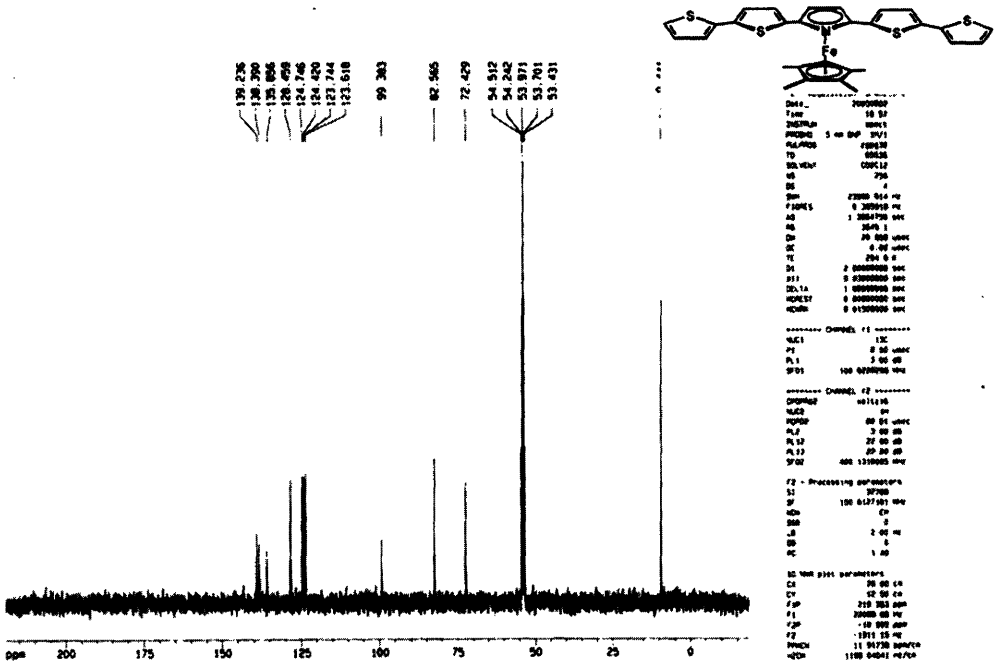

Compound **1b**

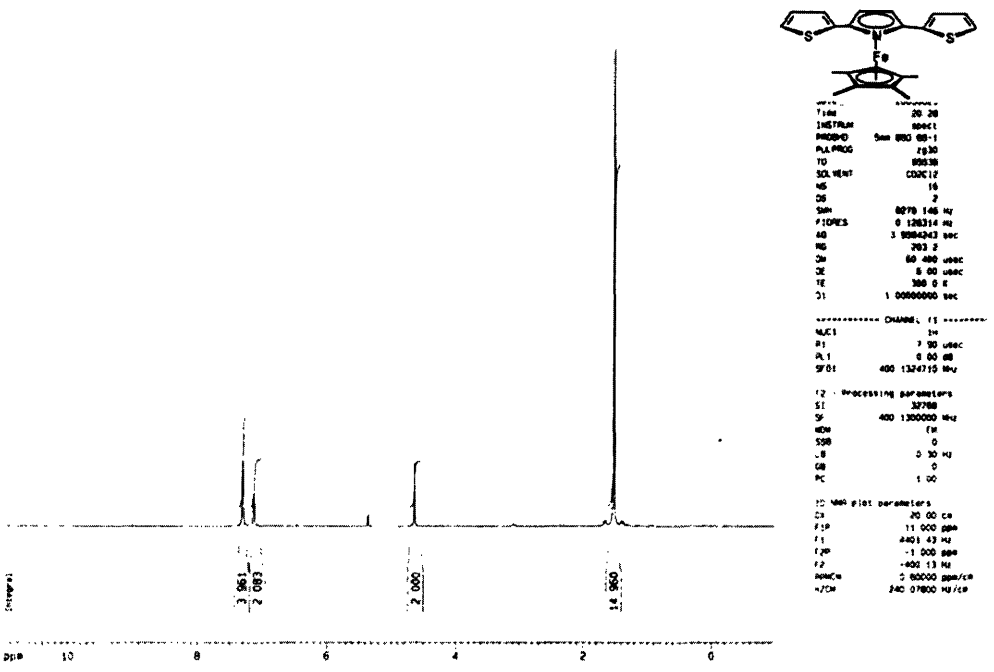

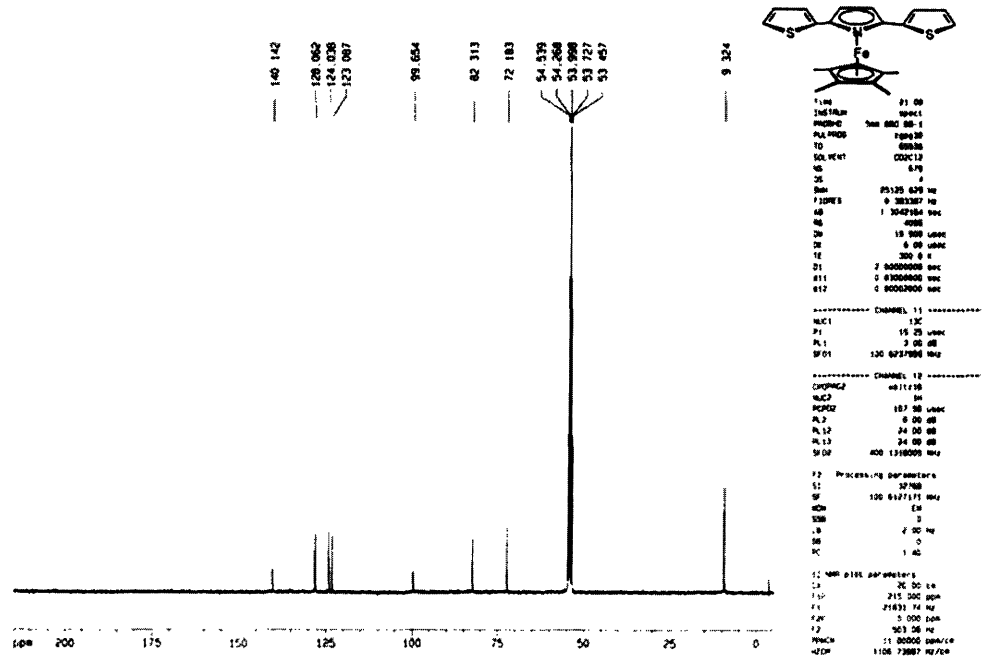

Compound **1c**

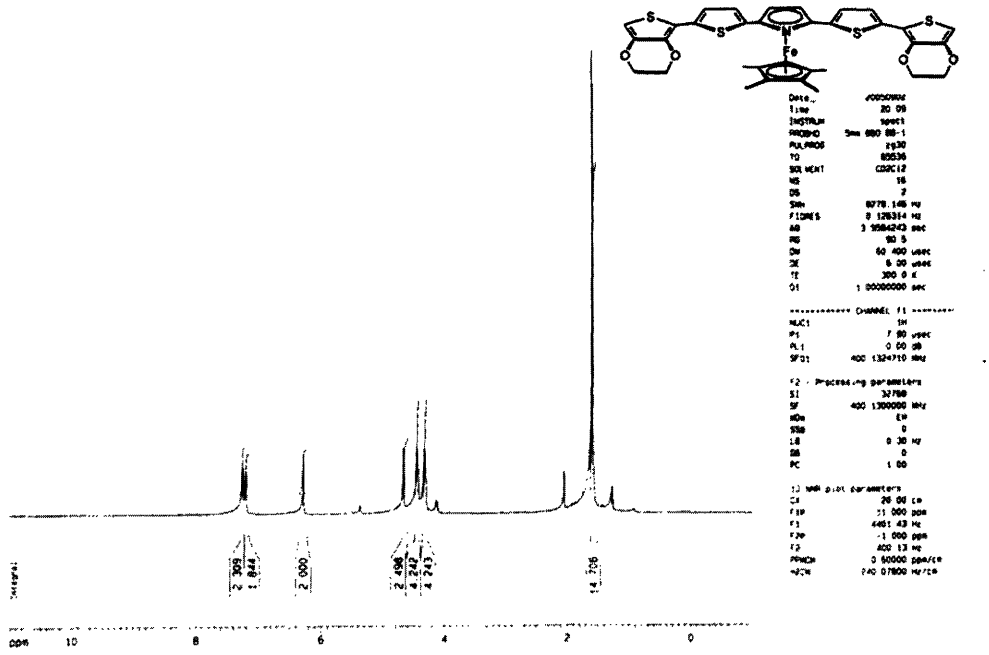

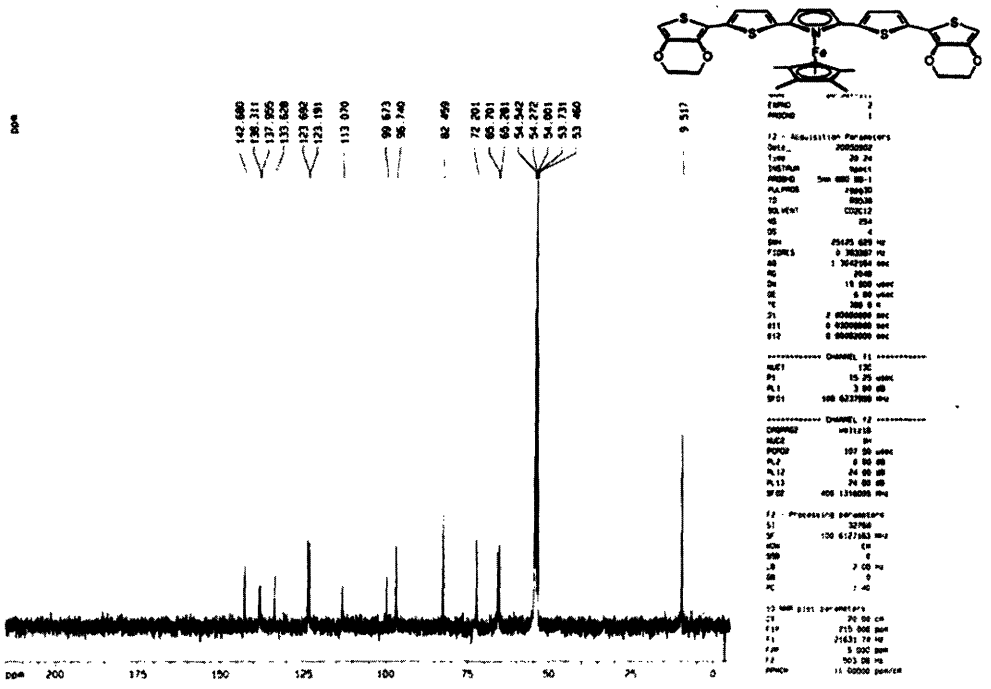

Compound **1d**

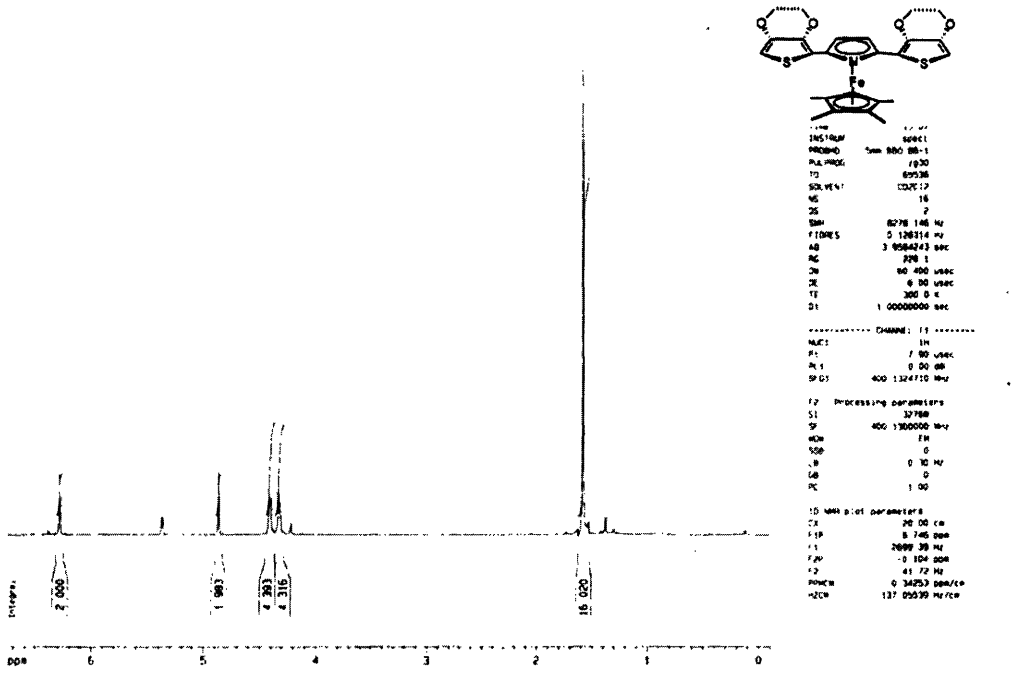

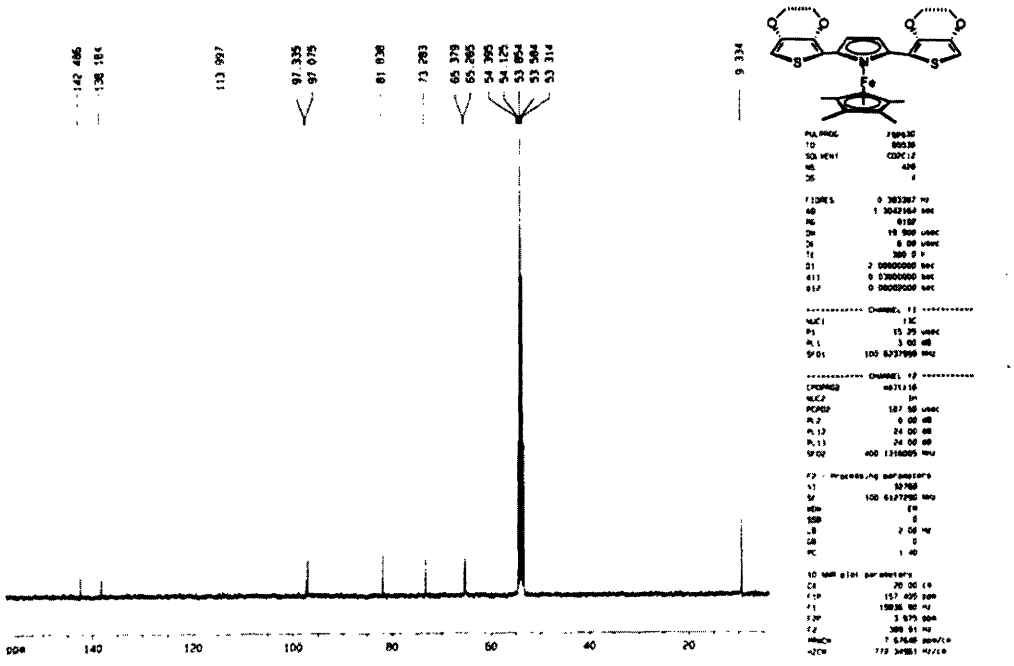

Compound **2a**

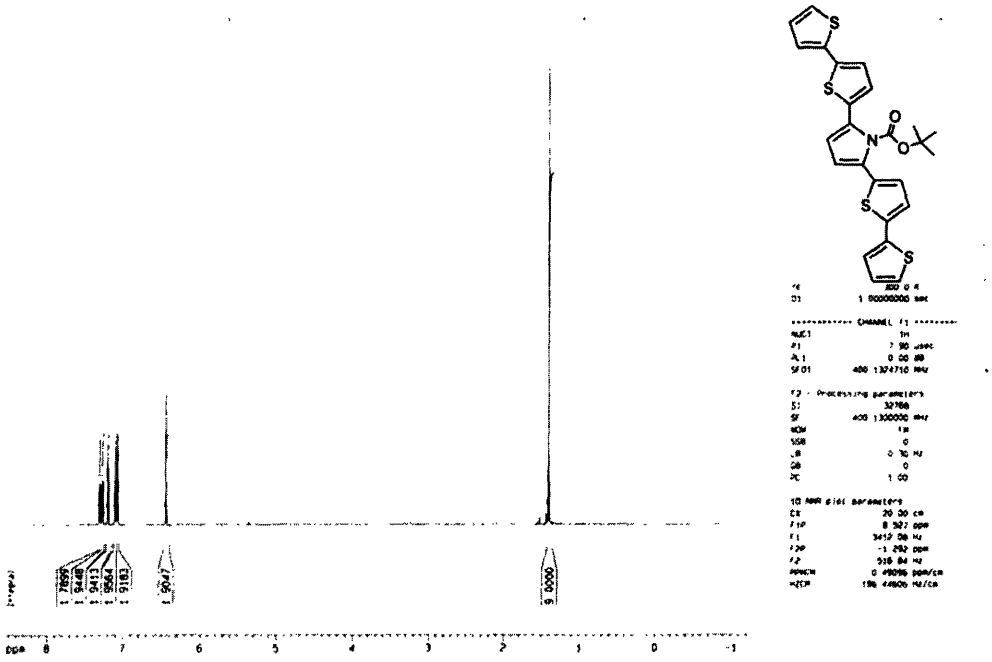

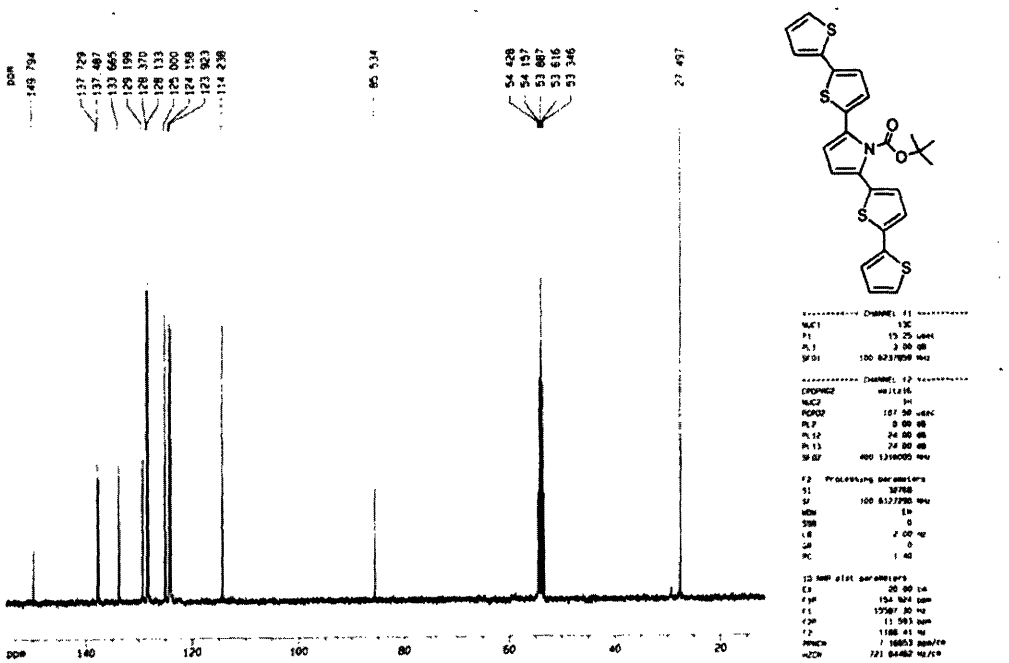

Compound **2b**

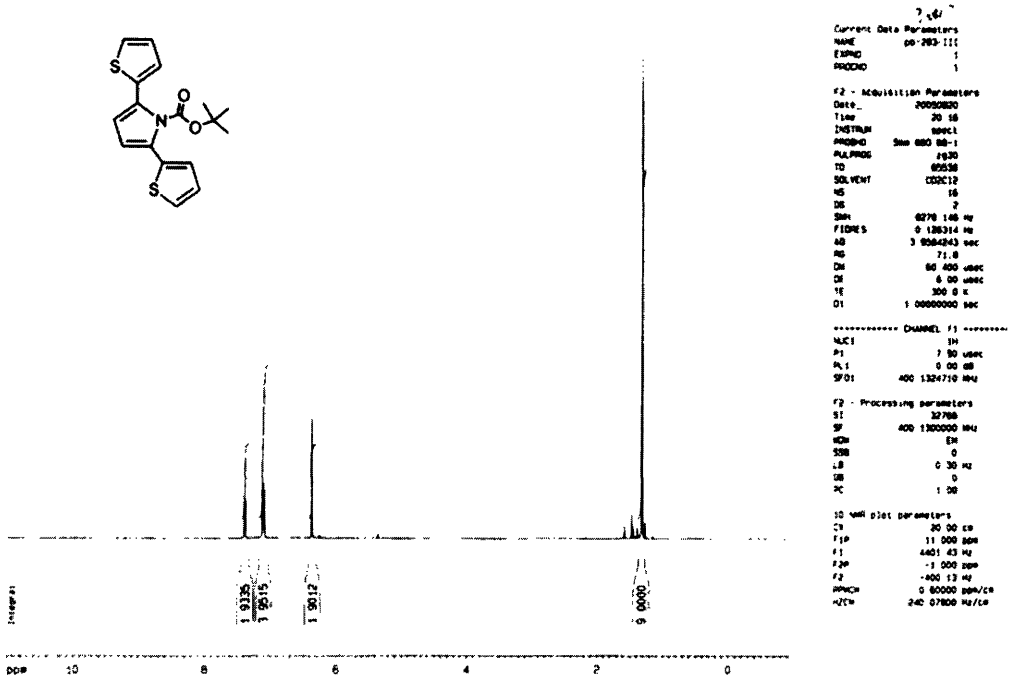

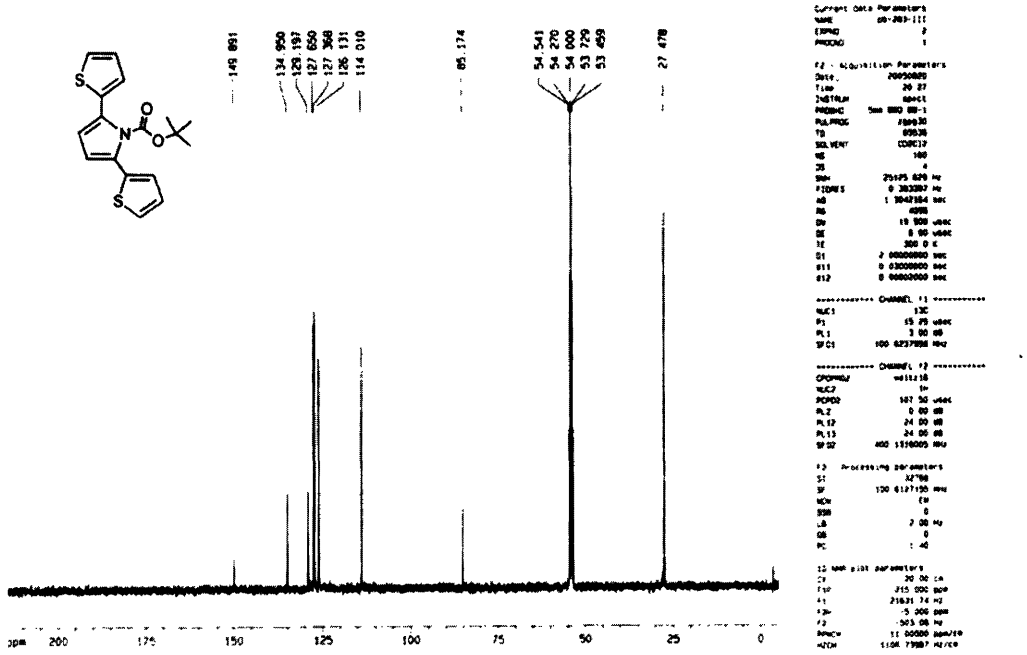

Compound **2c**

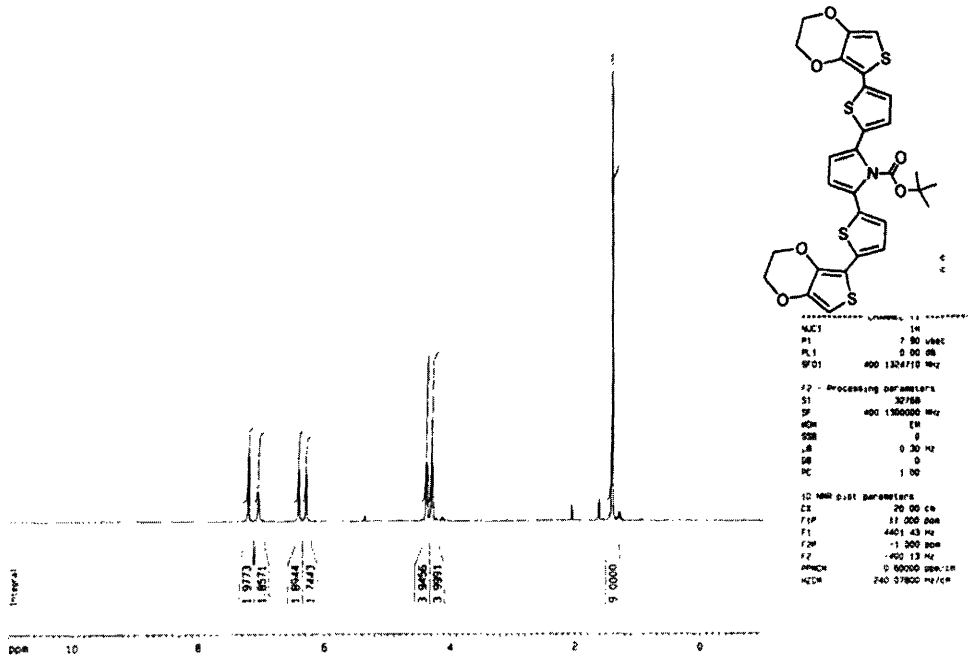

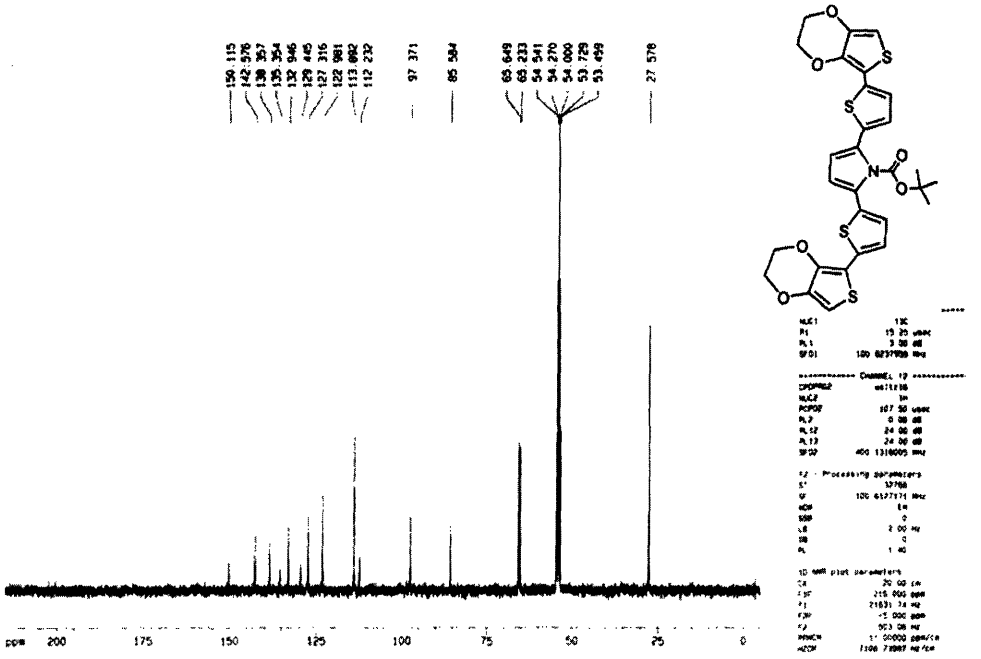

Compound **2d**

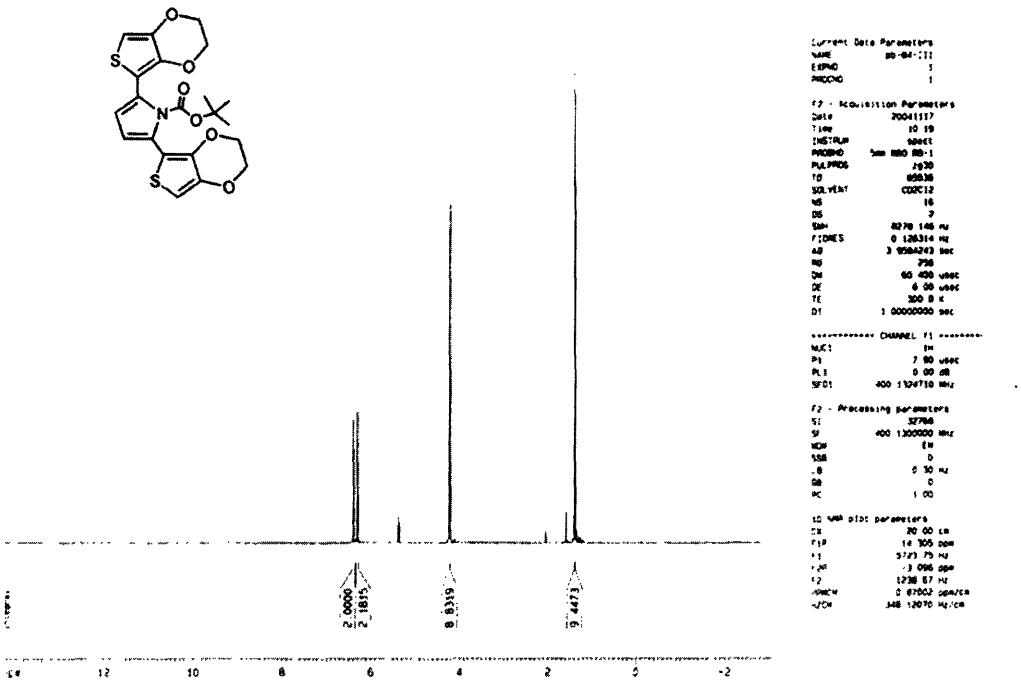

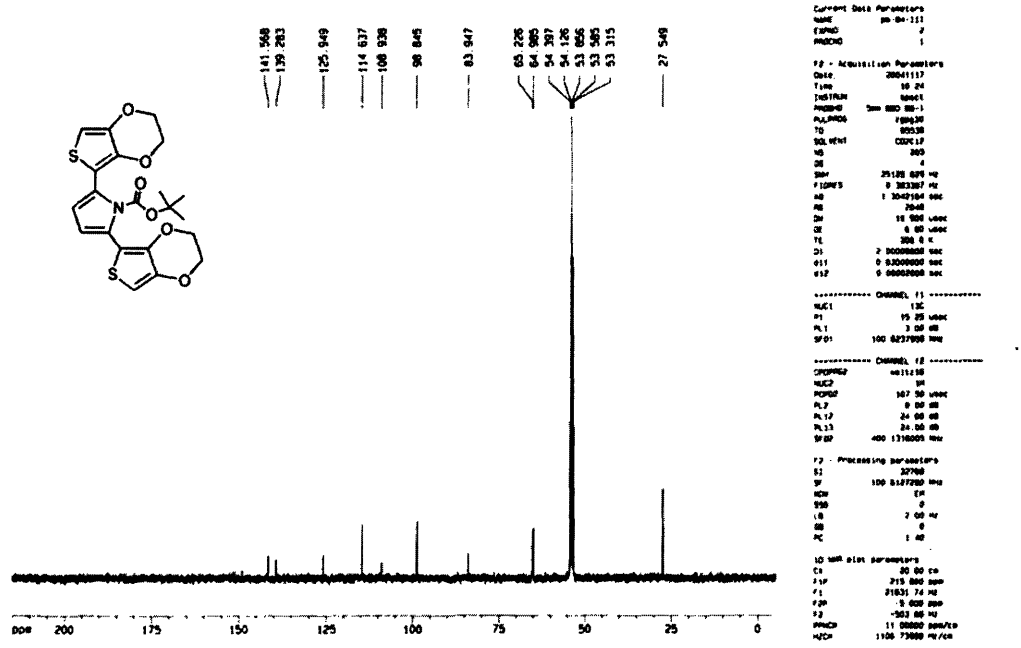

Compound **3**

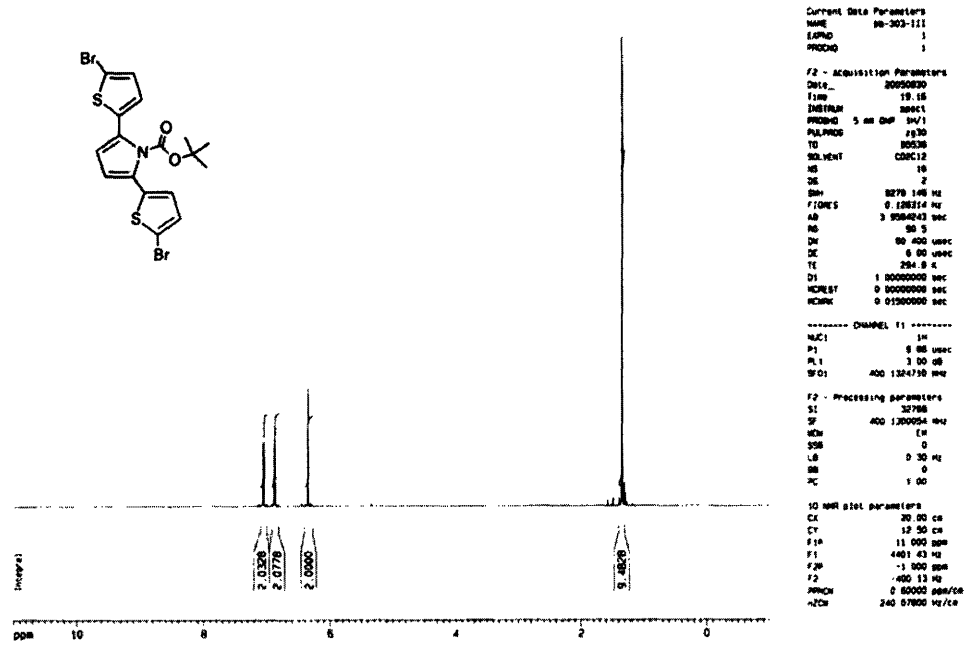
Br
S
N
O
O
S
Br
Integral
2.0326
2.0778
2.0000
9.4826
ppm
10
8
6
4
2
0

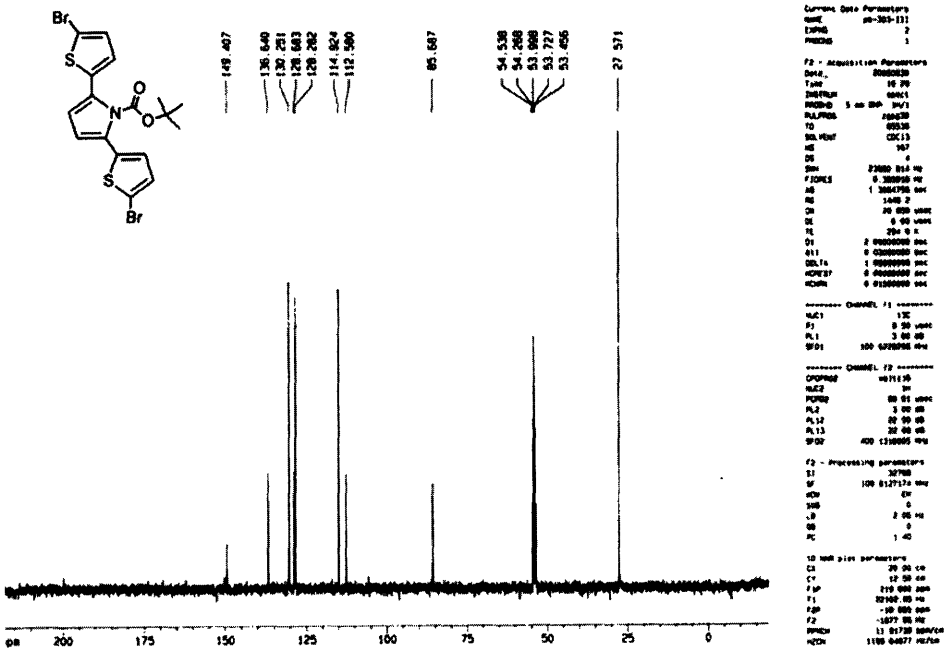
Br
S
N
O
O
S
Br
149.407
136.640
130.251
128.683
128.282
114.924
112.560
85.687
54.538
54.268
53.988
53.727
53.456
27.571
ppm
200
175
150
125
100
75
50
25
0

Appendix 6:
Chapter 5 NMR

Compound **2**

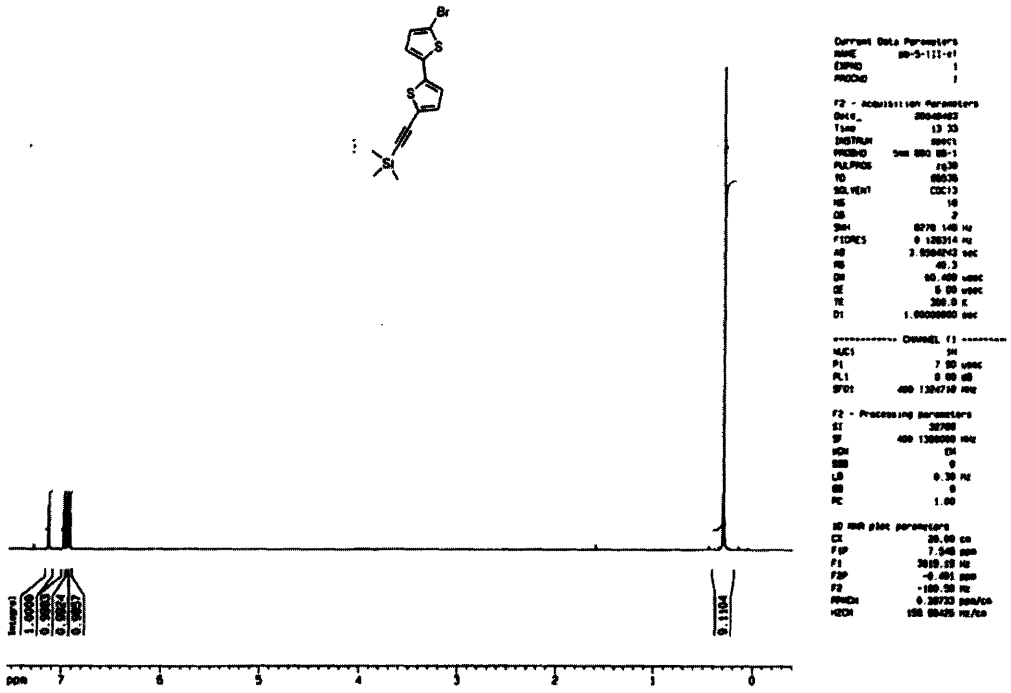

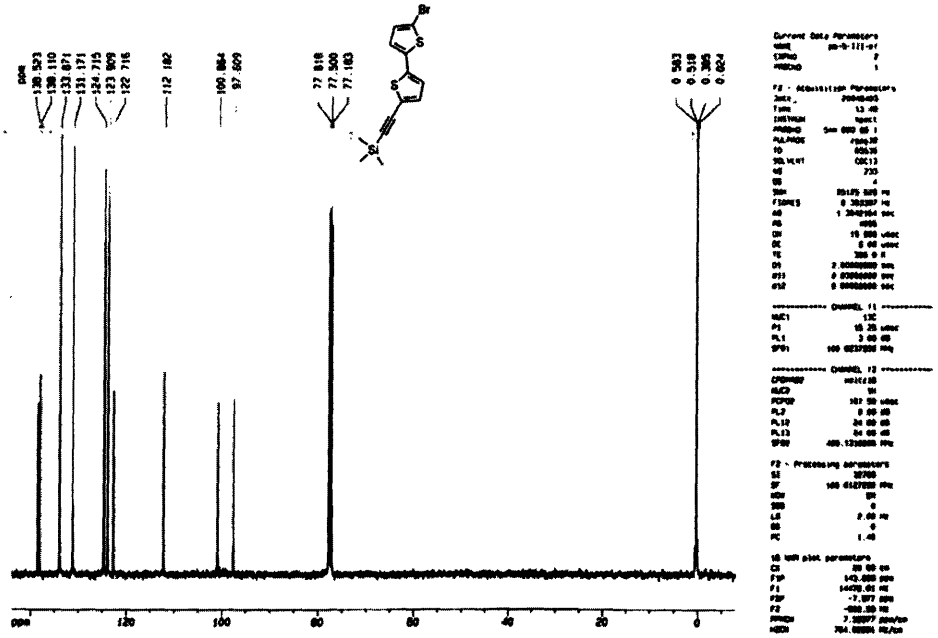

Compound 4

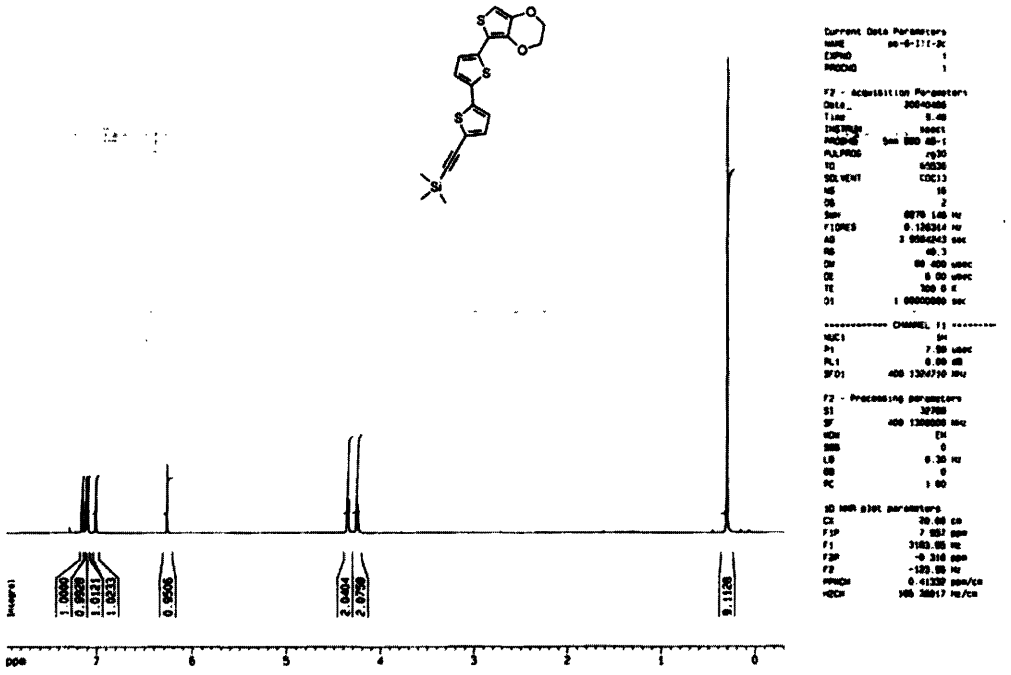

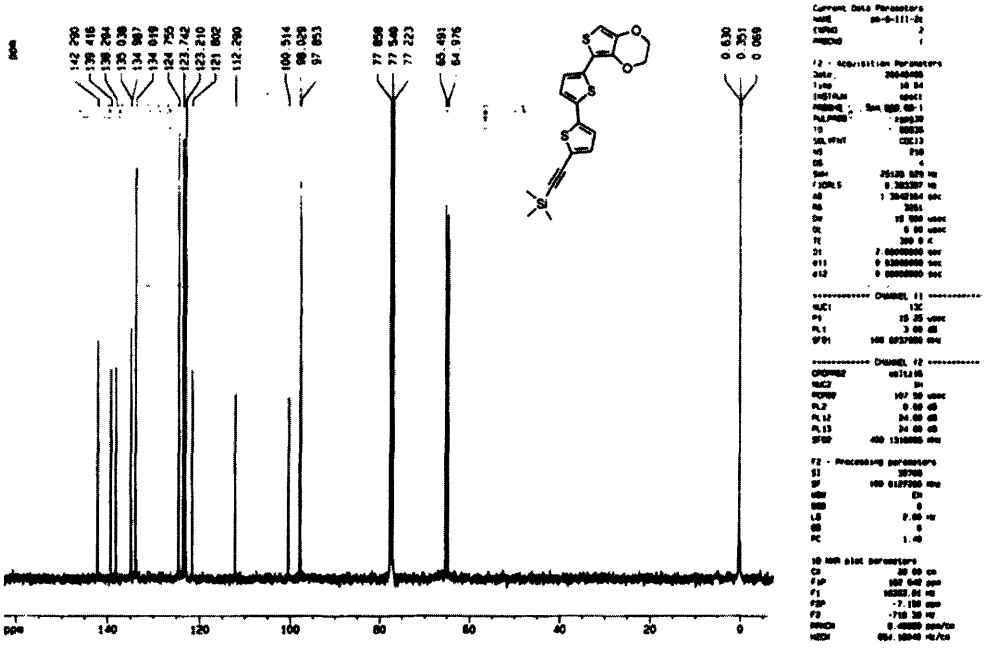

Compound **5**

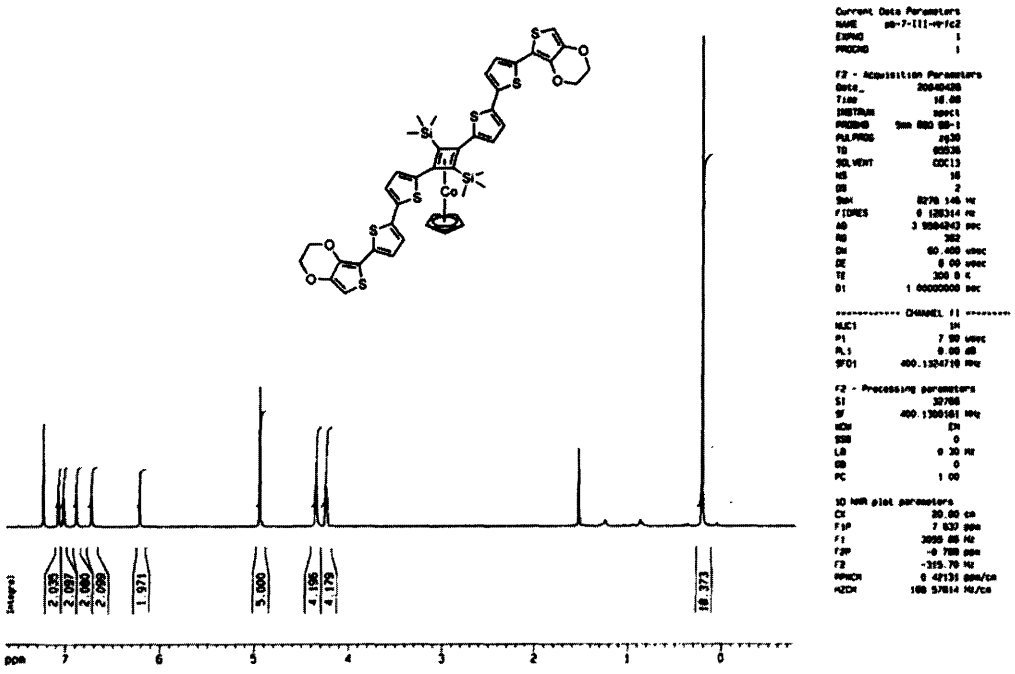

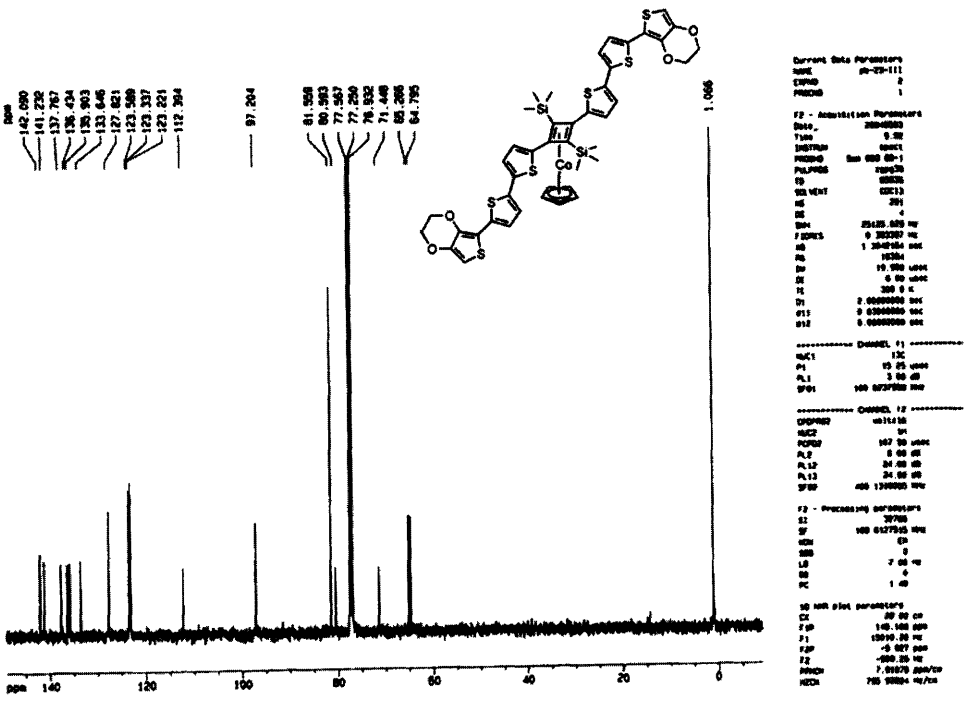

Compound **6**

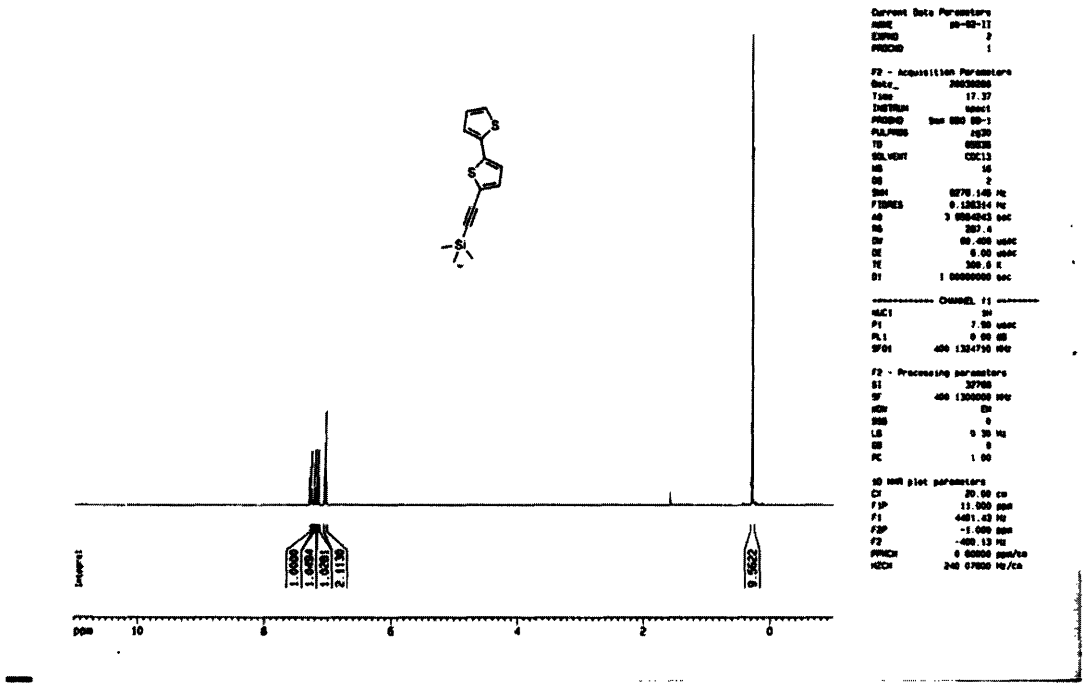

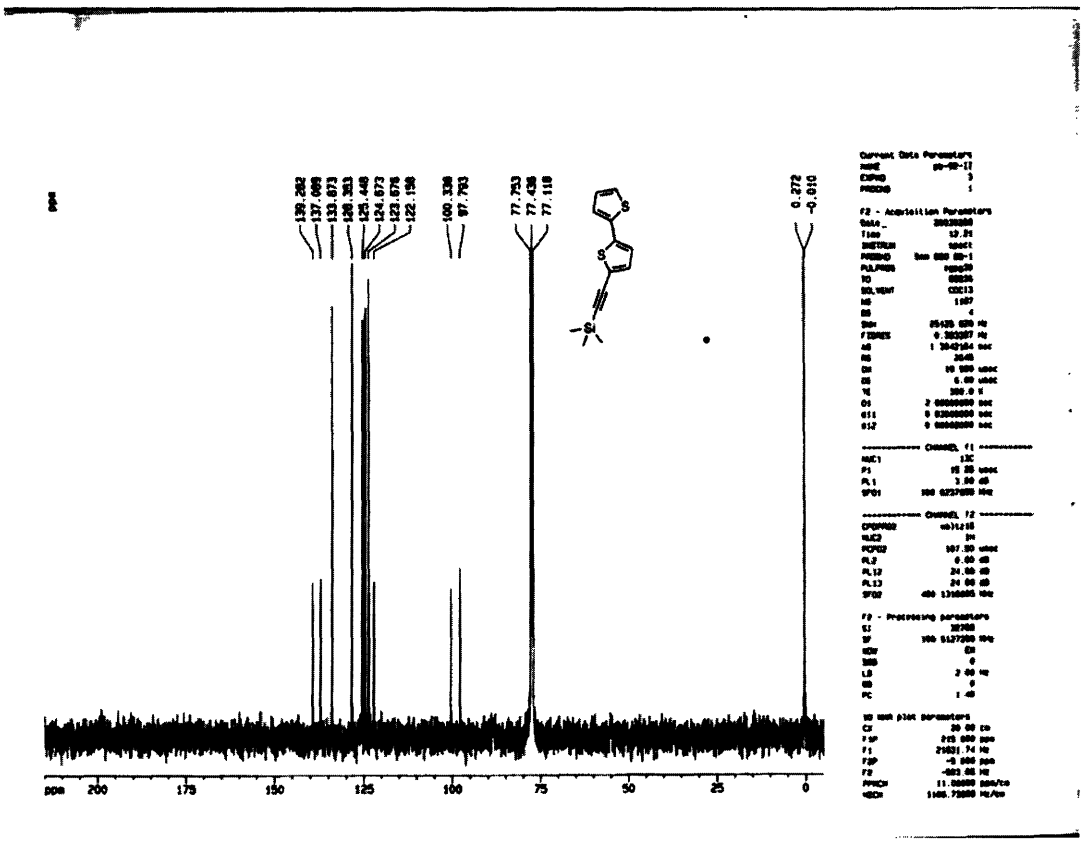

Compound 7

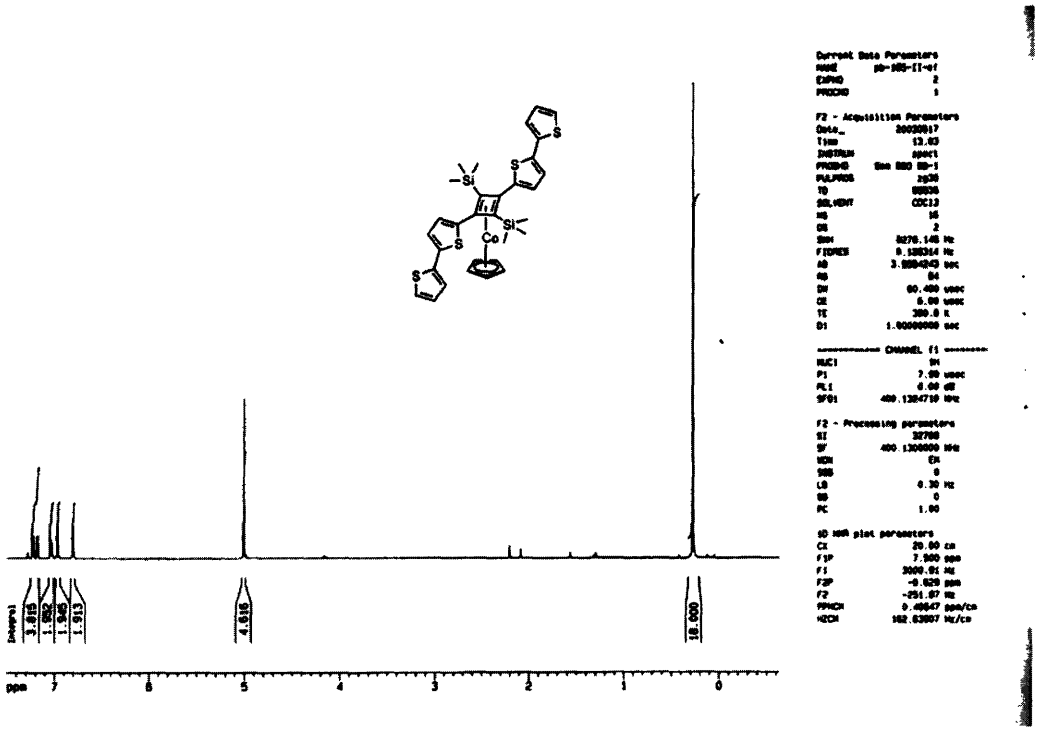

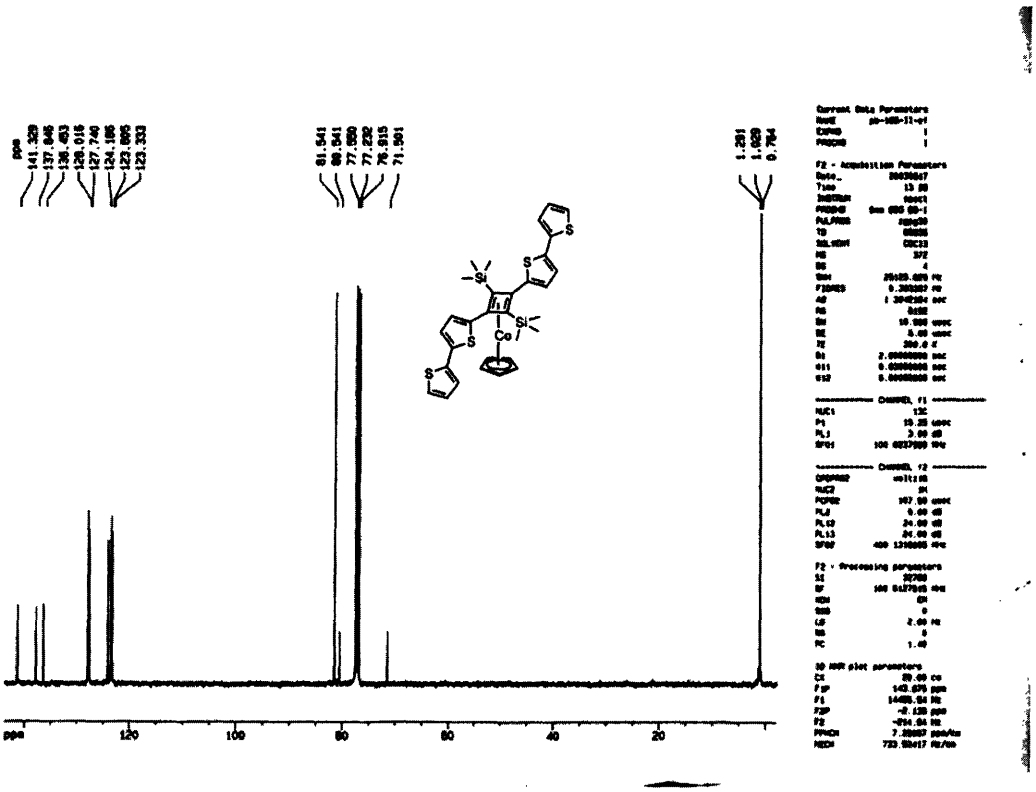

Compound **9**

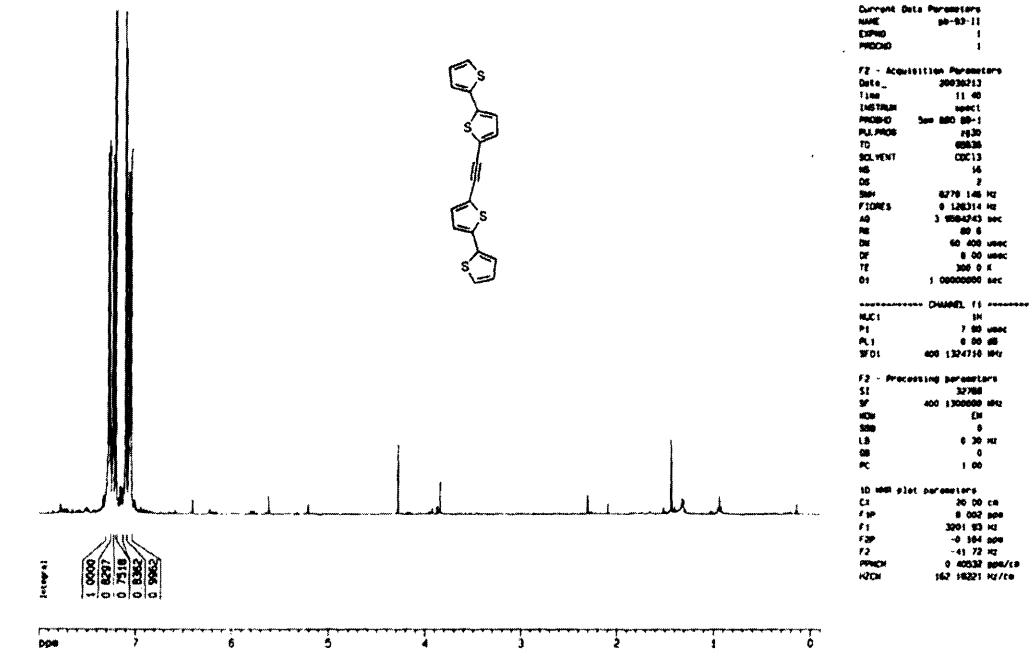

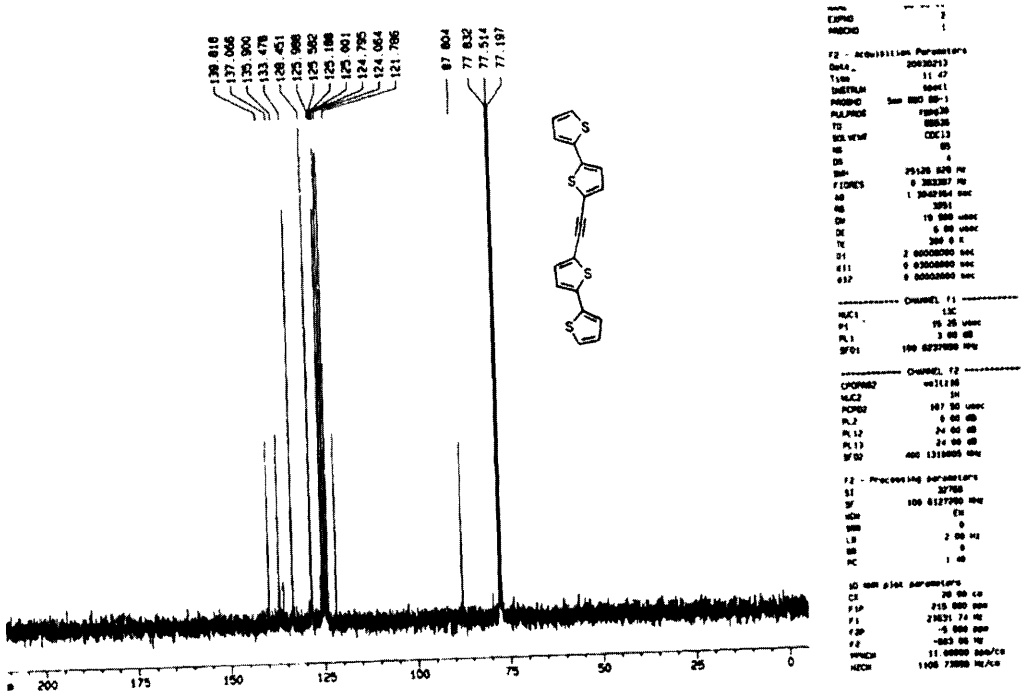

Compound **10**

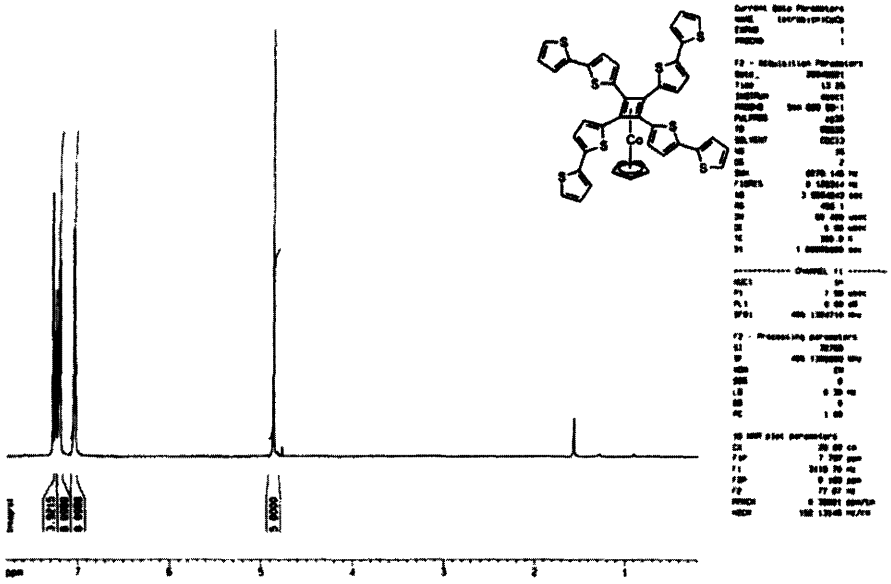

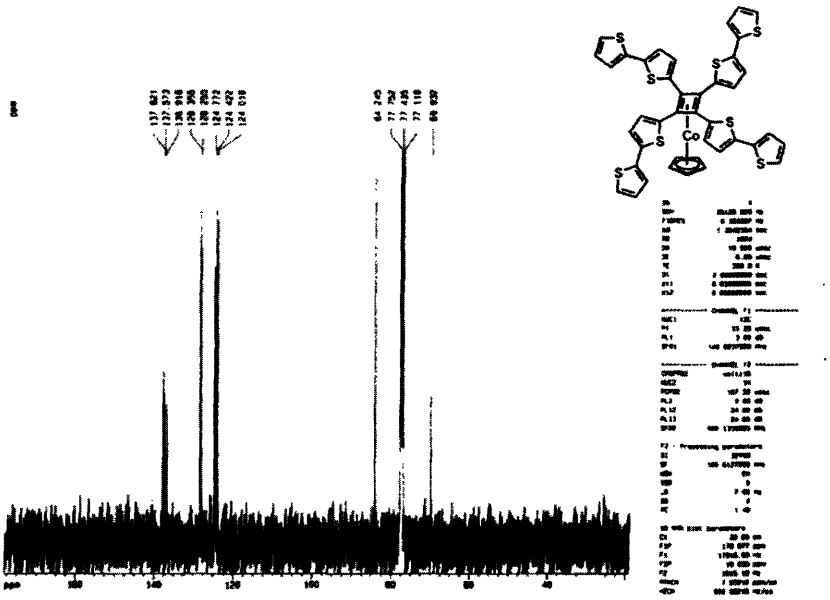

Compound **12**

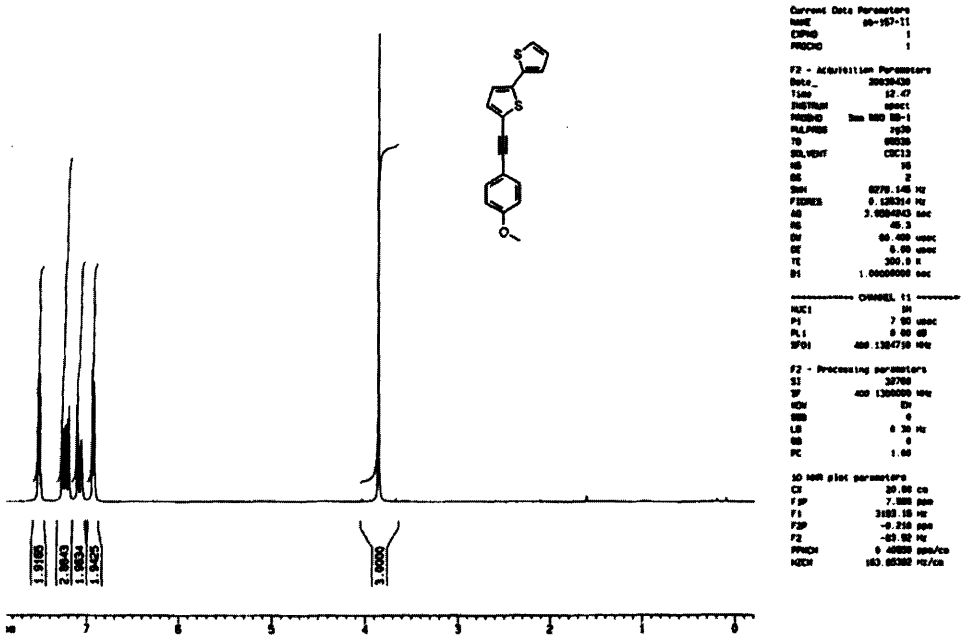

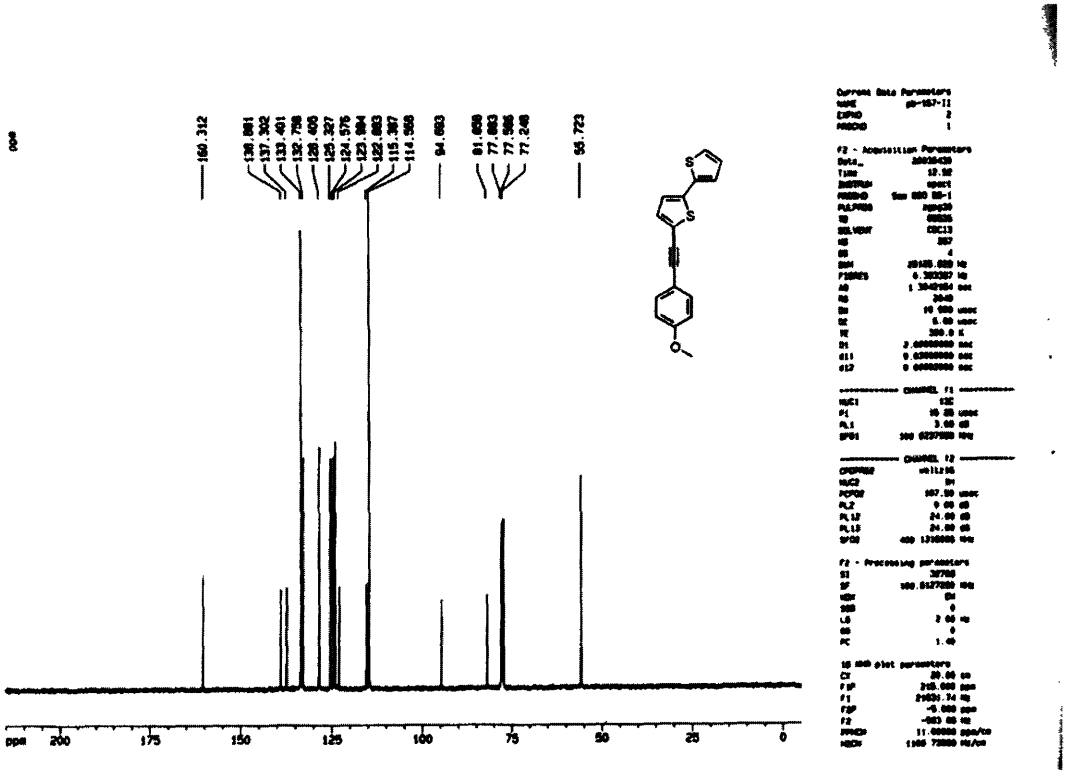

Compound **13**

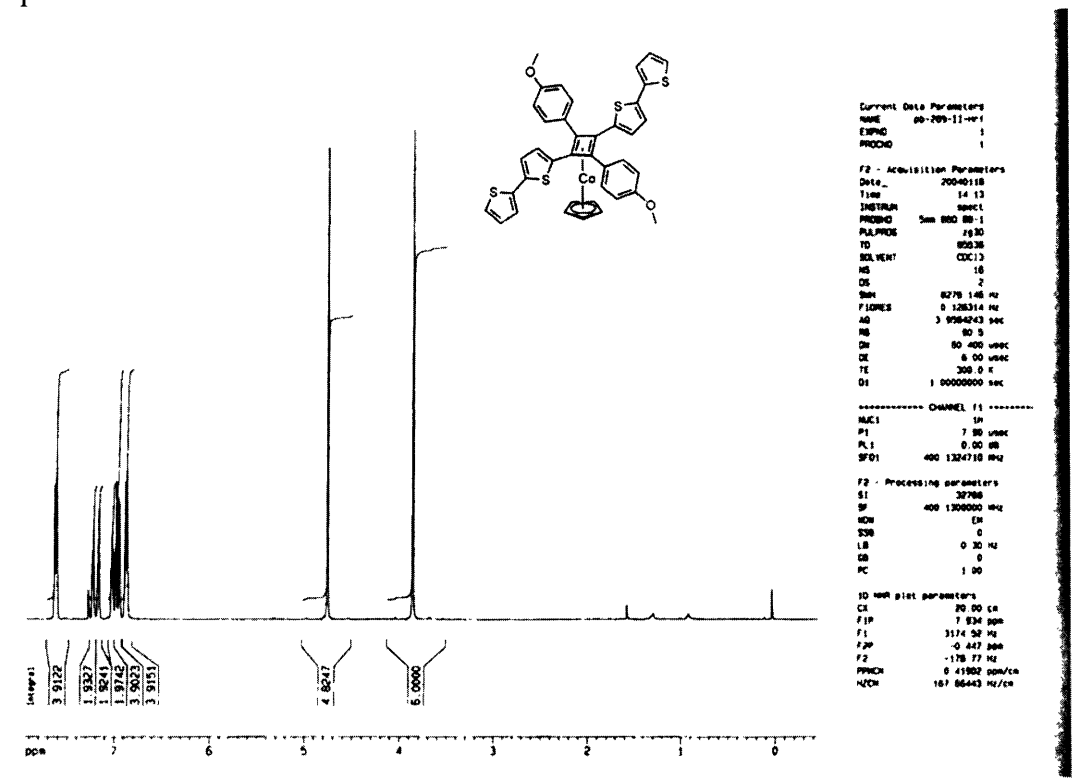

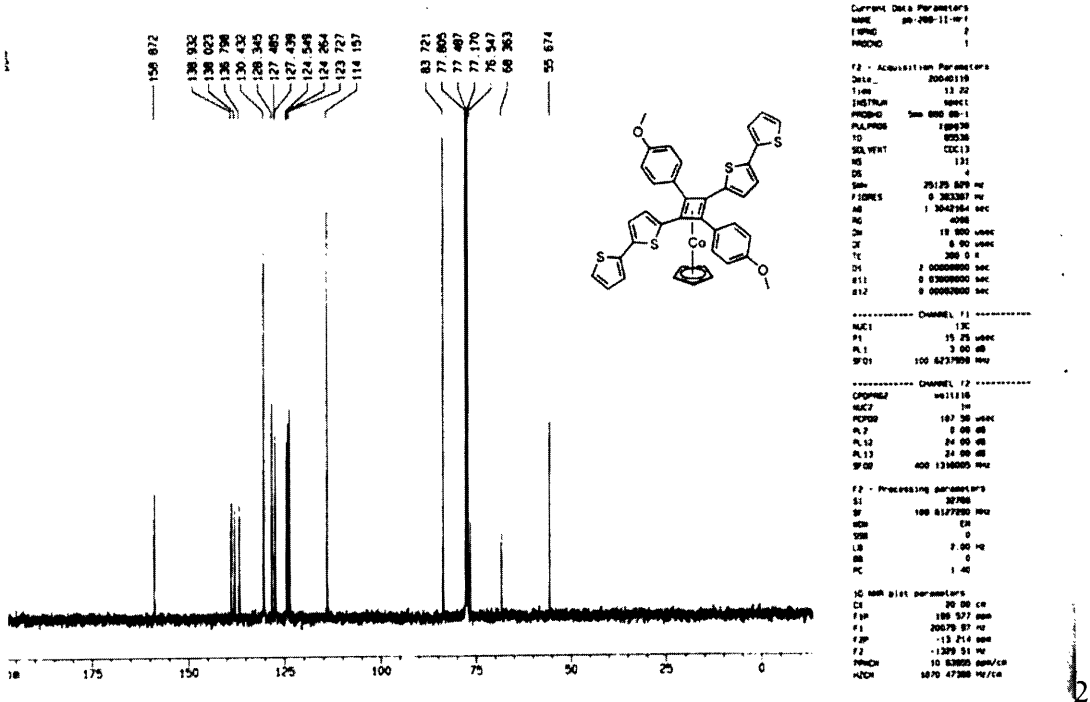

Compound **14**

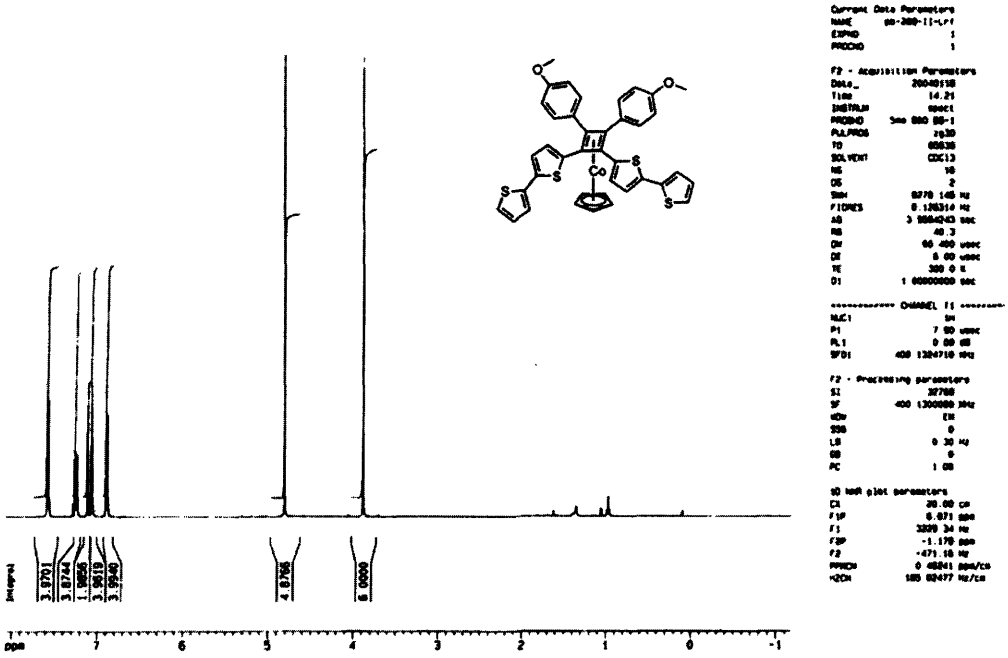

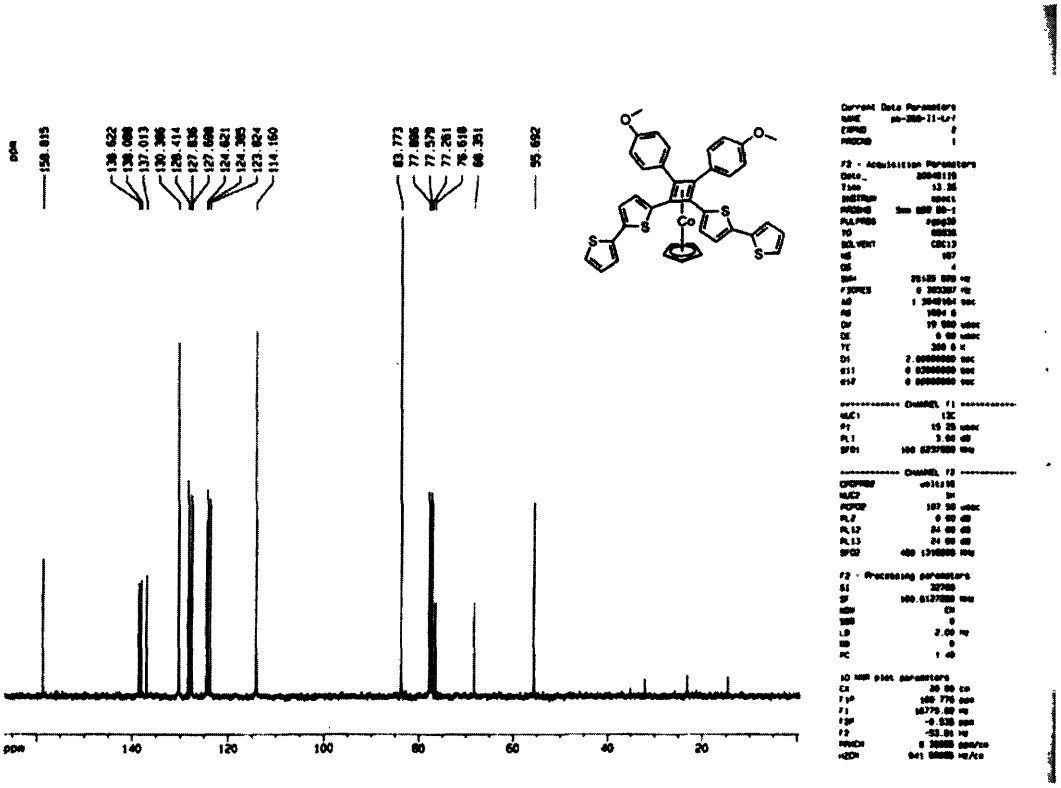

Compound **16**

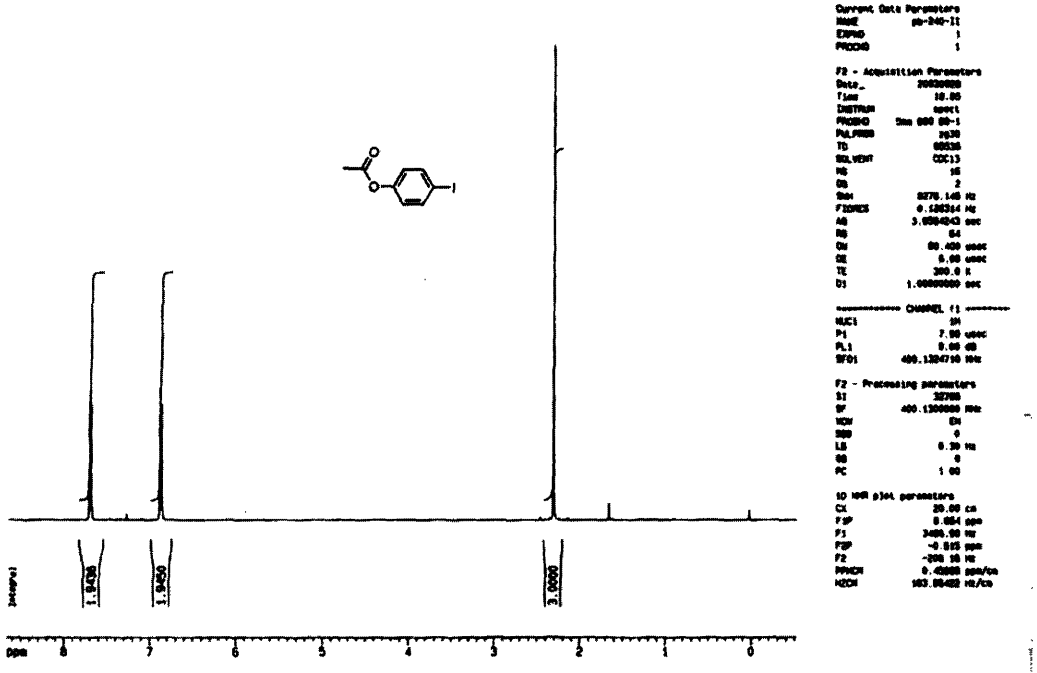

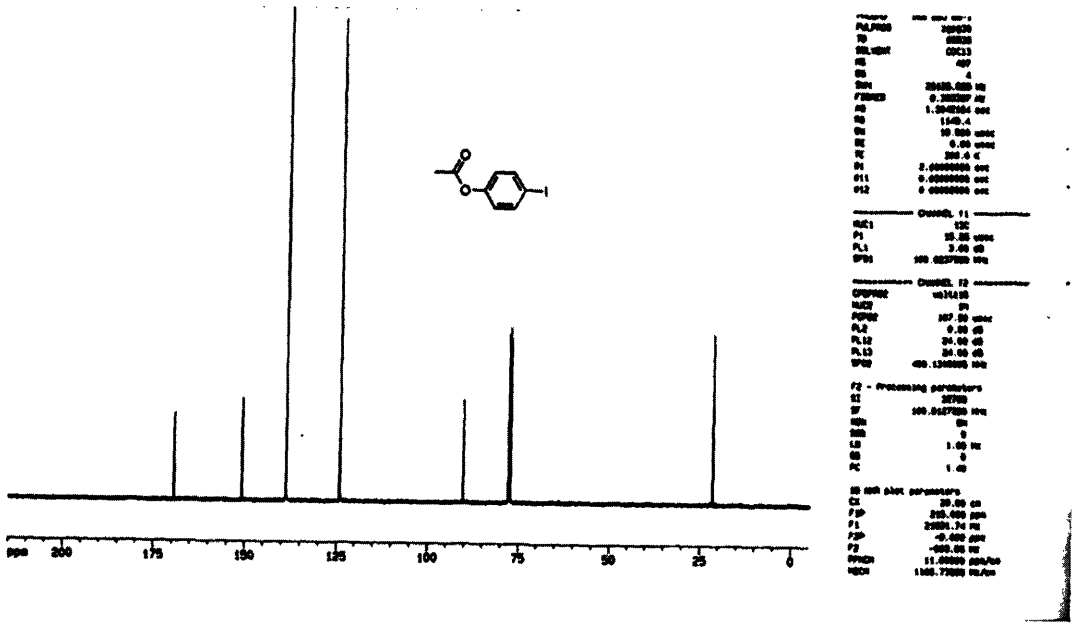

Compound **17**

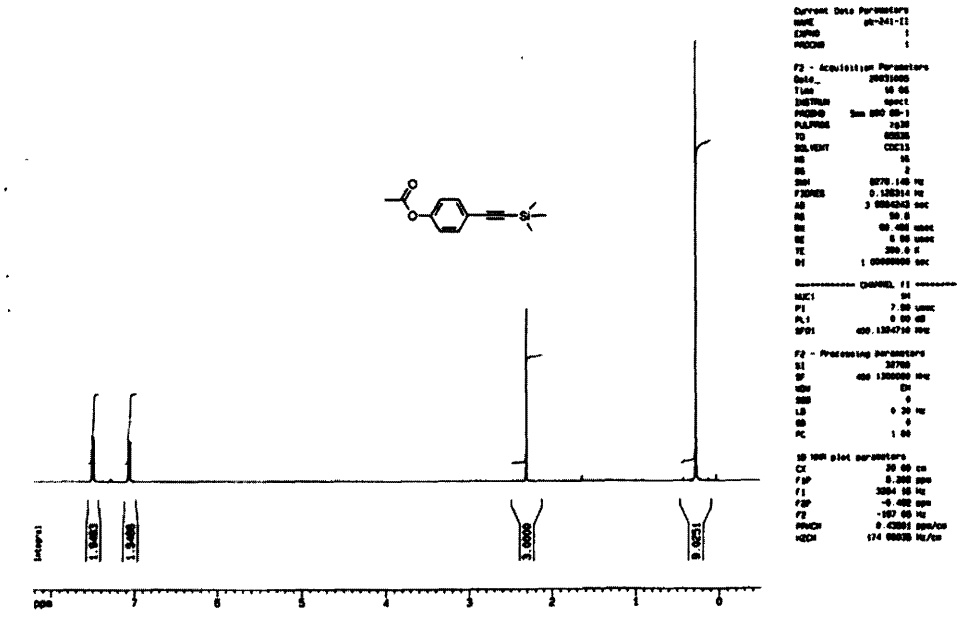

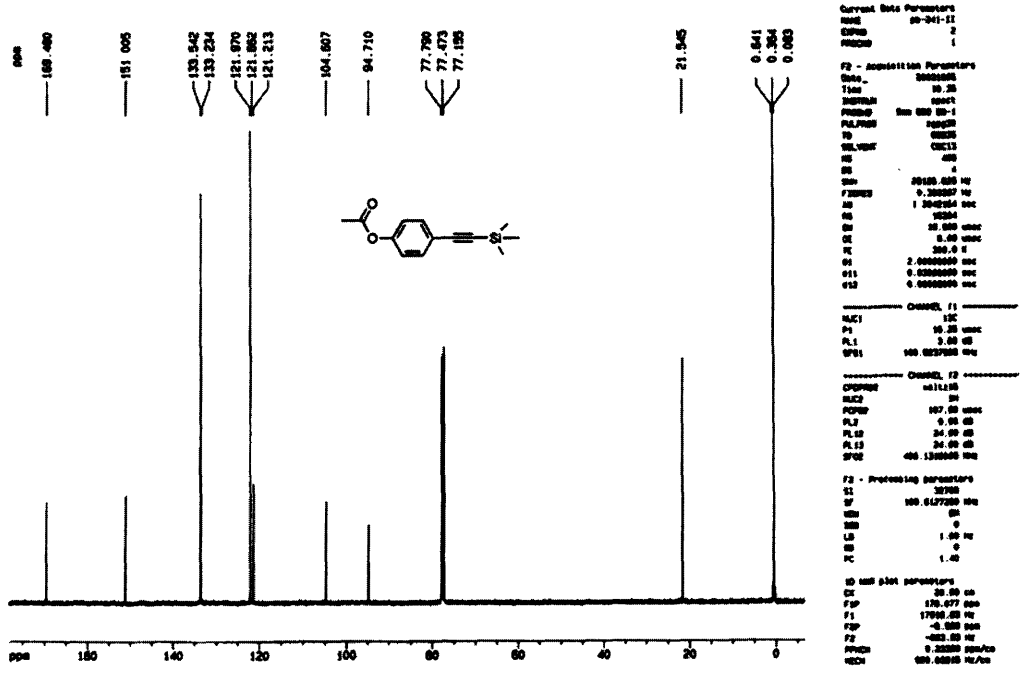

Compound **18**

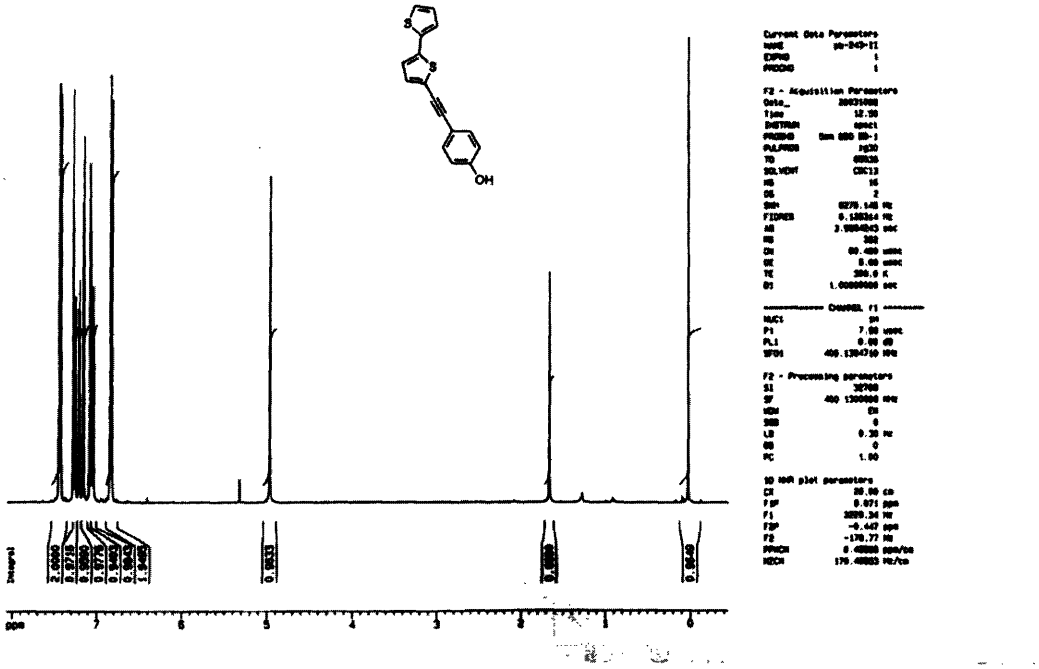

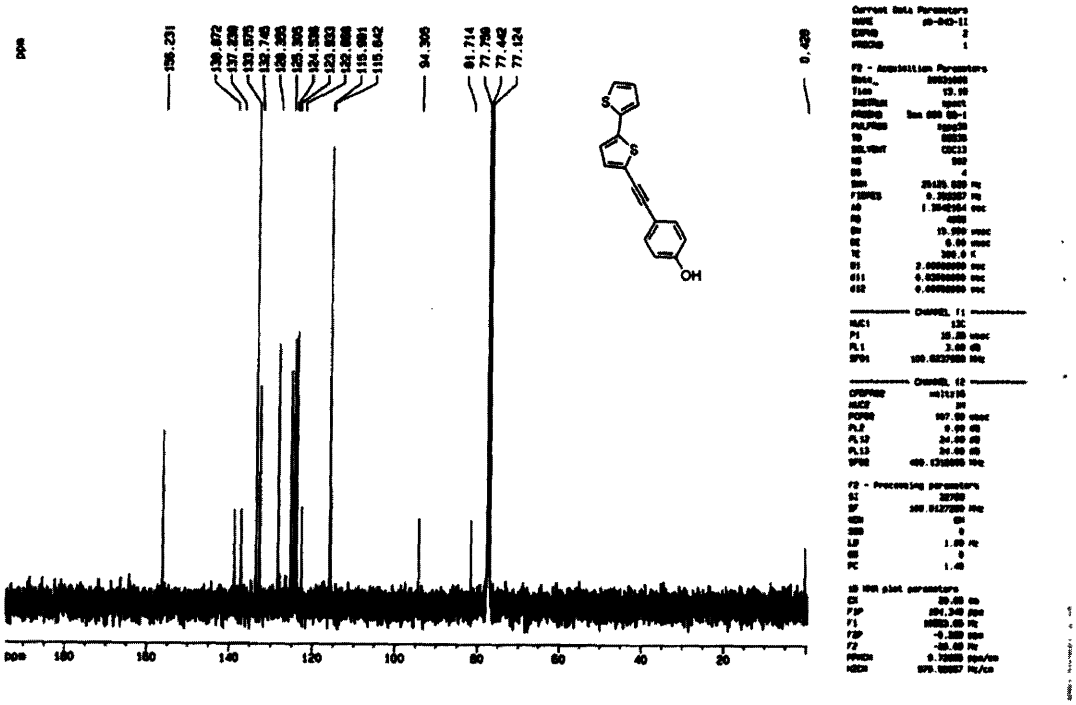

Compound **19**

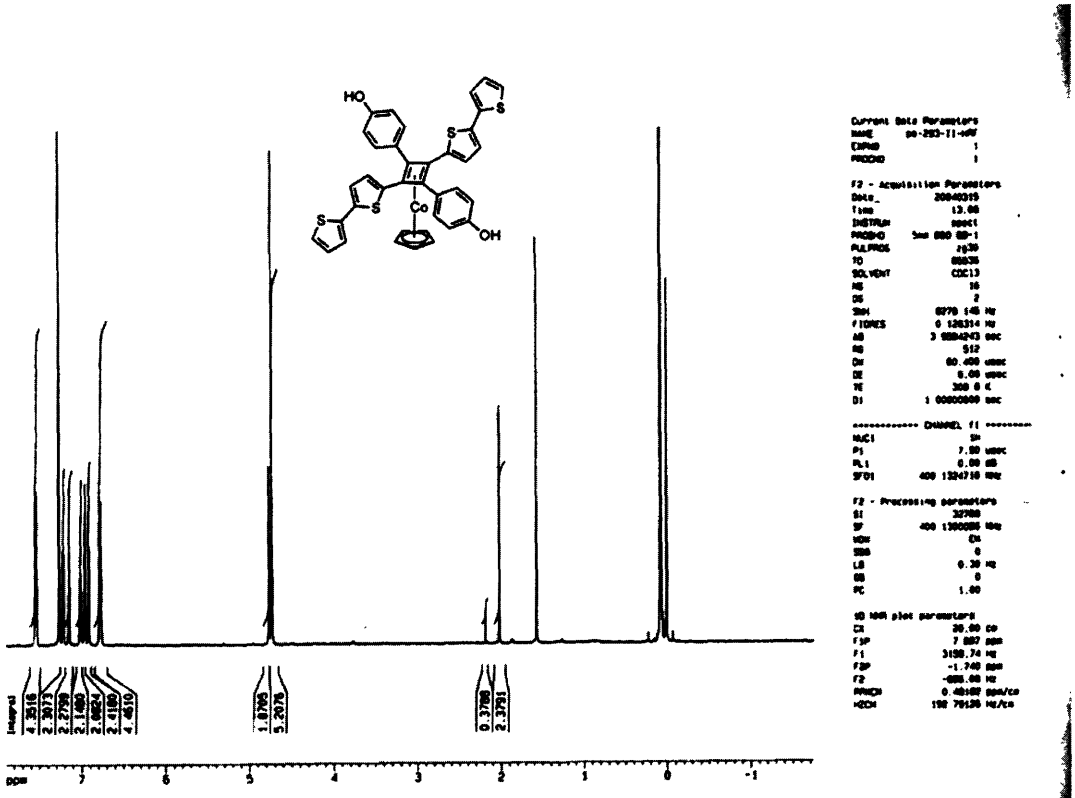

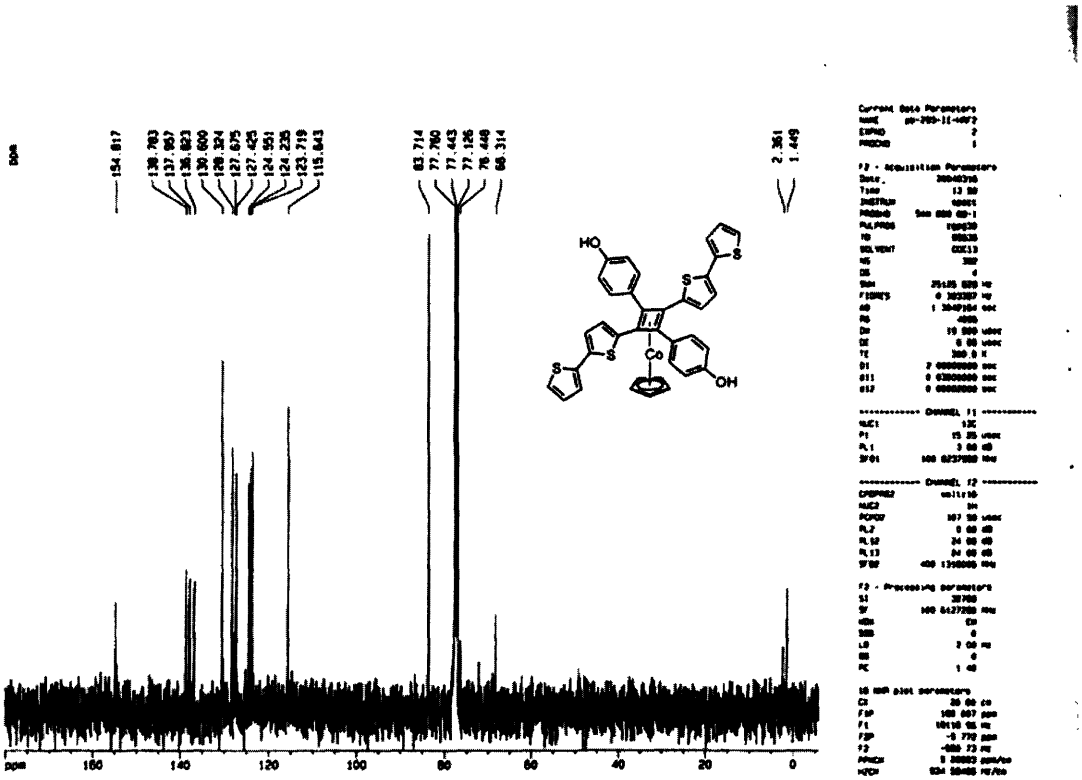

Compound **20**

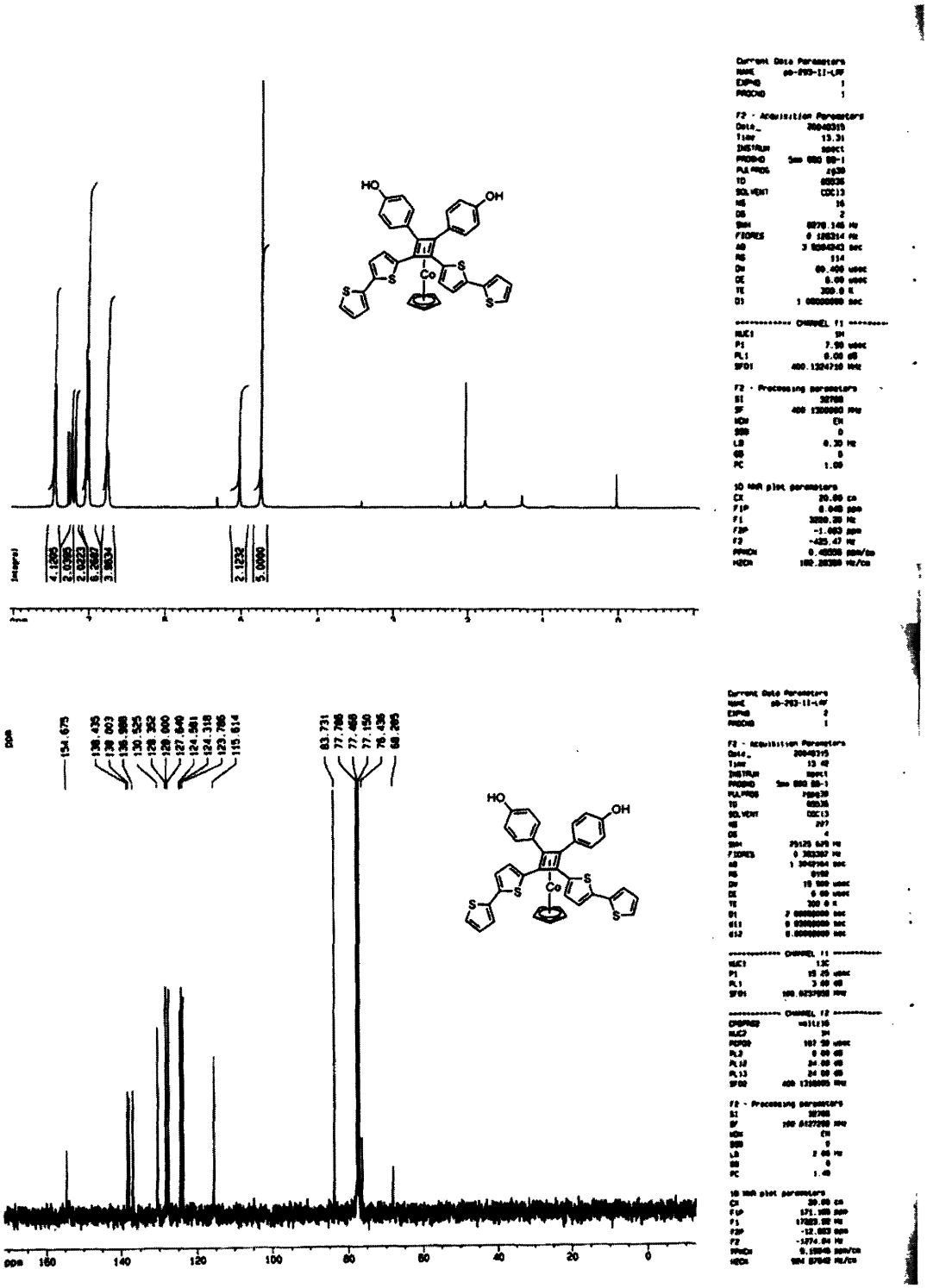

Compound **21**

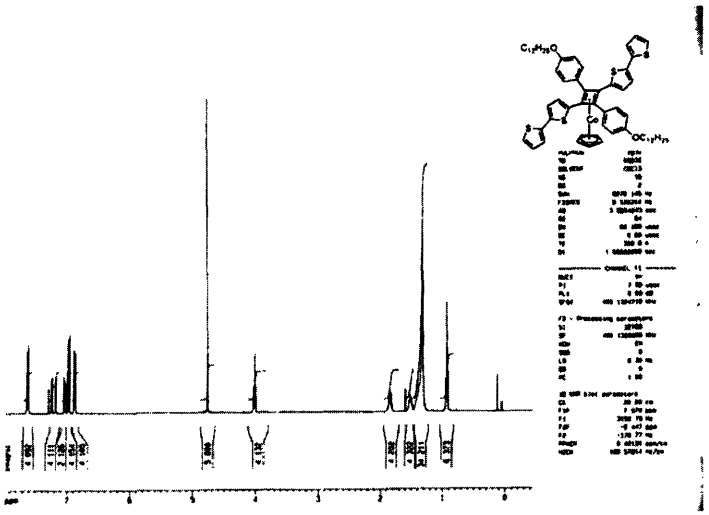

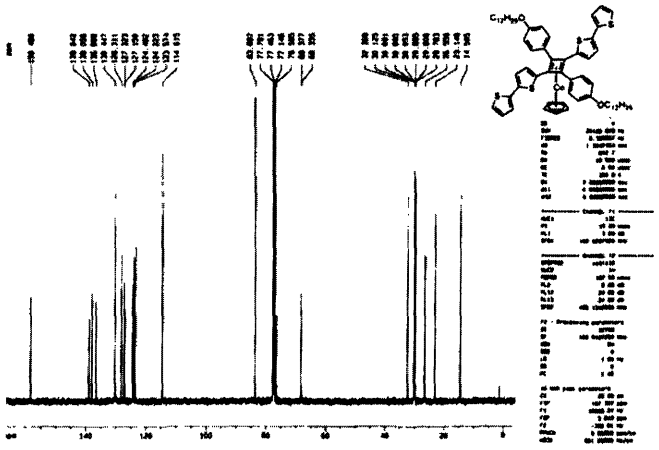

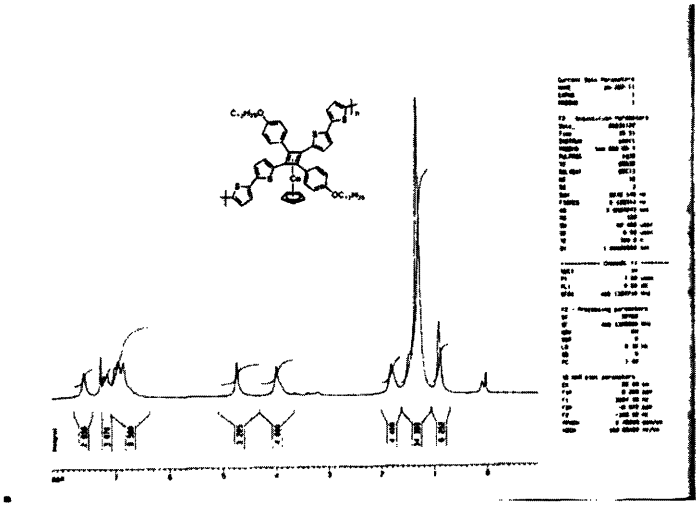

Compound **22**

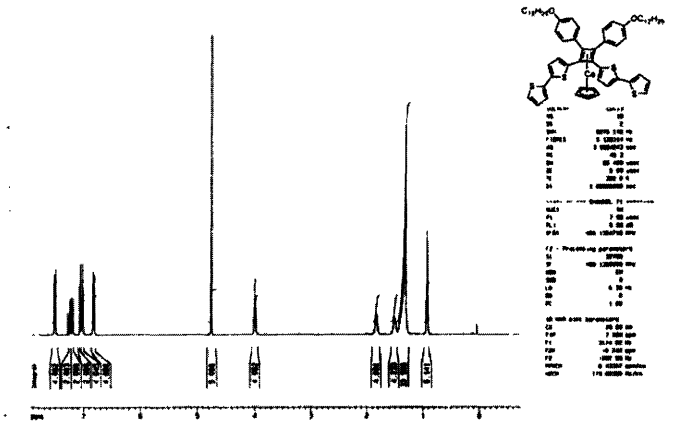

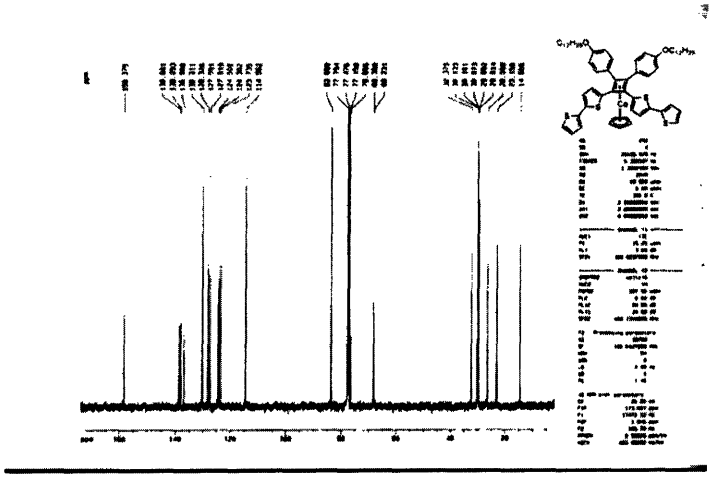

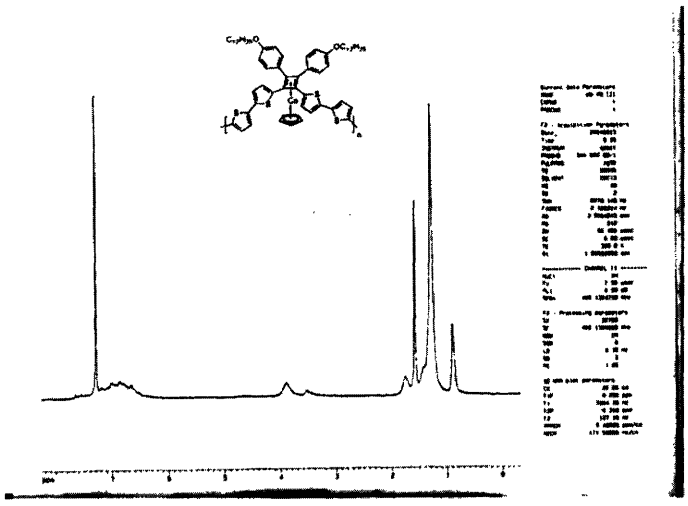

Compound **23**

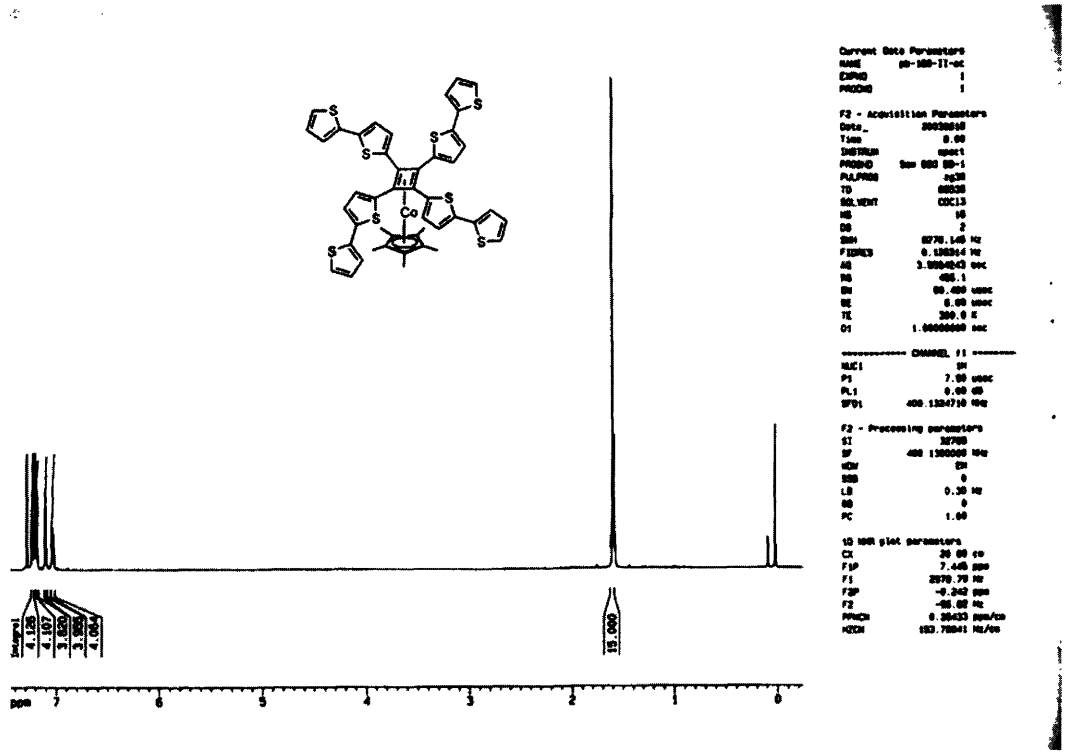

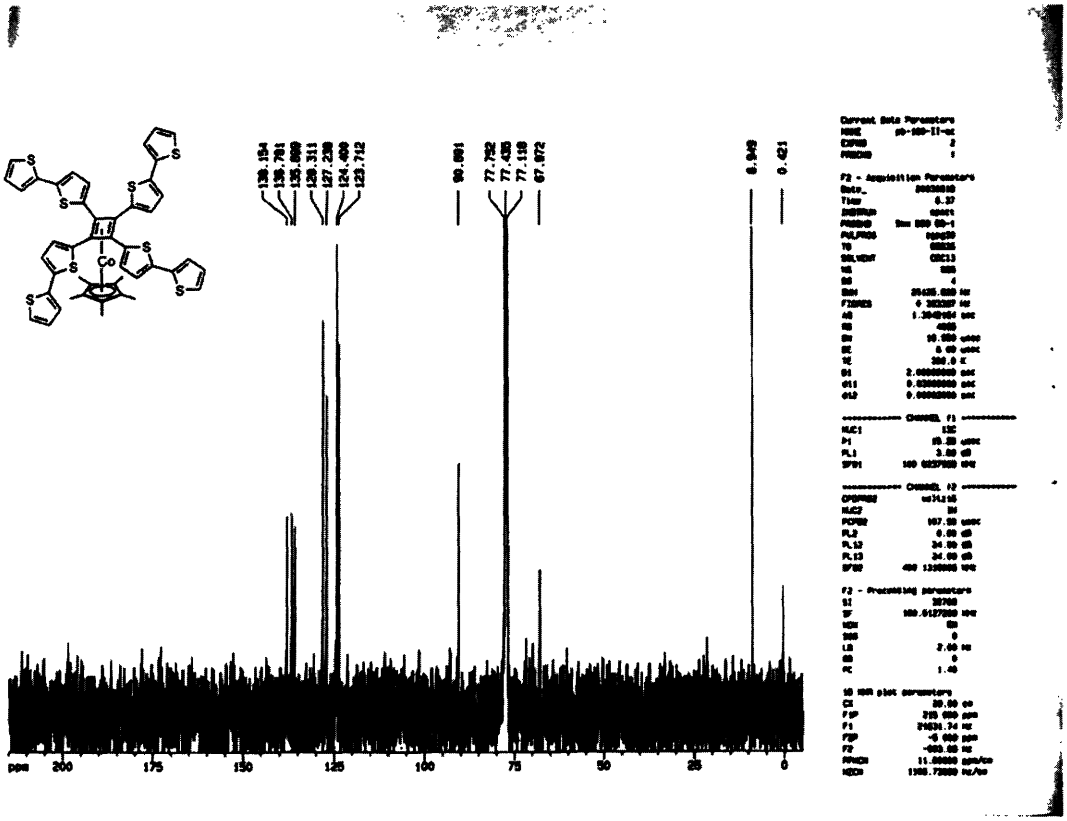

Compound **27**

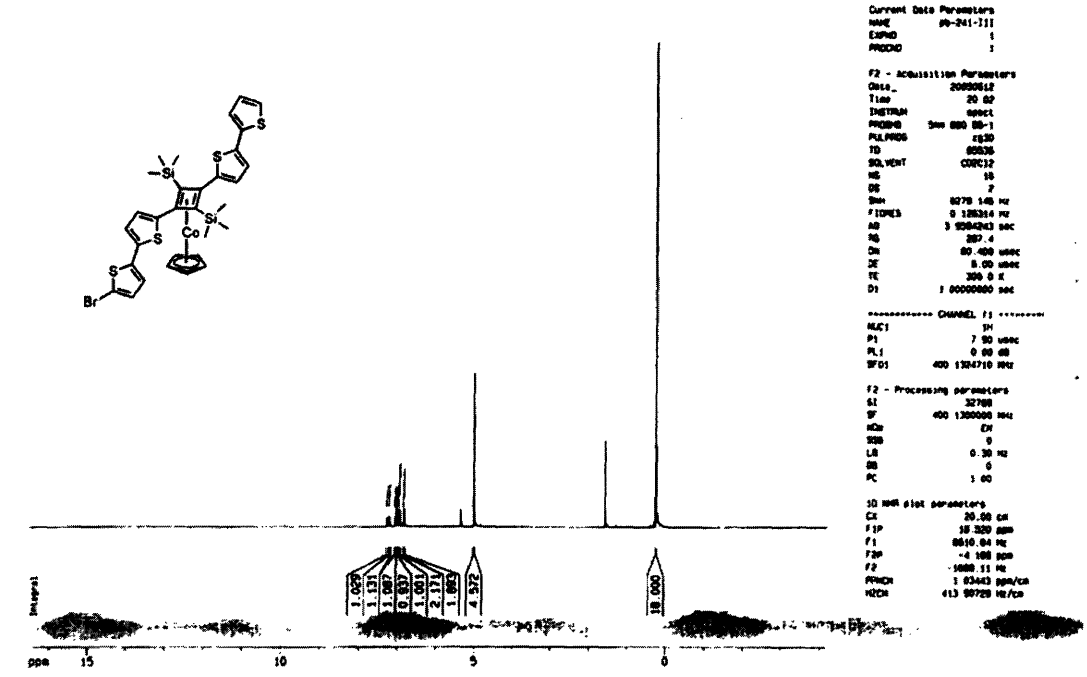

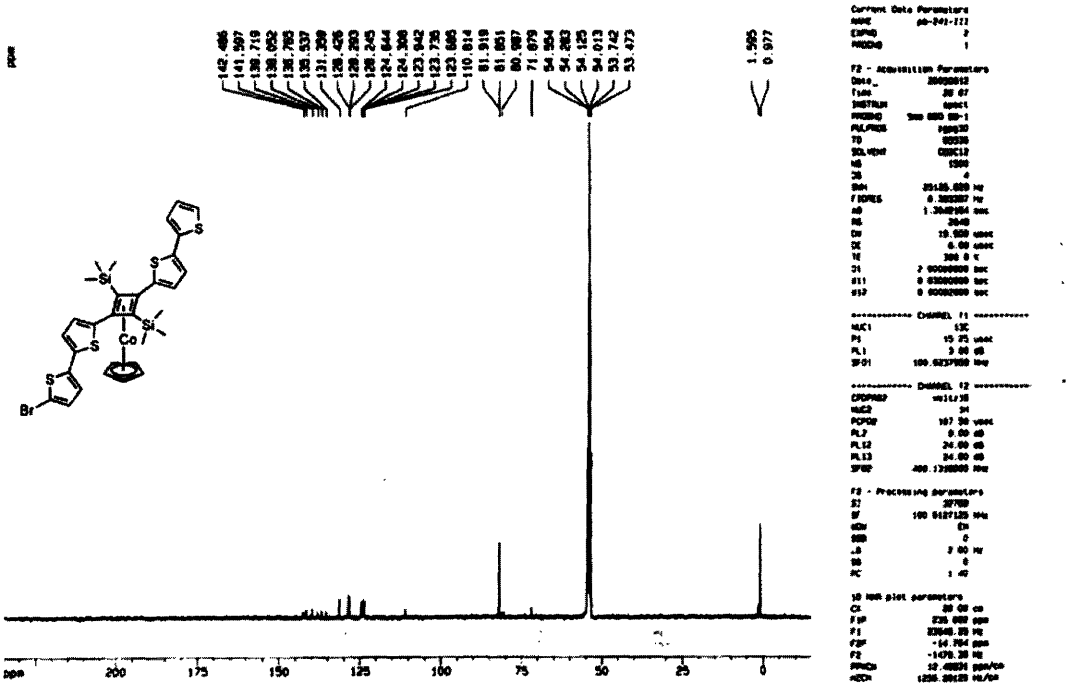

Compound **28**

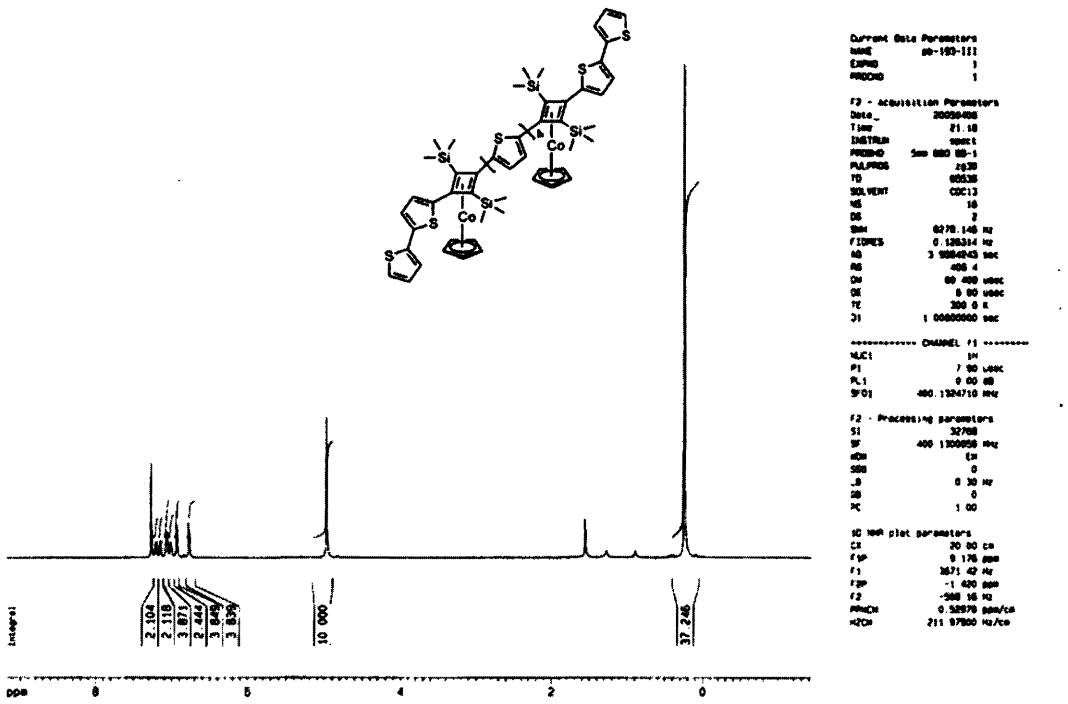

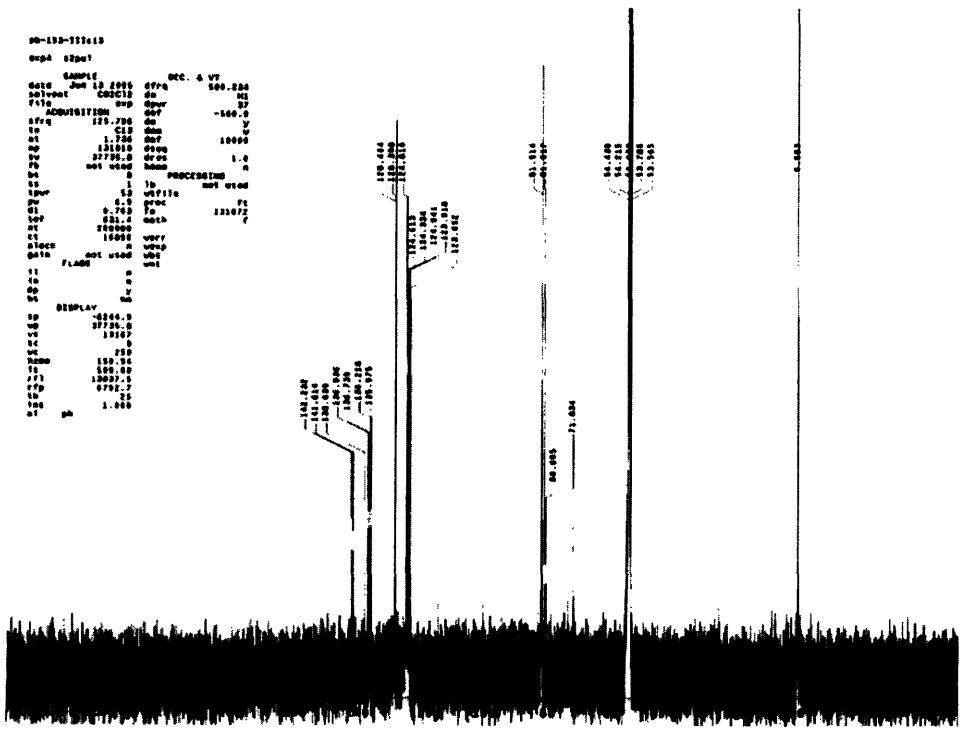

Compound **29**

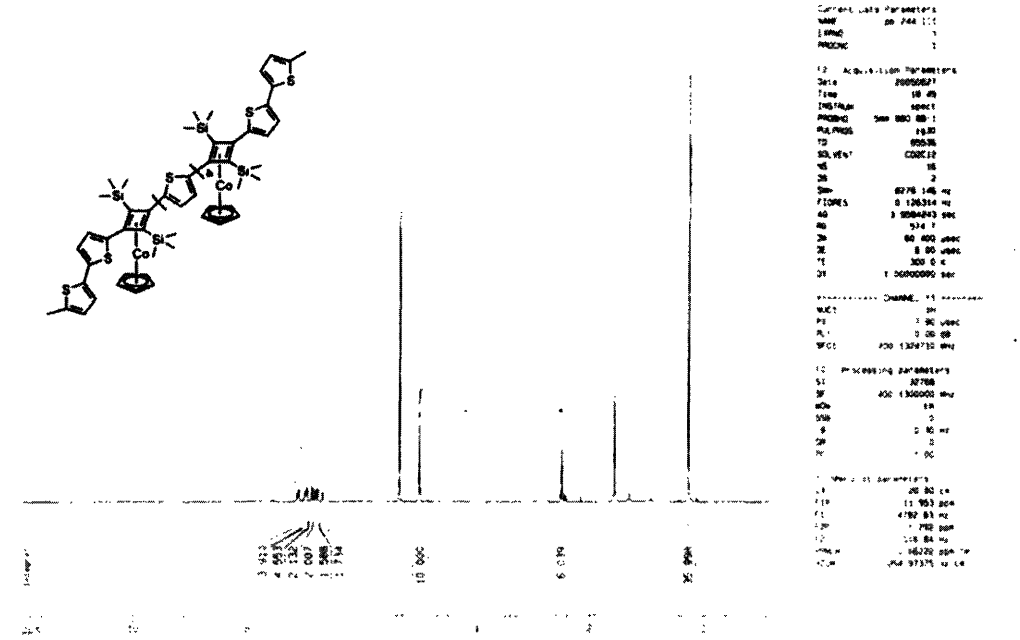

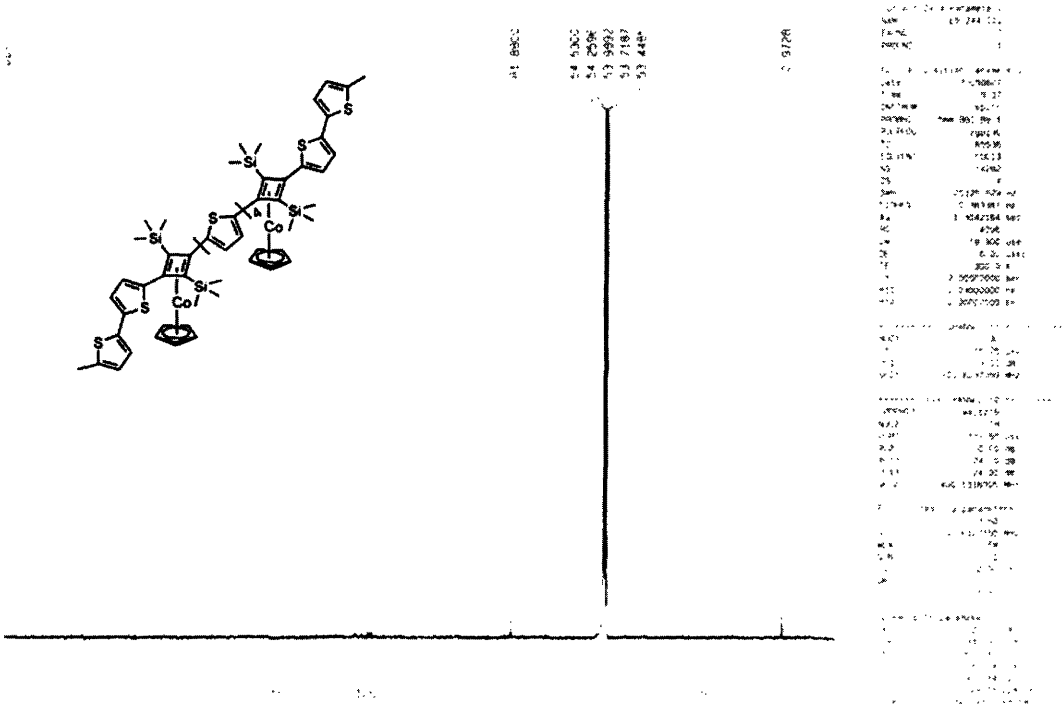

Compound **30**